DOCTOR OF PHILOSOPHY

Stimuli Responsive Hyperbranched Polymers for Anti-cancer Drug Delivery Synthesized Via RAFT Polymerization

Blackburn, Chester

Award date:
2021

Awarding institution:
Bangor University

DOCTOR OF PHILOSOPHY

Stimuli Responsive Hyperbranched Polymers for Anti-cancer Drug Delivery Synthesized Via RAFT Polymerization

Blackburn, Chester

Award date:
2021

Stimuli Responsive Hyperbranched Polymers for Anti-cancer Drug Delivery Synthesized Via RAFT Polymerization

Chester Blackburn BSc

School of Natural Sciences

Bangor University

A thesis submitted to Bangor University in partial fulfilment

for the degree of Doctor of Philosophy

Acknowledgements

The work published in this thesis would not have been possible without the help and support of so many people. Firstly, I would like to acknowledge the funding body Life Sciences Research Network Wales (NRN) for funding this PhD scholarship alongside Bangor University.

Secondly, without the support encouragement and insight of Dr Hongyun Tai I would not have pursued a PhD in the first place. Dr Tai is an incredible mentor and a fantastic woman who is wholly inspiring with the unique ability of turning every negative situation into a positive. It is through her warm words of support and guidance that this work was possible and her passion and drive for the subject that has guided me to where I am today, I hope one day to become a scientist as she has shown me, even 10% of her morals, characteristics and principles would make a truly inspiring scientist mentor and friend.

Thirdly, I would like to thank Edgar Hartsuiker, Martina Salerno and Angharad Wilkie from the North Wales Cancer Research Institute. Edgar has been a fantastic second supervisor with Martina and Angharad teaching me all I need to know about biology, coming from a person who didn't quite understand the structure of a cell I am now more than confident about performing biological analysis and assays myself. They are all dear friends and colleagues.

To Wenxin Wang and Xi Wang at University College Dublin and to Ian Ratcliffe and Chandra Senan at Wrexham Glydwr University. Without the help of these collaborations SEC and DLS analysis would not be possible, it is through collaborations such as these that science can blossom.

My family have been exceptionally supportive throughout my studies most notably my mother who despite my grievances has always pushed me to be the best I can be, and this was through her love, kindness and guidance, I hope to make her proud. These characteristics she has surely acquired from my grandmother who is equally inspiring in her own right and they are the two most important women in my life.

On the topic of family, it would be an insult to the vast chemistry family I have built throughout my years at Bangor if I didn't acknowledge them herein. Whilst there has been stress within the department and our family may no longer exist in its current form I would like to say my deepest thanks to all within the 501 society: Kenny, James, Mohammed, Sohad, Tom, Richard and David for all the support and guidance within chemistry they have shown me, whilst being amazing friends. Dr Paddy Murphy for many a lunch time putting the world to rights alongside Jamie and Dr Andrew Davies for keeping me up to date with the latest in the Sci-Fi world. Dr

Chris Gwenin has been throughout my time a fantastic tutor and friend and its through his straight to the point talking I have managed to overcome many hurdles and to the former technician Denis who I class as a dear friend to this day. To the rest of the academics, technicians and support staff, such as the cleaner Maggie whom with many a bacon roll was shared with and to whom I have not mentioned, as I believe this list would be endless, I want to thank you for being part of my family and giving me some of the happiest memories I will cherish.

I thank the Chem Tower itself, if I wasn't being trapped in elevators or having render from 10th floor falling upon me there was always something to make me smile. Be it failing fume hoods or leaks in the office, you have your charm and don't let anyone tell you any different!

A special thanks must go to Sara Little who has shown me love and support since I returned to Nottingham to embark on my write up. Through a serendipitous meeting a week after I returned there is seldom people you meet in life that can drag you up when you are down. It is with this vigor and lust for life you will become the most fantastic nurse and we will make the most amazing memories with a pink gin in one hand and no limitations in the other.

Finally, to the late Charles Nicholson, I hope you have a old fashioned for me up there in the clouds.

Diolch yn fawr.

Abstract

This thesis describes the development of novel pH responsive hyperbranched polymers via the Reversible Addition Fragmentation chain Transfer (RAFT) polymerisation technique, for the targeted drug delivery of cancer therapeutics via folate mediated endocytosis.

This thesis consists of four chapters, described as such: Chapter one introduces the common topics within the subject area, with a focus on the issues surrounding current drug efficacy and efficiency within cancer therapies. A broad review of the current state of the disease in the 21st century and current therapeutic developments regarding nanotechnology and targeted drug delivery are discussed. With an insight into a multitude of polymerisation and bioconjugation techniques including Free Radical Polymerisation (FRP), Atom Transfer Radical Polymerisation (ATRP), Nitroxide Mediated Polymerisation (NMP) and RAFT polymerisation, highlighting the advantages and disadvantages of each and the ability of “controlled/living” polymerisation techniques to synthesise materials with complex topology. Furthermore, an introduction into the world of “smart” materials and hyperbranched polymers is discussed, emphasising the advantages of stimuli responsive materials in drug delivery and beyond due to their ability to respond sharply to changes in the external environment facilitating actions such as drug release, gelation, changes in hydrophilic/hydrophobic character and self-assembly characteristics of the macromolecule.

Chapter two discusses the analytical methodologies adapted in detail with a background of the techniques and the methodology and hardware behind them. Additionally, contained within this chapter are all the calibration details and the details of standards run within an experimental section.

Chapter three focuses on the design and synthesis of novel hyperbranched polymers and the experimental and analytical methodology adopted discussed. Three monomers were chosen as the building blocks for RAFT co-polymerisation: 2-propyl acrylic acid (PAA) 2-(dimethylamino) ethyl methacrylate (DMAEMA) and disulfanebis(ethane-2,1-diyl) (DSDA) using 4-cyano-4-(((dodecylthio)carbonothioyl)thio)pentanoic acid as RAFT agent. The polymerisation

of this macromolecule was investigated at different monomer reaction feed ratio compositions to deduce the “sweet spot” for control and optimisation. Further work then investigated the control of molecular weight and dispersity via further experiments increasing RAFT agent ratio into reaction feeds. Characterisation was performed via Nuclear Magnetic Resonance (NMR), Size Exclusion Chromatography (SEC) and Dynamic Light Scattering (DLS). This is the foundation of the project, with further bio conjugation reactions via Steiglich esterification to modify the hyperbranched structures and biological studies assessing the design of the structure discussed in chapter three.

Chapter four, as previously stated focuses on the behaviour of the material post modification, with the synthesis Poly(ethylene glycol) (PEG) based linkers used to exploit high functionality associated with hyperbranched structures to covalently bond ligands or interest onto the structure. The experimental and analytical methodology are also discussed in this chapter. Folic acid was chosen as the targeting ligand, as to exploit folate mediated endocytosis, whilst the commonly used chemotherapeutic drug gemcitabine was used for drug efficacy and efficiency studies via the MTT cytotoxicity study. Characterisation of conjugates was performed via Fourier Transform Infra-Red (FTIR) Ultra Violet Visible Spectroscopy (UV-VIS), NMR and DLS. For biological investigations the HeLa cell line was chosen as the model cell line, for both cytotoxicity and cell uptake studies, which were characterised via UV-VIS and confocal microscopy respectively.

Chapter five acts as a summation of the results presented in this thesis and aims to draw rational conclusions from the data. The initial design is critiqued against alternatives, such as: alternative monomeric building block and alternative targeting moieties, whilst possible enhancements to the structure are discussed, as a basis for future work concerning this structure. Finally, the project aims, and project vision are evaluated against the results provided.

List of Abbreviations

5-Fu - 5-Flourouracil
ACVA - 4,4′-Azobis(4-cyanovaleric acid)

AFM - Atomic Force Microscopy

AIBN - Azobisisobutyronitrile

APC - Adenomatous Polyposis Coli gene

APCI - Atmospheric Pressure CI

ATP - Adenosine Triphosphate

ATR - Attenuated Total Reflectance

ATRP - Atom Transfer Radical Polymerization

BOC - Di-tert-butyl dicarbonate

BPY - 2,2’-bipyridine

BRCA - (BR)east (CA)ncer gene

BSA - Bovine Serum Albumin

CAM - Cell Adhesion Molecule

CDKN2A -Cyclin Dependent KiNase Inhibitor

CI - Chemical Ionisation

CLSM - Confocal Laser Scanning Microscopy

COSHH - Control Of Substances Hazardous to Health

CPP - Cell Pentrating Peptide

CPT - Camptothecin

CRP - Conventional Radical Polymerizations

CT - Computerized Tomography

CTC - S-Carboxymethylthiocysteamine

DAPI - (4′,6-diamidino-2-phenylindole)

DB - Degree of Branching

DCC - Dicyclohexylcarbodiimide

DCCu - DicyclohexylUrea

DCM - Dichloromethane

DDS - Drug Delivery System

DEAA - N,N-diethylacrylamide

dFdC - Gemcitabine

dFdCDP - Gemcitabine Diphosphate

dFdCMP - Gemcitabine Monophosphate

dFdCTP - Gemcitabine Triphosphate

DIAD - Diisopropylazodicarboxylate

DLS - Dynamic Light Scattering

DMAEMA - 2-(dimethylamino) ethyl methacrylate

DMAP - Dimethylaminopyridine

DMEM - Dulbecco's Minimum Essential Medium

DMF - Dimethylformamide

DMSO - Dimethylsulfoxide

DNA - Deoxyribonucleic Acid

DPBS - Dulbecco's Phosphate Buffered Saline

DSDA - Disulfanebis(ethane-2,1-diyl)

DSDMA - ((Disulfanediylbis(ethane-2,1-diyl) dimethacrylate

EDC - N'-ethylcarbodiimide

EGFR -Eepidermal Growth Factor Receptor

EI - Electron Impact

EPR- Enhanaced Permeation and Retention

ErbB - Erythroblastic Oncogene B

ESI - Electrospray Ionisation

FAB - Fast Atom Bombardment

FACS - Flourescence Assisted Cell Sorting

FBS - fetal bovine serum

FDA - Food and Drug Administration

FITC - Fluorescein

FR - Folate Receptor

FRP - Free Radical polymerization

FTIR - Fourier Transform Infra Red

GPC - Gel Permeation Chromatography

HBP - Hyperbranched Polymer

HDI - Human Development Index

HeLa - Henrietta Lacks Cell Line

HEMA - hydroxyethyl methacrylate

HPV - human papillomavirus

IMS - Industrial Methylated Spirits

IUPAC - International Union of Pure and Applied Chemistry

KDa - KiloDalton

LCD - Liquid Crystal Display

LC-MS - Liquid Chromatography Mass Spectrometry

LCST- Lower Critical Solution Temperature

LINAC - Linear Accelerator

L-L-C - Ligand-Ligand-Conjugate

LSM -Laser Scanning Microscope

mAb - Monoclonal Antibody

MALDI - Matrix Assisted Laser Desorption Ionisation

Mn - Number Averaged Molecular Weight

MRI - Magnetic Resonance Imaging

MS - Mass Spectrometry

mtDNA - Mitochondrial DNA

MTT - (3-(4,5-Dimethylthiazol-2-yl)-2,5-Diphenyltetrazolium Bromide)

Mw - Weight Averaged Molecular Weight

NCD - Non-communicable disease

NHS - N-hydroxysuccinimide

NIPAM - N-Isopropylacrylamide

NMP - Nitroxide Mediated Polymerization

NMR - Nuclear Magnetic Resonance

PAA - 2-Propyl Acrylic Acid

PBS - Phosphate Buffered Saline

PDI - Polydispersity Index

PEG - Poly(ehtylene glycol)

PEGDA - Poly(ethylene glycol diacrylate)

PEGdiPHT - PEG-dipthalamide

P-L-C - Polymer-Ligand-Conjugate

P-P-C - Polymer-Polymer-Conjugate

RAFT - Reversible Addition Fragmentation chain Transfer polymerization

RAFT agent -(((dodecylthio)carbonothioyl)thio)pentanoic acid

RDRP - Reversible-Deactivation Radical Polymerization

RI - Refractive Index

RME - Receptor Mediated Endocytosis

RNA - Ribonucleic Acid

RNR - Ribonucleotide Reductase

SEC - Size Exclusion Chromatography

SEM - Scanning Electron Microscopy

SLM - Spatial Light Modulators

TASC - Tumour Associated Stromal Cells

TEM - Transmission Electron Microscopy

TEMPO - ((2,2,6,6-Tetramethylpiperidin-1-yl)oxyl)

TFA - Triflouroacetic Acid

TLC - Thin Layer Chromatography

TMAEACl - Trimethylammoniumethyl acrylate chloride

TMEDA - Tetramethylethylenediamine

TNM - Tumour Node Metastasis

ToF - Time of Flight

TOP I/II - Topoisomerase I/II

TPEN - N,N,N',N'-tetrakis(2-pyridylmethyl)ethylenediamine

TQ - Triple Quad

TSG - Tumour Supressor Gene

UCST - Upper Critical Solution Temperature

UV-VIS - Ultra-Violet Visible

VEGF - Vascular Epithelial Growth Factor

VPF - Vascular Permeability Factor

List of Figures

List of Tables

Table of contents

Chapter One – An Introduction

1.1 Summary of introduction contents

The introduction to this thesis focuses on four main background themes integral to the planning and implementation of the core ideas behind this project. Firstly, the disease cancer is discussed in detail with both the genetic factors and environmental factors considered risk for cancer manifestation considered. Clinically, the classification of cancer is reported discussing both the advantages and disadvantages of the two classification systems, the number staging system and the Tumour, Node, Metastasis (TNM) system. Afterwards, the treatment of cancer of discussed, with both chemotherapy and radiotherapy considered in detail, as oppose to surgical removal, with the mechanisms of action of these treatments and the limitations discussed, and the impact on the cell cycle these treatments cause. Following on from this research in drug delivery systems is presented as an objective look at how researchers are aiming to overcome the limitations of chemotherapy in order to increase the targeting efficiency of the drugs in question, whilst also attempting to alleviate side effects caused by these high toxicity drugs. Additionally, the role of polymers is presented either synthesized via conventional methods to produce polymers of varying topology or via controlled radical methods. Synthetic methods are assessed and the limitations and positives from each approach are presented, whilst topological characteristics of polymers and the knock-on effect on polymer functionality and properties is discussed. Finally, stimuli responsive characteristics of polymers are discussed and route to synthetic production. The advantages of using so called “smart materials” is presented whilst blending themes from polymer synthesis, controlled polymerization methods and drug delivery strategies to look at contemporary macromolecules and their role in the fight towards drug delivery, with

advantages and drawbacks of using smart molecules rather than traditional drug delivery strategies.

1.2 Cancer onset, diagnosis and current treatments, a brief overview of current literature

This section aims to give the reader a brief overview of the current knowledge and some literature regarding cancer. Cancer is a huge subject and this section does not aim to give a definite and thorough review of the disease. However, for the remit of the thesis and the project it is important to understand how the disease is diagnosed, treated and current research regarding causation so that contributions to the fight against cancer can be made through research. Therefore, this section will cover briefly, how cancer is classed as a disease and the genetic and environmental factors suspected to play a role in onset, with brief case studies. Furthermore, treatments such as a chemo- and radiotherapy are discussed with their advantages and drawbacks. It is hoped that in this brief overview of the different aspects of cancer, the reader can acknowledge and get a feel for the complexities of the disease and the current direction of research, and understand as a chemist the appreciation that is required to be paid to multiple disciplines throughout this project. Therefore, being able to use this section of the introduction in order to be signposted, via references, to more substantial literature if they so desire.

1.2.1 Cancer as a Non-Communicable Disease throughout the developed and developing world

Cancer is widely regarded as a global burden and issue to humanity and the medical sector. 2018 estimates currently place an estimated 18.1 million new cancer diagnosed whilst 9.6 million deaths will occur from the disease [1]. As an ailment,

cancer is the result from malfunctions within cells leading to uncontrollable cell division and thus the formation of a large mass of tissue termed a tumour. In terms of cancers there are five main categories in which a cancer may fall into namely: carcinoma (cancer effecting the skin and tissues lining internal organs), sarcoma (cancers that develop and effect the bone, cartilage, fat and connective tissues), leukaemia (cancers of the blood and cancers effecting the bone marrow), lymphoma (cancers that effect the immune system and lymph nodes) and CNS cancers (cancers effecting the central nervous system encompassing the brain and the spinal cord). For example, breast cancer can be characterised as an invasive ductal carcinoma due to the cancer effecting the skin and tissue around the breasts themselves.

Furthermore, there is a general acknowledgement that within the developing world there is an increase of premature deaths (from the ages of 0-69) due to lack of facilities and medical care to accurately and efficiently diagnose and treat the disease, in addition recent studies report that in fact, cancer incidence is more prominent in the developed world than in the developing world[1].

Numerous factors could be attributed to this trend, for instance a form of relaxed natural selection. Due to the heightened medical care within countries with a high human development index (HDI) compared to those in the developing world, survival rates are increased at the expense of genetic defects that can lead to cancer being inherited throughout the bloodline [2]. Due to this reduction in mortality and an increasing fertility rate globally mutation-based natural selection may have been disturbed and distorted, allowing defects to accumulate within the gene pool, thus increasing the background effect of these mutations throughout lineage [3–7]. Cancer presents itself as one of the most widely known non-communicable diseases (NCDs) throughout the world. NCDs are defined as diseases that may or may not be caused by infection, however, they cannot be transmitted between person to person. For instance, the common cold is transmitted via infectious viral agents' and can be spread between people whereas cancer is self-contained within the body, whilst it may be triggered by infection it cannot be passed on to another as an infectious disease can. Cancer onset and progression is associated with two different gene types within the cell: oncogenes

and tumour suppressor genes (TSGs). Oncogenes are, in their non-mutated state, associated with the proteins needed for cell growth and differentiation, and compelling evidence on their effect on cancer onset within humans has been published throughout a variety of studies [8–16]. In the un-mutated form proto-oncogenes are completely benign and are involved in the normal regulation of the cell cycle, it is once activated they begin to cause malignant effects within the body.

TSGs similarly are completely benign within their unmutated form and act as a barrier against rapid cell proliferation preventing the onset of cancer by controlling aspects of cell division. Whereas oncogenes are known to cause cancer when mutations switch them on TSGs are only cancer causing when they are switched off via mutation.

1.2.2 Genetics and their link to cancer onset

As an oncogene, Her 2 was first implicated to be involved in the manifestation of human breast cancers in 1987 by Slamon et al. [16]. Structurally the erythroblastic oncogene B (ErbB) family of proteins (Her 1, Her 2, Her 3 and Her 4) consist of a binding site for extracellular ligands, a transmembrane domain with a juxatamembrane connected to a tyrosine kinase domain for intracellular operations, with a C-terminal tail [17] **(Figure 1-1**).

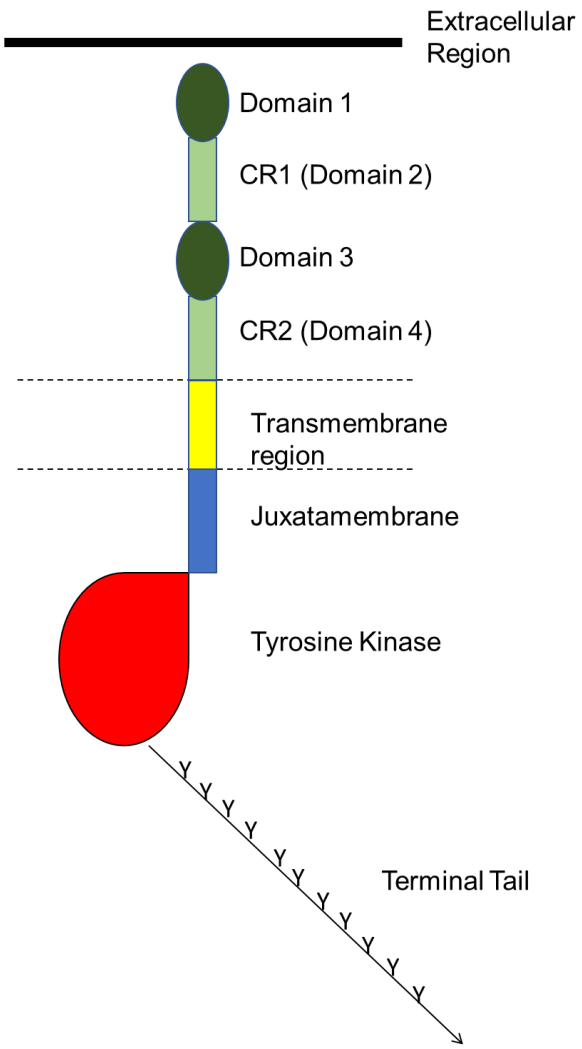

Figure 1- 1: Structural conformation of the ErbB family of genes

Her 2 has come under increasing interest as a foundation for the study of the oncogenic effect with respect to breast cancer in mammals (both human and non-human species) and has been established as an important biomarker for at least 30% of breast cancer patients [18], whilst it has also been observed to be present within gastric and salivary duct cancers. The ErbB family of proteins functionally are involved in the promotion of cellular proliferation pathways as oppose to the regulation of cells and the onset of apoptosis, and thus, when this gene is amplified aggressive and uncontrolled cell division may occur. Her 2 overexpression in cells can induce hyperactivation of ErbB signalling and thus promotion of this signalling pathway [17].

Thus, the clinical significance of oncogenes such as Her 2 is profound with associations to therapeutic resistance, whilst through research into Her 2 targeting methods there have been efforts to increase the rate at which Her 2 positive cancer is diagnosed. Thus, defining cancers as oncogenic positive can positively impact the course of action, providing extensive detail into the therapeutics that would provide the most potent response whilst also providing a road map for the possible resurgence of cancers and methodology in order to attempt to alleviate cancer onset post remission. In the case of breast cancer for instance, both men and women can undergo a mastectomy, in which either a single breast or both breasts are removed from the body entirely, either where the cancer is within a large surface area or has spread to the breast or as part of a pre-emptive strike due to high risk factors associated with possible somatic or germline mutations. Whilst this has obvious mental health effects to the patient themselves this procedure can dramatically reduce or eliminate the chance of either cancer resurgence or onset in the breast.

Her 2 however, is not the only growth oncogene associated with a high risk of cancer onset with the epidermal growth factor receptor (EGFR), which itself is closely related to Her, implicated in anal cancers [19]. Whilst signal transduction proteins (involved in the transmission of signals from cell receptors to the nucelus) such as the Ras family of proteins encompassing HRas, KRas and NRas implicated as a non-cancer specific oncogene.

Tumour suppressor genes on the other hand, are involved in the repression or dampening of the cell cycle in order to prevent mutations leading to carcinogenesis and are also involved in apoptosis of a cell, preventing the uncontrollable division of such cells. For instance, the tumour protein p53 is a known tumour suppressor gene and mutations with respect to this gene have been known to be extremely common in cancers [20].

Another key difference between the two is that whilst oncogene mutations occur only in somatic cells, TSGs can incur mutations in both the somatic and germ cell lines. Therefore, TSGs have a two-pronged approach in respect to mutations**,** with

comparisons of both oncogenes and tumour suppressor genes summarised (**Table 1-1)**.

Table 1- 1: Comparative summary of oncogenes and tumour suppressor genes

Oncogenes	Tumour Suppressor genes
Proto-Oncogenes are either turned ON gaining function, overexpressed or are inappropriately expressed and the resultant effect is cancerous characteristics in the cell,	TSGs are turned OFF and the resultant effect is cancerous characteristics in the cell
Commonly mutations only need to occur in one copy of the gene to increase the risk of cancer onset	Commonly both gene copies need to be turned off to incite cancerous characteristics within cell lines (both somatic and germline)
Acts as an accelerant of cancer onset increasing the rate at which cancerous characteristics appear	Turning off these genes allows the cell cycle to be performed unregulated.

Tumour suppressor genes, due to their function of regulation of the cell cycle and the prevention of uncontrolled cellular division can be catalogued into three main categories: caretakers, gatekeepers and landscapers [21], with each category of gene responsible for a different role within the cell cycle ensuring stability of the cell itself. Whilst the cell cycle will be discussed in greater detail within this chapter briefly the functionality of each gene type will be discussed alongside remarks on the implications of mutations within the genes themselves.

Caretaker genes are responsible for the coding the stabilisation of the genome, as the name suggests they “clean” the genome of the cell ensuring no oddities due to mutations appear. Due to the nature of cell replication there is an inherent risk of small

mutations from division to division to become fixed within the genome itself, and therefore risk both genomic and chromosomal instability. Therefore, caretakers act to reduce the amount of fixed mutations passed through the genealogy of the cell itself [22]. Therefore, the key mutations that occur in caretakers and indeed all tumour suppressor genes is the loss of function by turning off the gene itself. Caretakers due to their role in genomic and chromosomal stability are therefore a common route to cancer onset through mutations [23].

Gatekeeper genes work alongside caretaker genes in controlling cellular growth and aiming to prevent the bedding in of unwanted genetic mutations aiming to ensure the integrity and stability of the genetic material itself. Gatekeepers perform this task via two main routes: inhibiting the cell growth and division and inducing apoptosis [23]. Thus, as the name suggests gatekeeper genes act to control the influx of newly divided cells, reducing the “flow of traffic” of new cells being produced or forcing cell death. This can be exemplified when tissue damage occurs, damage to tissue undoubtedly leads to cell death and new cells are required to replenish the tissue to a healthy state. The role of the gatekeeper in this situation is to ensure that there is a healthy balance between cell death and cell growth, preventing “panic” and mass cell division which could lead to unwanted mutations and uncontrolled growth if not kept in check. This can be achieved by turning off apoptosis induction for a short while to allow the tissue to regenerate, although it is expected that the other checks for the cell cycle must be met to ensure the integrity of the genetical material contained within. Thus, mutations in the gene that allows for tissue regeneration via apoptosis arrest allows for uncontrolled proliferation if apoptosis cannot be switched back on, in turn leading to neoplasia and tissue of a cancerous nature. Both caretaker and gatekeeper genes encompass a wide variety of genes and proteins with some significant examples including the Adenomatous Polyposis Coli (APC) gene, which is involved in regulating cell division rates, adhesion and attachment to other cells to form tissue and the formation of the 3D structure of tissue [24]. CDKN2A, a Cyclin Dependent KiNase inhibitor which codes to produce numerous proteins needed for correct proliferation such as p16 and p14 [25]. BRCA, which has key implication in breast cancer much like Her 2 and as such is named the

(BR)east (CA)ncer gene and comes as either BRCA 1 or BRCA 2 and aid in the repair of DNA breakage [26].

Landscaper genes on the other hand are not actively associated with the growth of the cell in the same way caretaker and gatekeeper genes are. Landscapers are involved in providing an attractive environment for cell proliferation as oppose to controlling the proliferation process itself and encode the proteins required for the appropriate microenvironment. Therefore, upon mutation the landscaper genes provide a stromal environment escalating the growth of cancerous tissue [27]. Stromal cells, which themselves are not malignant, are connective tissue within organs, for instance the prostate or bone marrow, that aim to support the function of the organ itself. For instance, fibroblasts are known to produce collagen and the extracellular matrix and play a role in the wound healing process. However, it is the ability of cancerous cells to convert the normally benign supportive stromal cells into what has been termed tumour-associated stromal cells (TASC) [28]. These TASC cells provide the environment the neoplasia needs to proliferate at accelerated levels with overexpression of the Vascular Epithelial Growth Factor (VEGF) for example [28].

1.2.3 The 21st century environment and lifestyle and it's association with cancer

In addition to genetic inheritance and serendipitous mutation within genes, as discussed previously, environmental factors further contributing to an increased cancer incidence rate range from: tobacco smoking, urbanization, environmental pollution and changing diets throughout the decades with an increased amount of processed foods available, all of which can be linked via socioeconomic studies indicating higher mortality within deprived classes of individuals [29]. Additionally, the workplace can pose an additional risk to cancer onset with workers who require access to chemicals such as benzene, cadmium, formaldehyde, radon and vinyl chloride to name just a few

at risk from carcinogenic effects that these substances pose, and as such chemicals that pose a risk to health should be worked with in accordance with local guidelines such as safety data sheets, Control Of Substances Hazardous to Health (COSHH) assessments and risk assessments. How different environmental factors influence cancer onset varies from factor to factor there is an overarching theme that DNA damage as a direct result of the environment is the most probable cause for the development of neoplasia. In 1975 a study published by Armstrong and Doll in the International Journal of Cancer discussed the dietary factors surrounding cancer incidence in 23 countries worldwide focusing on 27 different variants of the disease [30]. Although the data obtained was crude and didn't reflect different time points throughout the study, such as before cancer incidence, there was a strong correlation between the consumption of meat and fat and incidence of colon, rectal and breast cancers, although it is stressed whilst there are secondary associations such as meat consumption combined with fat consumption in the case of colon cancer for instance meat consumption has a much stronger association to the onset of rectum cancers than fat consumption. Whilst this data in the current form isn't a comprehensive overview of the journey towards cancer there was some evidence for positive and negative relationships between some cancers and the diet of the nations researched. This research 45 years ago however, paved the way for more focused research into different factors affecting cancer onset.

In 2003 a further study was published by Boffetta and Nyberg discussing additional factors that could be implicated as having a positive correlation with cancer onset in the individual [31]. Asbestos, air pollution, tobacco smoke, radon and water pollutants such as chlorine, arsenic, nitrates & nitrites were studied. As with the study performed with Armstrong and Doll the authors suggest that whilst factors such as tobacco smoke, air pollutants, radionucleotides etc. can increase the risk of cancer the risk itself cannot be quantified however suggest a likely magnitude of risk.

Lifestyle choices by the individual therefore are one method of trying to mitigate risks associated with environmental factors correlated with cancer onset, although linking these factors to causation is difficult as the data is open to interpretation and

environmental factors should be treated with caution. Indeed, the National Health Service in the UK (NHS) suggests on their website lifestyle changes that may help to alleviate cancer onset [32]. Linking to a 2011 study by Parkin the most common risk factors towards cancer were tobacco (19.4%), diet (9.2%), being overweight or obese (5.5%) and alcohol (4%) [33]. Other risk factors were shown to be occupational hazards such as asbestos, excess intake of meat and lack of physical exercise [33]. However, the recurring theme of the data was that whilst these factors are somewhat avoidable there is uncertainty in whether the risk factors are a causation of cancer onset, however, give an indication of how the 21st century lifestyle could be changed in order to reduce the possible risks of cancer.

In summation, environmental factors are a form of risk for cancer onset however whether these same factors cause cancer is up for debate with great uncertainty over the data studies have produced over the past 45 years, although corroboration between studies with respect to tobacco smoking, meat and fat consumption have been found. Therefore, it is up to the individual to make informed choices based on advice given by the NHS, Cancer research UK, the American cancer society or indeed any other local health body in order to live in a healthy way to mitigate these risks.

1.2.4 Tumour localisation and metastasis – diagnosis and classification systems within the clinical environment

Cancer detection plays a pivotal role in diagnosing the cancer at early stages and preventing the spread of the cancer itself. Diagnosis of cancers may occur via a variety of different routes, for example a physical examination may be performed by a trained physician looking out for lumps and bumps within the body that may indicate the presence of cancer. Other changes such as skin pigment changes or enlargement of an organ in isolation may also provide information as to whether cancer is present within the body. Should the physical exam bring up abnormalities there may be a further need

for laboratory tests or imaging tests to corroborate whether cancer is present. Lab tests may occur in which urine or blood is taken in order to assess if there are changes within the internal environment caused by cancer. For instance, smear tests may be performed for cervical cancer; however, these are performed as preventative measures and do not indicate whether cancer itself has manifested, but if there is a high likelihood of cancer onset in the future. Therefore, the cervical smear test checks for the presence of high risk forms of human papillomavirus (HPV) as these have been suggested to be a cause of cervical cancer [34].

Should the patient be diagnosed as cancer positive classification within the clinical setting must occur in order to aid the treatment process and there are two main methods for the classification of cancers within the human body. As cancer progresses it may no longer be situated in isolation as a mass of tissue at the site of malfunction, and therefore as oppose to being termed a local cancer the cancer is deemed to have metastasized throughout the body. In general, the route for cancer spread is via the lymph nodes or via the bloodstream itself and involves rouge cells breaking away from the main tumour and migration to a different part of the body, for example a metastatic carcinoma may migrate via either the lymph nodes or the blood vessel system to infiltrate numerous different parts of the body, with certain cancers having a preferential site of invasion described by the “seed and soil theory” [35,36]. (**Figure 1-2**).

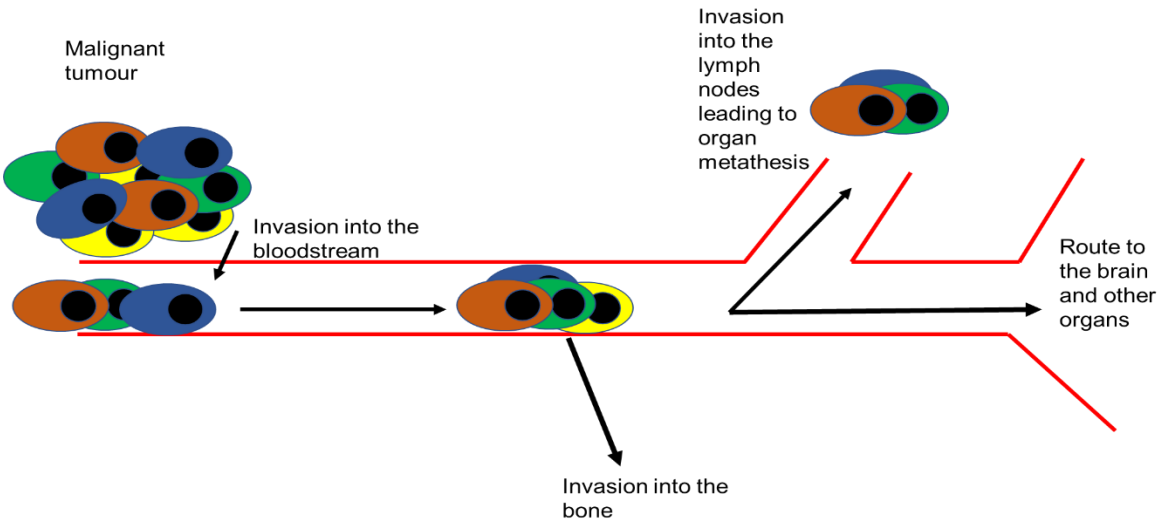

Figure 1- 2: Diagram depicting cancer migration throughout the body

In order to effectively migrate throughout the body, firstly a malignant cell needs to be able to break away from the site of the original tumour and enter either the lymph system or the blood vessels [35]. Upon migration there is then a need for the cell in question to be able to attach themselves to either system in order to effectively move without being degraded by the body or dying. Then, upon the site of migration the cell requires an environment that would allow it to thrive and grow. If all the above conditions are met, then the malignant cell can infiltrate healthy tissues and uncontrollably divide inducing tumour growth in a new location.

Cancers, therefore, due to their progression may become difficult to treat or indeed untreatable at all, with primary, advanced and terminal cancers coined in order to aid the clinician in the route of treatment needed. For instance, a primary cancer comprises of a cancer that is still localised within the site of cellular malfunction and is the first mass of malignant tissue to be produced. Advanced cancers and terminal cancers in some cases can be used interchangeably to describe cancers that have been able to spread throughout the body however this is not entirely true [37]. Advanced cancers are cancers that are no longer curable due to the aggressive nature of the cancer and the vast spread of the malignant tissue itself. Whilst terminal cancers share this same characteristic advanced cancer may respond to treatment to slow down the spread of the cancer or shrink the tissue itself, possibly prolonging the life of the patient. Terminal cancers on the other hand, will not respond to treatment and therefore there is a lack of treatments in order to either slow the spread of the cancer or shrink the tumour itself.

The terms primary, advanced and terminal cancer therefore give some indication as to the route of treatment required for the cancer itself however, they do not accurately describe the cancer in terms of whether metastasis has occurred. Therefore, the cancer staging system and the TNM system are widely used as a method of both diagnosis and description by the clinician in order to more accurately represent the state of the cancer. Firstly, the numbering system, in which cancers are classified as “stages”

depending on a variety of factors and the stages at which classification occurs is described below [38].

i. (Stage 0) The cancer is in situ and hasn't spread
ii. (Stage i) A relatively small tumour that is contained within the effected organ.
iii. (Stage ii) The tumour has begun to grow and is no longer considered stage i. The cancer has not yet moved into the surrounding tissues and the tumour is still contained within the effected organ. Dependant on the type of cancer, this stage can be used to describe tumours that have spread to lymph nodes close to the affected area, however this is purely on a case by case basis.
iv. (Stage iii) The tumour is large and may have begun the process to move into the area surrounding the affected organ. At this stage it is normal to see that the cancerous cells are diagnosed in the lymph nodes surrounding the area.
v. (Stage iv)The tumour has spread into a surrounding organ at this stage and metastasis has begun due to the ability of the cells to travel using either the lymph or blood system (or perhaps both).

Whilst this system provides a good description for cancer and description of the cancer progression itself there are cases where ambiguity and crossover between the stages may make it difficult for the clinician to accurately describe the tumour and thus the TNM system can much more accurately describe the size and nature of the cancer itself and is described as such [39]:

T – This refers to the size of the **T**umour. The physician will normally associate a number alongside the letter between 1 and 4. For instance a relatively small tumour would be described as T(1) whilst a large tumour T(4).

N – This refers to the lymph **N**odes and specifically whether the cancer cells have been able to manifest themselves within them. Again, numbers are used to associate the severity of which the cancer has spread to the nodes from 0 -3. i.e. a N(0) type cancer has effected no lymph nodes whereas a N(3) suggests a vast amount of lymph nodes contain cancerous cells.

M- This refers to the state of **M**etastasis (the spread of the cancer) and therefore is used to denote whether the cancer has been able to spread to surrounding organs and tissues. The nature of this means there are two number states associated 0 and 1 where 0 denotes no spread and 1 denotes metastasis has occurred.

The TNM system therefore can be used to describe tumours relatively easily and with a great amount of detail. For example, a T(2) N(1) M (0) cancer, is easily recognisable as a cancer that has a small tumour slightly larger than level 1 with spread to a small amount of lymph nodes without metastasis. The advantages of using this technique over the staging system is that more detail can be given and there is less room for ambiguity. For instance a stage ii cancer could be described as T(2) N(0) M(0) or T(2) N(1) M(0) depending on the type of cancer the lymph nodes may or may not be invaded by cancer cells.

Thus, post diagnosis, the importance of accurate classification and description is paramount. The correct classification method can allow for the clinician to describe a cancer as much more than primary, advanced and terminal. Indeed, should the cancer itself enter advanced stages an in-depth accurate classification of the cancer itself can greatly aid deciding on the route of treatment itself in order to shrink or delay the spread of the cancer itself.

1.2.5 Common clinical treatments for cancer: Radiotherapy, Chemotherapy and the Cell Cycle

Post diagnosis and classification, if possible, treating the cancer is the next stage throughout the clinical life cycle.

Cancer therapies can be divided into the following main categories: surgical operations to physically remove cancerous tissue, radiotherapy (subjecting the cells to high doses of radiation to kill them), chemotherapy, immunotherapy, hormone therapy, targeted drug therapy or a combination of any of the listed methods.

Furthermore, the stages of treatment may differ between patient to patient and cancer to cancer however, generally clinicians treat cancer in three main ways: primary treatment, adjuvant treatment and palliative treatments.

Primary treatments aim to remove the cancer from the body and kill the malignant tissues associated with the disease. Obviously, it would be tempting to perform surgery to remove the tumour itself however complications can occur depending on the stage of cancer and the location of the tumour itself. As such, cancers that have metastasized or are in the vicinity of tissues in which surgery would cause severe harm to organs do not generally become treated in this way. Alternatively, physical removal can be used in combination with other techniques in what is termed “debulking” of the tumorous tissue. This occurs when it is not possible to completely remove the tumour however, removing a significant portion leaves the tumour vulnerable to a greater response from other treatment methods.

1.2.5.1 Radiotherapeutic treatments for cancer

Radio and chemotherapy are some of the most publicly well-known associations with cancer. Radiotherapy is the practice of utilizing ionizing radiation (such as X-rays) in order to damage cancerous tissues and prevents further cell division and subsequent cell death. Radiotherapy itself can be divided into two distinct methods of delivery: internal radiotherapy and external beam radiotherapy [40,41]. Internal radiotherapy generally involves internalization of radioactive materials in either solid (implant) or liquid form into the human body in order to incite therapeutic effect to the area of interest. Internal radiotherapy is known to have a smaller side effect pool due to ionizing radiation being concentrated within the body, closer to the cancer as oppose to a large surface area. There are two methods of delivery for internal radiotherapy, implants and liquid therapeutics. Solid forms of isotopes are generally implanted into the body through Brachytherapy. Brachytherapy, also termed sealed source radiotherapy,

involves sealing the radioactive material into a wire, disc or seed and implanting the sealed source to the site of localized cancer, such as the womb, the prostate or the cervix for example [42–46]. The material is then left for a set period before removal and can be used in conjugation with other radio and chemotherapeutic techniques, with computerized tomography (CT) or ultrasound scanning beforehand in order to aid the clinician as to the appropriate locale to place the implant itself.

Liquid radiotherapy on the other hand is normally ingested via a drink or an injection. There are several radioactive nuclei that are used for this purpose such as I^{131}, P^{32}, Ra^{223} and St^{89} [47]. The radioactive isotope is sometimes conjugated to a ligand to ensure a targeted delivery towards the site of therapeutic interest, for instance, I^{131} is picked up by the thyroid regularly however it can be used for the treatment of neuroendocrine tumours via conjugation to meta-iodobenzylguanadine (MIBG) whilst also doubling up as a diagnostic tool for these types of tumours, through radio tracing [48].

External radiotherapy as the name suggests compromises of a radiation source and directs ionizing beams of radiation towards the tumour. Beforehand, similarly to internal treatments, X-rays, CT and magnetic resonance imaging (MRI) scanning is performed to identify the locale of the tumour so that the radiation source can be directed appropriately considering healthy tissue in neighbouring vicinities. For the treatment to be conducted a linear accelerator (LINAC) machine is used as the radiation source, with high energy X-rays and electrons generated as the ionizing radiation [49] (**Figure 1-3**). Furthermore, the course of radiotherapy can be divided into numerous smaller doses termed fractions to protect the healthy tissues giving them as low a dose as possible over the course of treatment.

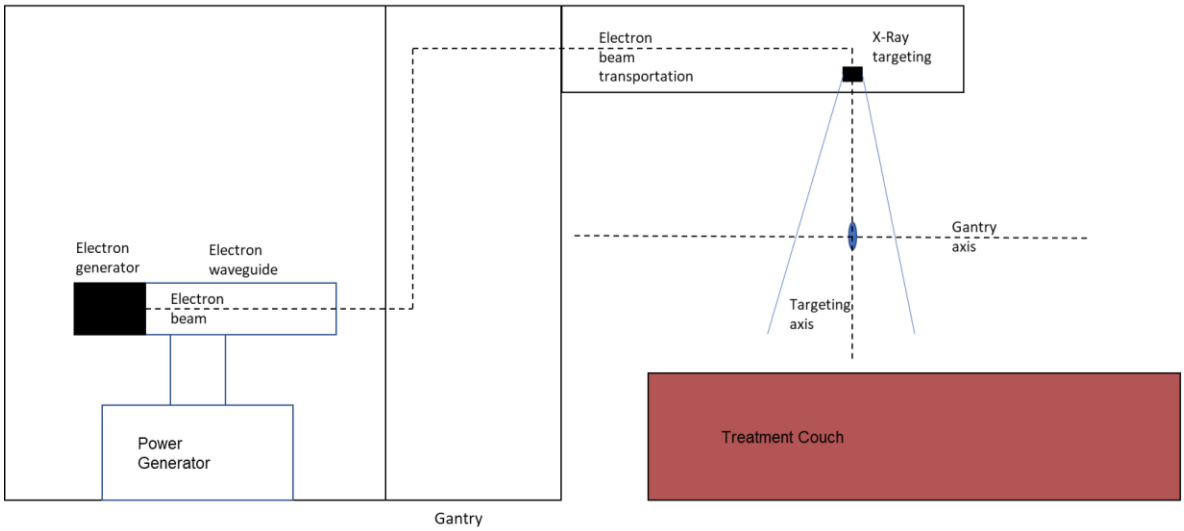

Figure 1- 3: LINAC machine schematic diagram noting the axes at which the X-ray targeting is directed

1.2.4.2 Chemotherapeutic treatments for cancer

Chemotherapeutic techniques for the treatment of cancer involve the treatment of malignant tissue by chemical means, with common drugs for the treatment of cancer including: capecitabine [50], carboplatin [51], *cis*-platin [52], gemcitabine [53], paclitaxel [54], docetaxel [55] and doxorubicin [56]. Initially, chemotherapy was first developed in the 1940s with nitrogen mustards used for the treatment of cancers. The use of nitrogen mustards was a progression from the use of mustard gas within the first world war, with the mustards developed further in the second world war at the Yale school of medicine [57]. It was observed that the use of these drugs supressed hematopoiesis (the formation of new blood components) and thus patients with lymphoma were given the drugs via an intravenous (IV) injection as oppose to inhalation of gas [57].

Since then chemotherapy has advanced vastly with both targeted and untargeted treatments. Chemotherapeutic agents can be classified based on their mechanism of action and the most common classifications are: alkylating agents (nitrogen mustards and platinum based drugs), topoisomerase or mitotic inhibitors and antimetabolites

(such as gemcitabine and capecitabine), whilst antibiotics, and antibodies can also be used, all of which will be discussed in detail herein.

Alkylating agents as the name suggests perform their therapeutic effects via alkylation to the DNA of malignant cells thus inhibiting replication of cells . *Cis*-platin is one of the most widely used alkylating agents for the use of chemotherapy and was first discovered in 1845 by Michele Peyrone and was termed Peyrone's chloride [58] however it wasn't until the late 1970s until it was approved for use in the clinical setting [59], and is currently delivered via IV injection. Alkylating agents such as *cis*-platin work in ways such as: the alkylation of DNA bases [52] and the cross-linking of DNA bases preventing separation of the double helix structure and hence preventing DNA replication [60].

Cis-platin has also been known to be used in conjugation with other drugs in a "combi" treatment with drugs such as gemcitabine [61], or in combination with either internal or external radiotherapy. Nitrogen mustards work in a similar way to *cis*-platin again alkylating [62].

Inhibitor drugs such as topoisomerase or mitotic inhibitors work as the name suggests by inhibiting key enzymes or processes in the cellular life cycle [63–65]. The cell cycle itself is a well-regulated process with numerous checkpoints involved in order to check the integrity of the cycle itself and the prevention of genetic defects. The three main checkpoints throughout the cycle however are G_1 phase, S phase, G_2 phase and the M checkpoint [66] (**Figure 1-4**).

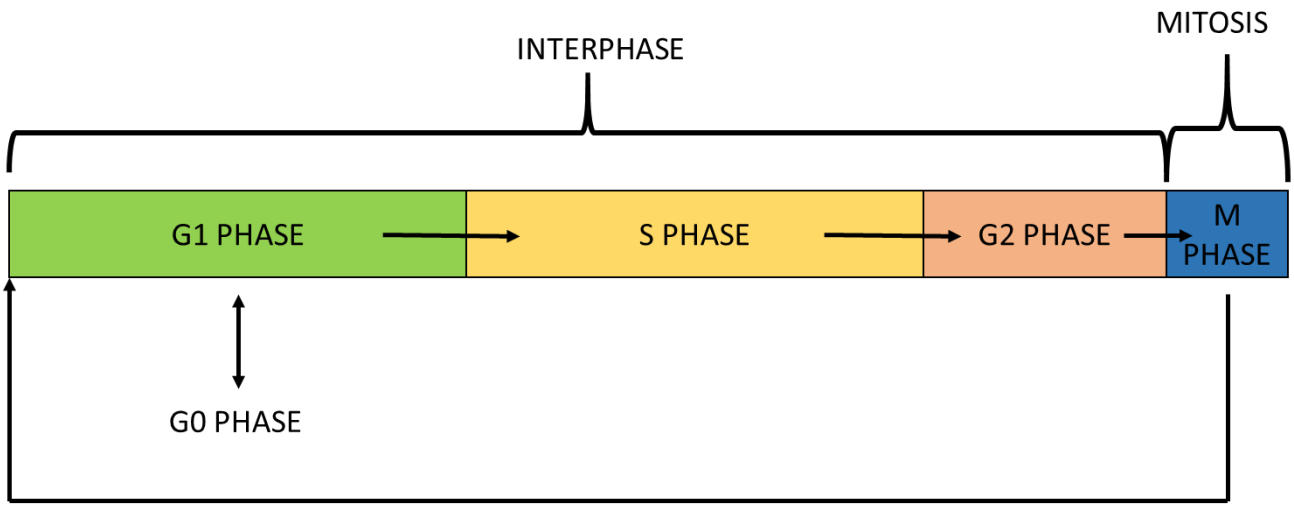

Figure 1- 4:The main checkpoints in the regulation of the cell cycle

G_1 phase, also commonly termed the restriction phase or the first growth phase, is the point in the cycle in which the cell "commits" to entering the cell cycle, via the activation of cyclin-CDK-dependant transcription, and it is at this stage that G_1 can be delayed or progression is allowed through to the S phase of DNA replication [67].

The E2F family of transcription factors are key for G_1-S transcription and transition, and it has been reported that mis regulation of the E2F family and subsequent malfunction of these factors has been observed within cancers suggesting strong links between oncogenesis and this section of the cell cycle [68]. The E2F family are responsible, alongside pocket proteins at different points of the cell cycle for binding to cell cycle promotors ensuring the proper expression of genes [69]. Ultimately, within G_1 phase the cell has three different routes that it can take to further progression throughout the cell cycle. Firstly, the cell can continue onto S phase if the conditions for progression are met. Secondly, the cell cycle may be stopped at this point and the cells may enter what is called G_0 phase in which differentiation is believed to occur, which is regulated by the restriction checkpoint in G_1 phase [70]. G_0 phase occurs outside the accepted normal cell cycle and has been termed the resting phase, however other reports indicate that G_0 may perhaps itself be considered an extension of G_1 phase itself, where cells are neither dividing nor making the preparations required for division

[71]. Finally, G_1 arrest may occur stagnating progression to S phase via G_0 phase initiation or the need to re-enter the cell cycle altogether [72] .

Should the requirements of G_1 phase be met, in which: the genetic code of the cell is free from malfunction, genetic expression is proper, the cell has grown in order to accommodate doubling of the genetic material contained within the cell and the p16 protein is no longer acting as a brake the cell then enters S phase. The p16 protein is a confirmed tumour suppressor gene and acts as a handbrake on the cyclin-CDK signalling pathway responsible for activating cell progression into S phase itself, and when defective p16 itself can act as a catalyst for uncontrolled cellular replication [34]. S phase deals with the replication of DNA and genetic material and completion of the phase is designated upon each chromosome being replicated and the daughter cells receiving the full complement of the hereditary material. Importantly, the pre-replication DNA complex (pre-RC_{DNA}) formed in G_1 consisting of Cdc6, Cdt1, ORC 1-6 and MCM 2-7 are removed within S phase [73]. The role of these complexes is to ensure that DNA replication begins at the appropriate start point however, they are removed before the commencement of replication itself. The stabilisation and retention of these pre-RC_{DNA} complexes would result in an excess of replications of DNA [73]. The resultant doubling of DNA situated within the cell then produces a full set of sister chromatids derived from an original chromosome, in effect each chromosome now consists of two sister chromatids attached to each other via the centromere. (**Figure 1-5**).

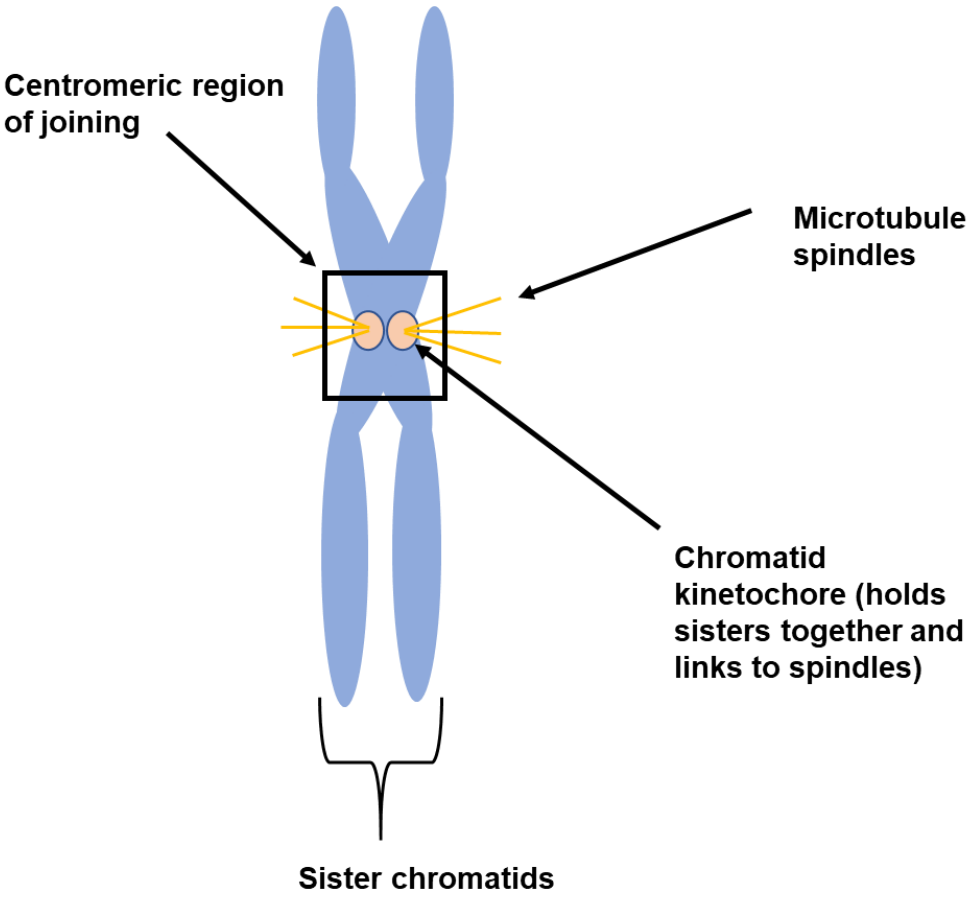

Figure 1- 5: Sister chromatids prior to mitosis demonstrating chromosome copies being joined at the centromere

Despite the replication of the chromosomes however the ploidy (completed sets of chromosomes) and number of chromosomes within the cell remain unchanged, with the key elements of this phase focusing on producing the chromosomes for the daughter cells upon cell division, therefore the S phase of the cell cycle presents itself as an exploitable process for the treatment of cancer [73].

The topoisomerase family of proteins are key for the unwinding and overwinding of the DNA double helix and have key implications in DNA replication and RNA transcription [74]. The winding of DNA often termed DNA supercoiling is key for the regulation of access to the genetic code and compacting DNA for replication [75]. Therefore, the function of topoisomerase is to modify and manipulate DNA topology to

facilitate the replication of DNA in a timely manner for the division of cells. Topoisomerases in eukaryotic cells can be sub-divided into two different forms topoisomerase I (TOP I) and topoisomerase II (TOP II), with different classes of drugs effective at disrupting the mechanism of action of these enzymes [76]. TOP I has implications in the breakage and formation of bonds within the DNA single strand, allowing rotation of the broken strand. Drugs such as camptothecin (CPT), discovered in 1966 [77], work as topoisomerase poisons directed towards this variant of the enzyme. This natural product has led to a plethora of CPT derivitised drugs used in the treatment of cancer today such as: irinotecan [75], topotecan [75] and belotecan [78] (**Figure 1-6**).

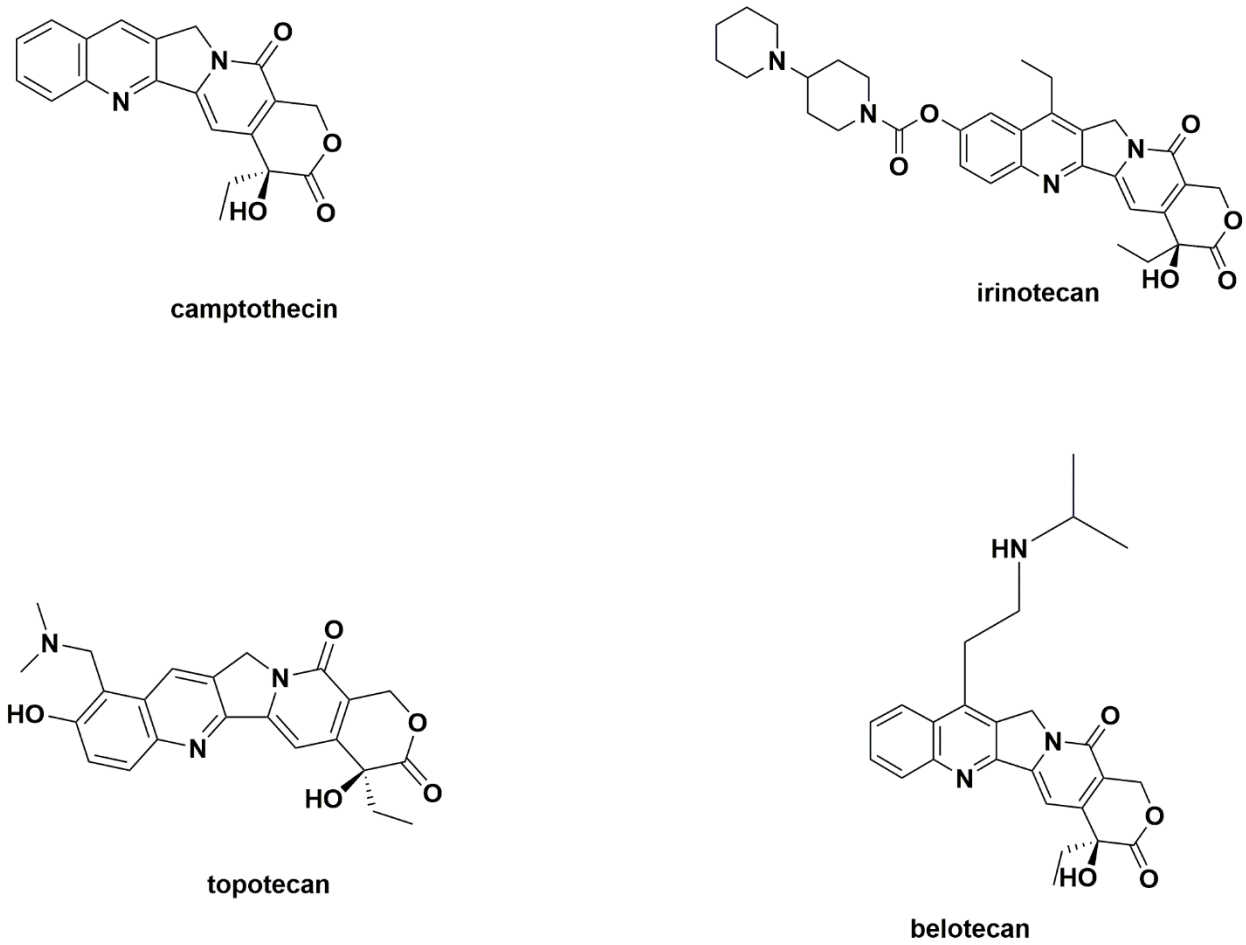

Figure 1- 6:The camptothecin family of topoisomerase I inhibitor drugs

CPT inhibits the action of the TOP I enzyme via complexation to the TOP I – DNA complex stabilizing the structure and thus preventing the formation of phosphate ester linkages between DNA strands required for re-ligation, this subsequently forces death of the cell [79].

Natural progression was then required in order to circumvent the limitations CPT chemotherapy presents and as such the indenoisoquinoline family of TOPO I inhibitors were developed by Cushman and Pommier [75]. The advantages these drugs presented over CPT were: an increase in blood stability through a lack of lactone formation; transport into the cell was found to be independent of membrane transporters and the drugs acted as inhibitors of the TOPO I complexation at distinct sites [80].

TOP II proteins, unlike the related TOPO I, are ATP dependent and are implicated in simultaneous cutting of both DNA strands, leading to a double strand break, managing the supercoiling effect. Supercoiling has key implications in genome packaging and gene expression [81]. Genome packaging is key within cells and is essential in ensuring that the genetic material can be contained within the cellular nucleus. Gene expression, whilst performed during the RNA transcription or replication process as DNA unzips [81].

Topology changes via twisting of the DNA double helix allows for the exposure of internal bases to the external environment allowing the genetic code to be read without the need for unzipping, with the genetic code itself affecting how DNA responds to the supercoiling process.

TOPO II inhibitors are split into two distinct categories depending on their mechanism of action: isomerase poisons (which target the DNA complex in order to disrupt isomerase activity) [82] or isomerase inhibitors (which disrupt the catalytic activity of topoisomerase II) [75]. One widely used isomerase poison in cancer chemotherapeutics is doxorubicin, which is within the anthracycline family of drugs [56,83,84]*(***Figure 1-7***).*

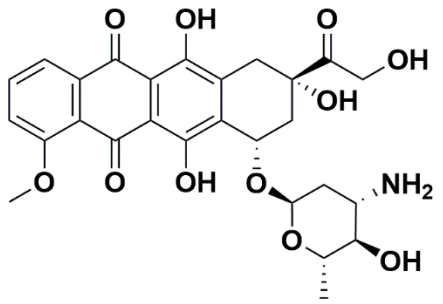

Doxorubicin

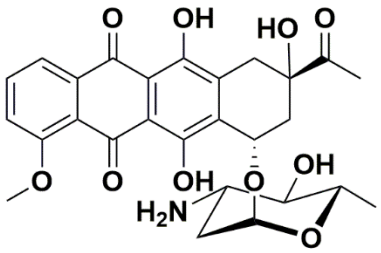

Daunorubicin

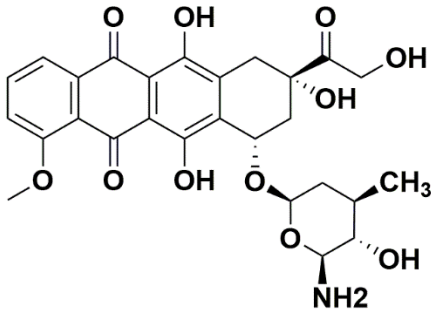

Epirubicin

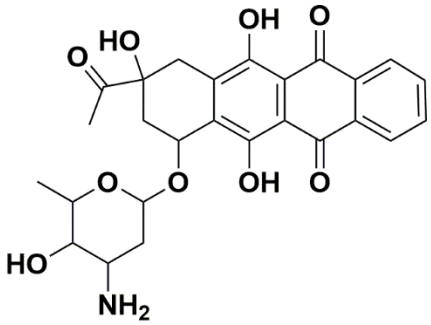

Idarubicin

Figure 1- 7:Structures of the anthracycline family of chemotherapeutics

Doxorubicin is today one of the most widely used chemotherapeutic treatments. As an isomerase poison the mechanism at which doxorubicin works is via intercalation within DNA and thus inhibits the biosynthetic pathways associated with DNA replication [85]. Doxorubicin therefore acts as a stabilizing agent upon the TOPO II-DNA complex upon DNA unzipping, preventing the resealing of the double helix (**Figure 1-8**).

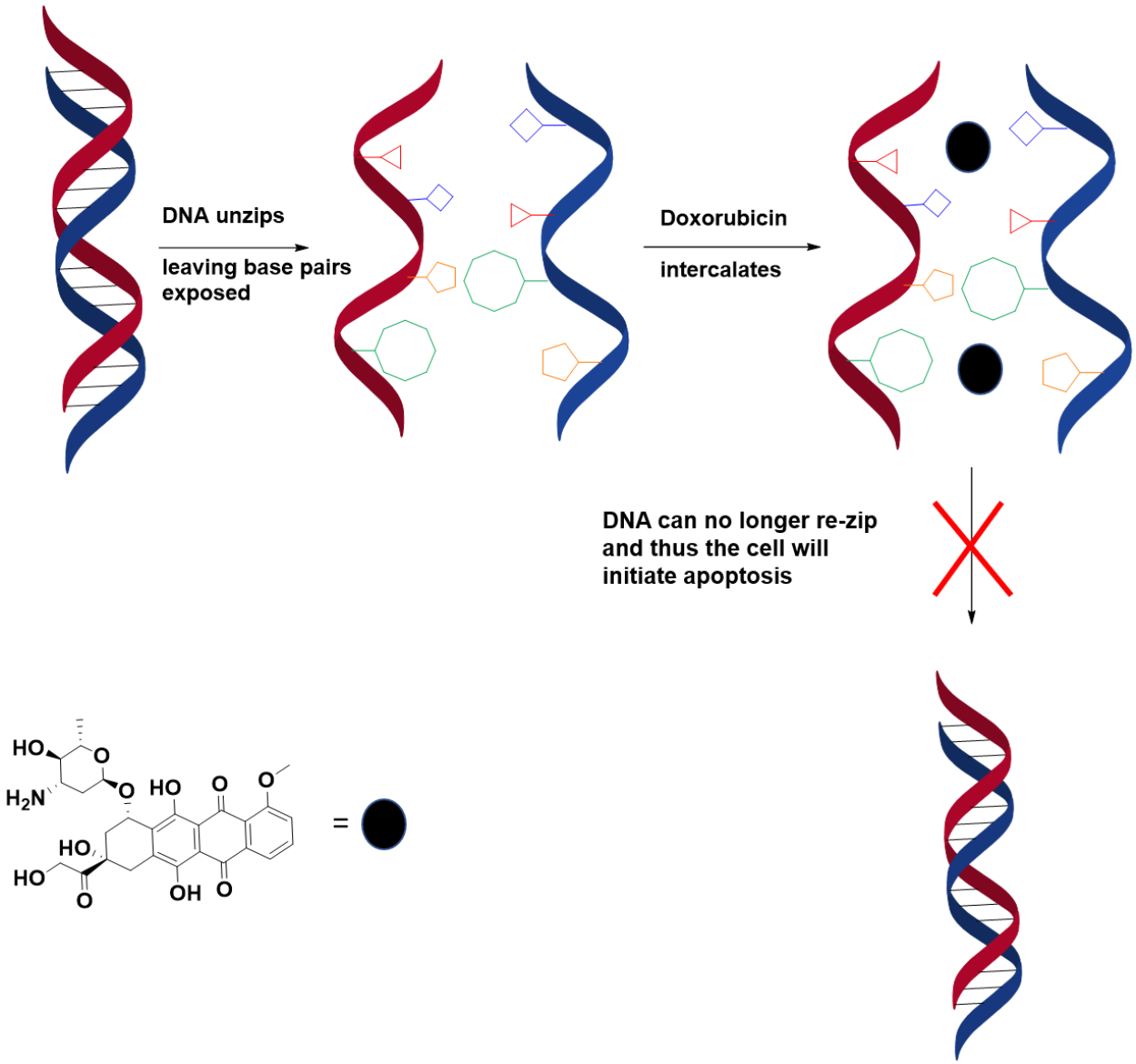

Figure 1- 8: Doxorubicin intercalation within DNA preventing the resealing of the double helix structure

Doxorubicin however is not the only drug to work in this way with amsacrine acting via an intercalation mechanism to poison the effects of the topoisomerase II enzyme [86].

Interestingly, TOPO II poisons can be further classified based on the cell type the drug preferentially targets with both eukaryotic and prokaryotic (bacterial) TOPO II poisons on the market today. Whilst eukaryotic poisons are used in cancer therapies such as doxorubicin and amsacrine; fluoroquinolones are implicated in the anti-bacterial

therapy market [87]. Fluoroquinolones such as ciprofloxacin however are indicated in a different mechanism of topoisomerase poisoning. As oppose to eukaryotic poisons, in which post unwinding intercalation prevents the resealing of the DNA double helix, this class of poisons prevents the DNA gyrase enzyme altogether thus preventing DNA replication via a different route [88]. However, these are currently not used as cancer therapies due to their bacterial preference but are interesting in their deviation from chemotherapeutic TOPO II poisons, nevertheless. G_2 phase follows on from S phase and is the secondary growth phase for the cell, preparing the needed materials for mitosis to occur [70]. It is within this phase that the cell begins reorganizing the microtubules contained within to form spindles, and the main regulatory checkpoint facilitated by the p53 tumour suppressor gene is performed [89]. The p53 protein ensures that the chromosomes and DNA contained within the cell contains no irregularities or mutations, ensuring the integrity of the genetic material. The p53 gene, much like the p16 gene, therefore, has implications in the facilitation of uncontrolled cellular division through malfunction [89]. Within healthy cells the p53 protein upon checking the genetic material either corrects mutations thereupon or triggers the process of apoptosis. However, defects within the protein, such as in some cancers, means that this vital checkpoint is neglected and cells with defective genetic material can replicate without barrier. If the cell passes through this checkpoint, then mitosis begins, and the replicated chromosomes begin to separate and new cells are formed (**Figure 1-9**).

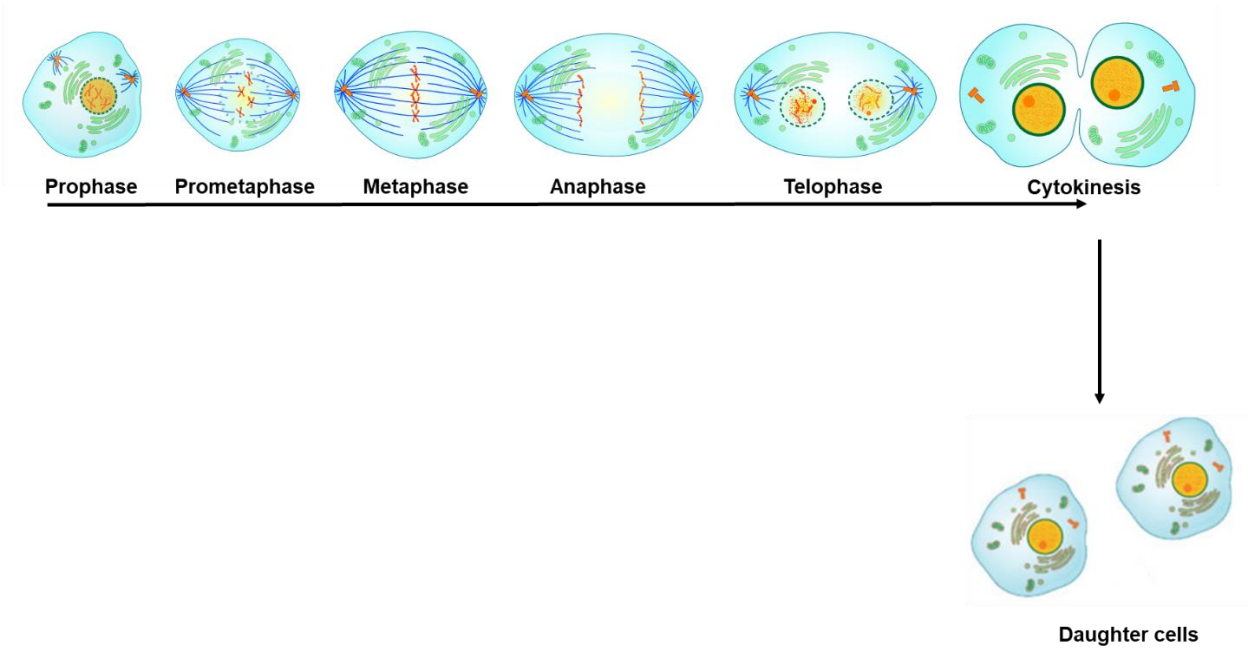

***Figure 1- 9: The mitotic cycle within the cell, cells were extracted from the public domain image under the creative commons licence* [90]**

Mitotic inhibitors act as therapeutics by causing mitotic arrest (i.e. preventing mitosis and the division of cells) [65]. Mitotic inhibitors widely used today are mainly derived from natural sources and are classed as alkaloids (nitrogen containing compounds derived of plant origin) [65]. Terpenes such as paclitaxel [91] or docetaxel [92] are also known to display anti-cancer properties **(Figure 1-10**).

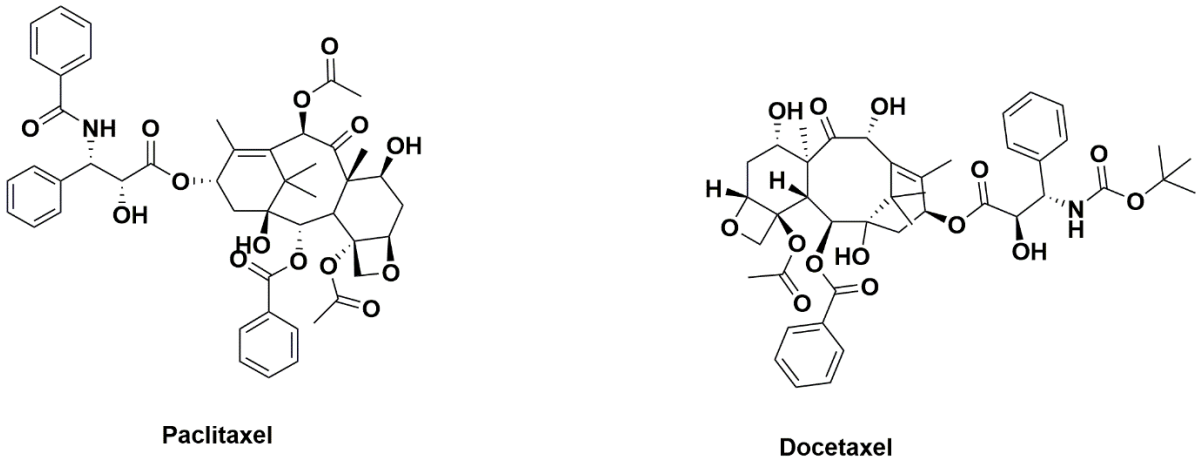

Figure 1- 10:Chemical structures of the therapeutics Paclitaxel and Docetaxel

The mechanism of mitotic inhibitors is well understood with binding towards tubulin preventing the polymerization process thought to be the main driving force towards their cytotoxic effects, as due to the stunted production of microtubules there is no capability for the cell to split chromosomes apart and thus produce daughter cells. Paclitaxel as a mitotic inhibitor targets tubulin and causes defects in mitotic spindle assembly, induces irregularities in chromosome segregation and arrests cell division, with tubulin mutations regarded as a huge resistance barrier to the drug itself [91]. Docetaxel acts similarly to paclitaxel by stabilizing the microtubules and preventing depolymerization [92]. As such docetaxel suppresses the microtubule assembly/disassembly processes in order to induce cytotoxic effects.

Anti-metabolites as a class of drug encompass therapeutics that interfere with DNA synthetic pathways. Whilst individual mechanisms may differ between drug to drug the general mechanism of action is that anti-metabolites are metabolized within the cell and either replace the nucleotide required for DNA synthesis acting as a chain terminator; forcing the abandonment of replication and subsequent cell death (such as in the case of gemcitabine) [93] ; or reduce the metabolization of key chemicals required for proliferation, via competition with metabolites or through inhibition of key enzymes required (capecitabine for example) [50].

Capecitabine itself is metabolized into 5-flourouracil (5-Fu) [94,95] and the metabolic pathway at which capecitabine is implicated within is well understood with two key steps involved before 5-Fu is produced, namely the production of 5’-deoxy-5-flourocytadine before 5’-deoxy-5’-flourouradine and subsequent metabolization to produce 5-flourouracil [96]. 5-Fu then undergoes metabolization to both fluorouridine monophosphate and further to fluorouracil diphosphate and fluorouracil triphosphate. It is the triphosphate form that becomes involves in RNA incorporation and upon incorporation into RNA forces apoptosis of the cell [97]. **Figure 1-11**.

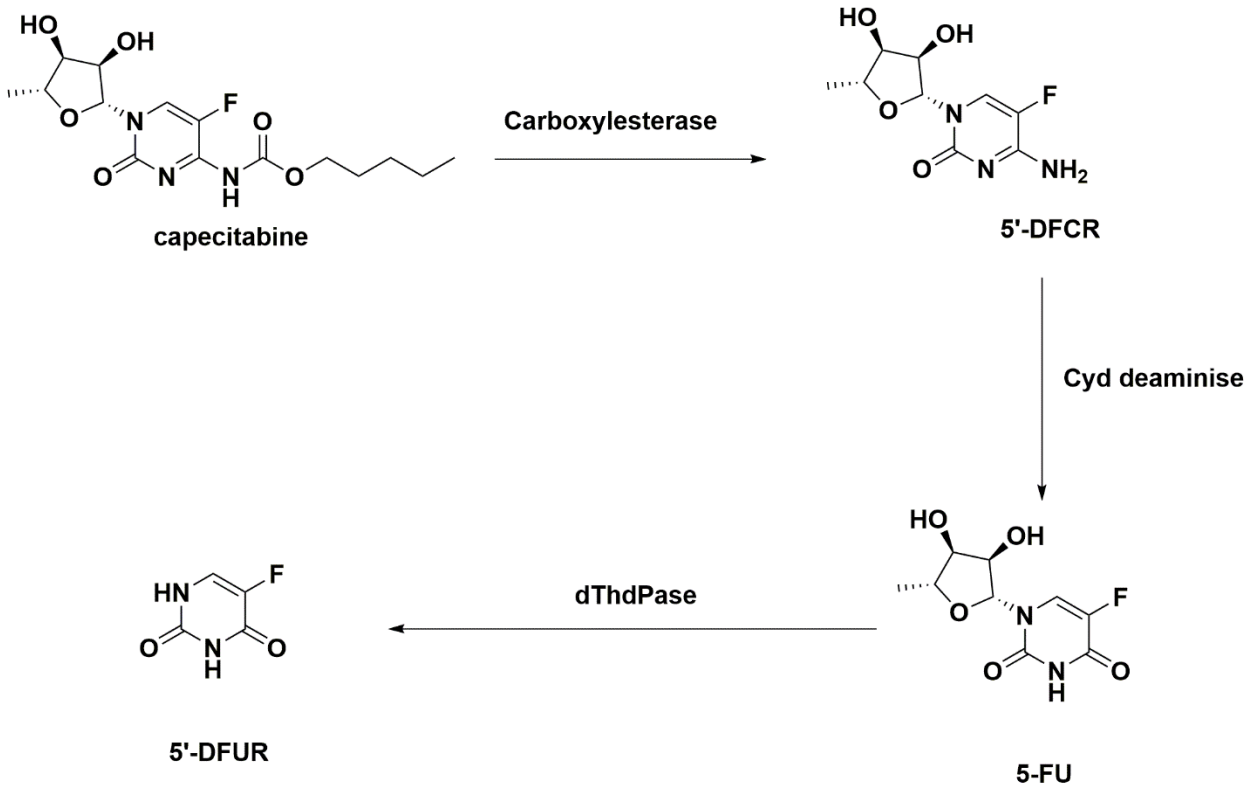

Figure 1- 11:Capecitabine metabolism in situ to form the commonly used therapeutic 5-flourouracil product and the subsequent metabolization of 5-Fu

Gemcitabine, similarly, to capecitabine, interferes with numerous biological pathways relating to DNA and RNA synthesis. Due to the hydrophilic nature of gemcitabine there are numerous nucleoside transporters implicated in the internalisation of the therapeutic into the cell, namely: SLC29A1, SLC28A1 and SLC28A3 [93]. Gemcitabine metabolization into either mono-, di- or tri-phosphorylated forms has a variety of mechanisms that all act to the detriment to the health of the cell. Firstly, the phosphorylation of gemcitabine into the monophosphate metabolite requires the enzyme deoxycytidine kinase and as such gemcitabine provides competition with cytidine for access to the phosphorylation pathways [93], with subsequent di- and tri-phosphorylation requiring UMP-CMP kinase [93]. The diphosphate form of gemcitabine acts as an inhibitor for the ribonucleotide reductase (RNR) enzyme, and as the primary focus of this enzyme is to synthesise nucleotides for RNA and DNA synthesis inhibition of this enzyme greatly impacts the ability of the cell to function correctly and efficiently. This inhibition acts as a positive feedback loop for gemcitabine, as the nucleotide

concentration within the cell is impacted by inhibition of the enzyme there is a need for nucleotides to be transported into the cell to meet the needs of the cell itself. This in turn promotes the uptake of gemcitabine into the cell thus increasing the inhibition of RNR [93]. The triphosphate form of gemcitabine also contributes to detriment of cell health, however, acts as a stealth nucleotide. Gemcitabine competes with the native nucleotide triphosphates for incorporation into DNA and once incorporated acts as a faulty sugar, with the ability to evade the cells correction facility [93].

Base-excision repair is a correction mechanism within the cell cycle that acts to repair damaged DNA as either long-patch or short-patch repair mechanisms [98]. In addition to evasion of base-excision repair gemcitabine has been shown to remain unaffected by the nucleoside excision repair mechanism which as the name suggests acts to repair damaged nucleosides as oppose to strands of DNA themselves [99]. This natural evasion of gemcitabine to two common repair mechanisms allows the anti-metabolite to become incorporated within DNA and act as a stealth chain terminator. Upon gemcitabine addition to DNA it is known that a further deoxynucleotide is added thereupon. However, after this subsequent addition of a further base DNA polymerase enzymes are no longer able to proceed with the function of the synthesis DNA molecules, thus stalling the process. This action leads to the “lock-in” of gemcitabine into DNA due to the now impaired ability of the proof-reading exonucleases to remove gemcitabine from the penultimate position in DNA and thus programmed cell death is commenced (apoptosis) [93].

1.2.4.3 Common side effects from treatments for cancer

With both radio and chemotherapy treatments however, there is a need to realise the side effects that any treatment can produce. Whilst the drugs and isotopes discussed beforehand in section 1.1.4.2 are not an exhaustive list, due to a plethora of different therapeutics on the market today, the side effects of treatments towards malignant tumours encompass not only the therapeutics discussed but also

those that have been neglected. Whilst side effects will be generalised throughout discussion, it is accepted that from patient to patient, cancer to cancer and indeed therapy to therapy there will differences in side effects; with underlying health issues, locale of the cancer, type of radio/chemotherapy being conducted etc. influencing the undesirable effects of therapy.

Radiotherapeutic treatments for cancer can lead to numerous side effects including: sore skin, tiredness, malaise and nausea, diarrhoea, muscular aches and stiffness and due to the nature of the treatment itself may induce the risk of developing a different type of cancer post remission.

Chemotherapy side effects are much more broad due to the circulation of drug within the human body there is much less control over where side effects may occur and as such these treatments can lead to: tiredness, malaise and nausea, hair loss (head, face, arms and legs), anaemia, bruising and bleeding due to reduced platelet count, loss of appetite, insomnia and diarrhoea or constipation. Whereas radiotherapeutic treatments induce certain side effects at the site of treatment only, chemotherapy drugs do not exclusively produce side effects related to the site of delivery itself, owing to their high toxicity yet low efficacy. These characteristics of chemotherapeutics have led to the strategy of drug delivery vehicles being researched in order to direct and deliver drugs to the site of interest, with the aim reducing their metabolization within the bloodstream, side effects caused by interaction with undesired sites and thus increasing their efficacy whilst keeping the inherent toxicity of the drugs intact.

1.3 Drug Delivery Techniques - efficiency, efficacy and progress

Numerous anti-cancer therapeutics suffer from low efficacy and high toxicity, leading to numerous side effects in the patient. Therefore, delivery of these to

increase efficacy towards the target site and reduce the overall toxicity and side effects shown is of great interest. Drug delivery of chemotherapeutics can be divided into 2 distinct targeting methods – passive targeting and active targeting [100]. The main difference of which is that whilst passive targeting exploits the tumour's pathophysiological microenvironment and the enhanced permeation and retention effect (EPR effect) [101], active targeting mechanisms involve ligands, antibodies and peptides (amongst other moieties), which are chosen against selected tumour confirmed targets and are often over expressed on the surface of such cells, to facilitate cellular uptake.

Currently, drug therapies for the combatting of cancer require a large dosage of drug in order to garner a therapeutic effect, such as the conventional chemotherapeutics as doxorubicin and gemcitabine as despite their high efficiency they suffer from low efficacy. The efficacy issue combined with the potent toxicity required for the removal of cancerous tissues therefore leads to a vast amount of side effects towards healthy tissues and the characteristic signs of cancer most people associate with the treatment of the disease.

The use of drug delivery systems aims to provide a solution to the issues surrounding efficacy and toxicity, by providing a route for the local accumulation of drug within target tissue, leading to a high concentration within the site of interest whilst also reducing the overall system concentration throughout the body [102,103].

The benefits therefore of an efficient drug delivery system are that drugs can be administered in a much lower quantity, with a much-simplified administration process and a reduced cost of treatment. In addition to the benefits for the medical professional, the large accumulation of drug within the target site and reduced system concentration overall will aid the reduction of side effects and could grant a greater quality of life to the patient.

Over the years there have been many attempts to provide drug delivery via a variety of different methods, such as the use of an external magnetic field to a

ferromagnetic drug carrier [104]. Using this method, the drug carrier accumulates within the site of interest due to magnetic attraction.

For the purpose of this chapter drug delivery via the EPR effect will be discussed in detail with respect to nanostructures and the topologies of such structures and their influence on the types of drugs suitable for loading and the advantages and disadvantages of such structures.

1.3.1 Nanoparticles as drug delivery vehicles – A polymer focused review

The term "*nanomedicine"* has been used to widely describe the use of nanotechnology for the enhancement of the pharmacological profiles of traditionally used drugs administered by a physician. Indeed, a vast array of different nanostructures are available to synthesise each with distinct advantages and disadvantages to one another that stem from their synthetic techniques and topology to kinetic stability and flexibility in functionalisation (**Table 1-2**).

Table 1- 2: Common nanostructures for drug delivery of polymer-based nanoparticles

Nanostructure	Advantages	Disadvantages	References
Micelles	Rapid, cheap production methods	Dilution may disrupt assembly, extravasation is slow, suitability is restricted to hydrophobic/lipophilic drugs	[105–110]
Liposomes	Biocompatible and biodegradable with a large versatility. Surface modification is possible. Freeze drying can be performed.	Drug release may be extended for a prolonged period, hydrophilic drugs may not be suitable due to possible leakage into solution.	[111–115]
Lipid based nanoparticles	Biocompatibility and good reproducibility. High drug loading can be afforded. Sterilization can be performed with ease.	Drug loading is limited via solubility in the melt. Polymeric transitions may result in drug expulsion.	[116–120]

Polymer based self-assembly	Smart drug release is possible. Chemistry is adaptable. Living controlled techniques allow for fine tuning of structures.	Synthesis can be costly depending on reagents. Biodegradability may become an issue. Polymer toxicity may become an issue.	[101,121–125]
Nano emulsions	Kinetically stable with a high drug loading capacity. Low cost of production with a slow and controlled payload release.	Fragile with most existing in suspension.	[126,127]

Whilst there is a vast array of different nanostructures available for the purpose of drug delivery vehicles there is currently no universal technique, in which a “universal courier approach” can be applied for any drug to be delivered to any site within the body, due to variations in solubility and hydrophilic/hydrophobic interactions stemming from the structure of the drug itself.

Within this section a heavy focus will be on the design, synthesis and characterisation of polymer-based nanoparticles as these fall within the remit of the project itself. However, other nanostructures such as gold and silver nanoparticles as an example of inorganic particles are within this scientific space. This brief review doesn’t aim on encompassing the entirety of these structure but to give a flavour of what polymer science can do in the modern day.

With that said current nanostructures have advanced considerably over the past few decades although limitations surrounding them exist such as:

a. The burst release of drugs is still a major concern. This type of behaviour is typical of drugs that are adsorbed onto the surface of nanocarriers and therefore, the therapeutic effect of the drug can be severely reduced whilst toxicity concerns are raised as the site of therapeutic need may not have been reached before payload delivery [128–131].
b. The difficulty of designing a functional nanostructure itself. Whilst novel structures have been developed major concerns arise from their biodegradability, general toxicity and accumulation in cells/tissues such as the liver. Thus, careful consideration needs to be paid to each individual aspect of the proposed nanostructure ranging from topology and surface charge to functionalization and composition, limiting the synthetic routes that can be taken by the chemist to produce a suitable nanostructure capable of performing the desired role with the appropriate therapeutic effect whilst ensuring kinetic stability and low toxicity. In this vein biodegradable drug delivery systems incorporating PEG and lactic acid for example have been of focus [106,132–134].

Whilst the design of nanostructures (either for the use in passive or active targeting systems) vary there are general guidelines to follow when the design conceptualisation and synthesis of such systems is implemented. Namely: the structure itself must be kinetically stable within the human body and remain stable within blood until the site of delivery is reached; to escape/ evade capture from the immune response within the body via stealth characteristics and finally to accumulate and penetrate the malignant tissues and interact with the cells and tissues in question exclusively.

Furthermore, the design of the nanostructure itself should prevent the payload from being degraded or metabolised by the extracellular environment, with protection from metabolism or excretion from the body before reaching the desired tissue, with the appropriate targeting method used to promote the accumulation of the structure in the tissues of interest.

If these guidelines are met, then the nanostructure has to potential to realise the “magic bullet” theory Paul Ehrlich suggested in the early 20th century. He states that there is a two-component approach to a drug targeting mechanism firstly, that the system seeks out and binds to the target of interest and secondly that there is a therapeutic effect at the site of interest [135].

1.3.2 Passively targeted approaches

Passive targeting of chemotherapeutic drugs does afford some advantages over an actively targeted approach. For instance, the need for post synthesis functionalisation of nanostructures is negated, due to the lack of targeting ligands required on the structure itself. Since the discovery of the EPR effect in the 1980s by Matsumura and Maeda [136] a vast amount of research has been conducted in order to understand how the phenomena could be exploited for therapeutic gain.

Predominately, the EPR effect itself is a result of the overexpression of the vascular epithelial growth factor (VEGF), which has also been known as the vascular permeability factor (VPF). Within the body the role of VEGF is simple, as a signal protein VEGF is used to stimulate the growth and formation of new blood vessels. For instance, in hypoxic conditions (when the supply of oxygen is inadequate to the tissues) VEGF forms part of the system that acts to restore oxygen levels to appropriate levels. Therefore, the role of VEGF in the growth of malignant tissues and cancer is to stimulate the formation of new blood vessels allowing the tumour to grow and metastasize [137].

The EPR effect therefore is directly related to the formation of the new blood vessels required for cancer angiogenesis, with abnormal architecture and form resulting in the lack of a smooth muscle layer and effective lymphatic drainage [138]. This leads the area of interest to become leaky to outside influence thus allowing nanostructures to infiltrate the tumorous tissue without threat of being removed effectively due to the lack of an efficient drainage system.

Despite all this the EPR effect does not necessarily promote the efficient delivery of drugs as one would assume. Due to the irregularity of the newly formed blood vessels there is a knock-on effect of irregularity within the growing cells themselves. This leads to hypoxic and necrotic regions of the tissue towards the core. Furthermore, as a further consequence of the leakiness of the malignant tissues there is a high observed interstitial pressure associated with cancerous tissue which can hinder the efficient release of drugs [139]. Furthermore, the assumption that all cancers can be targeted passively with the EPR effect isn't always true. Whilst the effect itself is present within almost all human cancers there is exceptions where the cancer is within a hypovascular environment (where there is a deficiency of blood vessels) [123].

In terms of passive targeting in action, the delivery system Caelyx is a medication for the treatment of a variety of cancers including breast and ovarian cancers and consists of the drug doxorubicin wrapped in a fatty liposome [140].

For such a delivery system to be effective there needs to be a long circulation time within the body as to allow the drug to accumulate in quantities to deliver the desired therapeutic effect within the target site. In the example of Caelyx to provide this long circulation time the use of the pegylation method was employed in order to induce stealth characteristics of the molecule, allowing for water solubilisation and preventing the opsonization (targeted for destruction by the immune system) of the system itself [140].

However, passive targeting cannot be considered a universal approach to the targeting of malignant tissues as the vascular endothelium may not be sufficiently permeable in all cases to ensure an efficient exploitation of the EPR effect. In these cases, a more active approach to targeting may be required to further enhance the exclusivity of the drug to the target tissue.

1.3.3 Actively targeted approaches

Whereas passive targeting of malignant tissues relies on the EPR effect for the permeation and retention of DDS actively targeted approaches build on this well-established observation in order to promote a greater exclusivity in the delivery of drugs to the target tissue. The main difference between a passive and active targeting system is the presence of a ligand on the DDS itself in order to interact with a specific receptor or protein overexpressed within the target tissue, promoting exclusivity in uptake, or the use of so called cell penetrating peptides such as the TAT peptide in order to promote the efficient cellular uptake of the DDS.

Direct coupling therefore of the drug to a targeting ligand is the easiest and most efficient method to facilitate the uptake of drug into target cells and such methods have been developed in a branch of delivery systems named immunotoxins [141].

The folate receptor has asserted itself as a prime target for exploitation and as such folic acid complexation to DDS has become commonplace due to the abundance of the folate receptor protein (FR) within cancerous tissues [142,143]. It is know that human cancer cells overexpress two forms of FR which have been termed α and β and these FRs bind to folic acid with high affinity and selectivity, kick starting folate mediated endocytosis internalizing the ligand into the cell [143]. It was the late Bart Kamen and his co-workers who first demonstrated the function and tumour distribution of the FRα and was the foundation for the numerous studies revolving around using folic acid as a ligand for the targeted delivery of therapeutics [144]. This has led to low molecular weight therapeutics, liposomes and drug encapsulated nanoparticles to be developed for the delivery of payloads to this site of therapeutic interest.

Whilst FRα has been shown to be overexpressed in epithelial tumours such as ovarian cancer and within cultured cell lines of this lineage the FRβ is often overexpressed in carcinoma that stem from non-epithelial lineage, although interestingly is absent from established cell lines of the same lineage [145].

However, folic acid is not the sole method of ligand based cellular internalization with other targeting strategies such as nicotinic acid (the oxidized form of nicotine) able to facilitate internalisation. However they may, necessitate the need to be biotinylated to a protein for example in order to function as a clathrin dependent receptor mediated endocytic delivery method [146].

Within the area of actively targeted approaches there are three main pathways in which molecules can be internalized within the cell. Receptor mediated endocytosis (RME), which includes the FR [147] and nicotinic acid pathways [148], fluid phase endocytosis [149] and cell adhesion molecule (CAM) directed approaches [150]. Within RME pathways there are two distinct families of proteins that regulate the internalization into cells: caveolin and clathrin, which exist in the pitted regions on the cell surface membrane [151] (**Figure 1-12**).

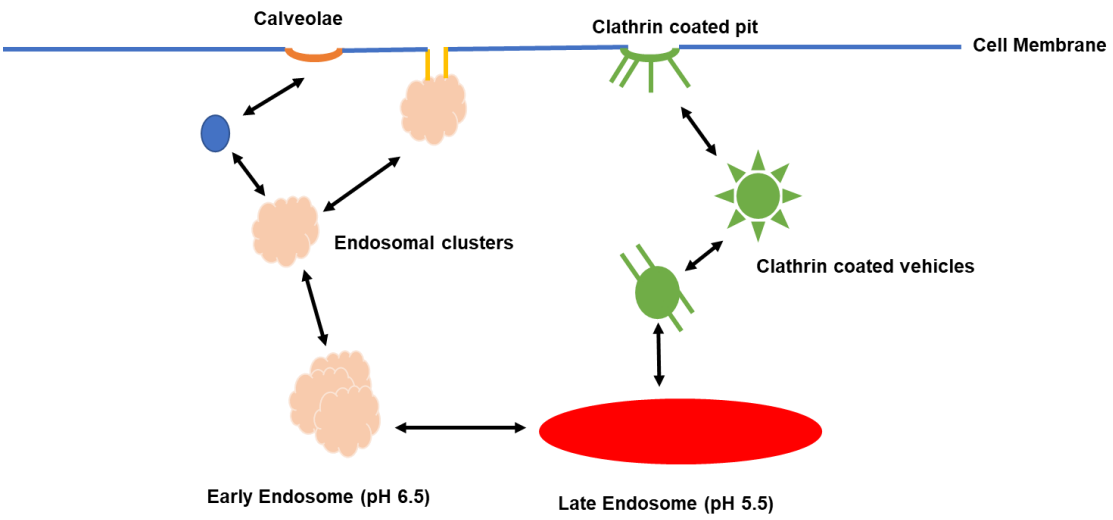

Figure 1- 12: : Calveolin and Clathrin mediated routes of cellular internalization for molecules

The method of FR internalization, however, is currently a hot topic for debate, in the early 1990s Rothberg et al. suggested that internalization did not require assistance from the clathrin mediated endocytosis pathway [144]. This led to the suggestion of potocytosis, in which molecules are transported across the plasma membrane of the cell and caveolae are responsible for assisting the transport of the molecule into the cytosol [152]. However, it was later suggested by Wu et al. in 1997 that whilst FR were situation on the plasma membrane there was no evidence to suggest that there was an association with caveolae [153]. Further work in 2001 reinforced this suggestion when Bridges and co-workers surmised that folate is internalized via a non-caveolar pathway, however, the localization of the FR within caveolar structures suggests there is a relationship between caveolin and the FR [154].

As oppose to direct conjugation of a complimentary ligand to the drug or drug carrier in question antibody-based techniques can be used to target receptors on the cell surface, with monoclonal antibodies the largest class of therapeutic proteins used for therapeutic gain in the sector today. Monoclonal antibodies (mAb) by nature are antibodies made via identical immune cells and as such are clones of the parent cell themselves, leading to an exceptionally high specificity in their binding towards epitopes

[18]. In terms of their mechanism of action antibody-based targeting therapeutics aim to directly conjugate to a specific cell receptor and stall the progress of certain cell signalling pathways and growth. For instance, ranibizumab is used as a treatment as an anti-VEGF antibody, and is used in order to treat the “wet” type of age-related macular degeneration [154]. In terms of oncological treatments with antibodies ipilimumab has been approved for use by the US food and drug administration (FDA) as an immune system activator by activating the cytotoxic T lymphocytes, which can seek out and destroy cancerous cells [155]. With respect to the immune system, briefly, the immune response is triggered via antibody conjugation onto “non-self” receptors either on eukaryote, prokaryote or viral cells which triggers the synthesis of receptor specific molecules required for the correct immune response and amplification of cells such as phagocytes in order to remove the alien cells from the host. Cancer cells, although malignant, are not “non-self” cells, and thus cancer antigens presented are either self or mutated self-receptors. Therefore, developing an immunity to cancer is a vastly complicated conundrum. Referring to the example of ipilimumab, targeting specific T cells within the human body are one way of triggering an immune response towards cancer cells themselves, effectively blowing the disguise off the cancer cells [155]. T cells have the ability to search for mutated cellular proteins that induce the onset of cancerous characteristics within the cell cycle, however the issue with relying on the T cells alone is the vast array of non-mutated cells and proteins that they are canvassing, leading to the mutated proteins generally becoming lost during the surveying process.

Cell penetrating peptides such as tat have also been explored for their use in targeting chemotherapeutics towards cancer cells [156]. The tat protein was first discovered as a protein encoded by the tat gene within the HIV-1 virus and is responsible for enhancing the efficiency of RNA transcription within cells, furthermore, the tat protein itself can act as a toxin towards cells not infected with HIV themselves, forcing apoptosis in uninfected T cells accelerating progression towards AIDS [157]. In terms of the cell penetrating abilities of the tat protein it aims to combat the issue of translocation through the plasma membrane of cells, which is a huge barrier to drug entry. The mechanism at which tat internalizes nanoparticles is believed to involve the

clatherin-dependent endocytosis mechanism [156]. The function of all cell penetrating peptides (CPPs) is to facilitate the entry of drugs that would otherwise have barriers to entry. CPPs although considered a targeted drug delivery technique isn't the most targeted method. Due to the nature of the peptide ligands conjugated onto the payload there is a lack of specificity as the peptides cannot actively distinguish between malignant and healthy cells. It is believed there are debated main methods of entry for CPP based systems into the cell: direct entry vs endocytosis, although the mechanism of entry is still not widely understood, these methods of cellular entry will be discussed briefly to give an overview of how CPPs are believed to work with the current research in mind.

Whether direct entry or endocytosis occurs is still a topic that is not well understood. Nevertheless, considering either entry route the key starting point is how the CPP itself interacts with the cellular membrane. The receptor rich membrane of the cell consists mainly proteoglycans such as herparin sulfate proteoglycans (HSPGs) and due to their negative charge and wide-reaching side chains they are an attractive proposition for peptide interactions [158].

In terms of internalization via the clathrin mediated pathways, this is known to be a type of receptor led approach, in which initialization of internalization occurs when ligand is bound to the corresponding receptor at the cell surface kick starting the recruitment of clathrin towards the plasma membrane [148]. Caveolin based uptake pathways have been discussed within the scientific literature as a method for CPP-cargo delivery [158]. Independent methods of entry, which do not require the assistance of either clatherin or calveolin has also been descirbed such as macropinocytosis [159].

Generally speaking, the take away message from the use of CPP cargo based delivery vehicles is there is a distinct lack of specificity, that either ligand based treatments or anitbody treatments can afford. Therefore, whilst CPP-cargo delivery may increase the chance of internalization in to the cell there is no way to accurately guide the payload to the appropriate site once treatment has been applied. Thus, greater research on the entry mechanisms of these CPPs is needed before they can become to

overcome the challenges associated with their unspecific approach. With this in mind, ligands such as folic acid are suggested to be used due to the research presenting an overexpression of the folate receptor in carcinomas.

1.4 Hyperbranched Polymers – Synthesis, theory and topology.

Hyperbranched polymers have become a vital player in the fight for better drug delivery treatments, due to their enhanced solubility and functionality over their linear counterparts to name a few advantages. This section focuses on the discovery of hyperbranched polymers and their related topologies. Focus then is paid to the synthetic techniques involved in the synthesis of polymers, be it radical or otherwise and how these approaches can be exploited by the researcher for the synthesis of desired compounds. Advancements in polymer synthesis are then discussed with respect to controlled polymerisation methods and the introduction of stimuli responsive smart materials. Finally, this section is concluded by discussing how these advancements in polymer technologies have impacted the drug delivery sector, with respect to cancer and delivery mechanisms previously discussed.

1.4.1 Characteristic elements of hyperbranched polymers

The terminology hyperbranched polymer (HBP) can be traced back to 1990 in Kim and Webster's publication describing the synthesis of Poly(phenylene) [160], although it was first in 1952 that Flory had predicted polymers with a high branching degree can be synthesised via the polycondensation of AB_n $(n \geq 2)$ type monomers [161] (**Scheme 1-1**), nearly 40 years prior to Kim and Webster's publication.

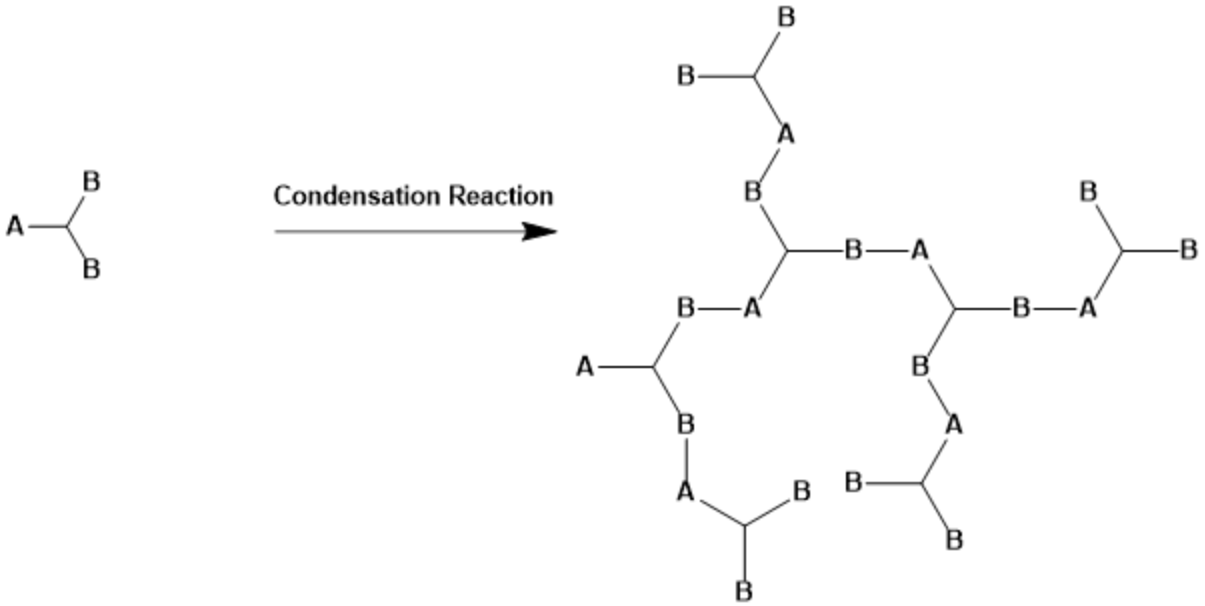

Scheme 1- 1: A condensation reaction of an AB2 monomer (eg. Phenylene) resulting in a highly branched structure

Since then hyperbranched polymers have been exploited for their unique characteristics and advantages, when compared to other polymer topologies, such as linear or even dendritic polymers [162,163]. These properties allow for the unique synthetic route of a branching polymer that is no more laborious to synthesise and purify than a linear type polymer, whilst enjoying the benefit of a 3D structure that would normally require multi-step synthesis and complex purification.

As suggested by the terminology "*hyperbranched"* HBPs benefit from a high degree of branching throughout, and the degree of branching (DB) is a distinct property of HBPs when compared to their linear counterparts. The degree of branching is the ratio of branched and terminal segments of the macromolecule compared to the linear segments, calculated via the molar fraction of each [164].

In general polymers are termed as linear or non-linear topologically speaking. As the name suggests linear polymers are a continuous chain of carbon-carbon bonds, such as poly(styrene), poly(vinylacetate) or poly(vinylalcohol) for example, with a lack of branching typifying linear structures. However, non-linear polymers are not so easily

classified with a plethora of different topologies such as dendritic, cyclic, star, brush and hyperbranched just a few examples of the variety of different non-linear structures [165] (**Figure 1-13**).

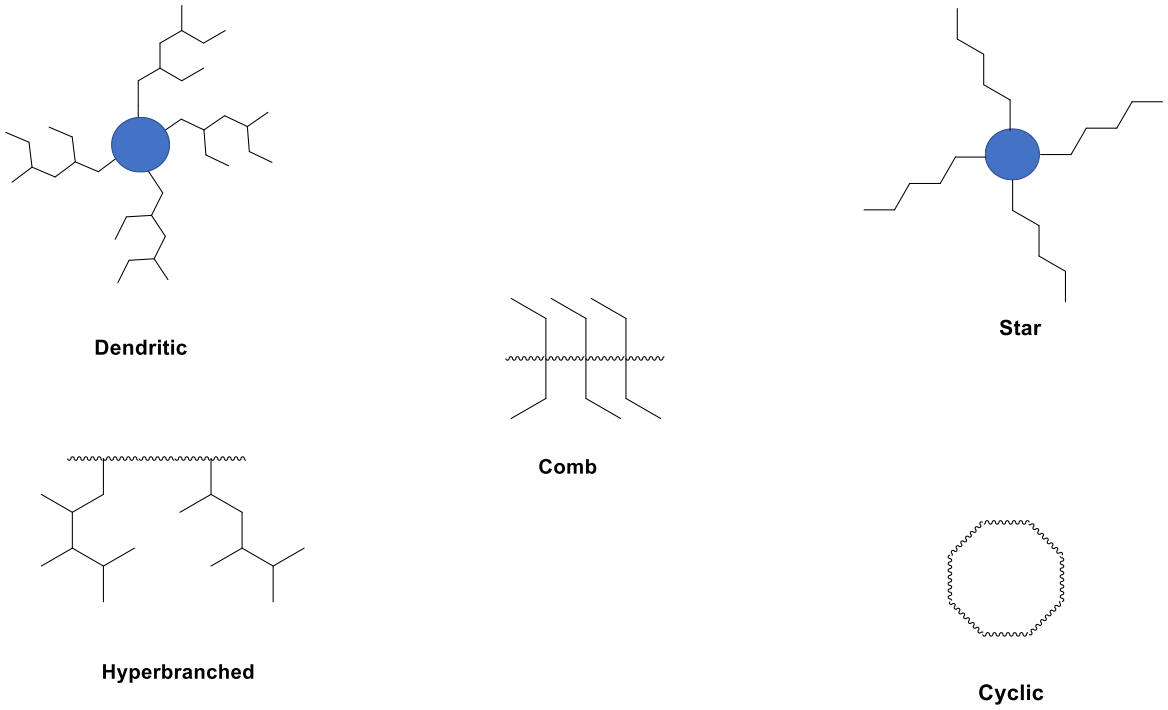

Figure 1- 13: Some examples of non-linear polymer topologies

Hyperbranched polymers can be therefore classed in some respects as a dendritic type architecture due to being repetitively branched in nature, with the origins for the classification stemming from the Greek word "*Dendron"* meaning tree. However, unlike dendrimers, which are generally symmetric from their core hyperbranched polymers can be synthesised in a random fashion or controlled via the use of block polymerisation techniques [163,166–169].

In terms of hyperbranching structure, their high degree of branching is the main characteristic that makes them unique from their linear relatives or cross-linked macromolecular structures. The degree of branching therefore is used to visualise the ratio of terminal and branched units considering dendritic (D), linear (L), initial (I) and terminal (T) units. Referring to the AB_2 type structure discussed (phenylene for eg.) the

(eq 1-1)

degree of branching can be calculated using the following mathematical formula [170] (eq. 1-1)

$$Degree\ of\ Branching\ = \frac{D+T}{D+T+L}$$

This equation can then be simplified should the macromolecule achieve a high degree of polymerization. Should this occur then the assumption is made that the number of D units are approximately equal to the number of T units. Thus, the following formula can be applied to such situations [170] (eq. 1-2).

$$Degree\ of\ Branching = \frac{2D}{2D+L} = \frac{1}{1+L/2D} \qquad \textit{(eq 1-2)}$$

Whilst it may not be possible to achieve accurate measurements of the structural units, linear and dendritic units can be approximated via the use of ^{1}H NMR spectroscopic analysis, with relative integrations compared for an accurate prediction of polymer repeat unit compositions.

A second consideration of hyperbranched polymers, and indeed a consideration for all polymers, is the molecular weight of the molecule itself, and the related poly dispersity index (PDI). The PDI of a polymer is determined as the uniformity of the polymer chains synthesized where 1 describes a polymer where all chains are indistinguishable between one another whilst values above one describes discrepancy between the polymer chains themselves [171]. Hyperbranched polymers and indeed all polymers therefore display their own unique PDI, which itself can alter between batches of the polymer itself. Therefore, it is generally accepted that the PDI of the synthesized macromolecule increases with the monomer conversion (as more chains are expected to be participating in the reaction), lack of controlled synthetic methods and a lack of classification-based purification methodology [172]. Therefore, to combat these factors in order to reduce PDI slow addition of monomers into the reaction vessel, copolymerization with core molecules themselves and classification based purification methods such as dialysis with a defined cut off point or precipitation designed to “crash out” molecules of molecular weight x and above, where x is the desired molecular

weight for the polymeric compound. Furthermore, the use of controlled polymerization methodologies can also aid the reduction in PDI [173,174].

1.4.2 Synthetic routes toward hyperbranched polymers

Within this section literature surrounding the common methods for the synthesis of polymers with a hyperbranched topology is discussed and the advantages and drawbacks of each technique. Both conventional uncontrolled free radical synthetic routes and their evolved controllable counterparts are therefore discussed to give the reader an understanding of the initial synthetic framework that led to the discovery and invention of more sophisticated methods such as RAFT. It is hoped that after reading this review the reader will gain a understanding and appreciation of the works over the past few decades involved in the synthesis of polymers with a defined topology and controllable characteristics and that literature cited will act to signpost the reader to current and significant historical literature in the field, if they so desire to do further reading.

1.4.2.1 Initiation and Free Radical Polymerizations

Hyperbranched polymers as previously mentioned benefit from ease of synthesis via facile one-step approaches either via controlled or completely random synthetic strategies. For instance, the use of multi-vinyl containing monomers such as Poly(ethylene glycol diacrylate) (PEGDA) facilitates chain growth at both alpha and omega monomer terminus – a direct result of the multi vinyl properties it displays [175].

The mechanism towards the synthesis of polymers can be explored in order to ascertain where control over the reaction can be afforded. Broadly speaking there are two routes towards the synthesis of macromolecules “Chain-growth polymerisation” and “step-growth polymerisation” techniques. Chain growth techniques generally utilise radicals in order to propagate the chain at vinylic terminus, such as in the synthesis of styrene [176,177], however, other chain growth mechanisms may utilise ionic bonds [178]. Furthermore, co-ordination chemistry has been employed as a chain growth methodology alongside ring opening techniques, such as the case in the synthesis of

Poly(ethyleneglycol) (PEG) [179] a widely used homo-polymer in the medicinal and cosmetic industry. PEG synthesis is relatively straightforward and requires the ring opening of the monomeric unit ethylene oxide and can be synthesised to a variety of different molecular weights depending on the amount of monomer feedstock used.

Step-growth polymerization techniques rely on the use of conjugation chemistry in order to form heteroatomic bonds, such as the amide bond present in nylon polymers [180]. Therefore, a general requirement for the synthesis of step-growth polymers is that there a is a bi-functional or multi-functional monomer, in order to induce reactions for homo-polymerizations. Another key difference between the two techniques is that within chain growth polymerizations only monomeric units may react and grow the chain whereas in step growth syntheses due to the heteroatomic nature of chain terminus two individual polymer chains may react with one another in order to grow the chain and the key differences between “chain-growth” and “step-growth” polymerization techniques are shown in **Figure 1-14.**

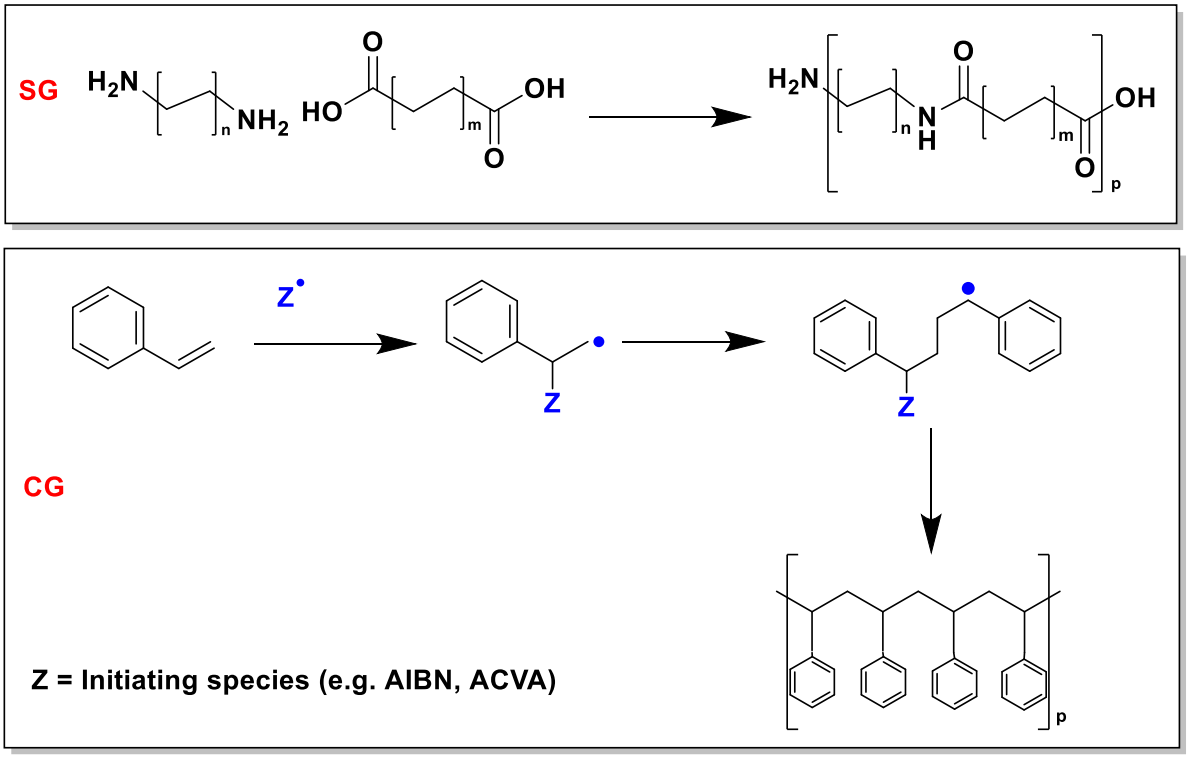

Where SG = Step-Growth polymerization and CG = Chain-Growth polymerization

Figure 1- 14: Chain Growth vs Step Growth polymerizations

Conventional radical polymerisations (CRP) has become one of the most widely used techniques in the modern day due to the vast variety of monomers that can be employed, whilst other small molecules can be modified to incorporate a vinyl bond in order to successfully be involved in the reaction mechanism. Radical polymerisation is a type of chain-growth polymerisation technique previously discussed and the mechanism comprises of three main components *initiation --> propagation --> termination.*

Firstly, in order to perform any CRP experiment the source of initiation needs to be strategically planned out, as there are a variety of different methodologies one can employ in order to generate the radicals required including: thermo-labile compounds (generally termed *azo-initiators or peroxy-initiators)* [181]*;* self-initiation [182] and redox [183] or photo (UV) initiation [184]. By large, the most common method of initiation for CRP reactions is the use of an azo initiator with commercially available compounds such as (AIBN) and (ACVA) being employed for this purpose, amongst many others. Such is the lability of the azo bond that two radicals are produced via thermolytic homofission (**Figure 1-15).**

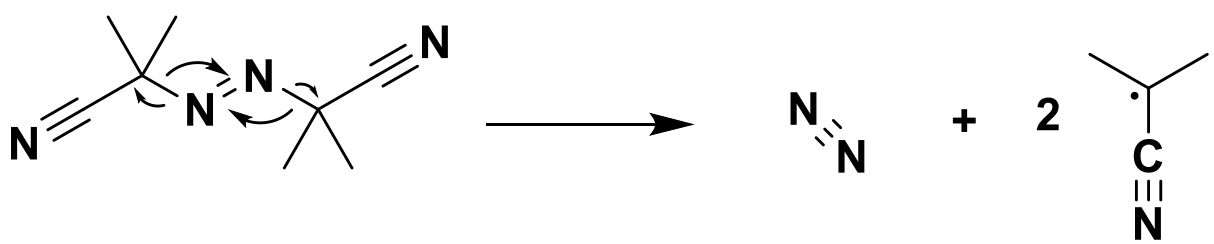

Figure 1- 15: Thermolytic homofission of AIBN (azo initiator) to produce radicals for CRP syntheses.

Additionally, as these primary radicals generate radicals within monomers via addition and kick start the chain transfer process there is an ideal situation where initiators can be functionalised in such a way (for instance ACVA incorporates a COOH group) that this functionality can be provided to the macromolecule itself. However, it is worth noting that the efficiency of the initiator (*f*) will alter depending on its structure as a

direct result from the rate at which initiator decomposition occurs [185], which is summarized in equation (eq.1-3).

$$f = \frac{Rate\ of\ initiation\ of\ propogating\ chains}{Rate\ of\ primary\ radical\ formation} \quad \textit{(eq 1-3)}$$

The decomposition rate constant (k_d) is then related to the half-life ($t_{1/2}$) by the following equation (eq. 1-4).

$$t_{1/2} = ln2/k_d \quad \textit{(eq 1-4)}$$

Whilst efficiency of the initiator can be calculated by the equations listed there will be an observed decrease in efficiency when compared to the calculated value, due to the solvent cage effect. The effect was first theorized by Franck and Rabinowich in the 1930s in which they described the effect free radicals and their relationship and collisions with other particles altering the photochemistry of solutions [186]. The solvent cage effect describes how for two radicals to interact they must first diffuse out of a cage containing identical molecules and diffuse into a cage containing a hetero species. Furthermore, it is also completely plausible that solvents can abstract hydrogen from radical species essentially de-activating the initiator and hence needs to also be considered. A list of commonly used initiators (both azo and peroxy based) and their decomposition and half-life are listed in **Table 1-3.**

Table 1- 3: Common initiators and their decomposition values[187]

Entry	Initiator	Solvent	Temp (°C)	K_d (S^{-1})	10 hr half-life C (Solvent)
1	tert-Amyl peroxybenzoate				99 (Benzene)
2	2,2'-Azobisisobutyronitrile	Benzene	50	2.2×10^{-6}	65 (Toluene)
			70	3.2×10^{-5}	
			100	1.5×10^{-3}	
3	4,4-Azobis(4-cyanovaleric acid	Acetone	70	4.6×10^{-5}	69 (Water)
		Water	69	1.9×10^{-5}	
		Water	80	9.0×10^{-5}	
4	1,1'-Azobis(cyclohexanecarbonitrile)	Benzene	60	2.2×10^{-6}	
			78	3.2×10^{-5}	
			100	1.5×10^{-3}	
5	1,1-Bis(tert-butylperoxy)cyclohexane	Benzene	93	1.9×10^{-5}	
6	tert-Butyl peroxide	Benzene	80	7.8×10^{-8}	125 (Benzene)
		Benzene	100	8.8×10^{-7}	
		Benzene	130	3.0×10^{-5}	
7	Cyclohexanone peroxide	Benzene			90 (Benzene)
8	Peracetic acid				135 (Toluene)

For the use of peroxide-based initiators the use of a redox reagent is required in order to generate the radicals required to kick start the polymerization process and as such common transition metal catalysts are employed for this role such as Cr^{2+} [188], Ti^{3+} [189] and Cu^{+} [190].

Self-initiation on the other hand means that only the monomer in question is needed within the reaction vessel alongside solvent, if so desired. One good example of a monomer that can induce self-initiation is styrene, which at elevated temperatures can undergo a Diels Alder cycloaddition and as such results in a free radical, which then behaves as the primary radical in the system, kick starting the propagation phase and thus chain growth, known as the mayo mechanism of styrene self-initiation [191]. However, this mechanism is disputed with the Flory mechanism of self-initiation, in which it is proposed that styrene first dimerizes and forms a diradical species before a third styrene molecule abstracts hydrogen forming monoracial species that are the primary radicals in the reaction [192]. (**Scheme 1-2**).

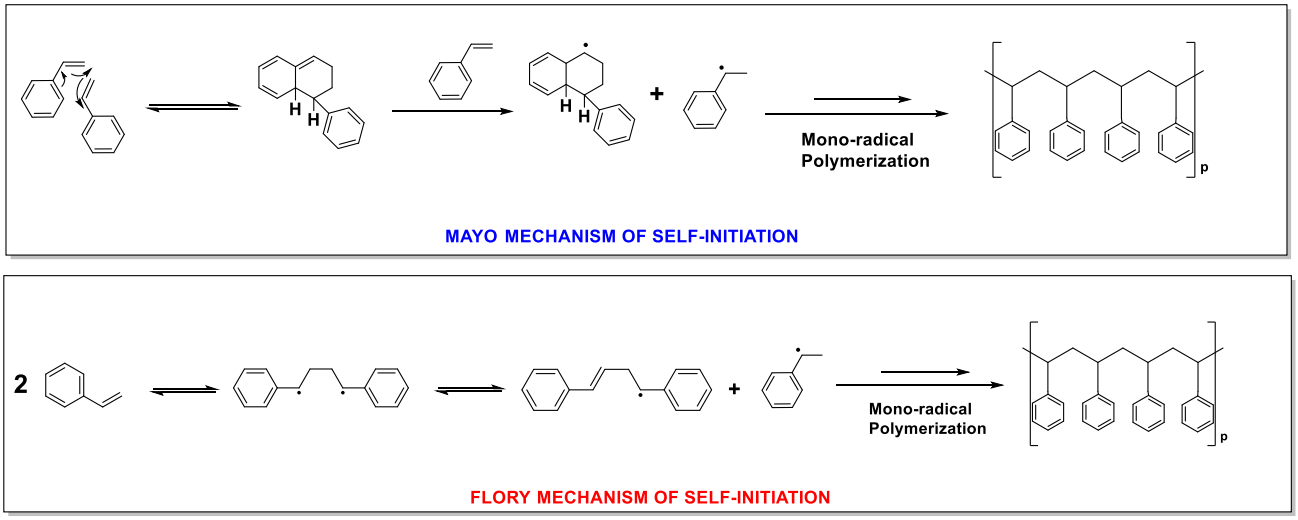

Scheme 1- 2: Mayo and Flory mechanisms of styrene self-initiation

The propagation phase of a radical polymerization is interchangeably termed the chain growth phase. Broadly speaking, the propagation phase is exclusively for the continued addition of polymeric radicals to vinylic bonds in order to produce molecules of a high molecular weight, resulting in a free radical on the product.

Furthermore, propagation tends to proceed at a much faster rate than other steps within the mechanism, and the rate at which propagation proceeds can be calculated with respect to temperature in the terms of the Arrhenius equation *(eq 1-5)*

$$K_{prop} = A \exp\left(-\frac{E_{act}}{RT}\right)$$

Where A is the pre-exponential factor, Ea is the activation energy R is the gas constant and T is the temperature.

The termination stage of the reaction results in the de-activation of propagating radicals primarily by combination, either via propagating chain radicals combining or primary radicals combining with radical chains. Termination in polymerization reactions comprises mainly of two different key reactions and is a reaction in which a chain carrier is converted into a non-propagating species without the formation of a new chain carrier. Essentially, active radicals are consumed in the reaction converting them into “dead” polymer chains or dead species with the necessity for initiation for them to propagate once again. Termination as a reaction step can be divided into two main categories of reaction exemplifying the complexity of this step. Firstly, recombination can occur. Recombination of radical species terminates the reaction by the formation of a new covalent bond. Two radical species react with one another to form a stable bond and consumes the radical on either side. For instance, two growing chains may react forming a much larger polymeric chain ($P_n + P_m \rightarrow P_{n+m}$). Alternatively, disproportionation may occur. In this reaction step two growing chain radicals are again involved however radical A may abstract a hydrogen from radical B resulting in two stable molecules a vinylic species and a saturated polymeric chain**.**

Additionally, a chain transfer reaction may also induce termination of a growing chain and involves a propagating radical reacting with a non-radical resulting in a dead polymer chain (I.e. no free radical) and a new radical capable of initiating a polymer chain**.**

With all steps considered a radical polymerization reaction and the mechanism of such can be defined as such (**Scheme 1-3).**

1. I → I*	(***Initiator radical generation)***	**CRP mechanism**
2. I* + M → IM*	(***Initiation)***	
3. IM* + M → IM_nM	(***Propogation)***	
4. IM_nM^* + IM_mM^* → IM_nM-MM_nI	(***Termination)***	
M* + M* → MH + $M_{vinylic}$	(***Disproportionation)***	**CRP side reactions**
M* + Solvent → M + Solvent*	(***Solvent transfer)***	
IM_mM^* + M → IM_mM + M*	(***Chain transfer)***	

Scheme 1- 3: Conventional Radical Polymerization Mechanism and Side Reactions

Heavy research has been conducted over the years in order to develop so called “living/controlled” polymerisation techniques, indeed the first example of a living mechanism was displayed by Micheal Szwarc in 1956 in the anionic polymerisation of styrene [193]. Essentially, Szwarc realised that upon addition of monomer viscocity of the system would increase indicative of monomer consumption, and upon 100% conversion viscosity would cease to increase. Furthermore, after addition of a second batch of monomer into the system the viscosity of the system would again increase indicating that the polymer chains were not dead and incapable of growth and hence never underwent the termination step of the reaction [193].

There have been some controversies regarding the use of the “living/controlled” terminology regarding controlled polymerization techniques. IUPAC has discouraged the use of such terms due to the nature of radical reactions themselves, in that termination steps cannot be eliminated from the mechanism, and thus the term “living” can be misleading due to the presence (even minor) of dead polymer chains. Hence, whilst the term “living/controlled” is widely used to describe controlled polymerizations it is generally accepted that the correct terminology in order to describe controlled techniques is “reversible-deactivation radical

polymerization" (RDRPs). Indeed, IUPAC defines RDRPs as "*Chain polymerization, propagated by radicals that are deactivated reversibly bringing them into an active/dormant equilibrium of which there might be more than one (radical)"* [194]. Bearing this strict definition RDRPs have advanced vastly since Szwarc's first discovery and these are discussed in detail herein.

1.4.2.2 Controlled Radical Polymerisation techniques – Nitroxide Medidiated Polymerisation

Advancements within the controlled approach to polymer synthesis firstly resulted in the Nitroxide Mediated Polymerisation technique (NMP), patented by Solomon et al in 1986 [195]. In this technique the chemist employs an alkoxyamine initiator in order to assert control over the reaction. Mechanistically, homolysis of the C-O bond occurs resulting in a carbon radical and a N-O radical which serve as the primary radicals within the reaction [196,197]. Thus, there is a purposefully designed steric hindrance on the nitrogen R groups with R^1 groups attached to the oxygen capable of forming stable radicals. Through this design there is a persistent radical effect observed within NMP reactions and the nitroxide radical itself acts as the mediator for the reaction. Whilst radicals are capable and do form on the oxygen with great stability, through resonance effects nitrogen can itself double bond on the oxygen abstracting the radical and inheriting the radical behaviour leading to the following mechanism of the reaction (**Scheme 1-4)**

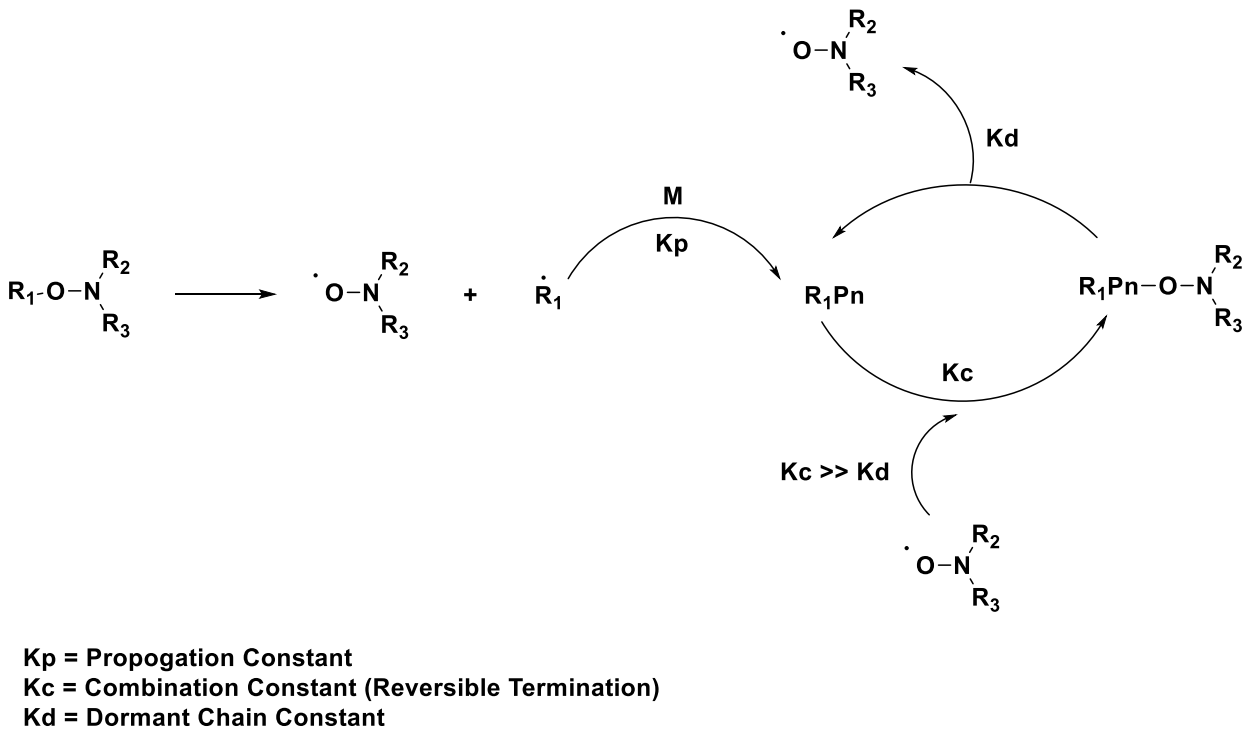

Scheme 1- 4: Mechanism of Nitroxide Mediated Polymerization (NMP)

Thus, due to the steric hinderance on the N atom itself this presents a huge barrier for radical coupling and thus contributes to the mediation of the reaction. A widely used molecule for the generation of nitroxide radicals is the initiator ((2,2,6,6-Tetramethylpiperidin-1-yl)oxyl) (TEMPO) and is used for inducing the polymerization of styrene [198]. However, it would be wrong to assume that there is a one-size fits all approach for the choice of nitroxide initiator in NMP reactions and careful consideration needs to be paid to the design and structure of the initiator in order to perform a successful reaction with sufficient control over the polymer chains. Generally there are three things to consider when choosing an efficient nitroxide initiator: solvent choice, such is the nature of the nitroxide formation it is suggested that a polar solvent be used for this purpose due to their inability to bind to the labile nitroxide and ring size.

NMP therefore has been used for the synthesis of a wide variety of polymers including acrylic acid polymers, styrene/acrylate copolymers, styrene derivative copolymers and acrylate copolymers [199].

Whilst the advantages of NMP include simplicity in reaction, a large versatility of compatible monomers, ease of obtaining polymer purity, whilst styrene synthesis utilising TEMPO is one of the simplest methods to produce polystyrene with a degree of control there are still drawbacks to consider when considering the use of NMP [199]. These include: the slow kinetics of the reaction leading to the need for high temperature and large reaction times, the use of methacrylate monomers may cause unwanted side reactions or recombination with the nitroxide, whilst the nitroxide synthesis themselves can be cumbersome and have such limited NMP to commercially available systems and the modifications of such [199].

1.4.2.3 Controlled Radical Polymerisation techniques – Atom Transfer Radical Polymerisation

Further advancements came when Kristof and Jin-Shan Wang published their work on Atom Transfer Radical Polymerisation (ATRP) as a new method for the control of radical polymerisation reactions in 1995 [200]. ATRP mechanistically relies on the formation of carbon-carbon bonds with the use of a transition metal catalyst. Interestingly that same year Mitsuo Sawamoto had independently reported the same polymerization mechanism via the use of a ruthenium catalyst [201]. ATRP came as a direct advancement of the previously studied Atom Transfer Radical Addition (ATRA) process, in which a transition metal catalyst is employed as a halogen carrier in a revisable redox reaction with alkyl halides [202].

Matyjewski discovered that halogen capped polymer chains existed in equilibria with the employed transition metal, of which Cu, Ru, Fe and Ni are commonly employed, in a reversible redox reaction and only when oxidation of the catalyst is performed is the polymer chain able to propagate [203] (**Scheme 1-5**).

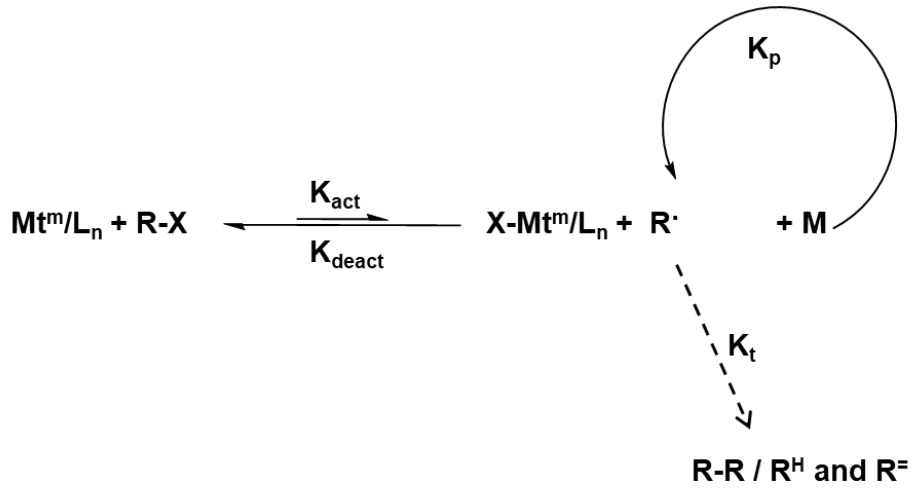

Mt^m = transition metal
L_n = Ligand for complexation
R- = Polymer Chain
X = Halide (normally Br or Cl)

Scheme 1- 5: ATRP proposed mechanism demonstrating a controllable polymerization process

The components of a general ATRP reaction include: monomer units, a alkyl halide initiator with the capacity to become involved in reversible redox reactions with a transition metal, a transition metal catalyst and a ligand [200]. Most important in the design of ATRP reactions is the choice of catalyst and indeed the associated ligand. The metal catalyst itself has select requirements that it needs to meet in order to facilitate the ATRP reaction itself, and as such influencing the equilibria between active and dormant species. It is of key importance to hit the “sweet spot” of the equilibrium constant between these two species, too large and there is a wide distribution of chain lengths, whilst a constant that is too low leads to inhibition or a reaction rate that is unfit for purpose (the reaction proceeds too slowly) [202,203]. Therefore, requirements for the catalyst include the following: the metal center must show an affinity towards halogens and as such the co-oridination sphere of the metal must be able to accommodate halogens upon oxidation; there must be two accessible oxidation states that can be differentiated by a single electron (for

instance Cu (I) → Cu (II) transitions) and this catalyst must not lead to significant side reactions that would otherwise prevent polymerization.

Additionally, the choice of ligand can have huge implications on the suitability of the catalyst for the role. For instance, a ligand can be employed in order to increase the solubility of the metal in the chosen solvent (water, toluene DMSO, DMF etc.), or to influence redox potentials allowing the metal to become much more easily involved in the reaction, or to limit redox involvement in order to impart control over the equilibrium constant. Some of the most common ligands utilized for an ATRP reaction with a copper complex involve 2,2'-bipyridine (BPY), N,N,N',N'-tetramethylethylenediamine (TMEDA) and N,N,N',N'-tetrakis(2-pyridylmethyl)ethylenediamine (TPEN) [203].

As stated previously, a key component of ensuring an efficiently controlled and feasible ATRP reaction relies on the equilibrium constant the reaction itself hinges upon. The equation for the constant is found below [204] (*eq 1-6).*

$$[R - P_n^{\cdot}] = K_{ATRP} * [R - P_n - X] * \frac{[Cu^{I}X/L]}{[Cu^{II}X_2/L]} \qquad \textit{(eq 1-6)}$$

Following this equation, the radical concentration can be obtained, whilst the K_{ATRP} value can be adjusted via catalyst modifications, temperature and solvent to influence the number of radicals within the reaction at any one time (T_1). Furthermore, as the K_{ATRP} value is dependent on the cleavage energy of the alkyl halide and the redox potential of the catalyst itself (with the associated ligand) the K_{ATRP} can be further defined as (eq. 1-7) within a system with two distinguishable alkyl halides and a further two disgustable ligands [204].

$$K_{ATRP}^{22} = \frac{K_{ATRP}^{12} * K_{ATRP}^{21}}{K_{ATRP}^{11}} \qquad \textit{(eq 1-7)}$$

Where K^{22}_{ATRP} refers to the K_{ATRP} for R^1-X and L^1 where R-X is an akyl halide and L is the ligand. Thus, by knowledge of three combinations the fourth can be calculated, and as such predicted values for K_{ATRP} constants can be calculated using literature knowledge of observed values.

Although, despite ATRP imparting advantages such as: a variety of monomers can be used and thus macromolecules synthesized, increased control over the molecular weight, polymer architecture and composition retaining a low dispersity with halogen capping also allowing for fast facile one pot modifications. There are some drawbacks to the technique that must be considered when designing polymers for specific roles. These include: a high concentration of transition metal catalyst required for successful reactions increasing cost with metal removal post synthesis cumbersome whilst also such catalysts are expensive limiting commercial viability [203]. Additionally, owing to the redox nature of the mechanism there are limitations on how the technique can be employed with air sensitivity a large stumbling block. Therefore, the need for the use of Schlenk techniques alongside freeze-pump-thaw cycles makes ATRP technically cumbersome in some settings. Whilst the transitional metal catalysts could themselves impart some toxicity.

1.4.2.4 Controlled Radical Polymerisation techniques – Reversible Addition Fragmentation chain-Transfer Polymerisation

The final controlled polymerization technique to be discussed was developed by the Commonwealth Scientific and Industrial Research Organisation (CSIRO) and they further advanced the field of controlled polymerisations with publications on the Reversible Addition Fragmentation Chain-Transfer (RAFT) polymerisation technique [205–207]. The RAFT technique allows for the controllability of the polymerisation reaction via the use of a RAFT agent, commonly dithiobenzoates, trithiocarbonates and dithiocarbamates are used for this purpose, and dependent on the reaction conditions and monomers used each RAFT agent has its own limitations. However, the beauty of RAFT is that due to a wide variety of RAFT agents on offer there is a large amount of versatility for a variety of different monomers and solvents to be used [207].

For instance, RAFT agents in general consist of a reactive C=S bond, a Z group (controllability over the C=S bond reactivity and thus influences the rate of radical addition and chain transfer/fragmentation), a weaker cleavable C-S bond and

a free radical leaving group R which has the ability to be able to reinitiate polymerisations [208] **(Figure 1-16).**

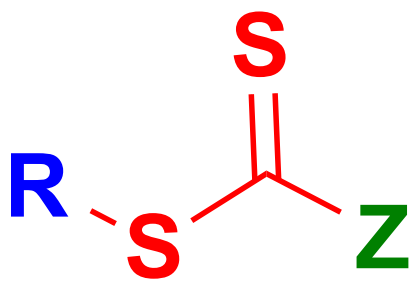

Figure 1- 16: General RAFT agent structure

Thus, it is due to both the Z and R groups present within RAFT agents that promotes the versatility of this approach. In fact, such is this versatility that it has been shown that the RAFT approach can be conducted within an aqueous environment, promoting the idea of green chemistry and limiting the need for potentially toxic solvents to be used throughout polymer synthetic processes [209,210].

RAFT polymerization therefore has become a leader in the controlled synthesis of polymers with complex architecture due to the advantages it possess such as versatility, the lack of potentially toxic transition metal catalysts, a much higher tolerance to oxygen (a Schlenk line isn't always required for a RAFT synthesis) and can be performed via a one-pot approach [207]. Mechanistically, the RAFT approach differs from other controlled polymerization methods as it relies on degenerative chain transfer for controllability **(Scheme 1-6).**

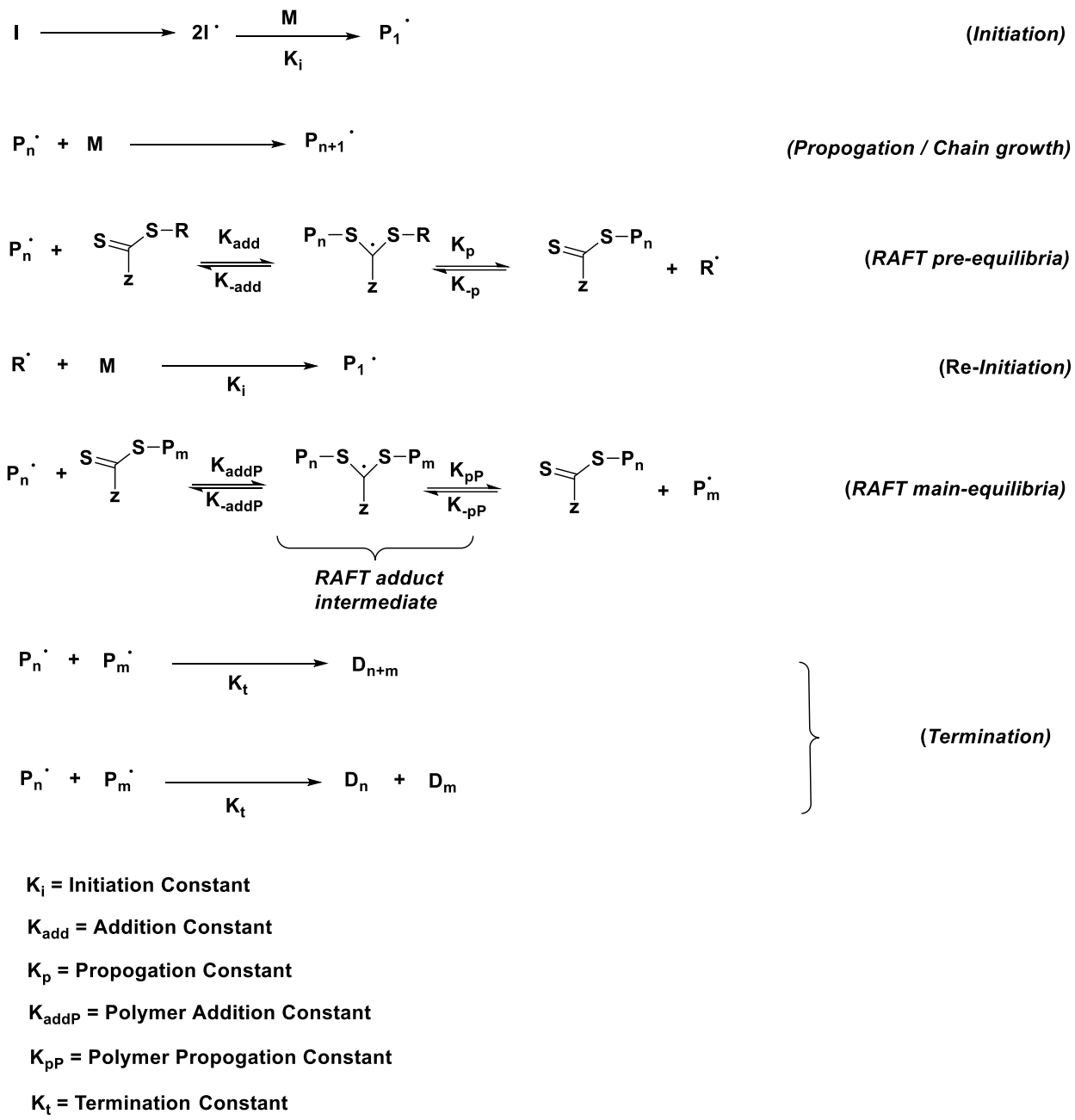

Scheme 1- 6: RAFT polymerization mechanism

This therefore incorporates RAFT agent end groups within the synthesized polymer molecule, which in turn can be exploited for bioconjugations for instance [205]. Additionally, due to the incorporation of such a group polymers synthesized via the RAFT technique generally adopt the coloration of the RAFT agent itself, which in turn can be exploited via UV-VIS for example to study a variety of effects on the polymer such as heat degradation, redox sensitivity and quantification of RAFT end

groups (and thus their associated functional group). RAFT end groups on the polymer back bone are described as being either α - end group or ω - end group.

Whilst either the α or ω - end groups of the polymer stemming from the RAFT process can be used for further modification via thermolysis [211], radical induced reduction [212], diels-alder reactions or a nucleophillic attack etc. [213,214].

Additionally, the thiocarbonylthio group can be readily reduced by a variety of agents such as amines to produce a free thiol at the ω terminus of polymers [215]. The thiol group can then be exploited for cross linking via micheal additions to vinylic groups such as acrylates in order to produce a dense network of polymers [216].

However, there may be occasion in which modification is required or preferred to eliminate sulfur altogether. For instance, the use of thermolysis completely de-sulfonates the polymeric terminus leaving an unsaturated chain end [211]. However, this methodology requires careful planning as the polymeric species itself needs to remain stable under the conditions required for thermolysis, alongside any functionality already incorporated into the material. Due to the nature of the technique there is no need for the addition of chemicals into the reaction and as such presents a relatively straight forward purification. Studies have shown that dithiobenzoates have the advantage of greater thermal stability when compared to trithiocarbonates or xanthates [217]. Furthermore, the reaction profile can be studied in situ via the use of thermogravimetric analysis allowing the researcher to monitor the degradation of the RAFT end group in real time. Despite these advantages, thermolysis sometimes results in the production of potentially toxic and generally malodourous compounds and as such there is a need for additional safety precautions to be taken when dealing with this methodology.

However, if thermolysis is not an option due to issues with thermal stability of the material itself one can introduce reductions via radicals in order to eliminate sulfur [213,214]. Such methodology generally requires the need for hypophosphite salts as the proton source however, the water-soluble nature of the byproducts (and the reagent itself for that matter) allow for removal from the polymer with great ease, assuming the polymer isn't water soluble itself. Whilst the thiocarbonylthio group can be exploited in hetero diels alder reactions due to the nature of the π bond , and as

such has been exploited for functionalization of polymers with a variety of dienes [214].

Furthermore, the use of nucleophiles to introduce functionality has been well studied and thiocarbonylthio reactions with excess amount amines was first reported in 1990 [218] and has been a method of choice for the cleaving of RAFT end groups from their parent molecule. This reaction is particularly interesting when designing a polymer. The use of monomeric compounds containing amines is nothing new as polymers containing DMAEMA and NIPAM for instance have garnered acclaim for either biocidal properties (in the case of DMAEMA) [219] or for the temperature “smart” properties of NIPAM containing polymers [220,221]. However, as has been discussed amines have the capability to reduce RAFT agents into thiols and as such careful design is needed to ensure that this unwanted side reaction does not occur.

Additionally, when the nucleophiles are used in order to produce thiol ended RAFT polymers the conditions of the reaction must eliminate oxygen. The thiol bond is known to readily oxidize in air to produce disulfide linkages [222] and therefore should oxygen be present this could result in higher molecular weight species being formed, resulting from thiol-thiol reaction from two different polymer chains, rather than recombination of the Z group. However, the exclusion of oxygen from the reaction may necessitate the use of Schlenk techniques or a positive pressure gradient of argon for example and therefore it may be possible to include reducing agents with the reaction mixture in order to combat unwanted disulfide formation.

In terms of α modifications, it is much easier to in fact modify the RAFT agent itself in order to incorporate functionality into the synthesized polymer via the R group. Incorporation of desired functionality (e.g. COOH or peptides) within the initiating radical therefore limits the need for post synthetic modification, producing a one-pot polymerization process with the ability for ligand incorporation. Indeed, this process of RAFT polymerization utilizing bioconjugate RAFT agents isn’t a new phenomenon with a plethora of studies utilizing this method for conjugations of folic acid via one pot polymerizations for example [173]. Bearing this in mind, it is much more common for polymers post synthesis to be functionalized via Z group modifications rather than alterations to the R group itself (**Scheme 1-7)**

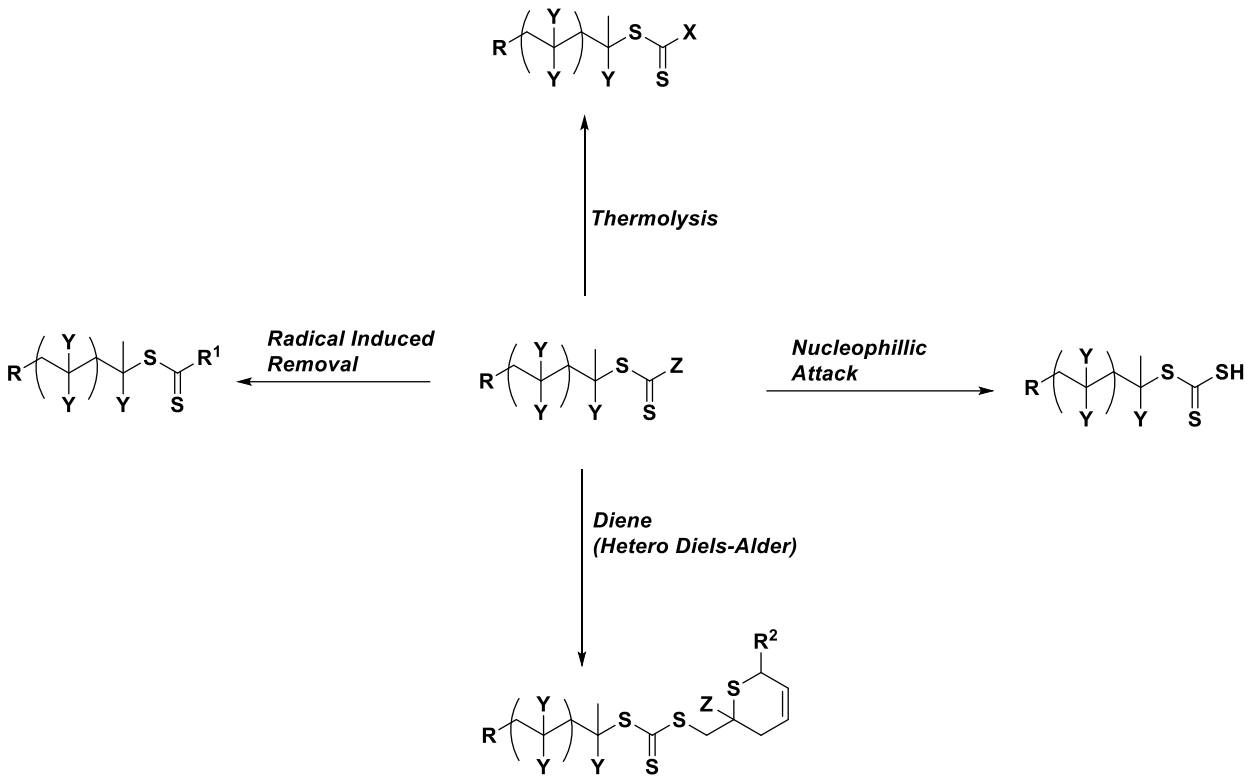

Scheme 1- 7: Examples of RAFT end group modification strategies

Whilst the controllability of RAFT is comparable to the ATRP and NMP there is a solid argument for the use of RAFT in being utilized for the synthesis of polymers of complex topology for clinical use. Primarily, for the synthesis of controlled macromolecular structures it is much more tempting to consider ATRP or RAFT based synthesis over NMP due to the complexity involved in nitroxide synthesis required for NMP synthetic techniques. However, the use of transition metal catalysts and alkyl halides required for ATRP could lead to concerns over the possible toxicity of such compounds and therefore the suitability within the clinical setting of the products obtained. Alongside these concerns RAFT imparts advantages over NMP and ATRP include a higher toleration of impurities whilst allowing for better compatibility with a broader range of monomers and reaction conditions [223].

These advantages over NMP and ATRP have led to RAFT synthesis becoming an attractive ready to scale polymerization processes due the only conversion of traditional conventional polymerization techniques being the

introduction of a RAFT chain transfer agent. Such is the growing interest commercially in the advantages RAFT polymerization provides commercial chemical supply companies such as Sigma-Aldrich and Strem chemicals have begun to produce RAFT agents for purchase albeit in small quantities or as a special made to order product.

With the advantages and disadvantages of the different strategies discussed, synthesized hyperbranched polymers have found a great use in drug delivery systems [105,111,175,224]. Previously, linear (mono-branched) cross-linked polymeric structures were researched for their potential in the drug delivery field, however, over the past 20 years there has been a shift towards well-characterized multi-functional hyperbranched or dendritic polymeric architectures for this purpose. These architectures have the potential to upgrade the therapeutic potential of current drugs or could even allow for currently unfeasible drugs to be clinically relevant due to control of bioactivity [225].

1.4.3 Stimuli Responsive "Smart" Architectures – Their Role in Cancer Therapy

Within this section the design, synthesis and characterization of "smart" materials will be discussed within the remit of cancer therapeutics. Their suitability to deliver drugs towards cancerous sites will be discussed with focus paid to the unique tumour environment and how careful design of polymeric structures can allow for exploitation. This brief overview does not have the intention to be an all encompassing review and acts a springboard so that the reader can gain an appreciation of the scientific space and can use this as a foundation for further research within the field through their own further literature searches.

1.4.3.1 Stimuli Responsive Topologies

pH responsive polymers have become an attractive choice for use in tumour selective targeting systems, in part due to the unique physiological environment attributed to the Warburg effect [226,227]. The tumour microenvironment presents itself as a unique area for exploitation by drug delivery systems, due to the hypoxic

nature of the tumour as it grows (oxygen starved) there is a reliance on anaerobic respiration in which the cell favours anabolic glycolysis and thus increases lactic acid production [227]. This, therefore, lowers the pH value of surrounding tissue (from around pH 5.8 – 6.5) with also an elevated temperature a result of mass cellular replication, all which Otto Warburg described [228]. Thus, the observed effect allows the cancerous environment to be ripe for exploitation.

Generally speaking, assembly of the polymer itself within the appropriate media will have an influence on the pH response exhibited, such as through micelle/reverse micelle formation or swelling/deswelling to give a few examples [124] (**Figure 1-17**).

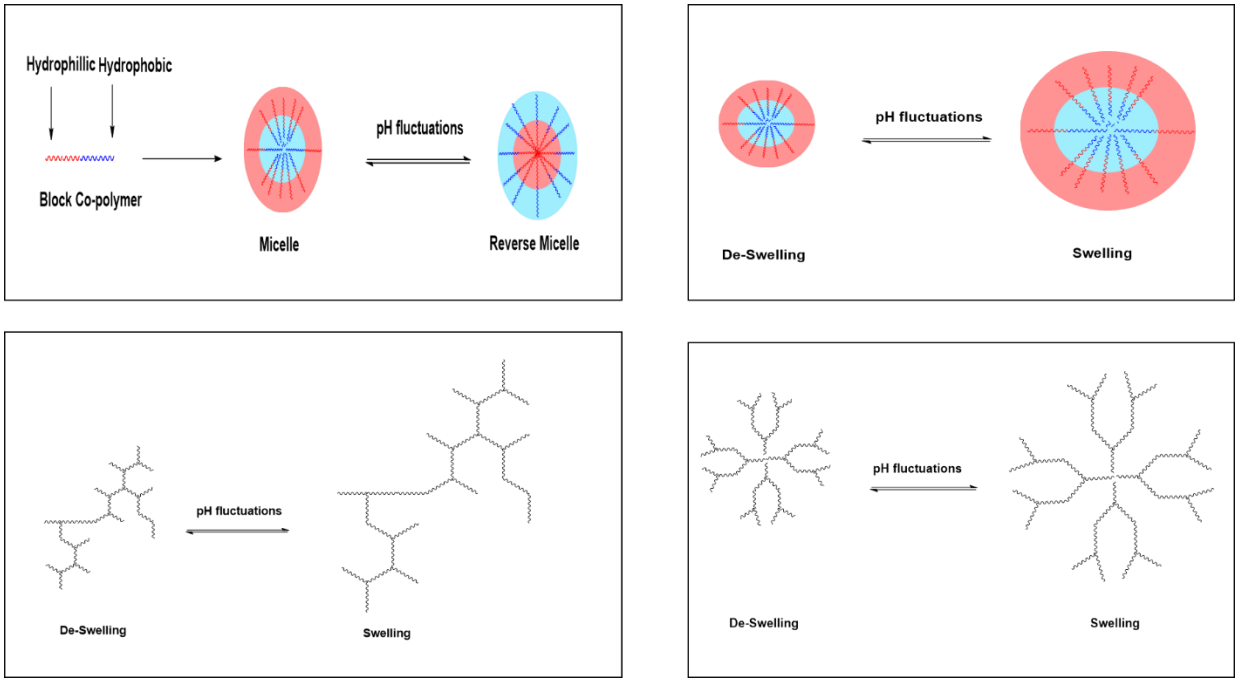

Figure 1- 17: pH responsive Micelle formation and swelling behavior of polymers

pH responsive polymers therefore can be defined as having a polyelectrolyte nature and therefore generally contain acidic or basic groups that can act as either proton donors or acceptors when fluctuations in the environmental pH present themselves. It is common to see groups such as carboxylic acids [124,224,229] and tertiary amines [122,230–232] employed in this role as ionization of the groups can

readily occur, influencing structural changes within the three-dimensional conformation of the macromolecule itself. Furthermore, this pH response can be fine-tuned through careful modification of the polymeric composition with basic monomers acting as proton acceptors in acidic conditions and acidic monomers the opposite, whilst a combination of different monomeric units can in theory allow for a dual pH response in both acidic and basic environments.

Conventionally, pH responsive polymers can be synthesized via either radical or step growth polymerization techniques, however due to a good control over particle size emulsion polymerization techniques have garnered momentum as a popular synthetic route for vinylic monomer polymerizations [126]. Whilst polymerizations in bulk or solvent are still widely used emulsion techniques generally consist of monomer units, water, water soluble imitators and catalysts (RAFT agents, nitroxides etc.) and a surfactant to act as the emulsifier. The main drawback of the technique itself, however, is the inclusion of a surfactant itself, which in some cases may need to be removed from the polymer and may require lengthy dialysis processes causing aggregation of the polymeric spheres themselves. One methodology developed to combat the need for surfactant removal is the use of persulfate initiator however, the solubility of monomers themselves need to be considered as modifications to the emulsion system may still be required in order to produce a stable emulsion system [233].

1.4.3.2 Stimuli Responsive building blocks – Acids and Bases

Commonly the use of carboxylic acids as pH responsive building blocks have revolved around the use of acrylic acids and alkylated variants such as meth/ethyl and propyl acrylic acids [131,229,234,235]. One monomer of interest is 2-propyl acrylic acid (PAA). PAA has been researched in depth by the Hoffman group as a potential building block for pH responsive drug delivery and imparts noticeable and desirable differences from other alkylacrylic acid counterparts [175,224,236,237]. Whilst poly(acrylic acid) (poly(AA)) has been known to display differing pH responsive properties depending on the molecular weight of the molecule itself [235]. Poly(PAA) on the other hand displays a longer propyl segment on the polymer

backbone and thus this raises the pK_a and allows pH induced phase transitions above pH 6 [175].

Whilst PAA at a first glance seems like a good building block for the synthesis of pH responsive macromolecules there have been reports about the unreactive nature of this monomer, with bulk polymerizations often needed in order to incorporate PAA in desired quantities into macromolecular structure [175]. This can lead to a tossup when designing structures with this monomer in mind and other desired monomeric units may need to be expelled from the design process due to incompatibility in synthetic methods.

Phosphorus containing molecules [238] and sulfonic groups [239] have also seen a great deal of attention, especially in hydrogel production. Hydrogels are a large network of cross-linked polymer that are hydrophilic in nature and have found uses in wound dressings [102,103,240] and drug delivery systems [241,242]. The ability of hydrogels to swell when they encounter water is highly desirable and can be exploited for the release of drugs, the filling of irregular wound shapes, donation of water or the absorption of aqueous waste. It is this pH response towards greater hydrophilic character than can be exploited for drug release properties. For example, Kim and co-workers published their work on their sulfonic acid-based hydrogel which was shown to respond to both electrical stimuli alongside fluctuations in pH [239]. The hydrogel they synthesized based on a co-polymer of Poly(2-acrylamido-2-methylpropane sulfonic acid)/hyaluronic acid and displayed reversible swelling and de-swelling character under electrical stimuli alongside pH dependent swelling behavior. This reversible swelling behavior lays the foundation for hydrogel-based drug delivery, with increased swelling of gels facilitating drug release.

Whilst the use of acidic groups has garnered a great deal of interest for drug delivery carriers on the opposite side of the spectrum it is common to see amines being utilized for their basic properties. Furthermore, tertiary amines can be exploited for their ability to form cations and thus are an ideal candidate for the ionic loading of anionic drug or gene molecules.

For instance, considering a simple polymeric structure in polystyrene Jiang and Thayumanavan demonstrated initial functionalization of the styrene monomers themselves to incorporate a primary amine group, protected by the BOC group, in

the synthesized nanoparticles [243]. In short, upon the construction of the nanostructure and deprotection of the amine groups themselves presented nanoparticles with free amines for coupling capabilities. Therefore, these free amines presented could be utilized alongside conventional coupling click chemistry to further functionalize these nanoparticles with drugs or genes. Whilst this is a simple demonstration of synthesizing amine functionalized polymers there are numerous different strategies in order to synthesize desired materials. Functionalization of a previously well used monomer may not be required as in the case of the tertiary amine monomer 2-dimethylaminoethylmethacrylate (DMAEMA), which has found as a variety of uses throughout the world due to its ability to impart basic properties to co-polymers [219,229,231,244] whilst also reactions with methyl chloride leads to the highly desired compound trimethylammoniumethyl acrylate chloride (TMAEACl) which is used in flocculants due to the pronounced cationic characteristics this compound displays [245] (**Scheme 1-8)**.

Scheme 1- 8: DMAEMA reaction with methyl chloride to synthesize the desired TMAEACl compound for flocculant use

Research groups therefore have exploited DMAEMA for its basic properties in the synthesis of different co-polymeric structures alongside traditional homopolymer based macromolecules. A prime example of the introduction of pH responsive properties within a co-polymeric structure was the work performed by Sun and colleagues at the Research Center for Engineering Technology of Polymeric Composites of Shangxi. In their work the monomer DMAEMA was utilized in order to introduce basic behavior in silver nanoparticles [239]. Firstly, they synthesized their block copolymer of phthalimide and DMAEMA, poly(DMAEMA-*b*-PPA), afterwards silver nitrate was reduced within the presence of this polymer in order to incorporate the macromolecule within the silver structure. Both the formation of the nanoparticles and pH responsiveness was characterized by Transmission Electron Microscopy (TEM), with zeta potential and UV-Vis measurements used to identify pH response exclusively. It was found that aggregation occurs as a result of pH with pH 8.9 and

12.5 shown to induce aggregation of the nanoparticles whilst acidification of the media to pH 2.5 inducing de-aggregation. Whilst the authors do not suggest this type of mechanism is to be applied as a drug delivery vehicle but instead as an optical biosensor it is a prime example of introduction of a monomer to induce pH responsive characteristics. In terms of the drug delivery sector amine based co-polymers Roointan and co-workers focused on the formation of pH responsive nanogel technology with the synthesis of their hydroxyethyl methacrylate (HEMA) and DMAEMA co polymer poly(HEMA-*co*-DMAEMA) again via the RAFT technique [246]. The pH responsive character of their product was then investigated using dynamic light scattering technology at the pH values of 5.5 and 7.4. In order to test the drug delivery capabilities of their compound interaction with the chemotherapeutic doxorubicin was tested and it was found drug release was increased fourfold (from 20% to 80%) in pH 5.5 when compared to pH 7.4 demonstrating the pH responsive nature of their structure within acidic environments. Other research groups have worked towards gene delivery therapies utilizing amine functionalities [244,247], whilst other groups have aimed to utilize amide based monomers such as N-isopropylacrylamide (NIPAM) in order to introduce temperature based responses into their macromolecules [111,122].

1.4.3.3 Stimuli Responsive building blocks – temperature responsive

Temperature responsive materials such as those homopolymers or co-polymers incorporating NIPAM have garnered great scientific interest. In brief, the ability of a polymer to respond to fluctuations in temperature stems from the Lower Critical Solution Temperature (LCST) or the Upper Critical Solution Temperature (UCST) of the material itself [248,249]. Both the LCST and the UCST are terms to describe whether the components of the mixture are miscible in all compositions, for example a polymer may exist in a homogenous mixture below the specific LCST of the molecule however when the temperature of the solution eclipses this value the polymer would then begin to precipitate out, exhibiting what is called as sol-gel character, which colloquially may be termed as the solution “cloud point” (**Figure 1-18**).

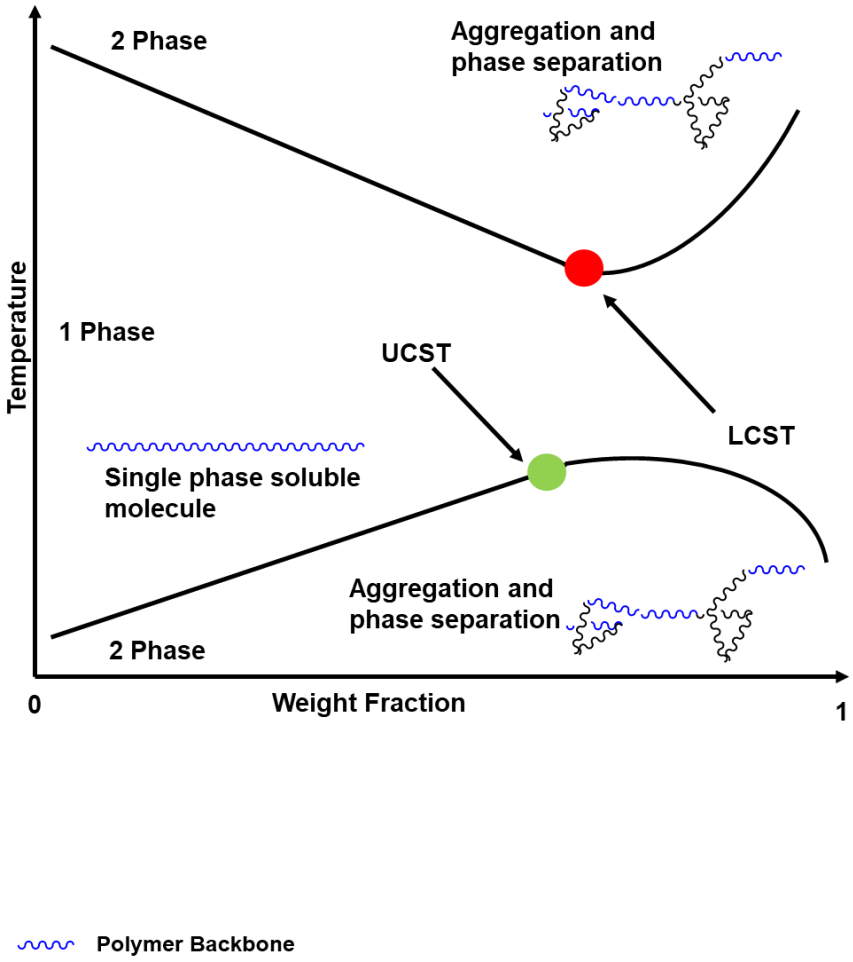

Figure 1- 18: How the LCST and UCST of a macromolecule effects solubility

This temperature responsive character of macromolecules therefore is a great weapon in the arsenal of the researcher. In knowing the specific temperature fluctuations of wounded tissue for example in comparison to the rest of the body wound healing devices such as hydrogels can be tailored to interact with the site exclusively as a result of specific temperature fluctuations, much in the same way as macromolecules can be designed to interact with sites with a distinct pH change. Temperature responsive polymers therefore generally incorporate NIPAM as the thermo responsive sub-unit within them due to the monomer itself being widely studied for this purpose [220,249]. NIPAM is known to exhibit a LCST of around 32°C within aqueous media [220], which of course can be manipulated with the correct co-polymerization technique, making it a good foundation for the use of

temperature response within polymers designed to interact with the human body (of which physiological temperature resides around 37°C). However, NIPAM is not the only monomer that can be exploited for thermo responsive properties with other such compounds like N,N-diethylacrylamide (DEAA) used due to favourable sol-gel transitions between 25°C and 35°C [250].

Other temperature responsive building blocks however have been exploited due to their favourable characteristics such as elastin side polymers, *N*-dimethylacrylamide and oligo(ethyleneglycol)-methacrylates. In terms of cancer and drug delivery therapies aside from the hydrogel technology Al-Ahmady and Kostarelos published an in-depth review into the building blocks required for such smart materials [251]. Uses however, range from temperature responsive micelles, temperature responsive magnetic nanoparticles and hydrogels alongside a plethora of other technologies.

In summation, the use of pH or thermo responsive polymers in so called “smart material” technology have greatly advanced the progress in drug delivery, lubricants, hydrogels amongst other technologies. Namely, the controlled drug delivery sector has achieved a variety of different products ranging from homopolymers or co-polymers consisting of acrylic acids, vinyl alcohols, acrylamides, ethylene glycols and methyl methacrylates to name but a few [102,124]. Overall, it is for the researcher to weigh up the different factors and characteristics required for the synthesis of these materials, taking into account structure and composition, distribution of the repeating units, functionality and end group inclusion, molecular weight and distribution of said molecular weight over the polymeric chains, topology, responsive nature and physiochemical and physical properties of the material (including but not inclusive to only: ionic strength, mechanical stresses, zeta potential etc.). pH responsive nature can be induced within polymeric chains through the addition of either acidic or basic groups, with widely used monomers for these responses encompassing acrylic acids, phosphates, sulfonic acids, amines and amides, whilst conventional monomers such as styrene or methyl methacrylate can be functionalised [232].

With the ever advancing progress in cancer diagnosis and cancer therapies, with the onset of cell penetrating peptides and immunotherapies as alternatives to conventional chemotherapy and in some cases radiotherapy, it is the opinion of this

author that the role polymers have to play in this ever growing global issue is enormous. With polymer technology allowing for the controlled synthesis of materials of complex topology and defined molecular weight, with an ever decreasing PDI in these materials due to the advancement of NMP, ATRP and RAFT technologies puts the versatility of polymers at the forefront of the fight for more efficient treatments for cancer. This thesis aims to draw on the research discussed within this introduction to develop a novel hyperbranched drug delivery system for the targeted delivery of drugs towards malignant cancer cells, encompassing the use of currently approved therapeutics and targeting systems in order to enhance the properties of the synthesized structure.

1.5 Bio-conjugation techniques

Whilst, the synthesis of a material capable of acting as a drug carrier is a major achievement in the progress of any project focusing on this aim there are times where further post-synthetic modifications may be required in order to provide either the passively or actively targeted approaches discussed in section 1.3.2 and1.3.3 respectively. Therefore, this section will discuss some of the commonly used bioconjugation techniques utilized commonly throughout research and the industry in order to give an insight into how synthetic methodology can be employed in order to optimize the pharmacological profiles of chemotherapeutics for their use in cancer therapies

1.5.1 PEGylation

PEGylation is one of the most common forms of drug, molecule and macromolecular structure alteration used today and involves the attachment (covalently or non-covalently) or the amalgamation of Poly(ethylene glycol) to the structure in question [252,253]. Thus, upon this modification the structure is then termed PEGylated. For instance, paracetamol upon conjugation to PEG would then be termed PEGylated paracetamol. In terms of the PEGylation process, linkage is formed via first derivitisation of PEG (if required) to a reactive and active form and subsequent reaction with the target molecule itself [254]. In terms of the advantages this can bring PEGylation can act as a “mask” giving stealth characteristics to the target mol-

ecule preventing unwanted immune response, inappropriate metabolism and an increased circulation time, due to an increase in the hydrodynamic volume of the molecule itself [254]. Additionally, whilst PEGylation affords these advantages there is also the advantage of PEGylated products increasing in their hydrophilic nature, allowing previously insoluble products to be dissolved in water (e.g. for IV injection of therapeutics) [254–257].

The advantages PEGylation affords molecules has led to this method becoming commonplace within the therapeutic industry. In terms of the conjugation process there are two generations of PEGylation that are in common use today: the non-specific random conjugation (1st generation PEGylation) and the site specific conjugation performed in 2nd generation PEGylations, both of which will be discussed in more detail herein, to give a good overview of PEGylation methodologies generally used today.

1.5.1.1 1st Generation PEGylation

1st generation PEGylation is defined as the random conjugation of PEG to a target molecule through non-site-specific means. PEG itself is formed by the polymerization of ethylene glycol molecules to form either a linear or branched structure, with subsequent modifications afforded to allow for conjugation onto the target molecule if required.

In terms of the 1st generation of PEGylation techniques PEGylation was commonly performed on polypeptide drugs and enzymes, with PEG forms restricted to their linear form. In the 1990s Adagen® became the first PEGylated drug to be FDA approved for use as therapeutics [258] and is an excellent example of a 1st generation PEGylated product. The drug itself consists of randomly PEGylated enzymes at multiple sites [258] (in excess of 60 distinct sites) and PEGylation itself was marketed by Enzon Pharamaceuticals Ltd.as an effective half-life extension technology. However, despite the successful marketing and approval of therapeutics such as these the 1st generation of PEGylation encountered numerous difficulties, attributed to the random nature of conjugation itself. For example, conjugation onto the ε terminus of lysine resulted in the modification of numerous lysine molecules, thus producing a non-uniform mixture of product with a large molecular weight

distribution of PEG isomers [259]. Indeed, it is the presence of these isomers that leads to poor clinical results due to the lack of reproducibility between different batches of drug itself.

1.5.1.2 2nd Generation PEGylation

Therefore, in order to combat the shortcomings with 1st generation PEGylation, namely isomer mixtures and diol contamination, site specific PEGylation was developed. The overarching objective of 2nd generation PEGylation is to improve the pharmacological properties of the drug and further optimize and improve on the properties observed when low molecular weight PEG has been employed [260,261].

In terms of the advantages site specific conjugation can bring, firstly there is a much greater control over the reaction reducing the presence of isomeric PEG molecules within the final batch, reducing the loss in biological activity and reducing the immunogenicity of the drug in question itself. Take for instance the example given of PEGylation to lysine molecules within a protein or peptide. The researcher can instead of targeting the amine situated on lysine focus on the targeting cysteine, more specifically the thiol groups present on this molecule, reducing over PEGylation and thus isomeric forms of the polypeptide [262]. Moreover, through genetic engineering technology, cysteine can be added to the polypeptide precisely where required further increasing the control over the PEGylation process [263].

In terms of 2nd generation PEGylated products on the market today there are a plethora of different health conditions, in which the patient involved has benefited from PEGylated therapeutics. Doxil for instance is a PEGylated doxorubicin and has found uses in the treatment of ovarian and breast cancers [140]. When compared to the alternative medication of topotecan, doxil requires a single IV infusion once a month whereas topotecan is generally administered daily over a half an hour session over a 5-day period once every three weeks.

1.5.2 Steglich Esterification

The Steglich esterification is a well-known technique discovered by Neises and Steglich in 1978 as a simple method for the esterification of carboxylic acids

[264]. Utilizing a carbodiimide in either the form of N'-ethylcarbodiimide (EDC) or N,N'-dicyclohexylcarbodiimide (DCC) the carboxylic acid in question is able to form a *O*-acylisourea intermediate which in turn a nucleophile is able to attack and esterification can be performed, due to presenting similar reactivity to the corresponding acid anhydride, with the mechanism described below via a DCC/ 4-Dimethylaminopyridine (DMAP) coupling reaction (**Figure 1-19**).

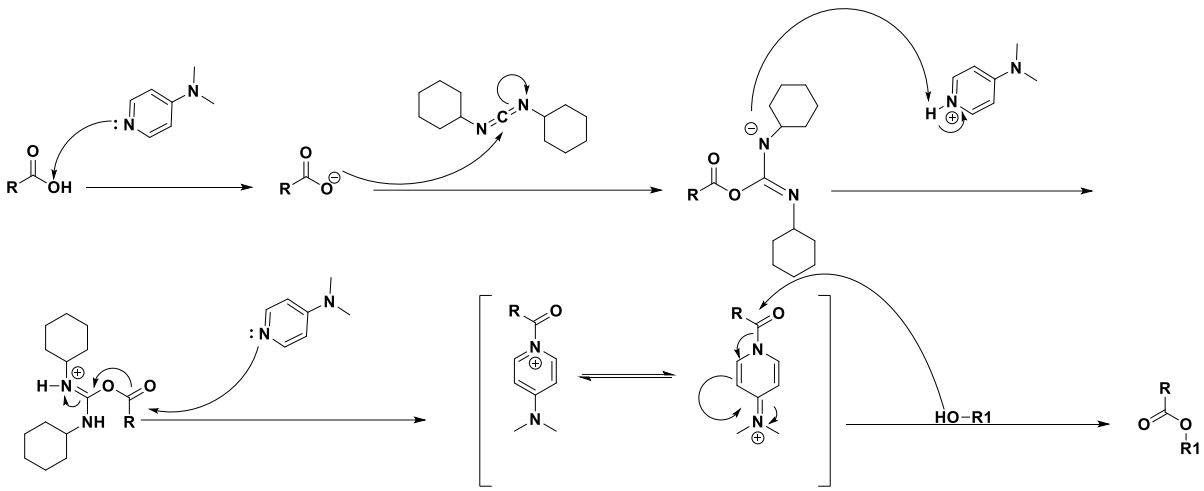

Figure 1- 19: Mechanism of a DCC/DMAP Steglich esterification reaction

Indeed, the simplicity of the reaction itself has led to this method becoming commonplace, with N-hydroxysuccinimide (NHS) occasionally introduced into the reaction to stabilize the intermediate by nucleophilic substitution upon the intermediate itself, before substitution to form the target molecule via a NHS/DCC route as oppose to the aforementioned DCC/DMAP [265–267].

In fact, lysine reactions with a NHS ester is a common reaction for bioconjugations, with the amine terminus of lysine participating in the reaction to form an amide linkage [268]. However, this type of conjugation is not limited to lysine alone, with amino acids, polymers, drugs and other molecules able to be conjugated together through the esterification process or through the formation of an amide bond with the aid of a NHS ester formed in the first instance.

1.5.3 Reactions of protein residues

Whilst PEGylation and esterification have been discussed other bioconjugation techniques focus on the modification, also termed programming, of

antibodies and proteins. Most commonly, the residues of this proteins presented on the surface are ripe for exploitation. With residues such as lysine, cysteine and tyrosine utilized in order to produce the desired target molecule, as well as the abundance of C and N terminus found on amino acids for example. The conjugation reactions involving these residues will be discussed briefly here with attention to the suitability of each residue to a desired outcome.

1.5.3.1 Reactions involving lysine

The lysine residue being nucleophilic in nature has been exploited via a variety of different methods for bioconjugation reactions, including the PEGylation [259] and Steglich esterification reactions [268].

Lysine conjugations are widely regarded as non-specific forms of conjugation due to the side chain ε-amino acid being nucleophilic [269]. Therefore, it has been utilized as a conjugation methodology for the linking of payloads to the protein surface, whilst the reactive nature of the residue means that modifications to the amine group through conjugation or function group interconversions can be performed.

Furthermore, research has also focused on site-specific lysine arylation as an alternative controlled bioconjugation strategy towards programmable antibodies and antibody-drug conjugates (ADCs). Hwang et al. recently published their research into this work, concluding that a proof of concept for the site-specific conjugation towards lysine is possible using methylsulfone oxadiazole derivatives [270]. They concluded that conjugation towards the lysine (Lys99) residue on the antibody h38C2 can be performed via this methodology and is compatible with the therapeutic utilities of this antibody, demonstrating that site specific conjugation towards lysine residues is possible, at least in this case.

1.5.3.2 Reactions involving cysteine

Cysteine, as oppose to lysine, is considered a much more site-specific approach to conjugation, due to the lack of abundance of this residue on the protein surface when compared to lysine [271]. Furthermore, the presence of a thiol group

within this residue allows for a variety of different chemical reactions to occur, allowing greater freedom in the choice of conjugation methodology to be employed, with either the production of disulfide bonds through thiol-thiol oxidation or deprotonation to form thiolate nucleophiles which in turn can react with electrophiles, forming a C-S bond through the conjugation process [272]. Due to the different reactions possible involving cysteine there is the possibility to produce either cleavable biodegradable bonds (S-S) or stable bioconjugates, rendering this method attractive to controlled release mechanisms through redox stimulation or for general purpose chemoselective ADC formation [272].

1.5.3.3 Reactions involving tyrosine

Tyrosine residues, unlike their lysine and cysteine counterparts are generally considered a last resort in protein bioconjugations due to their relatively unreactive nature. However, using aromatic electrophilic substitution reactions there has been some progress in tyrosine conjugations [273]. Furthermore, owing the nature of the reaction needed to perform tyrosine conjugations there is selectivity towards tyrosine, proving useful in the cases in which cysteine conjugation cannot be performed, with diazonium salts, 4-Phenyl-1,2,4-triazole-3,5-dione and the mannich reaction being employed for tyrosine conjugations, with selectivity afforded towards the carbon adjacent to the phenolic hydroxy group [273].

Despite the relative selectivity of both the cysteine and tyrosine approaches to protein conjugation there is requirement for the researcher to “do their homework” on the protein in question, through characterization such as mass spectrometry and crystallographic studies, alongside correct identification of the protein source. Hence, identifying the reactive landscape of the protein may require probing of the protein landscape itself, utilizing the mentioned reactions to conjugate fluorescent markers to protein residues for example. However, this trial and error towards correct identification can be time consuming and expensive, as over labelling of the protein can occur whilst selectivity to a specific residue can also be cumbersome. Therefore, genetic modification of proteins to overexpress desired residues can be performed in order to eliminate this process and this is a common practice in the introduction of cysteine residues for instance [262].

1.5.3.4 Choosing the most effective protein conjugation method

Paramount to the conjugation of proteins to target molecules is choosing the correct methodology to efficiently and effectively conjugate the desired molecules together to produce the target ADC for example. Therefore, should site specificity is not required then by far the easiest method for conjugation would be to exploit the lysine residues on the protein itself. However, once site specificity becomes a requirement the experimental design process becomes much more complicated and cumbersome. Stephanopoulos and Francis have described in their paper a easy to follow guide for the correct choice of protein conjugation method and this is described briefly herein [274]. Firstly, should the protein be situated within a complex mixture and isolation not possible labelling of the sites of interest with a reactive probe can be performed, however this is only useful in the case of enzyme families being targeted, if this isn't the case then cysteine may need to be introduced, peptides may need to be tagged onto the molecule or a new protein domain may need to be introduced. Should the protein be isolated then the process becomes much more streamlined, if specificity isn't required then lysine modification with a NHS ester can be performed, and any additional conjugations can then be evaluated using the following:

1. If the protein is isolated from a natural source, then cysteine or tyrosine can be targeted.
2. If the protein has been expressed then cysteine will need to be introduced if possible, if this isn't possible then N terminus reactions will need to be performed.

Should either of these routes yield no results then again new protein domains, peptide tagging, or further cysteine introduction will need to perform in order to facilitate conjugation.

Bearing all these factors in mind, it is apparent that protein conjugation requires much more in depth chemistry and knowledge of the overall structure as oppose to click chemistry methods such as esterifications and micheal addition type reactions and thus it is important that the researcher has a clear understanding of the route to conjugation as a key component of experimental plan when considering protein bioconjugations.

1.5.4 Bioorthagonal chemistry and Conjugation methods

Bioorthagonal chemistry was first presented by Bertozzi in 2003 and refers to the chemical reaction of molecules that can occur in a living system without interference to the natural biochemistry of the system itself [275]. This concept therefore has attracted great interest in the world of conjugation chemistry with a variety of different reactions able to demonstrate this property, varying from modification of aldehydes alongside named reactions such as the Cu catalyzed Huisgen reaction and the Staudinger reaction.

1.5.4.1 Carbonyl reactive techniques

Targeting of ketones and aldehydes is a common practice in conjugation chemistry, with a protein firstly attached to a carbonyl group through an oxidation reaction at the N terminus of the peptide residue. Then two distinct reactions can be performed in order to produce the appropriate compound needed for the conjugation towards either a ketone or an aldehyde, using either an alkoxyamine or hydrazine one can produce either an oxime or a hydrozone derivatized molecule respectively [276] (**Figure 1-20**).

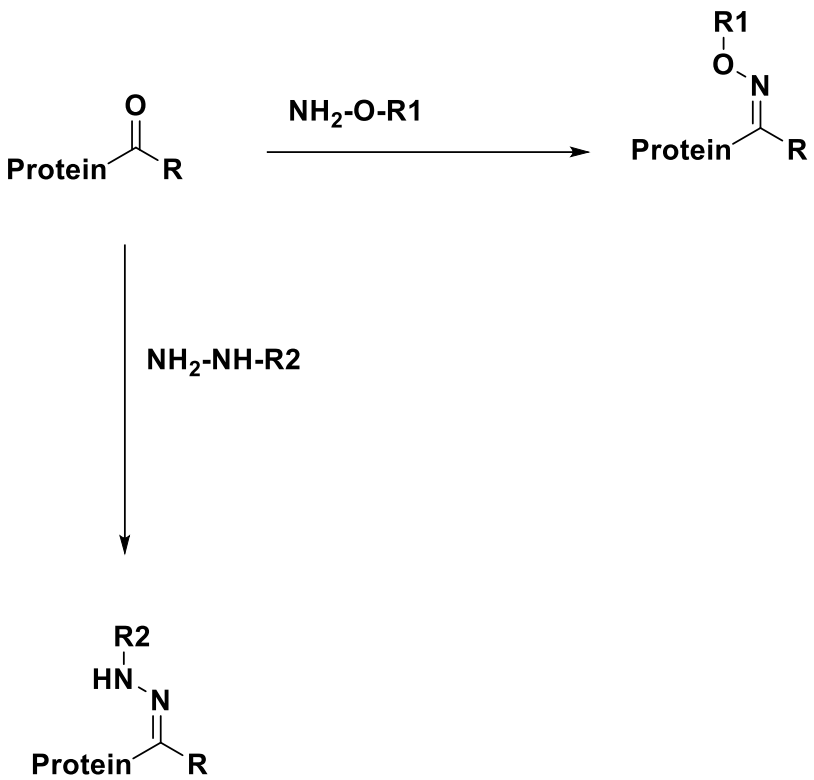

Figure 1- 20: Coupling via Carbonyl Chemistry

Additionally, it is possible to employ a catalyst within the alkoxyamine reaction in order to generate a Schiff base, allowing oxime ligation to be conducted at a much higher rate. Such catalysts employed for this role include the aromatic amine containing aniline, which can generate the required electrophile without competition with the product, whilst saline has also demonstrated acceleration of the oxime reaction [277].

1.5.4.2 Azide based conjugation methods, The Huisigen and Staudinger reactions

The Huisigen cycloaddition is a well known 1,3-dipolar addition reaction that has found uses in organic chemistry through the synthesis of ylides and the ozonolysis reaction to form carbonyl products [278]. Whilst there are numerous dipolar addition reactions the Huisigen reaction generally is used to describe the reaction between an organic azide and an alkyne to form the desired 1,2,3-triazole product. Biologically, the reaction has garnered interest through the Cu catalyzed variant. For example Bertozzi et al demonstrated the use of a copper catalyst in

order to successfully conjugate a probe to the surface of the cell via azide reactions [279].

Thus, azide conjugation has become a popular choice for protein modification however, the reaction still has limitations due to the high temperatures required and the production of regioisomers within the final product.

However, despite the use of protecting ligands there is still a general concern over the toxicity of Cu towards cells. As such the strain promoted Huigisen reaction was developed and demonstrated successfully by Bertozzi et al. Utilizing a strained cyclooctyne and an azide it was reported that the [3+2] cycloaddition can occur producing two regioisomeric products of the triazole product [279]. Furthermore, this reaction has been reported to occur at room temperature and as such can be used to modify living cells without risk of harm.

Furthermore, azides can be utilized in the Staudinger reaction, in which azides and phosphine are ligated to form a stable conjugate [280]. Due to the stable amide bond formed through the ligation the Staudinger ligation has found numerous uses in the modification of cell membranes and bioconjugation studies [281].

Whilst numerous different conjugation techniques have been discussed in brief here it is important to remember that this is not a one size fits all approach and thus, the protein, cell line, macromolecule and ligand need to be taken into account when planning experimental procedures. For instance, PEGylation is a completely viable method for improving the pharmacological properties of a chosen drug or protein, however modifications may be required to provide a site specific reaction reducing different molecular weight isomers, however it would be a viable choice for the conjugation of fluorescent markers to the cell surface, indeed in this scenario a azide based conjugation technique would be more adequately suited. Furthermore, the structure of the protein or drug itself may limit the researcher to a certain conjugation technique and thus due diligence and consideration needs to be paid in the planning process to ensure efficacy and value for money.

1.6 Gemcitabine – A nucleoside analog

Whilst numerous different chemotherapeutic techniques have been discussed throughout this chapter, special consideration is to be paid to the drug gemcitabine. This drug was chosen early throughout the project's life cycle as the model drug for assays pertaining to the drug delivery ability of any materials produced, whilst methods for detection of gemcitabine within DNA were already developed at Bangor University with the Edgar Hartsuiker group. Herein, the pharmacological properties of the drug will be discussed in detail with special consideration towards methods of treatment, mechanism of action and current scientific research into the role of gemcitabine in fighting cancer.

1.6.1 Gemcitabine history and route to approved treatment

As previously discussed in section 1.1.4.2 Gemciabine as a drug falls under the category of an anti-metabolite class of drug. Gemcitabine's action as a chemotherapeutic drug was founded serendipitously at the Eli Lilly and company, as initial tests were performed to deduce the anti-viral capabilities of the compound [282]. However, testing found that the drug had the ability to impart toxicity towards leukemia cells during pre-clinical testing shifting the focus of studies from the study of the anti-viral capabilities of the drug towards anti-cancer medication. Gemcitabine has since been approved for the treatment of pancreatic, lung and breast cancers, with numerous different brand names for the drug in use today.

1.6.2 Gemcitabine mechanism of action and pharmacology

Gemcitabine clinically is administered via intravenous drip (IV), as this has been shown to be the only form of treatment available to deliver a significant clinical impact on the patient. Previously, in section 1.1.4.2. it was discussed that gemcitabine falls under the category of anti-metabolite, alongside capecitabine for example [50,282]. Therefore, Gemcitabine is implicated in both the RNA and DNA synthesis cycles of the cell, directly interacting at these stages in order to cause cell death. As a hydrophilic drug gemcitabine itself relies on the use of cellular transporters in order to achieve internalization within the cell as this cannot occur through osmosis or diffusion for example. Indeed, these transporters termed human nucleoside transporters (hNTs) can be divided into two sub-classes equilibrative

transporters (hENTs) and concentrative transporters (hCNTs), with gemcitabine utilizing hENT1 (SLC29A1), hENT2 (SLC29A2), hCNT1 (SLC28A1) and hCNT3 (SLC28A3) [99]. Thus, the transporters themselves play a key role in the treatment of cancers via gemcitabine. In terms of activity gemcitabine requires metabolization via phosphorylation to provide therapeutic effects to the site in question with either the mono-,di- or triphosphate forms of gemcitabine capable of clinically significant actions resulting in cell death [93,99,283].

1.6.2.1 Gemcitabine Monophosphate (dFdCMP)

The first clinically significant form of gemcitabine is the mono-phosphate metabolite of the nucleoside analog and is facilitated by deoxycytidine kinase (DCK) enzyme [99], which is the rate determining step for the further metabolism of gemcitabine into active forms. Theoretically therefore, gemcitabine monophosphate has the potential to be administered via a drug delivery vehicle in order to circumvent the nucleoside transporters whilst also negating the rate limiting primary phosphorylation step. Furthermore, via delivery in this route there is further potential for an increase in efficacy of the drug, in cases where mutations in the DCK enzyme has led to gemcitabine resistance.

1.6.2.2 Gemcitabine Diphosphate (dFdCDP)

Following on from the initial phosphorylation gemcitabine monophosphate is then further metabolized into the diphosphate form via the UMP/CMP kinase (CMPK1) enzyme and it is within this form there are significant clinical effects on the cell observed [53,93,284]. Firstly, pharmacodynamically, dFdCDP depletes the cells natural pool of deoxyribonucleotide (dNTP) through the inhibition of the enzyme ribonucleotide reductase (RNR), which is responsible for the catalysis of deoxyribonucleotide formation from ribonucleotides within the nucleoside salvage pathway. The effect of this is that the cell no longer has the required precursors (or at least a much-depleted amount) for the synthesis of DNA. Furthermore, the depletion of these dNTP pools allow for an increase in favorability of gemcitabine uptake creating a feedback loop in which gemcitabine uptake is enhanced through dNTP depletion, however through this depletion DCK activity is increased producing

a higher concentration of gemcitabine monophosphate in what is termed the “self-potentiation behavior” of gemcitabine owing to its potency [285]. In this manner, gemcitabine is considered a first line chemotherapeutic treatment for appropriate cancers, either in tandem with other therapeutics or as a stand-alone medication.

1.6.2.3 Gemcitabine Triphosphate (dFdCTP)

Further phosphorylation of gemcitabine diphosphate into the triphosphate form is performed via the enzyme nucleoside-diphosphate kinase (NDPK, NME) and this form of gemcitabine is implicated in the integration of elongating DNA strands [93]. This in turn prevents the base-excision repair mechanism and allows for the integration of native dNTP to be added alongside thus, activating “masked chain termination” [53]. Effectively, masked chain termination works the way it does by having gemcitabine in the penultimate position. By the addition of the native dNTP alongside gemcitabine, the analog can no longer be detected at a efficient rate within the DNA strand and thus removed by exo nucleases or DNA repair enzymes. The cell then has inhibited DNA synthesis and begins the process of programmed cell death “apoptosis” [53,93].

1.6.3 Pharmacogenomics to be considered when treating with gemcitabine

Whilst the pharmacokinetic and pharmacodynamic properties of each metabolite of gemcitabine have been discussed in 1.6.2 it is not just a case of treating appropriate cancers with gemcitabine in order to achieve the desired effect. Genetic factors also play a huge role in whether the cell will itself respond to treatment to the drug or if a cocktail of treatments is required in order to achieve therapeutic gain. These factors will be discussed briefly focusing on the mechanisms of action of gemcitabine and how genomics play a huge role in drug resistance. Indeed, utilizing this knowledge dosage can be tailored patient to patient to ensure that the maximum therapeutic gain can be achieved whilst preserving the greatest quality of life to the patient themself.

1.6.3.1 The nucleoside transporters and variations thereof

With gemcitabine utilizing hENT1 (SLC29A1), hENT2 (SLC29A2), hCNT1 (SLC28A1) and hCNT3 (SLC28A3) nucleoside transporters for the delivery of drug into the cell there has been a wide array of studies documenting whether variations in these solute carrier (SLC) transporters can provide either resistance or sensitivity to gemcitabine itself. SLC29A1 for example has a high affinity for purines and pyrimidines and thus cells deficient in this transporter have been known to be highly resistant to gemcitabine, implicating this transporter as a key component for drug entry [286]. Indeed, on the other side, cells that have demonstrated an increased expression of this transporter have correlated with an increase in the survival rates of patients treated with gemcitabine [287]. The SLC29A2 transporter shares the same affinity for purines and pyrimidines [286] however there are scant studies investigating the relationship between this transporter and the effectiveness of gemcitabine treatment, and therefore further work on this transporter is required before any real judgements can be made on its effect on patient response levels.

The SLC28 family of transporters also have a high affinity for the transport of purines and pyrimidines intercellular [286]. SLC28A1 much like SLC29A1, has been observed in depleted levels providing resistance to gemcitabine treatment, although re-sensitization is possible through constitutive expression. Generally, located within the kidneys, intestine and the liver (SLC28A1 and SLC28A2) these transporters have been indicated in the absorption of nucleotides and their analogs whereas SLC28A3 has been reported to be distributed in a wide variety of different tissues [288]. Bearing this in mind the expression of the A1 and A2 variants of SLC28 varies from tissue type, between malignant and healthy cells and of course between individuals themselves.

1.6.3.2 Enzymes required for metabolization and variations thereof

Throughout the metabolic life cycle of gemcitabine upon entering the cell there are numerous enzymatic pathways required in order to facilitate the therapeutic abilities of the drug, which have been surmised in **Table 1-4**.

Table 1- 4: Enzymes required for gemcitabine metabolism

Enzyme	Role in gemcitabine metabolism	Reference
Cytidine deaminase (CDA)	Deamination of gemcitabine into 2'2' diflourodeoxyuridine (dFdU)	[93,99,288–290]
Deoxycytidine Kinase (DCK)	Catalysis of Phosphorylation into dFdCMP	[99,288,290–292]
Deoxycytidine deaminase (DCTD)	Inactivation of gemcitabine monophosphate into diflourodeoxyuridine monophosphate (dFdUMP)	[99,288,290, 292]
Cytidine mono-phosphate kinase 1 (CMPK1)	Catalysis Phosphorylation of dFdCMP into dFdCDP	[288]
5' Nucleotidases	Catalysis of the de-phosphorylation of dFdCMP back to gemcitabine	[288,290]

A concern with the use of cancer therapeutics is the need to balance the toxicity of the drug towards the cancer cells with the toxicity associated with general circulation towards non-target healthy cells. The enzymes reported in the above table are clinically significant when considering the treatment of cancer with gemcitabine.

The cytidine deaminase enzyme has a primary role in gemcitabine metabolism in deamination of the drug and hence reducing the efficacy via transformation into a less active form [93,99,288–290]. Therefore, decreased expression of this enzyme has been associated with an increase in the efficacy of the drug however a higher toxicity towards healthy cells is also observed [283].

Deoxycitidine Kinase enzymatically acts as a catalyst for the phosphorylation of gemcitabine to its monophosphate form [99,282,288,291]. It is understood that cell lines that have a long exposure to gemcitabine expression of this enzyme is decreased and thus resistance to the drug is built up over time [288]. One possible cause of this is the killing of cells expressing this protein with the *null* cells surviving and through division allowing inheritance of this *null* characteristic.

Deoxycytidine deaminase in a similar way to CDA acts as a deaminating agent for the monophosphate form of gemcitabine inactivating it from further metabolization through the desired pathways. However, there has been no strong evidence linking this enzyme and its expression to reception to gemcitabine treatment clinically or through the onset of neurophenia [288].

The cytidine monophosphate kinase 1 enzyme is responsible for the second phosphorylation of gemcitabine into the diphosphate form. The diphosphate form of gemcitabine has been shown to decrease the activity of ribonucleotide reductase, which in turn replenishes the stock of gemcitabine diphosphate itself within the feedback loop [93,99,288,290,293]. There have been some studies into this enzyme and the associated alleles in order to asses whether mutations in this enzyme can facilitate a greater patient response to gemcitabine however they require further investigation in order to come to a conclusive finding [288].

The 5’ Nucelotidases (2 and 3 variants) catalyse the dephosphorylation of gemcitabine monophosphate and hence an increased expression of this enzyme is associated with a greater resistance to drugs such as gemcitabine, due to an increase in deactivation of these drugs [288]. However, as studies has been performed on the association between this enzyme and gemcitabine clearance there has been positive associations between genetic variants of the enzyme and gemcitabine clearance. However further work is needed in this area in order to fully understand how to tailor treatment towards specific genetic variants displayed in patients.

In conclusion, the enzymes required for gemcitabine metabolization have been discussed briefly with the consensus that further work is required in this area to understand fully how different genetic variants in these proteins effect response to treatment. The takeaway message from the studies in these enzymes are that proteins such as DCK can promote sensitisation to gemcitabine whereas CDA can promote resistance. Therefore, through further studies in this area a greater understanding of dosages required for effective treatment can be attained and thus efficacy of the drug can be much more balanced alongside the inherent toxicity of the drug.

.

1.6.3.3 Targets for gemcitabine therapeutic effect and variations thereof

Whilst variants in the enzymatic pathways required for gemcitabine activation have been discussed, it is just as important that the targets for gemcitabine treatment and their genetic variations are discussed also. Should cells be sensitized to gemcitabine through the enzymes required it is of no importance if the targets for treatment are unresponsive. Thus, it is only through response in both metabolism and target proteins that treatment can be tailored appropriately, and a clinically significant response can be achieved. There is only one true target for gemcitabine to impart a therapeutic effect, ribonucleotide reductase (RNR). Thus, the effects of gemcitabine on the pathways facilitated by this enzyme will be discussed and of course how variations in this enzyme can provide hurdles in gemcitabine treatment.

The ribonucleotide reductase enzyme is responsible for the production of dNTPs from their respective ribonucleotides. The enzyme itself comprises of two subunits RR1 and RR2. Both subunits have specific roles to play in the production of dNTPs. The larger subunit RR1 is responsible for maintaining the number of dNTPs within the pool via the nucleoside salvage pathway and it is in this unit gemcitabine diphosphate binds and causes inhibition [93,293]. RR2 and its association with gemcitabine is less understood however, with most studies focussing on gemcitabine and its association with RR1 [288]. RR1 as well as acting as a mediator for the dNTP pools acts as a tumour suppressor, with studies demonstrating prolonged treatment to gemcitabine correlating with an increased expression of RR1, and thus an increased resistance to gemcitabine resistance. Studies therefore have concluded that a lowered expression of RR1 correlates with a greater reception to gemcitabine and a lower time for tumour progression [288].

Therefore, whilst the RNR enzyme plays an important role in gemcitabine treatment it must be stressed that diagnostic tools identifying expression of this protein is crucial for tailoring of dosages and the choice of drug to be used during treatment. Thus, metabolic enzyme and target enzyme expression together play an important role in reception to gemcitabine and resistance can be built up over time to the drug, despite being a key therapeutic drug further work is needed to identify the

mechanisms of action much more clearly so treatments can evolve over time to overcome hurdles that may occur genetically from patient to patient.

1.6.4 Current studies and research into gemcitabine

Gemcitabine has been discussed in terms of its proposed mechanism of action and the enzymes required to facilitate cellular response to the drug throughout this section. Finally, key research into gemcitabine will be discussed with respect to the up and coming prodrugs of the therapeutic and how these prodrugs can help alleviate issues discovered clinically with treatment, such as drug resistance and inherent toxicity.

Whilst gemcitabine itself is a pyrimidine prodrug there has been extensive research on gemcitabine modifications in order to circumvent metabolic pathways with three notable prodrugs discussed, H-gemcitabine, A-gem and TPGS-gemcitabine, in order to asses the different methods being utilised by researchers in order to improve the efficacy of the drug through combating different resistance pathways. And it will be discussed within these three case studies how further research into gemcitabine prodrugs can aid treatment with gemcitabine, with precis of relevant research papers and conclusions that can be drawn when considering modification of this drug for cancer treatment.

1.6.4.1 H-Gemcitabine

H-Gemcitabine has been termed as such due to the presence of the Hoechst conjugated to the molecule itself. The molecule itself consists of a cleavable disulfide and amide linkage linking the targeting moiety itself to the drug and was first reported by Dasari and co-workers [294].

The reasoning behind the synthesis of H-gemcitabine is that the Hoechst acts as a DNA targeting ligand due to its high affinity of DNA binding [295]. In their study, the authors examined the binding affinity of H-gemcitabine to bind to DNA and it was reported that the presence of gemcitabine did not impair the ability of the Hoechst to

bind to DNA, with no significant decrease in binding affinity when compared to the free Hoechst [294]. Furthermore, it was reported that the H-gemcitabine conjugate displayed similar binding characteristics to that of antibodies used for DNA targeting in cancer.

A second consideration the authors studied was the ability for the H-gemcitabine to circulate through the body, as should the drug be released via the cleavable linkers too early there is a risk that the drug is metabolized within the body to an inactive form, negating the positive effects of the linker itself. It was found via *in vivo* studies that within phosphate buffered saline (pH 7.4) the aromatic amide bond breaks releasing free gemcitabine with a half life of >11hrs suggesting a enough time for circulation through the body.

Membrane permeability and drug effectiveness were also studied by the authors. Permeability into the cell was discovered to be a major stumbling block, with methanol treated cells demonstrating a large increase in permeability as oppose to the live cells, suggesting that despite a high DNA binding affinity the characteristics of the drug are not adequate for a controlled release within the cell. These findings then correlated with a decrease in cellular toxicity in the HT29 cell line, with H-gemcitabine displaying a 80% survival rate over 30 days whereas the free gemcitabine displayed around 20% survival over the same period.

To summarize, targeting ligands can be used to increase DNA affinity of gemcitabine treatment however, stumbling blocks occur when it comes to cell permeability suggesting that modification of the drug in this way can interfere with the action of the transporters needed to facilitate uptake into the cell. Thus, whilst desirable characteristics are observed with respect to half life of the drug and DNA binding there is a considerable stumbling block when designing prodrugs that can carry over uptake characteristics.

1.6.4.2 A-gem – a Hydrogen Peroxide Activated Drug

The second case study to be discussed is the case of gemcitabine being activated via an external chemical as oppose to targeting ligands to increase affinity

of the drug. It has been previously studied that the levels of H_2O_2 are elevated within cancer cells and thus providing the trigger needed to release gemcitabine in the hope that the toxicity of the drug will be reduced.

Therefore, Matsushita and coworkers reported their hydrogen peroxide activated gemcitabine prodrug termed A-gem, which is hydrolyzed in the presence of hydrogen peroxide to produce the active form of gemcitabine [296].

The authors report that within 20 minutes of H_2O_2 stimulation there was a 95% recovery in gemcitabine and was then tested alongside other compounds used as a response to oxidative stress such as hydroxyl radicals, superoxide and hypochlorite and it was found that gemcitabine production was highly selective to hydrogen peroxide. Cytotoxicity was then assessed in both human pancreatic cell lines and non-cancerous cell lines and it was reported that A-gem retained selectivity to the cancerous cell lines as well as inducing cytotoxic effects. Additionally, it was reported that stimulation of H_2O_2 production within cells increased the cytotoxic effects of A-gem demonstrating their proposed mechanism in action with positive results.

This study therefore exemplifies that without the need for a targeting ligand selectivity in gemcitabine treatment can still be achieved. However, the lack of uptake studies within their research still leads to the suggestion that A-gem may not be as readily uptaken and therefore available to the cells through treatment. Furthermore, circulation studies were not performed and thus a half life of the drug through circulation could not be adequately quantified. Despite these lacks of findings this research shows the advances in prodrug technology with respect to gemcitabine and how through careful modifications selectivity towards cancer cells can be afforded by exploiting their unique metabolism and specific cellular environment.

1.6.4.3 TPGS-gemcitabine

TPGS-gemcitabine was reported by Khare and colleagues as a micellar pro-drug technology for the treatment of pancreatic cancer . As oppose to the other

methods discussed in this section this prodrug is unique as the topology of the drug itself is crucial to its effects, through a polymer drug conjugate. Chemically, the structure consists of a Tocopherol polyethylene glycol succinate (TPGS) polymer conjugated to gemcitabine via an amide linkage on the aromatic region of the nucleotide analog [297–299].

Micelles were then prepared by first dissolution into ethanol before dropwise addition into water and filtering. Freeze drying was then performed in order to preserve the micelles for future use, with a particle size of 15.09 ± 0.7 nm at 25°C however increasing the temperature at steps of 5°C to 40°C did not interfere with the size of the particles suggesting thermo stability with a zeta potential of -9.3 ± 0.61 mV, with a critical micelle concentration of 0.15 mg/ml further suggesting a high stability of the structures when dissolved in a large amount of blood in the body for example.

Drug release profiles were then studied, and it was observed that at 30°C there was a lessened drug release than at 37°C or 40°C although TPS-gemcitabine displayed a sustained release at all the temperatures tested. Most interestingly, TPGS-gemcitabine was tested alongside free gemcitabine with the CDA enzyme in order to asses whether this micellar structure could circumvent the metabolic pathway inactivating the drug and it was shown that over a 30 minute period TPGS-gemcitabine retained over 90% of gemcitabine whereas the free gemcitabine was assessed at around 15%. These promising results display how structural changes to gemcitabine can help reduce gemcitabine resistance in cells via the CDA pathway.

The increased stability of the prodrug correlated with an increase in cytotoxic effects studied by the MTT assay on the BxPC-3 cells at 24, 48 and 72 hr intervals. Interestingly, at 24hrs both TPGS micelles and TPGS-gemcitabine micelles showed the most toxic effects suggesting that at this time point toxicity was caused by the polymeric vehicle itself at all concentrations, whereas at 48 hr and 72 hrs gemcitabine displayed the highest toxicity between 0.0001 to 1 µmol concentrations before TPGS and TPGS-gemcitabine displayed more favorable toxicity towards cells. However, again it must be stressed at concentrations above 1 µmol it would appear toxicity is induced by the TPGS molecule itself rather than gemcitabine. Therefore,

whilst the CDA mechanism has been avoided there is a cost to pay in that the toxicity of the molecule in general circulation appears to have increased due to the attachment of TPGS, with free gemcitabine imparting a higher toxicity at the dosages required to negate TPGS toxicity.

Finally, the authors researched into both transporter inhibition and cellular uptake. In their MTT studies the cells were treated with dipyridamole in order to compete with the drug for the use of the transporter thus inhibiting the ability of free gemcitabine to enter the cell through this route. It was observed that the IC_{50} value (the amount of substance needed to inhibit 50% of biological processes) of cells treated with the dipyridamole treatment and gemcitabine had a 5 fold higher IC_{50} value than those cells treated with gemcitabine alone. Whereas, in the TPGS-gemcitabine treated cells no changes in the IC_{50} value were observed, suggesting that the micellar version did not require the transporters in order to enter the cell. This was then correlated with fluorescent microscopy suggesting that the micellar structure enters the cell via a different route.

To summarise, three different gemcitabine prodrugs have been discussed and the benefits and drawbacks of each reported. When designing a gemcitabine prodrug there is a tossup between drug activity and cell uptake. Whilst, it would be ideal to circumvent the natural resistance of cells to gemcitabine, or to reduce inherent toxicity to healthy cells it is problematic either due to lack of entry mechanisms through modifications (in the case of H-gem) or through inherent toxicity of conjugated molecules combined with a reduction in drug efficacy at appropriate concentrations (such as in the case of TPGS-gemcitabine). Therefore, further work is needed on both the mechanisms of action of gemcitabine and the pharmacogenomics pertaining to its use in treatment, whilst also more sophisticated prodrugs are required in order to effectively deliver gemcitabine in an active form reducing toxicity to healthy cells and increasing the efficacy of the drug.

1.7 Project Aims and Objectives

In conclusion, this introduction aimed to provide an insight into the current methodologies and challenges within the oncology sector today, with focus on drug

delivery vehicles as a method of solving unmet clinical needs. The current challenges facing the chemotherapeutic sector within the contemporary setting stem from the high toxicity and low efficacy of current treatments, leading to a multitude of side effects reducing the quality of life of the patient. It has been discussed how the use of drug delivery methods, either in the passive or active form, can act as a courier service within the body reducing the effects of some of the issues with chemotherapeutic treatments. However, there are still to this day side effects and issues to address despite the monumental effort from the scientific community, either due to pharmacological profiles of the drugs in question or due to a lack of an adequate delivery method for the drug in question.

1. This project aims to synthesise a novel hyperbranched structure, via the controlled RAFT approach, for the use in such drug delivery methods with bioconjugation of folic acid in order to provide an actively targeted vesicle for cancer therapeutics. Therefore, theoretical and practical elements will be employed from polymer chemistry, bioconjugation techniques, characterisation methodologies in a blended project alongside biological study. In this manner, the key performance indicators of the project are the following: The complete synthesis and purification of a novel hyperbranched polymer displaying both bio-degradable and “smart” stimuli responsive properties that can be characterised fully using Nuclear Magnetic Resonance and Size Exclusion Chromatography technology.
2. Demonstration of synthetic controllability via the RAFT approach. Allowing for the optimisation of the synthetic route towards the hyperbranched polymer with full characterisation.
3. If so required, the successful synthesis of a linker molecule in order to perform the bio-conjugation of folic acid onto the hyperbranched polymer, with optimised purification and quantification of the folate content, either via Ultra Violet spectroscopy or another means.
4. Bio-evaluations of both the “naked” and folate conjugated polymer assessing their suitability towards the drug delivery role, with key interest into their toxicity profile and cellular uptake with use of the HeLa cell line and tissue culture methodology.

5. Drug conjugation (for this project gemcitabine was chosen as the model drug) and further bio-evaluations of the molecule to assess whether drug delivery can be performed.

These performance indicators therefore will form the objective road map and thus scope of the project over the course of the three-year lifespan, with in depth discussions and results presentation relating to these objectives presented within this thesis. This project therefore aims to tie together previous research in polymer and bioconjugation chemistry alongside advancements in the oncological setting in order to produce a novel fit for purpose material capable of improving on treatments currently used in the modern day, with the design of such a material based on the widely studied 2-Propyl Acrylic Acid (PAA), due to its characterised pH responsive nature and a disulfide branching agent. With reduction capabilities lending this type of monomer appropriate for the bio-degradable criteria set within.

References

[1] F. Bray, J. Ferlay, I. Soerjomataram, R.L. Siegel, A. Jemal, Global Cancer Statistics 2018: GLOBOCAN Estimates of Incidence and Mortality Worldwide for 36 Cancers in 185 Countries, CA. Cancer J. Clin. 0 (2018) 1–31. https://doi.org/10.3322/caac.21492.

[2] C.N. Stephan, M. Henneberg, Medicine may be reducing the human capacity to survive, Med. Hypotheses. 57 (2001) 633–637. https://doi.org/10.1054/mehy.2001.1431.

[3] B.M. Henn, L.R. Botigué, C.D. Bustamante, A.G. Clark, S. Gravel, Estimating the mutation load in human genomes, Nat. Rev. Genet. 16 (2015) 333–343. https://doi.org/10.1038/nrg3931.

[4] D.F. Conrad, J.E.M. Keebler, M.A. Depristo, S.J. Lindsay, Y. Zhang, F. Casals, Y. Idaghdour, C.L. Hartl, C. Torroja, K. V. Garimella, M. Zilversmit, R. Cartwright, G.A. Rouleau, M. Daly, E.A. Stone, M.E. Hurles, P. Awadalla, Variation in genome-wide mutation rates within and between human families, Nat. Genet. 43 (2011) 712–714. https://doi.org/10.1038/ng.862.

[5] F.J. Rühli, M. Henneberg, New perspectives on evolutionary medicine: The relevance of microevolution for human health and disease, BMC Med. 11 (2013) 1–7. https://doi.org/10.1186/1741-7015-11-115.

[6] J.F. Crow, The origins, patterns and implications of human spontaneous mutation, Nat. Rev. Genet. 1 (2000) 40–47. https://doi.org/10.1038/35049558.

[7] M. Lynch, Mutation and human exceptionalism: Our future genetic load, Genetics. 202 (2016) 869–875. https://doi.org/10.1534/genetics.115.180471.

[8] I.B. Weinstein, A. Joe, Oncogene addiction, Cancer Res. 68 (2008) 3077–3080. https://doi.org/10.1158/0008-5472.CAN-07-3293.

[9] G.N. Rao, B.C. Berk, Active oxygen species stimulate vascular smooth muscle cell growth and proto-oncogene expression, Circ. Res. 70 (1992) 593–599. https://doi.org/10.1161/01.res.70.3.593.

[10] M. Park, M. Dean, C.S. Cooper, M. Schmidt, S.J. O'Brien, D.G. Blair, G.F. Vande Woude, Mechanism of met oncogene activation, Cell. 45 (1986) 895–904. https://doi.org/10.1016/0092-8674(86)90564-7.

[11] S. Collins, The HL-60 Promyelocytic Leukemia Cell Line: Proliferation, Differentation and Cellular Oncogene Expression, J. Am. Soc. Hematol. 70 (1987) 1233–1244.

[12] M.J. Bueno, I. Pérez de Castro, M. Gómez de Cedrón, J. Santos, G.A. Calin, J.C.C. Cigudosa, C.M. Croce, J. Fernández-Piqueras, M. Malumbres, Genetic and Epigenetic Silencing of MicroRNA-203 Enhances ABL1 and BCR-ABL1 Oncogene Expression, Cancer Cell. 13 (2008) 496–506. https://doi.org/10.1016/j.ccr.2008.04.018.

[13] J.F. Bromberg, M.H. Wrzeszczynska, G. Devgan, Y. Zhao, R.G. Pestell, C. Albanese, J.E. Darnell, Stat3 as an oncogene, Cell. 98 (1999) 295–303. https://doi.org/10.1016/S0092-8674(00)81959-5.

[14] K. Alitalo, M. Schwab, Oncogene amplification in tumor cells, Adv. Cancer Res. 47 (1986) 235–281. https://doi.org/10.1016/S0065-230X(08)60201-8.

[15] R.M. Hoffman, Altered methionine metabolism, DNA methylation and oncogene expression in carcinogenesis. A review and synthesis, BBA - Rev. Cancer. 738 (1984) 49–87. https://doi.org/10.1016/0304-419X(84)90019-2.

[16] D.J. Slamon, G.M. Clark, S.G. Wong, W.J. Levin, A. Ullrich, W.L. Mcguire, Human Breast Cancer: Correlation of Relapse and Survival with Amplification of the HER-2lneu Oncogene, Science (80-.). 235 (1987) 177–182.

[17] M.M. Moasser, The oncogene HER2: its signaling and transforming functions and its role in human cancer pathogenesis, Oncogene. 26 (2007) 6469–6487. https://doi.org/10.1038/sj.onc.1210477.

[18] Z. Mitri, T. Constantine, R. O'Regan, The HER2 Receptor in Breast Cancer: Pathophysiology, Clinical Use, and New Advances in Therapy, Chemother. Res. Pract. 2012 (2012) 1–7. https://doi.org/10.1155/2012/743193.

[19] F. Walker, L. Abramowitz, D. Benabderrahmane, X. Duval, V. Descatoire, D. Hénin, T. Lehy, T. Aparicio, Growth factor receptor expression in anal squamous lesions: modifications associated with oncogenic human papillomavirus and human immunodeficiency virus, Hum. Pathol. 40 (2009) 1517–1527. https://doi.org/10.1016/j.humpath.2009.05.010.

[20] P.A.J. Muller, K.H. Vousden, p53 mutations in cancer, Nat. Cell Biol. 15 (2013) 2–8. https://doi.org/10.1038/ncb2641.

[21] A. Ashworth, C.J. Lord, J.S. Reis-Filho, Genetic interactions in cancer progression and treatment, Cell. 145 (2011) 30–38. https://doi.org/10.1016/j.cell.2011.03.020.

[22] P. Deininger, Genetic Instability in Cancer: Caretaker and Gatekeeper Genes, Ochsner J. 1 (1999) 206 LP – 209. http://www.ochsnerjournal.org/content/1/4/206.abstract.

[23] S.A. Frank, Somatic mutation: Early cancer steps depend on tissue architecture, Curr. Biol. 13 (2003) 261–263. https://doi.org/10.1016/S0960-9822(03)00195-7.

[24] A.C. Lesko, K.H. Goss, F.F. Yang, A. Schwertner, I. Hulur, K. Onel, J.R. Prosperi, The APC tumor suppressor is required for epithelial cell polarization and three-dimensional morphogenesis, Biochim. Biophys. Acta - Mol. Cell Res. 1853 (2015) 711–723. https://doi.org/https://doi.org/10.1016/j.bbamcr.2014.12.036.

[25] S.I. Chiosea, L. Williams, C.C. Griffith, L.D.R. Thompson, I. Weinreb, J.E. Bauman, A. Luvison, S. Roy, R.R. Seethala, M.N. Nikiforova, Molecular characterization of apocrine salivary duct carcinoma, Am. J. Surg. Pathol. 39 (2015) 744–752. https://doi.org/10.1097/PAS.0000000000000410.

[26] R. Scully, Role of BRCA gene dysfunction in breast and ovarian cancer predisposition, Breast Cancer Res. 2 (2000) 1–7.

[27] O. De Wever, M. Mareel, Role of tissue stroma in cancer cell invasion, J. Pathol. 200 (2003) 429–447. https://doi.org/10.1002/path.1398.

[28] L. Raffaghello, F. Dazzi, Classification and biology of tumour associated stromal cells, Immunol. Lett. 168 (2015) 175–182. https://doi.org/10.1016/j.imlet.2015.06.016.

[29] N. Krieger, Social class, race/ethnicity, and incidence of breast, cervix, colon, lung, and prostate cancer among Asian, black, Hispanic, and white residents of the San Francisco Bay Area, 1988-92 (United States), Cancer Causes Control. 10 (1999) 525–537. https://doi.org/10.1023/A:1008950210967.

[30] B. Armstrong, R. Doll, Environmental factors and cancer incidence and mortality in different countries, with special reference to dietary practices, Int. J. Cancer. 15 (1975) 617–631. https://doi.org/10.1002/ijc.2910150411.

[31] P. Boffetta, F. Nyberg, Contribution of environmental factors to cancer risk, Br. Med. Bull. 68 (2003) 71–94. https://doi.org/10.1093/bmp/ldg023.

[32] N.H. Service, Lifestyle changes could slash cancer rates, Www.NHS.Co.Uk. (2011). https://www.nhs.uk/news/cancer/lifestyle-changes-could-slash-cancer-rates/ (accessed July 6, 2020).

[33] D.M. Parkin, Tobacco-attributable cancer burden in the UK in 2010, Br. J. Cancer. 105 (2011) S6–S13. https://doi.org/10.1038/bjc.2011.475.

[34] T. Sano, T. Oyama, K. Kashiwabara, T. Fukuda, T. Nakajima, Expression status of p16 protein is associated with human papillomavirus oncogenic potential in cervical and genital lesions, Am. J. Pathol. 153 (1998) 1741–1748. https://doi.org/10.1016/S0002-9440(10)65689-1.

[35] Y. Gao, I. Bado, H. Wang, W. Zhang, J.M. Rosen, X.H.F. Zhang, Metastasis Organotropism: Redefining the Congenial Soil, Dev. Cell. 49 (2019) 375–391. https://doi.org/10.1016/j.devcel.2019.04.012.

[36] I.J. Fidler, The pathogenesis of cancer metastasis: the “seed and soil” hypothesis revisited, Nat. Rev. Cancer. 3 (2003) 453–458. https://doi.org/10.1038/nrc1098.

[37] S.H. Kim, D.W. Shin, S.Y. Kim, H.K. Yang, E. Nam, H.J. Jho, E. Ahn, B.L. Cho, K. Park, J.H. Park, Terminal versus advanced cancer: Do the general population and health care professionals share a common language?, Cancer Res. Treat. 48 (2016) 759–767. https://doi.org/10.4143/crt.2015.124.

[38] N.H. Service, What do cancer stages and grades mean?, What Do Cancer Stages Grades Mean? (2018). https://www.nhs.uk/common-health-questions/operations-tests-and-procedures/what-do-cancer-stages-and-grades-mean/ (accessed July 7, 2020).

[39] F. Greene, C. Balch, I. Fleming, A. Fritz, D. Haller, M. Morrow, D. Page, General Information on Cancer Staging and End-Results Reporting, in: F. Greene (Ed.), AJCC Cancer Staging Handb., 6th ed., Springer US, New York, 2002: pp. 3–15.

[40] M.C. Support, Internal radiotherapy, Intern. Radiother. (2020). https://www.macmillan.org.uk/cancer-information-and-support/treatment/types-of-treatment/radiotherapy/internal-radiotherapy#what_is_internal_radiotherapy (accessed July 8, 2020).

[41] A. Dietrich, L. Koi, K. Zöphel, W. Sihver, J. Kotzerke, M. Baumann, M. Krause, Improving external beam radiotherapy by combination with internal irradiation, Br. J. Radiol. 88 (2015). https://doi.org/10.1259/bjr.20150042.

[42] H. Ragde, Modern prostate brachytherapy, Manag. Prostate Cancer Adv. Controv. (2004) 205–226. https://doi.org/10.3322/canjclin.50.6.380.

[43] S. Nag, D. Shasha, N. Janjan, I. Petersen, M. Zaider, The American Brachytherapy Society recommendations for brachytherapy of soft tissue sarcomas, Int. J. Radiat. Oncol. Biol. Phys. 49 (2001) 1033–1043. https://doi.org/10.1016/S0360-3016(00)01534-0.

[44] S. Nag, B. Erickson, S. Parikh, N. Gupta, M. Varia, G. Glasgow, The American Brachytherapy Society recommendations for high-dose-rate brachytherapy for carcinoma of the endometrium, Int. J. Radiat. Oncol. Biol. Phys. 48 (2000) 779–790. https://doi.org/10.1016/S0360-3016(00)00689-1.

[45] S. Nag, C. Chao, B. Erickson, J. Fowler, N. Gupta, A. Martinez, B. Thomadsen, The American Brachytherapy Society recommendations for low-dose-rate brachytherapy for carcinoma of the cervix, Int. J. Radiat. Oncol. Biol. Phys. 52 (2002) 33–48. https://doi.org/10.1016/S0360-3016(01)01755-2.

[46] R. Hudson, Brachytherapy treatments increasing among Medicare population, Heal. Policy Br. Am. Urol. Assoc. 9 (1999) 1.

[47] C.R. UK, Radioactive liquid treatment, Radioact. Liq. Treat. (2019). https://www.cancerresearchuk.org/about-cancer/cancer-in-general/treatment/radiotherapy/internal/radioactive-liquid-treatment (accessed July 9, 2020).

[48] R.J. Ott, D. Tait, M.A. Flower, J.W. Babich, R.M. Lambrecht, Treatment planning for 131I-mIBG radiotherapy of neural crest tumours using 124I-mIBG positron emission tomography, Br. J. Radiol. 65 (1992) 787–791.

[49] D.I. Thwaites, J.B. Tuohy, Back to the future: the history and development of the clinical linear accelerator, Phys. Med. Biol. 51 (2006) R343–R362. https://doi.org/10.1088/0031-9155/51/13/r20.

[50] C.M. Walko, C. Lindley, Capecitabine: A review, Clin. Ther. 27 (2005) 23–44. https://doi.org/10.1016/j.clinthera.2005.01.005.

[51] A.J. Wagstaff, A. Ward, P. Benfield, R.C. Heel, Carboplatin, Drugs. 37 (1989) 162–190. https://doi.org/10.2165/00003495-198937020-00005.

[52] P.D. Lawley, D.H. Phillips, DNA adducts from chemotherapeutic agents, Mutat. Res. - Fundam. Mol. Mech. Mutagen. 355 (1996) 13–40. https://doi.org/10.1016/0027-5107(96)00020-6.

[53] D. S Gesto, N. MFSA Cerqueira, P. A Fernandes, M. J Ramos, Gemcitabine: a critical nucleoside for cancer therapy, Curr. Med. Chem. 19 (2012) 1076–1087.

[54] E.K. Rowinsky, R.C. Donehower, Paclitaxel (Taxol), N. Engl. J. Med. 332 (1995) 1004–1014. https://doi.org/10.1056/NEJM199504133321507.

[55] K.A. Lyseng-Williamson, C. Fenton, Docetaxel, Drugs. 65 (2005) 2513–2531. https://doi.org/10.2165/00003495-200565170-00007.

[56] J. V. McGowan, R. Chung, A. Maulik, I. Piotrowska, J.M. Walker, D.M. Yellon, Anthracycline Chemotherapy and Cardiotoxicity, Cardiovasc. Drugs Ther. 31 (2017) 63–75. https://doi.org/10.1007/s10557-016-6711-0.

[57] J.E. Fenn, R. Udelsman, First use of intravenous chemotherapy cancer treatment: Rectifying the record, J. Am. Coll. Surg. 212 (2011) 413–417. https://doi.org/10.1016/j.jamcollsurg.2010.10.018.

[58] G. Kauffman, Michele Peyrone (1813–1883), Discoverer of Cisplatin, Appl. Catal. 54 (2010) 250–256. https://doi.org/10.1016/S0166-9834(00)80742-3.

[59] J. Fischer, G.. Ganellin, Licensed Antineoplastic and Immunomodulating Agents, in: IUPAC, J. Fischer, G.. Ganellin (Eds.), Analog. Drug Discov., John Wiley & Sons, Ltd, 2006: p. 513.

[60] P.D. Lawley, P. Brookes, Interstrand cross-linking of DNA by difunctional alkylating agents, J. Mol. Biol. 25 (1967) 143–160. https://doi.org/10.1016/0022-2836(67)90285-9.

[61] J. Weigt, P. Malfertheiner, Cisplatin plus gemcitabine versus gemcitabine for biliary tract cancer, Expert Rev. Gastroenterol. Hepatol. 4 (2010) 395–397. https://doi.org/10.1586/egh.10.45.

[62] M.R. Osborne, D.E.V. Wilman, P.D. Lawley, Alkylation of DNA by the Nitrogen Mustard Bis(2-chloroethyl)methylamine, Chem. Res. Toxicol. 8 (1995) 316–320. https://doi.org/10.1021/tx00044a018.

[63] D. Ormrod, C.M. Spencer, Topotecan, Drugs. 58 (1999) 533–551. https://doi.org/10.2165/00003495-199958030-00020.

[64] L.R. Wiseman, A. Markham, Irinotecan, Drugs. 52 (1996) 606–623. https://doi.org/10.2165/00003495-199652040-00013.

[65] N. Jiang, X. Wang, Y. Yang, W. Dai, Advances in Mitotic Inhibitors for Cancer Treatment, Mini-Reviews Med. Chem. 6 (2006) 885–895. https://doi.org/10.2174/138955706777934955.

[66] Z. Darzynkiewicz, G. Juan, E. Bedner, Determining Cell Cycle Stages by Flow Cytometry, Curr. Protoc. Cell Biol. 1 (1999). https://doi.org/10.1002/0471143030.cb0804s01.

[67] C.J. Sherr, G1 phase progression: Cycling on cue, Cell. 79 (1994) 551–555. https://doi.org/10.1016/0092-8674(94)90540-1.

[68] H.-Z. Chen, S.-Y. Tsai, G. Leone, Emerging roles of E2Fs in cancer: an exit from cell cycle control, Nat. Rev. Cancers. 9 (2009) 785–797. https://doi.org/10.1038/jid.2014.371.

[69] S. Gaubatz, G.J. Lindeman, S. Ishida, L. Jakoi, J.R. Nevins, D.M. Livingston, R.E. Rempel, E2F4 and E2F5 play an essential role in pocket protein-mediated G1

control, Mol. Cell. 6 (2000) 729–735. https://doi.org/10.1016/S1097-2765(00)00071-X.

[70] Y. Li, O. Barbash, J.A. Diehl, Regulation of the Cell Cycle, Mol. Basis Cancer Fourth Ed. (2014). https://doi.org/10.1016/B978-1-4557-4066-6.00011-1.

[71] T.H. Cheung, T.A. Rando, Molecular regulation of stem cell quiescence, Nat. Rev. Mol. Cell Biol. 14 (2013) 329–340. https://doi.org/10.1038/nrm3591.

[72] S. Ren, B.J. Rollins, Cyclin C/Cdk3 promotes Rb-dependent G0 exit, Cell. 117 (2004) 239–251. https://doi.org/10.1016/S0092-8674(04)00300-9.

[73] P. Nurse, Ordering S phase and M phase in the cell cycle, Cell. 79 (1994) 547–550.

[74] A.B. Khodursky, B.J. Peter, M.B. Schmid, J. DeRisi, D. Botstein, P.O. Brown, N.R. Cozzarelli, Analysis of topoisomerase function in bacterial replication fork movement: Use of DNA microarrays, Proc. Natl. Acad. Sci. U. S. A. 97 (2000) 9419–9424. https://doi.org/10.1073/pnas.97.17.9419.

[75] Y. Pommier, Topoisomerase I inhibitors: camptothecins and beyond, Nat. Rev. Cancer. 6 (2006) 789–802. https://doi.org/10.1038/nrc1977.

[76] S.M. Vos, E.M. Tretter, B.H. Schmidt, J.M. Berger, All tangled up: how cells direct, manage and exploit topoisomerase function, Nat. Rev. Mol. Cell Biol. 12 (2011) 827–841. https://doi.org/10.1038/nrm3228.

[77] M.E. Wall, M.C. Wani, C.E. Cook, K.H. Palmer, A.T. McPhail, G.A. Sim, Plant Antitumor Agents. I. The Isolation and Structure of Camptothecin, a Novel Alkaloidal Leukemia and Tumor Inhibitor from Camptotheca acuminata1,2, J. Am. Chem. Soc. 88 (1966) 3888–3890. https://doi.org/10.1021/ja00968a057.

[78] G.M. Kim, Y.S. Kim, Y.A. Kang, J.-H. Jeong, S.M. Kim, Y.K. Hong, J.H. Sung, S.T. Lim, J.H. Kim, S.K. Kim, B.C. Cho, Efficacy and Toxicity of Belotecan for Relapsed or Refractory Small Cell Lung Cancer Patients, J. Thorac. Oncol. 7 (2012) 731–736. https://doi.org/https://doi.org/10.1097/JTO.0b013e31824b23cb.

[79] Y. Onishi, Y. Azuma, Y. Sato, Y. Mizuno, T. Tadakuma, H. Kizaki, Topoisomerase inhibitors induce apoptosis in thymocytes, Biochim. Biophys. Acta. 1175 (1993) 147–154. https://doi.org/10.1016/0167-4889(93)90017-J.

[80] Y. Pommier, M. Cushman, The indenoisoquinoline noncamptothecin topoisomerase I inhibitors: update and perspectives, Mol. Cancer Ther. 8 (2009) 1008 LP – 1014. https://doi.org/10.1158/1535-7163.MCT-08-0706.

[81] R.N. Irobalieva, J.M. Fogg, D.J. Catanese Jr, T. Sutthibutpong, M. Chen, A.K. Barker, S.J. Ludtke, S.A. Harris, M.F. Schmid, W. Chiu, L. Zechiedrich, Structural diversity of supercoiled DNA, Nat. Commun. 6 (2015) 8440. https://doi.org/10.1038/ncomms9440.

[82] A. Fedier, V.A. Schwarz, H. Walt, R.D. Carpini, U. Haller, D. Fink, Resistance to topoisomerase poisons due to loss of DNA mismatch repair, Int. J. Cancer. 93 (2001) 571–576. https://doi.org/10.1002/ijc.1356.

[83] R.B. Weiss, The anthracyclines: will we ever find a better doxorubicin?, in: Semin. Oncol., 1992: p. 670.

[84] G. Aubel-Sadron, D. Londos-Gagliardi, Daunorubicin and doxorubicin, anthracycline antibiotics, a physicochemical and biological review, Biochimie. 66 (1984) 333–352. https://doi.org/https://doi.org/10.1016/0300-9084(84)90018-X.

[85] G.E. Kellogg, J.N. Scarsdale, F.A. Fornari Jr, Identification and hydropathic characterization of structural features affecting sequence specificity for doxorubicin intercalation into DNA double-stranded polynucleotides, Nucleic Acids Res. 26 (1998) 4721–4732. https://doi.org/10.1093/nar/26.20.4721.

[86] L.P.G. Wakelin, P. Chetcuti, W.A. Denny, Kinetic and Equilibrium Binding Studies of Amsacrine-4-carboxamides: A Class of Asymmetrical DNA-Intercalating Agents Which Bind by Threading through the DNA Helix, J. Med. Chem. 33 (1990) 2039–2044. https://doi.org/10.1021/jm00169a039.

[87] S.A. BROWN, Fluoroquinolones in animal health, J. Vet. Pharmacol. Ther. 19 (1996) 1–14. https://doi.org/10.1111/j.1365-2885.1996.tb00001.x.

[88] A. Smith, P.M. Pennefather, S.B. Kaye, C.A. Hart, Fluoroquinolones, Drugs. 61 (2001) 747–761. https://doi.org/10.2165/00003495-200161060-00004.

[89] A.M. Oliveira, J.S. Ross, J.A. Fletcher, Tumor Suppressor Genes in Breast Cancer: The Gatekeepers and the Caretakers, Pathol. Patterns Rev. 124 (2005) S16–S28. https://doi.org/10.1309/5XW3L8LU445QWGQR.

[90] LadyofHats, Mitosis cells sequence - Creative Commons Licence, Wikimedia - Free Media Repos. (2008).

https://commons.wikimedia.org/wiki/File:Mitosis_cells_sequence.svg (accessed May 10, 2020).

[91] B.A. Weaver, How Taxol/paclitaxel kills cancer cells, Mol. Biol. Cell. 25 (2014) 2677–2681. https://doi.org/10.1091/mbc.E14-04-0916.

[92] D.P. Figgitt, L.R. Wiseman, Docetaxel, Drugs. 59 (2000) 621–651. https://doi.org/10.2165/00003495-200059030-00015.

[93] J. Ciccolini, C. Serdjebi, G.J. Peters, E. Giovannetti, Pharmacokinetics and pharmacogenetics of Gemcitabine as a mainstay in adult and pediatric oncology: an EORTC-PAMM perspective, Cancer Chemother. Pharmacol. 78 (2016) 1–12. https://doi.org/10.1007/s00280-016-3003-0.

[94] B. Reigner, K. Blesch, E. Weidekamm, Clinical Pharmacokinetics of Capecitabine, Clin. Pharmacokinet. 40 (2001) 85–104. https://doi.org/10.2165/00003088-200140020-00002.

[95] H. Ishitsuka, Capecitabine: Preclinical Pharmacology Studies, Invest. New Drugs. 18 (2000) 343–354. https://doi.org/10.1023/A:1006497231579.

[96] Y. Tsukamoto, Y. Kato, M. Ura, I. Horii, H. Ishitsuka, H. Kusuhara, Y. Sugiyama, A Physiologically Based Pharmacokinetic Analysis of Capecitabine, a Triple Prodrug of 5-FU, in Humans: The Mechanism for Tumor-Selective Accumulation of 5-FU, Pharm. Res. 18 (2001) 1190–1202. https://doi.org/10.1023/A:1010939329562.

[97] T. Inada, A. Ichikawa, T. Kubota, Y. Ogata, A.R. Moossa, R.M. Hoffman, 5-FU-induced apoptosis correlates with efficacy against human gastric and colon cancer xenografts in nude mice., Anticancer Res. 17 (1997) 1965.

[98] D. Fu, J.A. Calvo, L.D. Samson, Balancing repair and tolerance of DNA damage caused by alkylating agents, Nat. Rev. Cancer. 12 (2012) 104–120. https://doi.org/10.1038/nrc3185.

[99] E. Mini, S. Nobili, B. Caciagli, I. Landini, T. Mazzei, Cellular pharmacology of gemcitabine, Ann. Oncol. 17 (2006) v7–v12. https://doi.org/10.1093/annonc/mdj941.

[100] Q. Xu, S.P. Kambhampati, R.M. Kannan, Nanotechnology approaches for ocular drug delivery., Middle East Afr. J. Ophthalmol. 20 (2013) 26–37. https://doi.org/10.4103/0974-9233.106384.

[101] H. Maeda, Polymer therapeutics and the EPR effect, J. Drug Target. 25 (2017) 781–785. https://doi.org/10.1080/1061186X.2017.1365878.

[102] M.A. Ward, T.K. Georgiou, Thermoresponsive polymers for biomedical applications, Polymers (Basel). 3 (2011) 1215–1242. https://doi.org/10.3390/polym3031215.

[103] V.G. Kadajji, G. V. Betageri, Water soluble polymers for pharmaceutical applications, Polymers (Basel). 3 (2011) 1972–2009. https://doi.org/10.3390/polym3041972.

[104] M.O. Aviles, A.D. Ebner, J.A. Ritter, Ferromagnetic seeding for the magnetic targeting of drugs and radiation in capillary beds, J. Magn. Magn. Mater. 310 (2007) 131–144.

[105] M.H. Stenzel, RAFT polymerization: An avenue to functional polymeric micelles for drug delivery, Chem. Commun. (2008) 3486–3503. https://doi.org/10.1039/b805464a.

[106] M. Nakayama, T. Okano, T. Miyazaki, F. Kohori, K. Sakai, M. Yokoyama, Molecular design of biodegradable polymeric micelles for temperature-responsive drug release, J. Control. Release. 115 (2006) 46–56. https://doi.org/https://doi.org/10.1016/j.jconrel.2006.07.007.

[107] E.S. Lee, K. Na, Y.H. Bae, Doxorubicin loaded pH-sensitive polymeric micelles for reversal of resistant MCF-7 tumor, J. Control. Release. 103 (2005) 405–418. https://doi.org/10.1016/j.jconrel.2004.12.018.

[108] H.-C. Shin, A.W.G. Alani, D.A. Rao, N.C. Rockich, G.S. Kwon, Multi-drug loaded polymeric micelles for simultaneous delivery of poorly soluble anticancer drugs, J. Control. Release. 140 (2009) 294–300. https://doi.org/https://doi.org/10.1016/j.jconrel.2009.04.024.

[109] J. Akimoto, M. Nakayama, T. Okano, Temperature-responsive polymeric micelles for optimizing drug targeting to solid tumors, J. Control. Release. 193 (2014) 2–8. https://doi.org/https://doi.org/10.1016/j.jconrel.2014.06.062.

[110] L. Qin, F. Zhang, X. Lu, X. Wei, J. Wang, X. Fang, D. Si, Y. Wang, C. Zhang, R. Yang, Polymeric micelles for enhanced lymphatic drug delivery to treat metastatic tumors, J. Control. Release. 171 (2013) 133–142.

[111] T. Ta, A.J. Convertine, C.R. Reyes, P.S. Stayton, T.M. Porter, Thermosensitive liposomes modified with poly(N-isopropylacrylamide-co-

propylacrylic acid) copolymers for triggered release of doxorubicin, Biomacromolecules. 11 (2010) 1915–1920. https://doi.org/10.1021/bm1004993.

[112] K. Maruyama, Intracellular targeting delivery of liposomal drugs to solid tumors based on EPR effects, Adv. Drug Deliv. Rev. 63 (2011) 161–169. https://doi.org/10.1016/j.addr.2010.09.003.

[113] B. Uziely, S. Jeffers, R. Isacson, K. Kutsch, D. Wei-Tsao, Z. Yehoshua, E. Libson, F.M. Muggia, A. Gabizon, Liposomal doxorubicin: antitumor activity and unique toxicities during two complementary phase I studies., J. Clin. Oncol. 13 (1995) 1777–1785. https://doi.org/10.1200/JCO.1995.13.7.1777.

[114] R.J. Lee, P.S. Low, Folate-mediated tumor cell targeting of liposome-entrapped doxorubicin in vitro, BBA - Biochim. Biophsica Acta. 1233 (1995) 134–144. https://doi.org/10.1016/0005-2736(94)00235-H.

[115] Y. Patil, H. Shmeeda, Y. Amitay, P. Ohana, S. Kumar, A. Gabizon, Targeting of folate-conjugated liposomes with co-entrapped drugs to prostate cancer cells via prostate-specific membrane antigen (PSMA), Nanomedicine Nanotechnology, Biol. Med. 14 (2018) 1407–1416. https://doi.org/10.1016/j.nano.2018.04.011.

[116] A.D. Miller, Lipid-based nanoparticles in cancer diagnosis and therapy, J. Drug Deliv. 2013 (2013).

[117] A. Puri, K. Loomis, B. Smith, J.-H. Lee, A. Yavlovich, E. Heldman, R. Blumenthal, Lipid-based nanoparticles as pharmaceutical drug carriers: from concepts to clinic, Crit. Rev. Ther. Drug Carr. Syst. 26 (2009).

[118] D. Landesman-Milo, D. Peer, Altering the immune response with lipid-based nanoparticles, J. Control. Release. 161 (2012) 600–608.

[119] W. Li, F.C. Szoka, Lipid-based Nanoparticles for Nucleic Acid Delivery, Pharm. Res. 24 (2007) 438–449. https://doi.org/10.1007/s11095-006-9180-5.

[120] J.E. Schroeder, I. Shweky, H. Shmeeda, U. Banin, A. Gabizon, Folate-mediated tumor cell uptake of quantum dots entrapped in lipid nanoparticles, J. Control. Release. 124 (2007) 28–34. https://doi.org/10.1016/j.jconrel.2007.08.028.

[121] V. Khare, A. Singh, G. Mahajan, N. Alam, S. Kour, M. Gupta, A. Kumar, G. Singh, S.K. Singh, A.K. Saxena, D.M. Mondhe, P.N. Gupta, Long-circulatory nanoparticles for gemcitabine delivery: Development and investigation of pharmacokinetics and in-vivo anticancer efficacy, Eur. J. Pharm. Sci. 92 (2016) 183–193. https://doi.org/10.1016/j.ejps.2016.07.007.

[122] A. Chilkoti, M.R. Dreher, D.E. Meyer, D. Raucher, Targeted drug delivery by thermally responsive polymers, Adv. Drug Deliv. Rev. 54 (2002) 613–630. https://doi.org/https://doi.org/10.1016/S0169-409X(02)00041-8.

[123] H. Maeda, G.Y. Bharate, J. Daruwalla, Polymeric drugs for efficient tumor-targeted drug delivery based on EPR-effect, Eur. J. Pharm. Biopharm. 71 (2009) 409–419. https://doi.org/https://doi.org/10.1016/j.ejpb.2008.11.010.

[124] G. Kocak, C. Tuncer, V. Bütün, pH-Responsive polymers, Polym. Chem. 8 (2017) 144–176. https://doi.org/10.1039/C6PY01872F.

[125] D. Wang, Y. Jin, X. Zhu, D. Yan, Synthesis and applications of stimuli-responsive hyperbranched polymers, Prog. Polym. Sci. 64 (2017) 114–153. https://doi.org/10.1016/j.progpolymsci.2016.09.005.

[126] C. Solans, P. Izquierdo, J. Nolla, N. Azemar, M.J. Garcia-Celma, Nano-emulsions, Curr. Opin. Colloid Interface Sci. 10 (2005) 102–110. https://doi.org/https://doi.org/10.1016/j.cocis.2005.06.004.

[127] N. Anton, T.F. Vandamme, Nano-emulsions and Micro-emulsions: Clarifications of the Critical Differences, Pharm. Res. 28 (2011) 978–985. https://doi.org/10.1007/s11095-010-0309-1.

[128] K.E. Broaders, S.J. Pastine, S. Grandhe, J.M.J. Fréchet, Acid-degradable solid-walled microcapsules for pH-responsive burst-release drug delivery, Chem. Commun. 47 (2011) 665–667. https://doi.org/10.1039/c0cc04190d.

[129] X. Huang, C.S. Brazel, On the importance and mechanisms of burst release in matrix-controlled drug delivery systems, J. Control. Release. 73 (2001) 121–136. https://doi.org/https://doi.org/10.1016/S0168-3659(01)00248-6.

[130] B.J. Boyd, Characterisation of drug release from cubosomes using the pressure ultrafiltration method, Int. J. Pharm. 260 (2003) 239–247. https://doi.org/https://doi.org/10.1016/S0378-5173(03)00262-X.

[131] J. Pillai, A.K. Thulasidasan, R. Anto, D. Chithralekha, A. Narayanan, G.S. Kumar, Folic acid conjugated cross-linked acrylic polymer (FA-CLAP) hydrogel for site specific delivery of hydrophobic drugs to cancer cells, J. Nanobiotechnology. 12 (2014) 25. https://doi.org/10.1186/1477-3155-12-25.

[132] P. Grossen, D. Witzigmann, S. Sieber, J. Huwyler, PEG-PCL-based nanomedicines: A biodegradable drug delivery system and its application, J. Control.

Release. 260 (2017) 46–60. https://doi.org/https://doi.org/10.1016/j.jconrel.2017.05.028.

[133] A. Smith, Ian M. Hunneyball, Evaluation of poly(lactic acid) as a biodegradable drug delivery system for parenteral administration, Int. J. Pharm. 30 (1986) 215–220. https://doi.org/https://doi.org/10.1016/0378-5173(86)90081-5.

[134] L. Di Silvio, W. Bonfield, Biodegradable drug delivery system for the treatment of bone infection and repair, J. Mater. Sci. Mater. Med. 10 (1999) 653–658. https://doi.org/10.1023/A:1008995926566.

[135] K. Strebhardt, A. Ullrich, Paul Ehrlich ' s magic bullet concept : 100 years of progress, Nat. Rev. Cancer. 8 (2008) 473–480. https://doi.org/10.1038/nrc2394.

[136] Y. Matsumura, H. Maeda, A New Concept for Macromolecular Therapeutics in Cancer Chemotherapy: Mechanism of Tumoritropic Accumulation of Proteins and the Antitumor Agent Smancs, Cancer Res. 46 (1986) 6387 LP – 6392. http://cancerres.aacrjournals.org/content/46/12_Part_1/6387.abstract.

[137] H.F. Dvorak, L.F. Brown, M. Detmar, A.M. Dvorak, Vascular permeability factor/vascular endothelial growth factor, microvascular hyperpermeability, and angiogenesis, Am. J. Pathol. 146 (1995) 1029–1039. https://pubmed.ncbi.nlm.nih.gov/7538264.

[138] J. Fang, H. Nakamura, H. Maeda, The EPR effect: Unique features of tumor blood vessels for drug delivery, factors involved, and limitations and augmentation of the effect, Adv. Drug Deliv. Rev. 63 (2011) 136–151. https://doi.org/10.1016/j.addr.2010.04.009.

[139] H. Kobayashi, R. Watanabe, P.L. Choyke, Improving conventional enhanced permeability and retention (EPR) effects; what is the appropriate target?, Theranostics. 4 (2013) 81–89. https://doi.org/10.7150/thno.7193.

[140] T. Tejada-Berges, C.O. Granai, M. Gordinier, W. Gajewski, Caelyx/Doxil for the treatment of metastatic ovarian and breast cancer, Expert Rev. Anticancer Ther. 2 (2002) 143–150. https://doi.org/10.1586/14737140.2.2.143.

[141] R.J. Kreitman, Immunotoxins for targeted cancer therapy, AAPS J. 8 (2006) E532–E551. https://doi.org/10.1208/aapsj080363.

[142] G.L. Zwicke, G.A. Mansoori, C.J. Jeffery, Targeting of Cancer Nanotherapeutics, Nano Rev. 1 (2012) 1–11.

[143] A.R. Hilgenbrink, P.S. Low, Folate receptor-mediated drug targeting: From therapeutics to diagnostics, J. Pharm. Sci. 94 (2005) 2135–2146. https://doi.org/10.1002/jps.20457.

[144] K.G. Rothberg, Y.S. Ying, J.F. Kolhouse, B.A. Kamen, R.G. Anderson, The glycophospholipid-linked folate receptor internalizes folate without entering the clathrin-coated pit endocytic pathway., J. Cell Biol. 110 (1990) 637–649. https://doi.org/10.1083/jcb.110.3.637.

[145] J. Sudimack, R.J. Lee, Targeted drug delivery via the folate receptor, Adv. Drug Deliv. Rev. 41 (2000) 147–162. https://doi.org/https://doi.org/10.1016/S0169-409X(99)00062-9.

[146] K.K. Jain, Use of nanoparticles for drug delivery in glioblastoma multiforme, Expert Rev. Neurother. 7 (2007) 363–372. https://doi.org/10.1586/14737175.7.4.363.

[147] B. a Kamen, a Capdevila, Receptor-mediated folate accumulation is regulated by the cellular folate content., Proc. Natl. Acad. Sci. U. S. A. 83 (1986) 5983–7. https://doi.org/10.1073/pnas.83.16.5983.

[148] L.M. Bareford, P.W. Swaan, Endocytic mechanisms for targeted drug delivery, Adv. Drug Deliv. Rev. 59 (2007) 748–758. https://doi.org/https://doi.org/10.1016/j.addr.2007.06.008.

[149] G.R. Ogden, Alcohol and oral cancer, Alcohol. 35 (2005) 169–173. https://doi.org/https://doi.org/10.1016/j.alcohol.2005.04.002.

[150] F. van Roy, G. Berx, The cell-cell adhesion molecule E-cadherin, Cell. Mol. Life Sci. 65 (2008) 3756–3788. https://doi.org/10.1007/s00018-008-8281-1.

[151] J. Rejman, A. Bragonzi, M. Conese, Role of clathrin- and caveolae-mediated endocytosis in gene transfer mediated by lipo- and polyplexes, Mol. Ther. 12 (2005) 468–474. https://doi.org/https://doi.org/10.1016/j.ymthe.2005.03.038.

[152] C. Mineo, R.G. Anderson, Potocytosis, Histochem. Cell Biol. 116 (2001) 109–118. https://doi.org/10.1007/s004180100289.

[153] M. Wu, J. Fan, W. Gunning, M. Ratnam, Clustering of GPI-Anchored Folate Receptor Independent of Both Cross-Linking and Association with Caveolin, J. Membr. Biol. 159 (1997) 137–147. https://doi.org/10.1007/s002329900277.

[154] C.C. Bridges, A. El-Sherbeny, P. Roon, M. Shamsul Ola, R. Kekuda, V. Ganapathy, R.S. Cameron, P.L. Cameron, S.B. Smith, A Comparison of Caveolae

and Caveolin-1 to Folate Receptor α in Retina and Retinal Pigment Epithelium, Histochem. J. 33 (2001) 149–158. https://doi.org/10.1023/A:1017991925821.

[155] I. Mellman, G. Coukos, G. Dranoff, Cancer immunotherapy comes of age, Nature. 480 (2011) 480–489. https://doi.org/10.1038/nature10673.

[156] J.P. Richard, K. Melikov, H. Brooks, P. Prevot, B. Lebleu, L. V. Chernomordik, Cellular uptake of unconjugated TAT peptide involves clathrin-dependent endocytosis and heparan sulfate receptors, J. Biol. Chem. 280 (2005) 15300–15306. https://doi.org/10.1074/jbc.M401604200.

[157] M.F. Laspia, A.P. Rice, M.B. Mathews, HIV-1 Tat protein increases transcriptional initiation and stabilizes elongation, Cell. 59 (1989) 283–292. https://doi.org/10.1016/0092-8674(89)90290-0.

[158] A. Fittipaldi, A. Ferrari, M. Zoppé, C. Arcangeli, V. Pellegrini, F. Beltram, M. Giacca, Cell Membrane Lipid Rafts Mediate Caveolar Endocytosis of HIV-1 Tat Fusion Proteins, J. Biol. Chem. 278 (2003) 34141–34149. https://doi.org/10.1074/jbc.M303045200.

[159] J.P. Lim, P.A. Gleeson, Macropinocytosis: an endocytic pathway for internalising large gulps, Immunol. Cell Biol. 89 (2011) 836–843. https://doi.org/10.1038/icb.2011.20.

[160] Y.H. Kim, O.W. Webster, Water-Soluble Hyperbranched Polyphenylene; “A Unimolecular Micelle”?, J. Am. Chem. Soc. 112 (1990) 4592–4593. https://doi.org/10.1021/ja00167a094.

[161] P.J. Flory, Molecular Size Distribution in Three Dimensional Polymers. VI. Branched Polymers Containing A-R-Bf-1 Type Units, J. Am. Chem. Soc. 74 (1952) 2718–2723. https://doi.org/10.1021/ja01131a008.

[162] D.A. Tomalia, J.M.J. Fréchet, Discovery of dendrimers and dendritic polymers: A brief historical perspective, J. Polym. Sci. Part A Polym. Chem. 40 (2002) 2719–2728. https://doi.org/10.1002/pola.10301.

[163] D. Wang, T. Zhao, X. Zhu, D. Yan, W. Wang, Bioapplications of hyperbranched polymers, Chem. Soc. Rev. 44 (2015) 4023–4071. https://doi.org/10.1039/c4cs00229f.

[164] T. Higashihara, Y. Segawa, W. Sinananwanich, M. Ueda, Synthesis of hyperbranched polymers with controlled degree of branching, Polym. J. 44 (2012) 14–29. https://doi.org/10.1038/pj.2011.99.

[165] Y. Tezuka, H. Oike, Topological Polymer Chemistry: Systematic Classification of Nonlinear Polymer Topologies, J. Am. Chem. Soc. 123 (2001) 11570–11576. https://doi.org/10.1021/ja0114409.

[166] R. Dong, Y. Zhou, X. Zhu, Supramolecular dendritic polymers: From synthesis to applications, Acc. Chem. Res. 47 (2014) 2006–2016. https://doi.org/10.1021/ar500057e.

[167] S. Lee, K. Saito, H.R. Lee, M.J. Lee, Y. Shibasaki, Y. Oishi, B.S. Kim, Hyperbranched double hydrophilic block copolymer micelles of poly(ethylene oxide) and polyglycerol for pH-responsive drug delivery, Biomacromolecules. 13 (2012) 1190–1196. https://doi.org/10.1021/bm300151m.

[168] H. Tai, A. Tochwin, W. Wang, Thermoresponsive hyperbranched polymers via in Situ RAFT copolymerization of peg-based monomethacrylate and dimethacrylate monomers, J. Polym. Sci. Part A Polym. Chem. 51 (2013) 3751–3761. https://doi.org/10.1002/pola.26779.

[169] H. Tai, W. Wang, T. Vermonden, F. Heath, W.E. Hennink, C. Alexander, K.M. Shakesheff, S.M. Howdle, Thermoresponsive and photocrosslinkable PEGMEMA-PPGMA-EGDMA copolymers from a one-step ATRP synthesis, Biomacromolecules. 10 (2009) 822–828. https://doi.org/10.1021/bm801308q.

[170] Y. Zheng, S. Li, Z. Weng, C. Gao, Hyperbranched polymers: advances from synthesis to applications, Chem. Soc. Rev. 44 (2015) 4091–4130. https://doi.org/10.1039/C4CS00528G.

[171] M. Rogošić, H.J. Mencer, Z. Gomzi, Polydispersity index and molecular weight distributions of polymers, Eur. Polym. J. 32 (1996) 1337–1344. https://doi.org/10.1016/S0014-3057(96)00091-2.

[172] A. Goto, T. Fukuda, Effects of radical initiator on polymerization rate and polydispersity in nitroxide-controlled free radical polymerization, Macromolecules. 30 (1997) 4272–4277. https://doi.org/10.1021/ma9702152.

[173] D.S.W. Benoit, S. Srinivasan, A.D. Shubin, P.S. Stayton, Synthesis of folate-functionalized RAFT polymers for targeted siRNA delivery, Biomacromolecules. 12 (2011) 2708–2714. https://doi.org/10.1021/bm200485b.

[174] J. Loiseau, N. Doërr, J.-M. Suau, J.B. Egraz, M.F. Llauro, C. Ladaviere, J. Claverie, Synthesis and Characterization of Poly (acrylic acid) Produced by RAFT

Polymerization . Application as a Very Efficient Dispersant of CaCO 3 , Kaolin , and TiO 2, Macromolecules. 36 (2003) 3066–3077. https://doi.org/10.1021/ma0256744.

[175] H. Tai, C.L. Duvall, P.S. Stayton, A.S. Hoffman, W. Wang, pH-Responsive Hyperbranched Copolymers from One-pot RAFT Copolymerization of Propylacrylic Acid and Poly (Ethylene Glycol Diacrylate), Adv. Sci. Technol. 77 (2013) 333–342. https://doi.org/10.4028/www.scientific.net/AST.77.333.

[176] D. Kukulj, T.P. Davis, Mechanism of catalytic chain transfer in the free-radical polymerisation of methyl methacrylate and styrene, Macromol. Chem. Phys. 199 (1998) 1697–1708. https://doi.org/10.1002/(SICI)1521-3935(19980801)199:8<1697::AID-MACP1697>3.0.CO;2-Z.

[177] D. Stewart, C.T. Imrie, Role of C60 in the free radical polymerisation of styrene, Chem. Commun. (1996) 1383–1384. https://doi.org/10.1039/CC9960001383.

[178] S. Koltzenburg, M. Maskos, O. Nuyken, Ionic Polymerization BT - Polymer Chemistry, in: S. Koltzenburg, M. Maskos, O. Nuyken (Eds.), Springer Berlin Heidelberg, Berlin, Heidelberg, 2017: pp. 245–292. https://doi.org/10.1007/978-3-662-49279-6_10.

[179] A. Furuta, K. Okada, T. Fukuyama, Efficient Anionic Ring Opening Polymerization of Ethylene Oxide under Microfluidic Conditions, Bull. Chem. Soc. Jpn. 90 (2017) 838–842. https://doi.org/10.1246/bcsj.20170073.

[180] S.C.H.J. Turk, W.P. Kloosterman, D.K. Ninaber, K.P.A.M. Kolen, J. Knutova, E. Suir, M. Schürmann, P.C. Raemakers-Franken, M. Müller, S.M.A. de Wildeman, L.M. Raamsdonk, R. van der Pol, L. Wu, M.F. Temudo, R.A.M. van der Hoeven, M. Akeroyd, R.E. van der Stoel, H.J. Noorman, R.A.L. Bovenberg, A.C. Trefzer, Metabolic Engineering toward Sustainable Production of Nylon-6, ACS Synth. Biol. 5 (2016) 65–73. https://doi.org/10.1021/acssynbio.5b00129.

[181] E.J. Lee, H.J. Park, S.M. Kim, K.Y. Lee, Effect of Azo and Peroxide Initiators on a Kinetic Study of Methyl Methacrylate Free Radical Polymerization by DSC, Macromol. Res. 26 (2018) 322–331. https://doi.org/10.1007/s13233-018-6047-6.

[182] H. Riazi, A. A. Shamsabadi, M.C. Grady, A.M. Rappe, M. Soroush, Experimental and Theoretical Study of the Self-Initiation Reaction of Methyl Acrylate in Free-Radical Polymerization, Ind. Eng. Chem. Res. 57 (2018) 532–539. https://doi.org/10.1021/acs.iecr.7b04648.

[183] C. Chen, Redox-Controlled Polymerization and Copolymerization, ACS Catal. 8 (2018) 5506–5514. https://doi.org/10.1021/acscatal.8b01096.

[184] J. Zhou, X. Allonas, A. Ibrahim, X. Liu, Progress in the development of polymeric and multifunctional photoinitiators, Prog. Polym. Sci. 99 (2019) 101165. https://doi.org/https://doi.org/10.1016/j.progpolymsci.2019.101165.

[185] M. Buback, H. Frauendorf, F. Günzler, F. Huff, P. Vana, Determining initiator efficiency in radical polymerization by electrospray-ionization mass spectrometry, Macromol. Chem. Phys. 210 (2009) 1591–1599. https://doi.org/10.1002/macp.200900237.

[186] J. Franck, E. Rabinowitch, Some Remarks About Free Radicals and, Trans. Faraday Soc. 30 (1934) 120–130.

[187] J. Brandrup, E.. Immergut, E.. Grulke, Polymer Handbook, 4th ed., John Wiley & Sons, Ltd, New York, 1999.

[188] P.L. Nayak, R.K. Samal, Polymerization of acrylonitrile initiated by thiourea–chromium(VI) redox system, J. Polym. Sci. Polym. Chem. Ed. 15 (1977) 2603–2611. https://doi.org/10.1002/pol.1977.170151106.

[189] C.K.A. Gregson, V.C. Gibson, N.J. Long, E.L. Marshall, P.J. Oxford, A.J.P. White, Redox Control within Single-Site Polymerization Catalysts, J. Am. Chem. Soc. 128 (2006) 7410–7411. https://doi.org/10.1021/ja061398n.

[190] P. Garra, A. Kermagoret, A. Al Mousawi, F. Dumur, D. Gigmes, F. Morlet-Savary, C. Dietlin, J.P. Fouassier, J. Lalevée, New copper(i) complex based initiating systems in redox polymerization and comparison with the amine/benzoyl peroxide reference, Polym. Chem. 8 (2017) 4088–4097. https://doi.org/10.1039/c7py00726d.

[191] Y.K. Chong, E. Rizzardo, D.H. Solomon, Confirmation of the Mayo Mechanism for the Initiation of the Thermal Polymerization of Styrene, J. Am. Chem. Soc. 105 (1983) 7761–7762. https://doi.org/10.1021/ja00364a058.

[192] A. Ferrando, G. Goffredi, P.L. Cantini, E. Bencini, Identification of cis- and trans-1-phenyl-2-cyano-cyclobutane in the thermal copolymerization of styrene and acrylonitrile, Eur. Polym. J. 32 (1996) 899–908. https://doi.org/https://doi.org/10.1016/0014-3057(96)00004-3.

[193] M. Szwarc, M. Levy, R. Milkovich, POLYMERIZATION INITIATED BY ELECTRON TRANSFER TO MONOMER. A NEW METHOD OF FORMATION OF

BLOCK POLYMERS1, J. Am. Chem. Soc. 78 (1956) 2656–2657. https://doi.org/10.1021/ja01592a101.

[194] A.D. Jenkins, R.G. Jones, G. Moad, Terminology for reversible-deactivation radical polymerization previously called “controlled” radical or “living” radical polymerization (IUPAC recommendations 2010), Pure Appl. Chem. 82 (2010) 483–491. https://doi.org/10.1351/PAC-REP-08-04-03.

[195] D.H. Solomon, E. Rizzardo, P. Cacioli, Polymerization process and polymers produced thereby, (1986).

[196] V. Sciannamea, R. Jérôme, C. Detrembleur, In-situ nitroxide-mediated radical polymerization (NMP) processes: Their understanding and optimization, Chem. Rev. 108 (2008) 1104–1126. https://doi.org/10.1021/cr0680540.

[197] C.J. Hawker, A.W. Bosman, E. Harth, New polymer synthesis by nitroxide mediated living radical polymerizations, Chem. Rev. 101 (2001) 3661–3688. https://doi.org/10.1021/cr990119u.

[198] T.J. Connolly, J.C. Scaiano, Reactions of the “stable” nitroxide radical TEMPO. Relevance to “living” free radical polymerizations and autopolymerization of styrene, Tetrahedron Lett. 38 (1997) 1133–1136. https://doi.org/https://doi.org/10.1016/S0040-4039(96)02461-6.

[199] J. Nicolas, Y. Guillaneuf, C. Lefay, D. Bertin, D. Gigmes, B. Charleux, Nitroxide-mediated polymerization, Prog. Polym. Sci. 38 (2013) 63–235. https://doi.org/https://doi.org/10.1016/j.progpolymsci.2012.06.002.

[200] J.-S. Wang, K. Matyjaszewski, Controlled/" living" radical polymerization. atom transfer radical polymerization in the presence of transition-metal complexes, J. Am. Chem. Soc. 117 (1995) 5614–5615.

[201] M. Kato, M. Kamigaito, M. Sawamoto, T. Higashimura, Polymerization of methyl methacrylate with the carbon tetrachloride/dichlorotris-(triphenylphosphine) ruthenium (II)/methylaluminum bis (2, 6-di-tert-butylphenoxide) initiating system: possibility of living radical polymerization, Macromolecules. 28 (1995) 1721–1723.

[202] T. Pintauer, K. Matyjaszewski, Atom transfer radical addition and polymerization reactions catalyzed by ppm amounts of copper complexes, Chem. Soc. Rev. 37 (2008) 1087–1097. https://doi.org/10.1039/b714578k.

[203] K. Matyjaszewski, Atom Transfer Radical Polymerization (ATRP): Current status and future perspectives, Macromolecules. 45 (2012) 4015–4039. https://doi.org/10.1021/ma3001719.

[204] D.R. D'hooge, D. Konkolewicz, M.-F. Reyniers, G.B. Marin, K. Matyjaszewski, Kinetic Modeling of ICAR ATRP, Macromol. Theory Simulations. 21 (2012) 52–69. https://doi.org/10.1002/mats.201100076.

[205] G. Moad, E. Rizzardo, S.H. Thang, Living radical polymerization by the RAFT process, Aust. J. Chem. 58 (2005) 379–410.

[206] G. Moad, E. Rizzardo, S.H. Thang, Living radical polymerization by the RAFT process–a second update, Aust. J. Chem. 62 (2009) 1402–1472.

[207] G. Moad, E. Rizzardo, S.H. Thang, Living radical polymerization by the RAFT process–a third update, Aust. J. Chem. 65 (2012) 985–1076.

[208] D.J. Keddie, G. Moad, E. Rizzardo, S.H. Thang, RAFT Agent Design and Synthesis, Macromolecules. 45 (2012) 5321–5342. https://doi.org/10.1021/ma300410v.

[209] M. Semsarilar, V. Ladmiral, A. Blanazs, S.P. Armes, Cationic polyelectrolyte-stabilized nanoparticles via RAFT aqueous dispersion polymerization, Langmuir. 29 (2013) 7416–7424.

[210] N.J. Warren, S.P. Armes, Polymerization-induced self-assembly of block copolymer nano-objects via RAFT aqueous dispersion polymerization, J. Am. Chem. Soc. 136 (2014) 10174–10185.

[211] A. Postma, T.P. Davis, G. Moad, M.S. O'Shea, Thermolysis of RAFT-synthesized polymers. A convenient method for trithiocarbonate group elimination, Macromolecules. 38 (2005) 5371–5374.

[212] Y.K. Chong, G. Moad, E. Rizzardo, S.H. Thang, Thiocarbonylthio end group removal from RAFT-synthesized polymers by radical-induced reduction, Macromolecules. 40 (2007) 4446–4455.

[213] G. Moad, E. Rizzardo, S.H. Thang, End-functional polymers, thiocarbonylthio group removal/transformation and reversible addition–fragmentation–chain transfer (RAFT) polymerization, Polym. Int. 60 (2011) 9–25.

[214] H. Willcock, R.K. O'Reilly, End group removal and modification of RAFT polymers, Polym. Chem. 1 (2010) 149–157.

[215] X.P. Qiu, F.M. Winnik, Facile and efficient one-pot transformation of RAFT polymer end groups via a mild aminolysis/michael addition sequence, Macromol. Rapid Commun. 27 (2006) 1648–1653. https://doi.org/10.1002/marc.200600436.

[216] H. Shih, C.-C. Lin, Cross-linking and degradation of step-growth hydrogels formed by thiol–ene photoclick chemistry, Biomacromolecules. 13 (2012) 2003–2012.

[217] T.M. Legge, A.T. Slark, S. Perrier, Thermal stability of reversible addition–fragmentation chain transfer/macromolecular architecture design by interchange of xanthates chain-transfer agents, J. Polym. Sci. Part A Polym. Chem. 44 (2006) 6980–6987.

[218] C. Pino, V.H. Saez, L.H. Tagle, J.C. Vega, Aminolysis of 4-(alkoxythiocarbonylthio) benzenesulphonates and derivatives supported on anion exchangers, React. Polym. 12 (1990) 51–58.

[219] G. Lu, D. Wu, R. Fu, Studies on the synthesis and antibacterial activities of polymeric quaternary ammonium salts from dimethylaminoethyl methacrylate, React. Funct. Polym. 67 (2007) 355–366. https://doi.org/10.1016/j.reactfunctpolym.2007.01.008.

[220] Y.J. Liu, A. Pallier, J. Sun, S. Rudiuk, D. Baigl, M. Piel, E. Marie, C. Tribet, Non-monotonous variation of the LCST of light-responsive, amphiphilic poly(NIPAM) derivatives, Soft Matter. 8 (2012) 8446–8455. https://doi.org/10.1039/c2sm25959a.

[221] J.-F. Lutz, Ö. Akdemir, A. Hoth, Point by Point Comparison of Two Thermosensitive Polymers Exhibiting a Similar LCST: Is the Age of Poly(NIPAM) Over?, J. Am. Chem. Soc. 128 (2006) 13046–13047. https://doi.org/10.1021/ja065324n.

[222] J.L. García Ruano, A. Parra, J. Alemán, Efficient synthesis of disulfides by air oxidation of thiols under sonication, Green Chem. 10 (2008) 706–71. https://doi.org/10.1039/b800705e.

[223] C. Boyer, V. Bulmus, T.P. Davis, V. Ladmiral, J. Liu, S. Perrier, Bioapplications of RAFT polymerization, Chem. Rev. 109 (2009) 5402–5436.

[224] X. Yin, A.S. Hoffman, P.S. Stayton, Poly(N-isopropylacrylamide-co-propylacrylic acid) copolymers that respond sharply to temperature and pH, Biomacromolecules. 7 (2006) 1381–1385. https://doi.org/10.1021/bm0507812.

[225] G. Jiang, W. Chen, W. Xia, Environmental-Sensitive Hyperbranched Polymers as Drug Carriers, Des. Monomers Polym. 11 (2008) 105–122. https://doi.org/10.1163/156855508X298017.

[226] B.F. Palmer, D.J. Clegg, Oxygen sensing and metabolic homeostasis, Mol. Cell. Endocrinol. 397 (2014) 51–58. https://doi.org/https://doi.org/10.1016/j.mce.2014.08.001.

[227] M.G. Vander Heiden, L.C. Cantley, C.B. Thompson, P. Mammalian, C. Exhibit, A. Metabolism, Understanding the Warburg Effect : Cell Proliferation, Science (80-.). 324 (2009) 1029–1034. https://doi.org/10.1126/science.1160809.

[228] O. Warburg, Injuring of Respiration the Origin of Cancer Cells, Science (80-.). 123 (1956) 309–14. https://doi.org/10.1126/science.123.3191.309.

[229] Z. Xiong, B. Peng, X. Han, C. Peng, H. Liu, Y. Hu, Dual-stimuli responsive behaviors of diblock polyampholyte PDMAEMA-b-PAA in aqueous solution, J. Colloid Interface Sci. 356 (2011) 557–565. https://doi.org/10.1016/j.jcis.2011.01.067.

[230] J.I. Amalvy, E.J. Wanless, Y. Li, V. Michailidou, S.P. Armes, Y. Duccini, Synthesis and characterization of novel pH-responsive microgels based on tertiary amine methacrylates, Langmuir. 20 (2004) 8992–8999.

[231] B. Wang, X.D. Xu, Z.C. Wang, S.X. Cheng, X.Z. Zhang, R.X. Zhuo, Synthesis and properties of pH and temperature sensitive P(NIPAAm-co-DMAEMA) hydrogels, Colloids Surfaces B Biointerfaces. 64 (2008) 34–41. https://doi.org/10.1016/j.colsurfb.2008.01.001.

[232] S. Dai, P. Ravi, K.C. Tam, pH-Responsive polymers: synthesis, properties and applications, Soft Matter. 4 (2008) 435–449.

[233] C.P. Roe, P.D. Brass, The rate of particle growth in persulfate initiated emulsion polymerization, J. Polym. Sci. 24 (1957) 401–416.

[234] N. Murthy, J.R. Robichaud, D.A. Tirrell, P.S. Stayton, A.S. Hoffman, The design and synthesis of polymers for eukaryotic membrane disruption, J. Control. Release. 61 (1999) 137–143. https://doi.org/10.1016/S0168-3659(99)00114-5.

[235] T. Swift, L. Swanson, M. Geoghegan, S. Rimmer, The pH-responsive behaviour of poly(acrylic acid) in aqueous solution is dependent on molar mass, Soft Matter. 12 (2016) 2542–2549. https://doi.org/10.1039/c5sm02693h.

[236] G. Chen, A.S. Hoffman, graft copolymers of N-isopropylacrylamide and acrylic acid, Macromol. Rapid Commun. (1995) 175–182.

[237] and P.S.S. Jessica C. Garbern, Allan S. Hoffman, Injectable pH- and temperature-responsive poly(N- isopropylacrylamide-co-propylacrylic acid) copolymers for delivery of angiogenic growth factors, Biomacromolecules. 11 (2011) 1833–1839. https://doi.org/10.1021/bm100318z.Injectable.

[238] I. Anil, S.T. Gunday, A. Bozkurt, O. Alagha, Design of Crosslinked Hydrogels Comprising Poly (Vinylphosphonic Acid) and Bis [2-(Methacryloyloxy) Ethyl] Phosphate as an Efficient Adsorbent for Wastewater Dye Removal, Nanomaterials. 10 (2020) 131.

[239] S.J. Kim, C.K. Lee, S.I. Kim, Electrical/pH responsive properties of poly(2-acrylamido-2-methylpropane sulfonic acid)/hyaluronic acid hydrogels, J. Appl. Polym. Sci. 92 (2004) 1731–1736. https://doi.org/10.1002/app.20133.

[240] B. Balakrishnan, M. Mohanty, P.R. Umashankar, A. Jayakrishnan, Evaluation of an in situ forming hydrogel wound dressing based on oxidized alginate and gelatin, Biomaterials. 26 (2005) 6335–6342.

[241] G.W. Ashley, J. Henise, R. Reid, D. V Santi, Hydrogel drug delivery system with predictable and tunable drug release and degradation rates, Proc. Natl. Acad. Sci. 110 (2013) 2318–2323.

[242] T.R. Hoare, D.S. Kohane, Hydrogels in drug delivery: Progress and challenges, Polymer (Guildf). 49 (2008) 1993–2007. https://doi.org/10.1016/j.polymer.2008.01.027.

[243] J. Jiang, S. Thayumanavan, Synthesis and characterization of amine-functionalized polystyrene nanoparticles, Macromolecules. 38 (2005) 5886–5891.

[244] B. Newland, H. Tai, Y. Zheng, D. Velasco, A. Di Luca, S.M. Howdle, C. Alexander, W. Wang, A. Pandit, A highly effective gene delivery vector - Hyperbranched poly(2-(dimethylamino)ethyl methacrylate) from in situ deactivation enhanced ATRP, Chem. Commun. 46 (2010) 4698–4700. https://doi.org/10.1039/c0cc00439a.

[245] W.O.S. Doherty, C.M. Fellows, S. Gorjian, E. Senogles, W.H. Cheung, Flocculation and sedimentation of cane sugar juice particles with cationic homo-and copolymers, J. Appl. Polym. Sci. 90 (2003) 316–325.

[246] A. Roointan, J. Farzanfar, S. Mohammadi-Samani, A. Behzad-Behbahani, F. Farjadian, Smart pH responsive drug delivery system based on poly (HEMA-co-DMAEMA) nanohydrogel, Int. J. Pharm. 552 (2018) 301–311.

[247] T. Zhao, H. Zhang, B. Newland, A. Aied, D. Zhou, W. Wang, Significance of branching for transfection: Synthesis of highly branched degradable functional poly(dimethylaminoethyl methacrylate) by vinyl oligomer combination, Angew. Chemie - Int. Ed. 53 (2014) 6095–6100. https://doi.org/10.1002/anie.201402341.

[248] M.I. Gibson, R.K. O'Reilly, To aggregate, or not to aggregate? considerations in the design and application of polymeric thermally-responsive nanoparticles., Chem. Soc. Rev. 42 (2013) 7204–13. https://doi.org/10.1039/c3cs60035a.

[249] A. Hoth, Point by Point Comparison of Two Thermosensitive Polymers Exhibiting a Similar LCST : Is the Age of Poly (NIPAM) Over ?, J. Am. Chem. Soc. 128 (2006) 13046–13047. https://doi.org/10.1021/ja065324n.

[250] I. Idziak, D. Avoce, D. Lessard, D. Gravel, X.X. Zhu, Thermosensitivity of Aqueous Solutions of Poly(N,N-diethylacrylamide), Macromolecules. 32 (1999) 1260–1263. https://doi.org/10.1021/ma981171f.

[251] Z. Al-Ahmady, K. Kostarelos, Chemical Components for the Design of Temperature-Responsive Vesicles as Cancer Therapeutics, Chem. Rev. 116 (2016) 3883–3918. https://doi.org/10.1021/acs.chemrev.5b00578.

[252] G. Pasut, F. Canal, L. Dalla Via, S. Arpicco, F.M. Veronese, O. Schiavon, Antitumoral activity of PEG-gemcitabine prodrugs targeted by folic acid, J. Control. Release. 127 (2008) 239–248. https://doi.org/10.1016/j.jconrel.2008.02.002.

[253] A.A. Gabizon, Pegylated Liposomal Doxorubicin: Metamorphosis of an Old Drug into a New Form of Chemotherapy, Cancer Invest. 19 (2001) 424–436. https://doi.org/10.1081/CNV-100103136.

[254] A. Jain, S.K. Jain, PEGylation: An approach for drug delivery. A review, Crit. Rev. Ther. Drug Carrier Syst. 25 (2008) 403–447. https://doi.org/10.1615/CritRevTherDrugCarrierSyst.v25.i5.10.

[255] M.C. Parrott, J.M. DeSimone, Relieving PEGylation, Nat. Chem. 4 (2012) 13–14. https://doi.org/10.1038/nchem.1230.

[256] V. Khare, A. Singh, G. Mahajan, N. Alam, S. Kour, M. Gupta, A. Kumar, G. Singh, S.K. Singh, A.K. Saxena, D.M. Mondhe, P.N. Gupta, Long-circulatory nanoparticles for gemcitabine delivery: Development and investigation of

pharmacokinetics and in-vivo anticancer efficacy, Eur. J. Pharm. Sci. 92 (2016) 183–193. https://doi.org/10.1016/j.ejps.2016.07.007.

[257] Z. Liu, J.T. Robinson, X. Sun, H. Dai, PEGylated Nanographene Oxide for Delivery of Water-Insoluble Cancer Drugs, J. Am. Chem. Soc. 130 (2008) 10876–10877. https://doi.org/10.1021/ja803688x.

[258] M. Vellard, The enzyme as drug: application of enzymes as pharmaceuticals, Curr. Opin. Biotechnol. 14 (2003) 444–450. https://doi.org/https://doi.org/10.1016/S0958-1669(03)00092-2.

[259] J.K. Dozier, M.D. Distefano, Site-specific pegylation of therapeutic proteins, Int. J. Mol. Sci. 16 (2015) 25831–25864. https://doi.org/10.3390/ijms161025831.

[260] M. Swierczewska, K.C. Lee, S. Lee, What is the future of PEGylated therapies?, Expert Opin. Emerg. Drugs. 20 (2015) 531–536. https://doi.org/10.1517/14728214.2015.1113254.

[261] J.M. Harris, R.B. Chess, Effect of pegylation on pharmaceuticals, Nat. Rev. Drug Discov. 2 (2003) 214–221. https://doi.org/10.1038/nrd1033.

[262] S. Hadadian, H. Mirzahoseini, D.N. Shamassebi, M.A. Shokrgozar, S. Bouzari, S. Asgari, Chemoselective pegylation of cysteine analogs of human basic fibroblast growth factor (hbFGF) - Design and expression, Trop. J. Pharm. Res. 13 (2014) 1601–1607. https://doi.org/10.4314/tjpr.v13i10.5.

[263] L.H. Belén, C. de O. Rangel-Yagui, J.F. Beltrán Lissabet, B. Effer, M. Lee-Estevez, A. Pessoa, R.L. Castillo, J.G. Farías, From Synthesis to Characterization of Site-Selective PEGylated Proteins , Front. Pharmacol. . 10 (2019) 1450. https://www.frontiersin.org/article/10.3389/fphar.2019.01450.

[264] B. Neises, W. Steglich, Simple Method for the Esterification of Carboxylic Acids, Angew. Chemie Int. Ed. English. 17 (1978) 522–524. https://doi.org/10.1002/anie.197805221.

[265] A. Jafarizad, A. Taghizadehgh-Alehjougi, M. Eskandani, M. Hatamzadeh, M. Abbasian, R. Mohammad-Rezaei, M. Mohammadzadeh, B. Toğar, M. Jaymand, PEGylated graphene oxide/Fe 3O 4 nanocomposite: Synthesis, characterization, and evaluation of its performance as de novo drug delivery nanosystem, Biomed. Mater. Eng. 29 (2018) 177–190. https://doi.org/10.3233/BME-171721.

[266] H.S. Yoo, T.G. Park, Folate receptor targeted biodegradable polymeric doxorubicin micelles, J. Control. Release. 96 (2004) 273–283. https://doi.org/https://doi.org/10.1016/j.jconrel.2004.02.003.

[267] H.S. Yoo, T.G. Park, Folate-receptor-targeted delivery of doxorubicin nano-aggregates stabilized by doxorubicin–PEG–folate conjugate, J. Control. Release. 100 (2004) 247–256. https://doi.org/https://doi.org/10.1016/j.jconrel.2004.08.017.

[268] C.C. Ward, J.I. Kleinman, D.K. Nomura, NHS-Esters As Versatile Reactivity-Based Probes for Mapping Proteome-Wide Ligandable Hotspots, ACS Chem. Biol. 12 (2017) 1478–1483. https://doi.org/10.1021/acschembio.7b00125.

[269] A.H.K. Al Temimi, H.I.V. Amatdjais-Groenen, Y.V. Reddy, R.H. Blaauw, H. Guo, P. Qian, J. Mecinović, The nucleophilic amino group of lysine is central for histone lysine methyltransferase catalysis, Commun. Chem. 2 (2019) 1–14. https://doi.org/10.1038/s42004-019-0210-8.

[270] D. Hwang, K. Tsuji, H. Park, T.R. Burke, C. Rader, Site-Specific Lysine Arylation as an Alternative Bioconjugation Strategy for Chemically Programmed Antibodies and Antibody–Drug Conjugates, Bioconjug. Chem. 30 (2019) 2889–2896. https://doi.org/10.1021/acs.bioconjchem.9b00609.

[271] C.D. Spicer, B.G. Davis, Selective chemical protein modification, Nat. Commun. 5 (2014) 4740. https://doi.org/10.1038/ncomms5740.

[272] A. Sochaj, K. Świderska, J. Otlewski, Current methods for the synthesis of homogeneous antibody-drug conjugates, Biotechnol. Adv. 26 (2015). https://doi.org/10.1016/j.biotechadv.2015.05.001.

[273] D. Alvarez dorta, david deniaud, M. Mével, S.G. Gouin, Tyrosine conjugation methods for protein labelling, Chem. – A Eur. J. n/a (2020). https://doi.org/10.1002/chem.202001992.

[274] N. Stephanopoulos, M.B. Francis, Choosing an effective protein bioconjugation strategy, Nat. Chem. Biol. 7 (2011) 876–884. https://doi.org/10.1038/nchembio.720.

[275] E.M. Sletten, C.R. Bertozzi, Bioorthogonal chemistry: fishing for selectivity in a sea of functionality, Angew. Chemie Int. Ed. 48 (2009) 6974–6998.

[276] S.D. Tilley, N.S. Joshi, M.B. Francis, Proteins: Chemistry and Chemical Reactivity, Wiley Encycl. Chem. Biol. (2008) 1–16. https://doi.org/doi:10.1002/9780470048672.wecb493.

[277] A. Dirksen, T.M. Hackeng, P.E. Dawson, Nucleophilic Catalysis of Oxime Ligation, Angew. Chemie Int. Ed. 45 (2006) 7581–7584. https://doi.org/10.1002/anie.200602877.

[278] O.İ. Şentürk, Peptide-based bioinspired functional materials, (2016).

[279] N.J. Agard, J.A. Prescher, C.R. Bertozzi, A strain-promoted [3+ 2] azide−alkyne cycloaddition for covalent modification of biomolecules in living systems, J. Am. Chem. Soc. 126 (2004) 15046–15047.

[280] W.Q. Tian, Y.A. Wang, Mechanisms of Staudinger Reactions within Density Functional Theory, J. Org. Chem. 69 (2004) 4299–4308. https://doi.org/10.1021/jo049702n.

[281] C.I. Schilling, N. Jung, M. Biskup, U. Schepers, S. Bräse, Bioconjugation viaazide–Staudinger ligation: an overview, Chem. Soc. Rev. 40 (2011) 4840–4871. https://doi.org/10.1039/C0CS00123F.

[282] S. Noble, K.L. Goa, Gemcitabine, Drugs. 54 (1997) 447–472. https://doi.org/10.2165/00003495-199754030-00009.

[283] H. Ueno, K. Kiyosawa, N. Kaniwa, Pharmacogenomics of gemcitabine: can genetic studies lead to tailor-made therapy?, Br. J. Cancer. 97 (2007) 145–151.

[284] L. De Sousa Cavalcante, G. Monteiro, Gemcitabine: Metabolism and molecular mechanisms of action, sensitivity and chemoresistance in pancreatic cancer, Eur. J. Pharmacol. 741 (2014) 8–16. https://doi.org/10.1016/j.ejphar.2014.07.041.

[285] W. Plunkett, P. Huang, Y.Z. Xu, V. Heinemann, R. Grunewald, V. Gandhi, Gemcitabine: metabolism, mechanisms of action, and self-potentiation, Semin. Oncol. 22 (1995) 3—10. http://europepmc.org/abstract/MED/7481842.

[286] J. Zhang, F. Visser, K.M. King, S.A. Baldwin, J.D. Young, C.E. Cass, The role of nucleoside transporters in cancer chemotherapy with nucleoside drugs, Cancer Metastasis Rev. 26 (2007) 85–110.

[287] R. Maréchal, J. Bachet, J.R. Mackey, C. Dalban, P. Demetter, K. Graham, A. Couvelard, M. Svrcek, A. Bardier–Dupas, P. Hammel, Levels of gemcitabine transport and metabolism proteins predict survival times of patients treated with gemcitabine for pancreatic adenocarcinoma, Gastroenterology. 143 (2012) 664–674.

[288] M.L. Alvarellos, J. Lamba, K. Sangkuhl, C.F. Thorn, L. Wang, D.J. Klein, R.B. Altman, T.E. Klein, PharmGKB summary: Gemcitabine pathway, Pharmacogenet. Genomics. 24 (2014) 564–574. https://doi.org/10.1097/FPC.0000000000000086.

[289] J. Ciccolini, C. Serdjebi, G.J. Peters, E. Giovannetti, Pharmacokinetics and pharmacogenetics of Gemcitabine as a mainstay in adult and pediatric oncology: an EORTC-PAMM perspective, Cancer Chemother. Pharmacol. 78 (2016) 1–12. https://doi.org/10.1007/s00280-016-3003-0.

[290] L. De Sousa Cavalcante, G. Monteiro, Gemcitabine: Metabolism and molecular mechanisms of action, sensitivity and chemoresistance in pancreatic cancer, Eur. J. Pharmacol. 741 (2014) 8–16. https://doi.org/10.1016/j.ejphar.2014.07.041.

[291] S. Ohhashi, K. Ohuchida, K. Mizumoto, H. Fujita, T. Egami, J. Yu, H. Toma, S. Sadatomi, E. Nagai, M. Tanaka, Down-regulation of deoxycytidine kinase enhances acquired resistance to gemcitabine in pancreatic cancer, Anticancer Res. 28 (2008) 2205–2212.

[292] D.Y. Bouffard, J. Laliberté, R.L. Momparler, Kinetic studies on 2’, 2’-difluorodeoxycytidine (Gemcitabine) with purified human deoxycytidine kinase and cytidine deaminase, Biochem. Pharmacol. 45 (1993) 1857–1861.

[293] E. Artin, J. Wang, G.J.S. Lohman, K. Yokoyama, G. Yu, R.G. Griffin, G. Bar, J. Stubbe, Insight into the mechanism of inactivation of ribonucleotide reductase by gemcitabine 5′-diphosphate in the presence or absence of reductant, Biochemistry. 48 (2009) 11622–11629.

[294] M. Dasari, A.P. Acharya, D. Kim, S. Lee, S. Lee, J. Rhea, R. Molinaro, N. Murthy, H-Gemcitabine: A New Gemcitabine Prodrug for Treating Cancer, Bioconjug. Chem. 24 (2013) 4–8. https://doi.org/10.1021/bc300095m.

[295] J. Bucevičius, G. Lukinavičius, R. Gerasimaitė, The use of hoechst dyes for DNA staining and beyond, Chemosensors. 6 (2018) 18.

[296] K. Matsushita, T. Okuda, S. Mori, M. Konno, H. Eguchi, A. Asai, J. Koseki, Y. Iwagami, D. Yamada, H. Akita, T. Asaoka, T. Noda, K. Kawamoto, K. Gotoh, S. Kobayashi, Y. Kasahara, K. Morihiro, T. Satoh, Y. Doki, M. Mori, H. Ishii, S. Obika, A Hydrogen Peroxide Activatable Gemcitabine Prodrug for the Selective Treatment of Pancreatic Ductal Adenocarcinoma, ChemMedChem. 14 (2019) 1384–1391. https://doi.org/10.1002/cmdc.201900324.

[297] V. Khare, W. Al Sakarchi, P.N. Gupta, A.D.M. Curtis, C. Hoskins, Synthesis and characterization of TPGS–gemcitabine prodrug micelles for pancreatic cancer therapy, RSC Adv. 6 (2016) 60126–60137.

[298] V. Khare, W. Al Sakarchi, P.N. Gupta, A.D.M. Curtis, C. Hoskins, Correction: Synthesis and characterization of TPGS–gemcitabine prodrug micelles for pancreatic cancer therapy, RSC Adv. 7 (2017) 12598.

[299] V. Khare, W. Al Sakarchi, P.N. Gupta, A.D.M. Curtis, C. Hoskins, Further correction: Synthesis and characterization of TPGS–gemcitabine prodrug micelles for pancreatic cancer therapy, RSC Adv. 7 (2017) 17367.

Chapter Two – Analytical Techniques and Characterisation Methodology

2.1 Overview

This chapter describes the basic principles of the analytical techniques and characterisation methodology utilised in this thesis in order to obtain the results described in the results chapters following. Therefore the mathematical basis of these techniques will be described so that a greater understanding of the resulting spectra in the following can be obtained. These include Nuclear Magnetic Resonance (NMR), Gel Permeation Chromatography (GPC), Fourier Transform Infra-Red (FTIR), Ultra Violet Spectroscopy (UV), Mass Spectrometry (MS), Dynamic Light Scattering (DLS) and imaging techniques (confocal). Experimental procedures for the synthesis of polymers, linkers and other materials used throughout the project can be found in their respective chapter. Therefore, the focus herein is to introduce these analytical techniques to the reader, through their mathematical foundations so that a better understanding of the results presented and discussed hereafter can be obtained. Conclusions will be drawn after each subsection highlighting how the technique was used and will signpost to relevant literature showcasing the importance of the technique on similar materials.

2.2 Charaterisation Techniques

2.2.1 Nuclear Magnetic Resonance (NMR)

Nuclear magnetic resonance was first described in 1938 by Isidor Rabi [1]. Whilst traditional NMR machines were difficult to operate and vastly too expensive for average chemist to afford, hardware associated with the technique has advanced greatly up to the current day and can be found in most organic based laboratories. The

principles behind the use of NMR first described by Rabi, has led to NMR becoming the one of the main techniques used for structure elucidation owing to the ability for the collection of chemical, physical, structural and electronic data relating to molecules via the "chemical shift" obtained and it's use with a variety of nuclei with some of the most commonly used NMR spectroscopic techniques involve the following: ^{1}H, ^{13}C, ^{15}N, ^{19}F and ^{31}P, although there is a plethora of NMR active nuclei, with frequency tuning of the instrument to specific nuclear resonance required in order to generate useful spectra [2].

First and foremost, in order to generate "chemical shift" data, which is notated as p.p.m (parts per million) [3] nuclear spin within the sample to be analysed are subjected to an external magnetic field (B_0), in order to remove the random spin states within the sample and thus nucleus either align themselves with or against the external field. This then allows energy transfer within the nucleus (ΔE) from a ground to excited state, upon relaxation electromagnetic energy is released and detected by the machine, resulting in NMR spectra. With this in mind, the emitted electromagnetic energy is directly proportional to the field applied via the following equation (eq. 2-1).

$$v = \frac{\gamma B_0}{2\pi} \qquad \textit{(eq. 2- 1)}$$

Where B_0 is the external magnetic field and γ related to the magnetogyric ratio. Although this equation does not take into account "shielding" of the magnetic field by electrons in the local nuclei environment and therefore can be re-written as such (eq. 2-2).

$$v = \frac{\gamma}{2\pi} B_0(1 - \sigma) \qquad \textit{(eq. 2-2)}$$

Where σ directly relates to the shielding constant. This then relates to chemical shift via the following equation (eq. 2-3) [2].

$$\delta = \frac{Frequency\ of\ observed\ signal - Frequency\ of\ refence}{Spectrometer\ Frequency}\ x\ 10^6 \qquad \textit{(eq. 2-3)}$$

Whilst chemical shift can allow for structure elucidation of molecules, more complex samples may require further more comprehensive analysis. Therefore, both spin-spin coupling and the associated coupling constant can allow for identical groups to be distinguished via their chemical neighbours, via identifiable splitting patterns within peaks such as doublets, triplets and multiplets. Where the integrations of

presented peaks (both those that display coupling patterns and those that do not) represent the number of nuclei that correspond to that peak, with respect to the other peaks in the spectra. For instance, a peak with an integration of 2 when compared to a peak of integration 1 suggests that the former has twice as many nuclei within that chemical environment as the latter. Hence, it is imperative that the analyst has a clear understanding of the proposed structure so that such a ratio can be used effectively when deducing structures via this method.

Furthermore, as the name suggests Nuclear Magnetic Resonance deals with only nuclei of the compound in question, but more specifically the nuclear spins they present, and as such it is possible for nuclei in neighbouring chemical environments on the same structure to interact with one another. Whilst chemically identical nuclei do not present spin-spin coupling, non-equivalent nuclei will. For simplicity ^{1}H NMR spin-spin couplings will be discussed, with magnetic nucleus A coupling to N equivalent nuclei with spin I. Splitting patterns therefore can be deduced prior to NMR analysis using the following equation.

Taking into account the spin of hydrogen at $\pm\frac{1}{2}$ [2] coupling to three N nuclei (eg. Methyl group) the following equation would then solve as (eq. 2-4):

$$2 * 3 * \frac{1}{2} + 1 = 4\, peaks \qquad \textit{(eq. 2- 4)}$$

Therefore, as the hydrogen is coupling to 3 N nuclei and splitting into 4 peaks this is commonly called the N+1 rule. Furthermore, intensities of peaks when split into corresponding coupling patterns can be further validated via “Pascal’s Triangle” (**Table 2-1)**. In this way it is possible to deduce further whether a coupling patterns occurs as a result of a single coupling pattern such as a quintet (5 splits) or occurs as a result of a doublet and triplet in close proximity. Furthermore, coupling patterns such as a doublet of doublet can be deceiving as a quartet and thus, by use of the Pascal’s Triangle technique researchers can ensure that their analysis is robust and accurate by use of simple analytical methods.

Table 2- 1: Splitting patterns of NMR peaks and corresponding peak intensities

Splitting Pattern	Ratio of Peak intensity
Singlet	1
Doublet	1:1
Triplet	1:2:1
Quartet	1:3:3:1
Quintet	1:4:6:4:1
Sextet	1:5:10:10:5:1

It is worth noting however, as spins within nuclei become more complex (e.g. ^{17}O has a spin of 5/2) it cannot be as simple as N+1. For instance taking into account ^{17}O coupling to 1 N nuclei and inserting into the formula solves as such (eq. 2-5):

$$2 * 1 * \frac{5}{2} + 1 = 6\ peaks \qquad \textit{(eq. 2-5)}$$

In addition to the splitting pattern generated via coupling, the analyst can use the J constants generated in order to further deduce the location of chemically distinguishable nuclei within a product. The J constant in ^{1}H NMR for instance is the measure of the interaction between a pair of protons and is written as an output in Hz. It can be used to determine which peaks within an NMR spectra are coupling with one

another or whether hydrogens sit *cis* or *trans* along a pi bond, whilst germinal hydrogens may also be characterised using the same technique [4]. (**Figure 2-1)**.

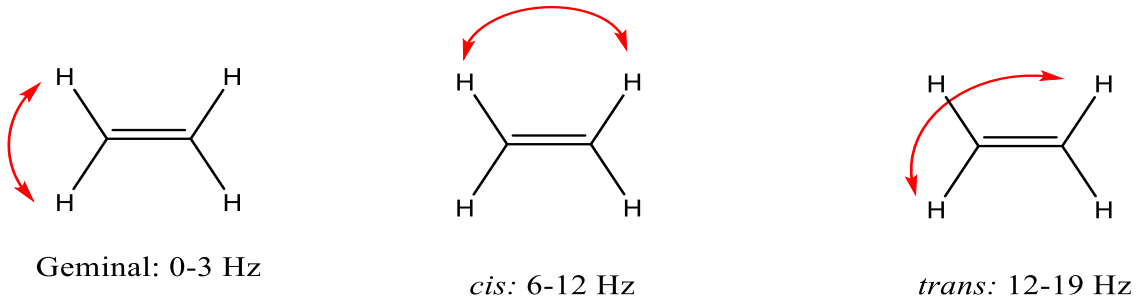

Figure 2- 1: J value estimations for pi bonded hydrogens

For sample preparation in NMR spectroscopy it is always advised to use a deuterated solvent for dissolution of the material to be analysed. This provides two main advantages, when compared to using non-deuterated solvents (i.e. $CDCl_3$ is used in lieu of $CHCl_3$). Firstly, by use of deuterated solvent the NMR spectrum is not “swamped” and heavily dampened due to solvent peak allowing the spectrum to be readily analysed without peaks being lost to background noise and good resolution of splitting patterns, although since most deuterated solvents contain 97%+ of deuterium and are never 100% isotopically switched there will be a residual solvent peak present within the obtained spectrum. Therefore, the use of $CDCl_3$ as a NMR solvent will generally yield a chloroform peak at 7.26 p.p.m. [5]. Secondly, by use of deuterium the NMR machine is able to “lock” to deuterium and accurately predict 0 ppm (TMS peak) as the difference between the two is well known, thus eliminating the need for TMS to be added to deuterated solvents or samples during the sample preparation process. With this in mind, the spectrometer also uses the lock to deuterium in order to accurately assess the required field strength throughout the experiment. Therefore,

the NMR spectrometer can measure the deuterium absorption of the solvent and adjust the field strength in order to keep it constant throughout the experiment.

Throughout this thesis a Bruker Ultrasheild Plus 400 NMR machine was used for the NMR characterisation of compounds with a sample concentration of 10 mg/ml for 16 scans unless otherwise specified (**Image 2-1)**.

Image 2- 1: The Bruker 400 MHz Nuclear Magnetic Resonance machine used predominately throughout this project

NMR throughout this project was therefore used to obtain ^{1}HNMR spectra for the compounds synthesized. This section therefore has neglected to go into detail on 2D NMR techniques as these sat outside the remit of the project. Briefly, 2D techniques such as correlation spectroscopy (COSY) plot spectra on both a horizontal and vertical axis and are useful for ascertaining which protons are coupling with one another, such as in NMR spectra of carbohydrates[6–8]. NMR of polymeric compounds does encounter some difficulties due to the vast amount of hydrogens and carbons chains contained within. Therefore, it is commonplace to see low resolution of NMR spectra of polymeric compounds where splitting patterns are absent or indistinguishable from a singlet peak. Thus, good knowledge of the NMR spectra of monomeric building blocks is required with accurate predictions of peak losses (such as vinylic hydrogens being consumed) is required in order to accurately characterize compounds. A good example of polymer NMR characterization is found within this paper by Tochwin et al. where characteristic monomer peaks were used in order to aid NMR interpretation [9]

2.2.2 Size Exclusion Analysis (SEC)

Polymers in general can have varying properties, product to product, despite an identical monomer composition [10–12]. For instance, Polystyrene can be found in either a liquid, as a viscous oil, or solid state at room temperature; and this variation is due to the differences in the molecular weight alongside distributions and dispersity of the individual polymer chains [13]. Therefore, a key factor in the characterisation of macromolecules is the observation of the molecular weight and the distribution of such. Two methods of reporting the molecular weight are commonly reported by researchers the number average molecular weight (M_n) and the weight average molecular weight (M_w) and the ratio of these two values allows the calculation of the poly dispersity index within the macromolecular product (Đ). Therefore, accurate calculations of each are vital to elucidate the properties of the given polymer with

respect to the molecular weights and dispersity. Hence, M_n can be calculated as such (eq. 2-6) and M_w (eq. 2-7)

$$M_n = \frac{w}{\sum_{i=1}^{\infty} N_i} = \frac{\sum_{i=1}^{\infty} w_i}{\sum_{i=1}^{\infty} N_i} = \frac{\sum_{i=1}^{\infty} N_i M_i}{\sum_{i=1}^{\infty} N_i}$$

$$M_w = \frac{\sum_{i=1}^{\infty} w_i M_i}{\sum_{i=1}^{\infty} w_i} = \frac{\sum_{i=1}^{\infty} N_i M_i^2}{\sum_{i=1}^{\infty} N_i M_i} \qquad \textit{(eq. 2-7)}$$

(eq. 2-6)

Where w_i, N_i and M_i correspond to the weight, number of molecules and the molecular weight of each species present (i) respectively. In this respect N_i indicates the number of molecules with mass M_i present.

Once these have been calculated the dispersity is as follows (eq. 2–8):

$$Đ = \frac{M_w}{M_n} \qquad \textit{(eq. 2-8)}$$

Owing to the nature of the calculations, dispersity is presented as a number ≥1, where 1 presents itself as a completely uniformed distribution of polymer chains, as M_n is equal to M_w [14]. Where living polymerisation techniques such as ATRP [15,16], NMP [17,18] and RAFT [19,20] polymerisations tend to achieve dispersity values towards 1, owing to enhanced controlled when compared to free radical polymerisations.

The primary source of characterisation and data collection for this purpose therefore is the use of Size Exclusion Chromatography, also known as Gel Permeation Chromatography as both terminologies are used interchangeably. The principle behind this technique separation in relation to size of molecule, which directly correlates to the hydrodynamic volume of the sample rather than the molecular weight itself. Thus, the researcher is not collecting data on the sample mass per say, such as

expected in mass spectroscopy techniques, but the size of the molecule to garner a relative molecular weight, compared to known calibration standards.

SEC is a rapid separation technique, where polymers are separated through a column packed with highly porous beads. As the polymer sample is pumped through alongside the carrier solvent the beads within the column act as sieves. Larger molecules as they cannot pass through the beads are quickly eluted as they travel in the gaps between pores whereas smaller molecules are retarded in their elution time due to their ability to pass through pores, hence elongating travel time **(Figure 2-2).**

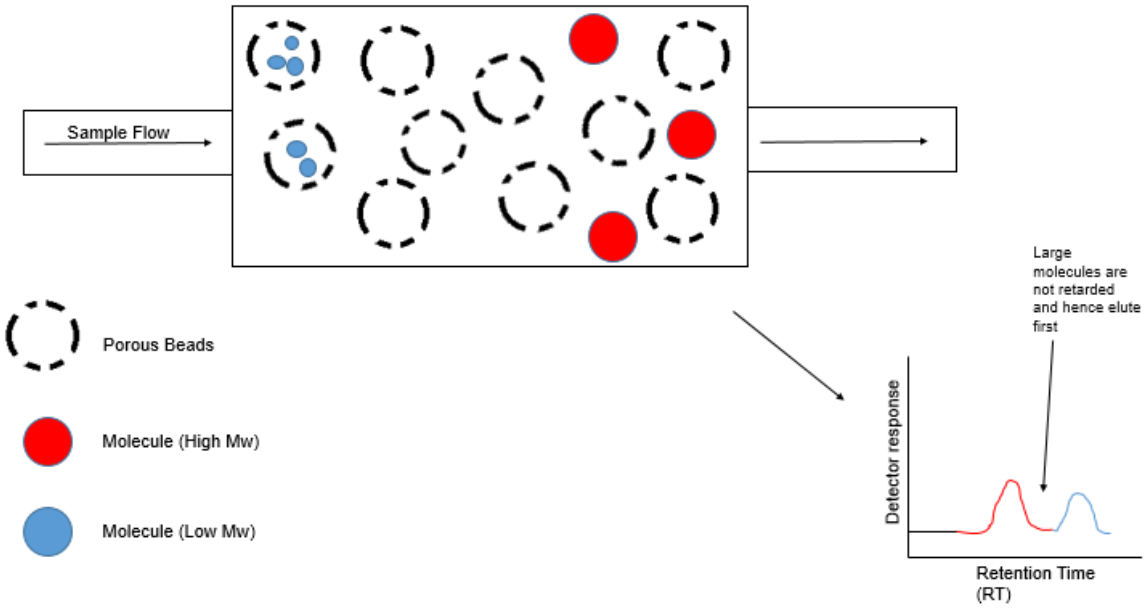

Figure 2- 2: Separation of molecules within a single sample based on size

In their current use it is not unusual to see SEC machines equipped with a variety of different detectors such as: Refractive Index (RI), Ultra-Violet (UV), Viscometer, Dynamic Light Scattering (DLS), Fluorescence and IR/Raman. It is therefore beneficial to use “triple” or “double” detection when the analysis of macromolecules is taking place as to ensure that there is more accuracy within SEC results. In addition to this whilst detection using methods such as RI garner a relative molecular weight, as in the molecular weight of the sample is relative to the calibrations ran previously and the curve established, methods such as DLS allow for an absolute molecular weight of a compound to be established. Throughout this project samples were kindly run in University College Dublin via the Prof. Wenxin Wang group on their

Agilent 1260 Infinity machine equipped with PolarGel-M, 7.5 x 300 mm, 8 µm, HPLC column (dual) and PolarGel-M, 7.5 x 50 mm, 8 µm guard column (Agilent Technologies Ltd.) utilising DMF as the eluent solvent system (additive 0.1% w/v LiBr). Flow rate was set at 1 ml/min using single detection via RI at an operating temperature of 40°C. With the RI detection technique polymers are characterised by use of measurement of their refractive index compared to the solvent system used, whilst this had led to I becoming a "universal detector" as it can detect any compound that causes a fluctuation in refractive index low sensitivity is the trade-off analysts must pay, meaning an increase in concentration of analyte is generally required. In principal a RI detector works via the use of a flow cell with two compartments a solvent compartment and an analyte compartment. Light is show and the difference of refractive index between the two compartments is measured and when a difference between the two is established the data is logged, which is visible to analyst as a peak in the chromatogram, it is also worth noting that the refractive index of DMF is 1.429. Hence, calibration curves were established via the use of poly(methylmethacrylate) PMMA standards (Agilent Technologies Lts.) and these curves can be found in **Tables 2-2, 2-3.**

Table 2- 2: Calibration data for GPC curve 08_02_17

Point	Retention Time (mins)	M_w (g/mol)	Log M_w	Percent error
1	10.68333	955000	5.980003	-1.37
2	11.16667	569000	5.755112	1.46
3	11.66667	332800	5.522183	0.10
4	12.73333	121600	5.084934	0.14
5	13.4	67400	4.82866	-0.68
6	14.36667	31110	4.4929	4.26
7	15.23333	13300	4.123852	-4.81
8	15.88333	7360	3.866878	-3.09
9	17.18333	1950	3.290035	3.15
10	17.75	1010	3.004321	7.77
11	18.08333	550	2.740363	-7.86

Table 2- 3: Calibration data for GPC curve 08_07_18

Point	Retention time (mins)	M_w (g/mol)	Log M_w	Percent error
1	10.86667	955000	5.980003	-3.87
2	11.41667	569000	5.755112	-4.11
3	11.93333	332800	5.522183	-9.68
4	13.03333	121600	5.084934	-7.06
5	13.71667	67400	4.82866	-1.80
6	16.26667	7360	3.866878	14.57
7	17.61667	1950	3.290035	9.02
8	18.18333	1010	3.004321	-3.27

Both calibration curves displayed error within 10% with the exception of point 6 in curve 08_07_18 which had an error of ~14%. For HBP3070 HBP4060 and HBP5050 discussed in more detail in chapter 3 calibration curve 08_02_17 was used. For all materials thereafter curve 08_07_18 was used.

2.2.3 Fourier Transform Infra-Red (FTIR)

FTIR has been established as a versatile technique to obtain the spectrum of absorption or emission from a molecule in gaseous, liquid or the solid state. The basis of this vibrational spectroscopic technique relies on the absorption, transmittance or reflectance of light, however, as oppose to dispersive absorption techniques such as Ultra Violet spectroscopy, in which beam of light is shone at a single wavelength for a set period of time, IR spectroscopy shines a combination of wavelengths at the sample records the data and then shines a different combination until completion. Furthermore, with the aid of a Michealson interferometer the monochromatic beam of light is split so that each “arm” of light passes to either the fixed or the movable mirror, afterwards they are reflected back and combined resulting in an interferogram. Once this has passed through the sample (which may either absorb or emit light) and

reached the detector, Fourier-Transform converts the data into spectra [21]. (**Figure 2-3).**

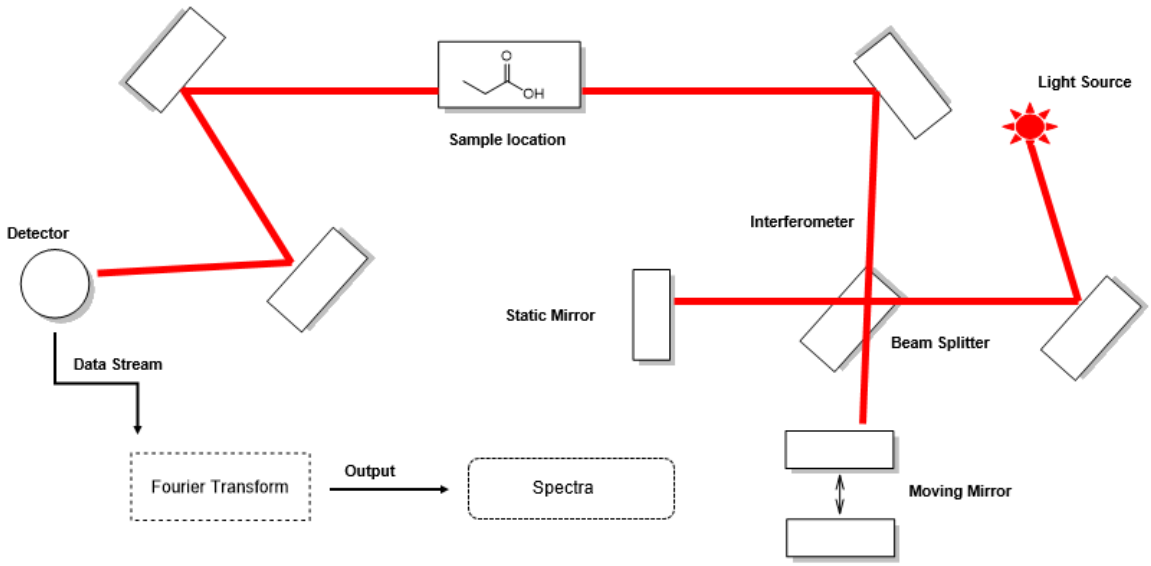

Figure 2- 3: The internal schematic of a conventional FTIR machine irrespective of sample preparation.

Furthermore, the versatility of IR allows a variety of different samples to be analysed, with techniques such as KBr pelleting and Attenuated Total Reflection (ATR) allowing samples in the solid state to be measured, other techniques such as dissolution within appropriate media, such as nujol or chloroform, and sandwiching between NaCl discs mean that IR is exceptionally versatile to sample state and is not a one size fits all for sample preperation. Therefore, the need for technique specific sample preparation is not present within FTIR allowing samples to be characterised readily and easily either as part of the reaction mixture or as a purified solid.

Throughout this project a Bruker Alpha FTIR machine was used equipped with an ATR attachment, as to allow sample analysis and retrieval with the greatest ease. ATR-FTIR has due to its simplicity and ease of sample revival, become one of the most popular ways to analyse samples via IR spectroscopy and involves placing the sample directly onto a crystal, upon which a head is lowered down and analysis is

performed. Upon completion the sample can be easily removed from the crystal and stored for further analysis or synthetic work.

Within this project FTIR was used in order to ascertain functional groups within compounds when NMR spectroscopy would not be useful, due to interference etc. Therefore, the main use of FTIR was when gemcitabine was loaded onto hyperbranched structures and the aromatic peaks of folic acid would cause sufficient interference to dampen this signal. Due to the C-F peaks within gemcitabine FTIR was a good indicator as to whether drug was loaded onto structures, other research has used this method such as in this paper by Parsian et al. in which the characteristic peaks of gemcitabine were signposted [22].

2.2.4 Ultra Violet Visible Spectroscopy

Ultra Violet Visible Spectroscopy (UV-VIS) is a versatile dispersive analytical technique for both qualitative and quantitative measurements of compounds that absorb or reflect within the ultra-violet spectrum. For instance, it can be used in the food industry to detect the amount of caffeine present in coffee beans [23].

The basis of the technique relies on the absorption on light within the ultra-violet and adjacent visible spectrum of light in order to excite electrons from their ground state to an excited state. Therefore, in general, compounds that are subject to UV-Vis analysis normally have a degree of unsaturation, are on occasion coloured (such as in transition metal complexes due to *d* electron excitement) and are soluble in an appropriate solvent (one that will not interfere with expected λ_{max} values). However, unsaturation is not a hard and fast rule for a compound to be UV active in fact any bonding or non-bonding electrons are capable of absorbing energy to their higher anti-

bonding orbitals (HOMO → LUMO transitions), however their absorption may be limited. (**Figure 2-6)**.

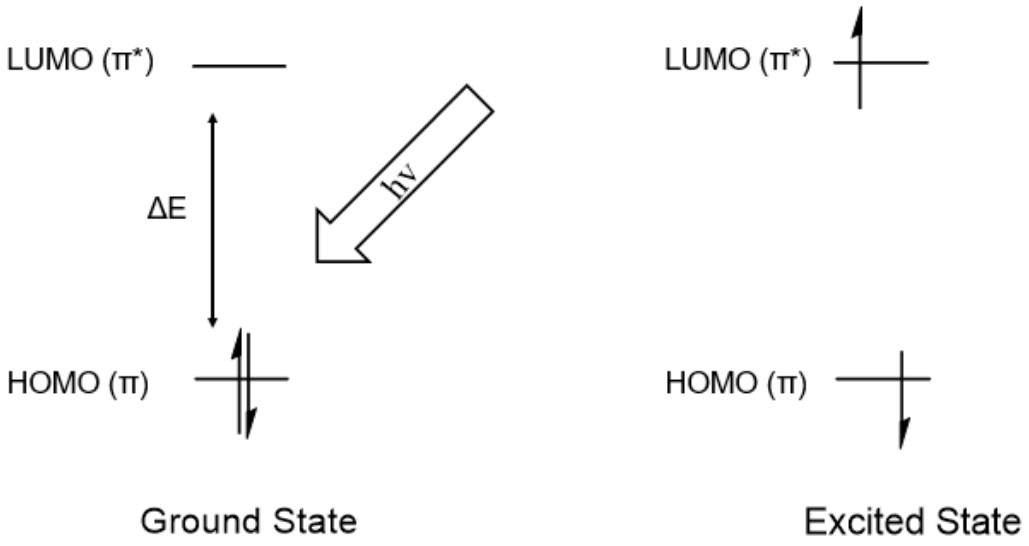

Figure 2- 4: Diagram showing the electronic principle behind UV-Vis spectroscopy (π excitations)

As previously mentioned, UV-Vis spectroscopy deals with the absorption of light in order to excite electrons and as such can be used complimentary alongside fluorescent spectroscopy, which is used to analyse the reverse i.e. the wavelengths of light emitted from excited state to ground state.

In terms of operation, a UV-Vis spectrophotometer contains two positions where cuvettes can be placed, a “blank” sample i.e. the solvent the sample is dissolved into and a “sample” position. Before analysis of the sample it is recommended to run the blank sample alongside another blank sample in order to accurately calculate the baseline for the spectrum, every time a new solvent is introduced into the system per batch of samples. Thereafter, upon analysis of samples the blank absorption can be accounted giving a true indication of only the compound absorption and the spectra

produced can be treated as a true indication of electron excitement within the sample, as seen within the following equation (eq 2-9) .

$$A = log_{10}\frac{I_0}{I} \qquad \text{(eq. 2-9)}$$

Where A is the observed absorption, I_o is the intensity of the light passing through the reference “blank” cell at a specific wavelength and I is the intensity of light passing through the sample at that same wavelength.

Upon receipt of spectra, it can be easy to believe an increase in absorbance at the λ_{max} between one samples to the next is indicative of change however, this is not always reliable as factors such as sample concentration need to be taken into account. Thus, λ_{max} can be a useful tool for the analysis of molecules such as gold nanoparticles for example, as the λ_{max} observed and intensity of absorption is directly related to the size of the molecule [24]. Making UV-Vis an accurate tool for the size analysis of such materials.

Hence, in the quantification of UV active compounds where concentration is unknown a calibration curve must be established, at the λ_{max} of the compound to be quantified. Though the use of a calibration curve, a researcher can readily and easily deduce the molar amount of chemical within the sample, taking into account the concentration of the sample (e.g. 2 moles of compound in a 2 ml solution would be a 1 mole/ml concentration) via use of the Beer-Lambert law (eq. 2-10).

$$A = \varepsilon l c \qquad \text{(eq. 2-10)}$$

Where A is absorption ε is molar extinction co-efficient, l is the path length i.e. the length the light passes through the sample in the cuvette (generally this is 1 cm), and c is the concentration. Therefore, where c is unknown the formula can be rearranged as such to solve for c with the aid of previously ran controls.

Throughout this project UV-Vis was used for the quantification of folic acid successfully conjugated onto polymer molecules and the calibration curves used can be found in **Figures 2-5, 2-6.**

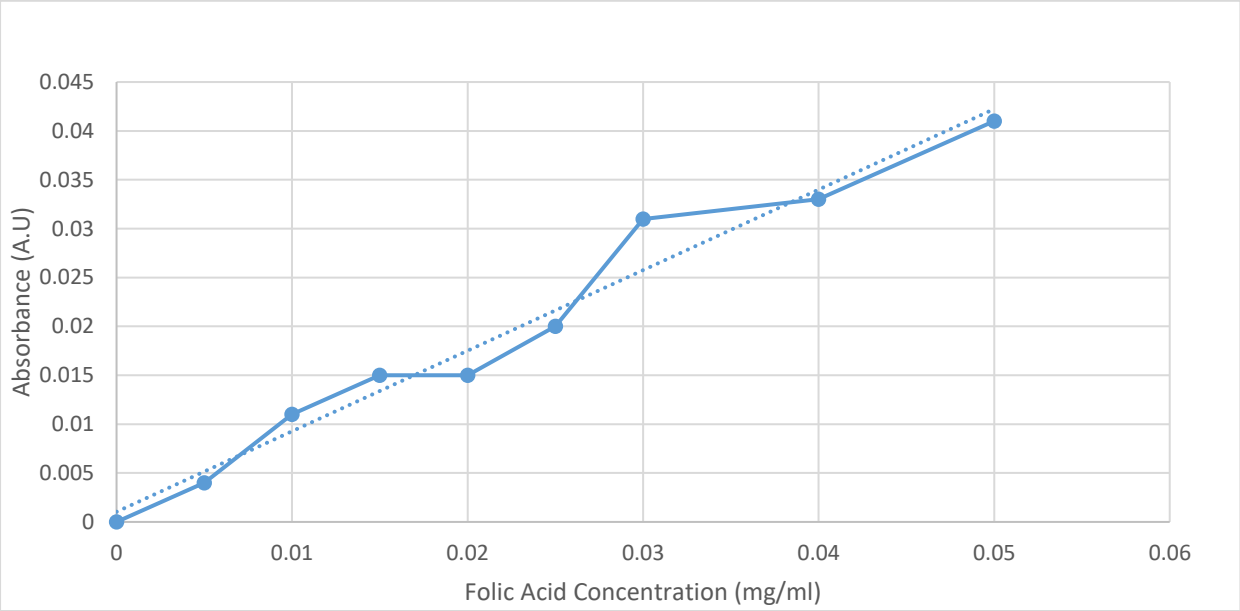

Figure 2- 5: Folic acid Calibration Curve 31_01_18

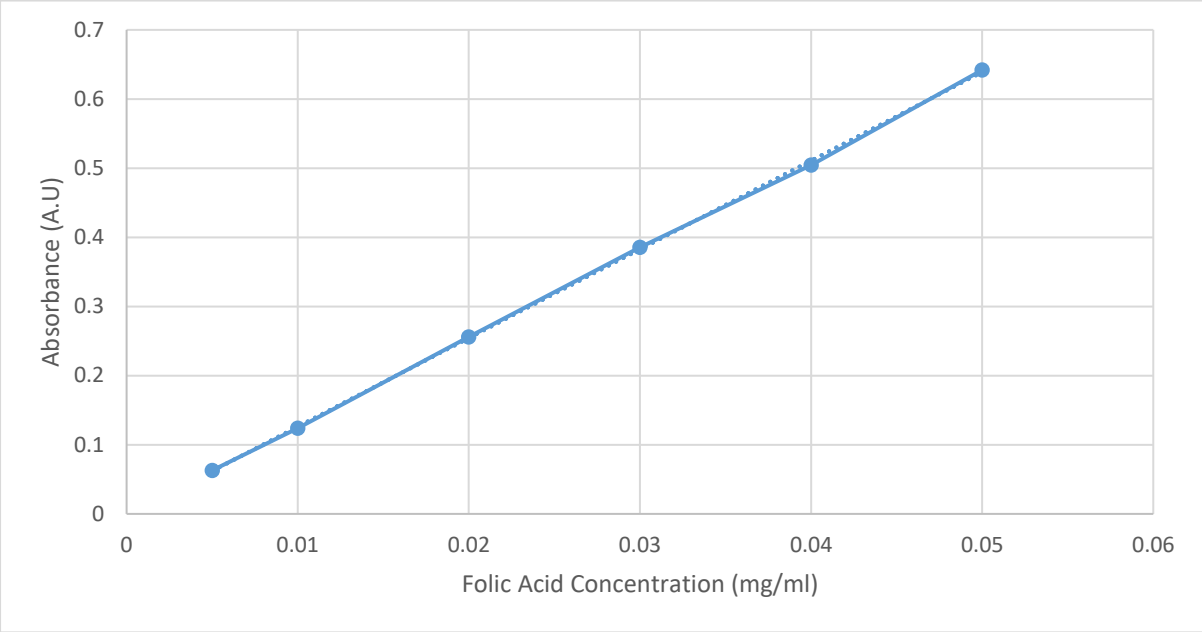

Figure 2- 6: Folic acid calibration curve 09_11_18

Two calibration curves were used as samples were tested at two different time points, therefore as to ensure that accurate measurements were made calibrations were established beforehand. For both curves the R^2 values were above 0.95 and were recorded as 0.9688 and 0.9998 respectively. As these values were above the 0.95 threshold and at least 6 points were used in each curve these were deemed sufficient and accurate for quantification purposes. Calibration curve 31_08_18 was established for the analysis of HBP4060, $HBP4060_{ethyf}$ and $HBP4060_{pegf}$. All other materials quantified for their folate content were assessed using curve 09_11_18. Samples of unknown were ran at appropriate concentrations so that absorbance was harmonious with calibration curves in a 1 ml sample volume and folate concentration was calculated via the Beer-Lambert law taking sample concentration into account. All samples and standards were run after a “blank” run of solvent DMF. DMF showed no absorbance in any region of the spectra and baseline values were calculated from the DMF spectra. Calibration curves were established at 362 nm as the λ_{max} of folic acid

at 256, 283 were interfered with due to presence of RAFT agent peaks within the spectra, which a point of further discussion in chapter 3.

Furthermore, UV-Vis spectroscopy was used in order to quantify the amount of Rhodamine and Fluorescein (FITC) linked to materials and their respective calibration curves can be found in **Figures 2-7, 2-8.** Both curves again showed a R^2 value above 0.95 at 0.9975 and 0.9936 respectively.

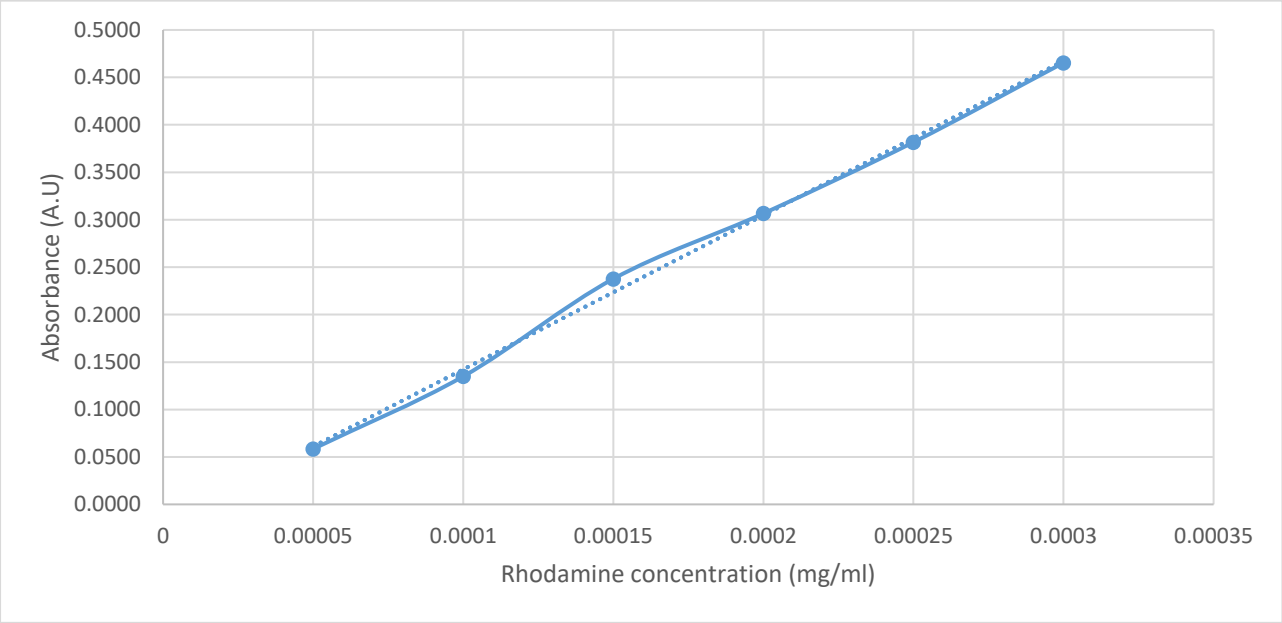

Figure 2- 7: Rhodamine calibration curve

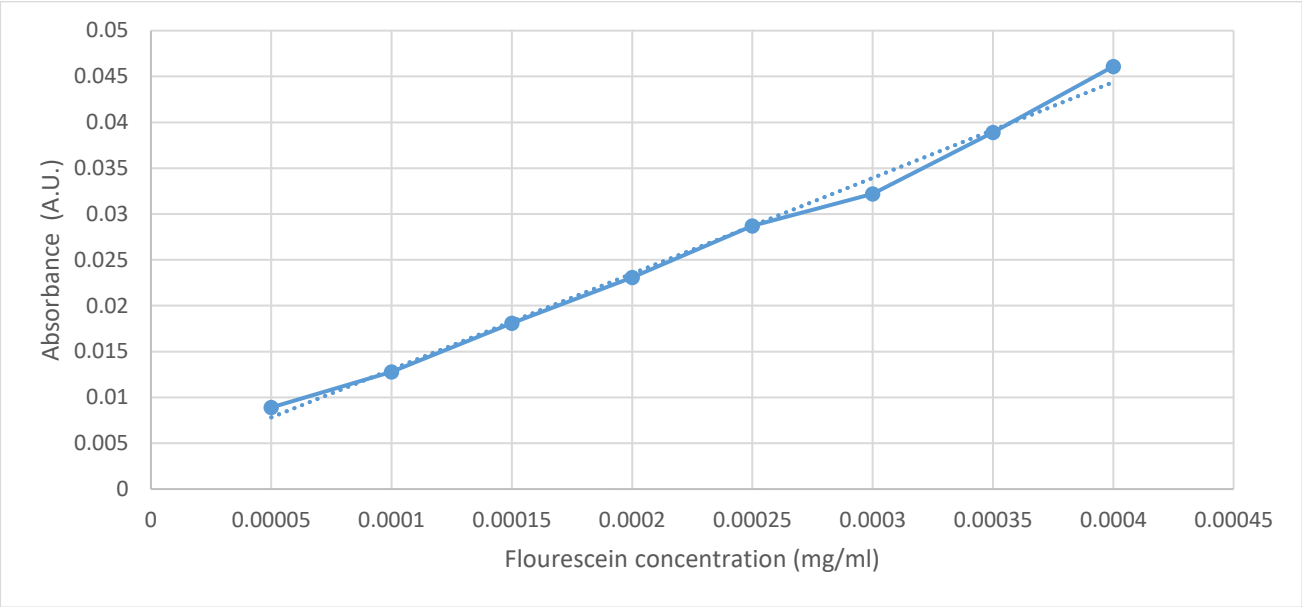

Figure 2- 8: FITC calibration curve

Throughout this thesis two spectrophometer were used for quantification purposes, HBP4060, $HBP4060_{pegf}$ and $HBP4060_{ethyf}$ were analysed using a Perkin Elmer Lambda 35 UV-Vis Spectrophotometer in 10mm Quartz cells in DMF at ambient temperature. UV-Vis electron absorption spectra for all other materials were recorded using a shimadzu UV-3600 spectrophometer in 10mm Quartz cells in DMF at ambient temperature and used for quantification for the amount of folic acid. For the quantifications of rhodamine and fluorescein linked onto HBPs a shimadzu UV-3600 spectrophotometer performed analysis on samples in 10mm polystyrene cells in distilled water at ambient temperature.

The reason for switching instrumentation between was due to the initial folic acid calibration curve shown in figure 2-5. As shown the data appears erratic and there was much more difficulty in gaining a calibration curve that was acceptable, although personal fault through technical and pipetting errors cannot be ruled out. Therefore, a newer more sophisticated instrument was used with the kindness of the Igor

Peripichka group, in the hope that instrumental errors can be removed. UV was then used for quantification purposes alone.

2.2.5 Confocal Laser Scanning Microscopy (CLSM)

Confocal microscopy is used within a wide range of life science and material science research as an optical imaging technique for the capture of two-dimensional images at different depths. Conventional microscopy relies on light travelling through a specimen to the maximum penetration in order to generate an image whereas in confocal microscopy a smaller beam of light, at one specified depth per unit of time, therefore achieving a much more controlled albeit very limited depth of focus. However, this method allows for much enhanced resolutions, as through the use of pinholes, any emission that is “out-of-field” is rejected ensuring that there is an improvement in both lateral and axial resolutions. As oppose to wide-field techniques there is therefore a much depleted interference from fluorescence emitted by the sample that is not within the focal plane of the objective. As confocal microscopy therefore displays fluorophore emission as one of the most important factors to generate an image of high quality it is at the discretion of the analyst to choose the appropriate fluorophores [25].

In terms of the technique itself and the hardware associated, there are three types of confocal microscopy in wide use today and they include: laser scanning microscopes in which a laser scans over the sample and the emission generated from the sample is collected and used to construct the image; spinning disc microscopes that operate via an electric motor, therefore when the disc is in operation and spinning an array of lasers can be directed through the pinhole in order to scan the image and data is collected and finally programmable array microscopes; in which Spatial Light Modulators (SLM) produce a moving set of pinholes. As the name suggests, the SLM can be programmed to vary properties each pixel situated within displays such as opacity, optical rotation and the reflectivity, much like as in Liquid Crystal Display

(LCD) monitors. In this way, the sample can be scanned in a variety of ways in order to produce an image.

Of course, with each different scanning technique in confocal microscopy there are advantages and disadvantages and they range from intensity of light needed, frame rate and resolution. For instance, when considering laser scanning microscopy the images constructed have a high resolution, this is however at the expense of frame rates which are in general quite low. If a high frame rate therefore is desired spinning disc microscopes have a much higher scanning frame rate. In the case of live cell imaging it is advantageous to use a spinning disc as oppose to a laser scanning microscope as images can be collected much faster and hence exposure time to the light source is greatly depleted, reducing the risk of photo bleaching so that samples can be imaged at a later time point if so desired, whilst also allowing cells to be returned to incubators much faster. Whereas in fixed cells, a laser scanning microscope can be employed as the time spent on image capture is not a vital requirement and higher resolution images can be produced as a result of this.

Throughout this project a Zeiss Laser Scanning Microscope (LSM) 710 was used in order to obtain cellular images. These types of microscopes, as previously mentioned, use multiple mirrors along the X and Y axes in order to scan the source

laser across the sample and subsequently “descan” the image across a fixed pinhole and detector (**Figure 2-9**).

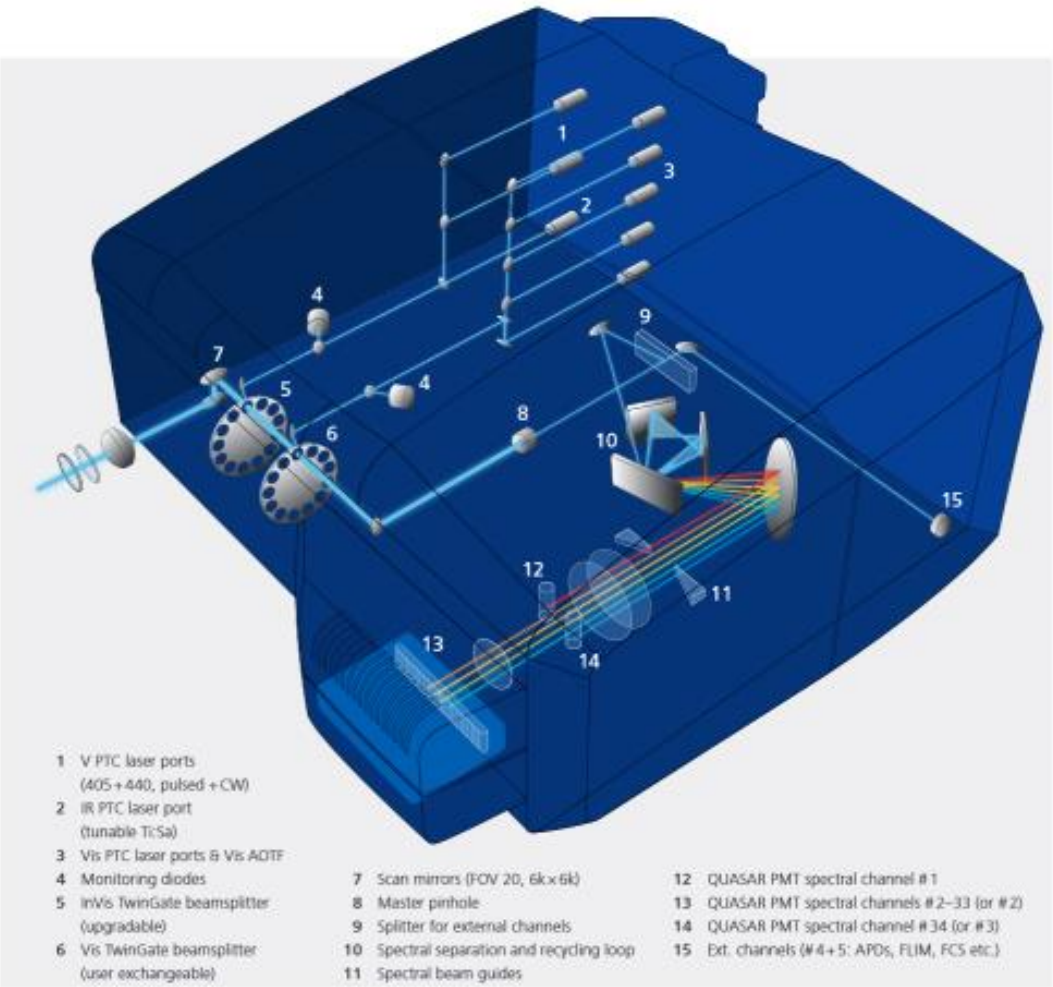

Figure 2- 9: Internal schematics of the Zeiss LSM 710 confocal microscope [26]

Such is the versatility of confocal microscopy it has been used for an array of different reasons such as the imaging of uptake of payload in cells [27–29], with multiple light sources used either in isolation or simultaneous operation that allow specific compound fluorescence. Therefore, cell specific organelles can be visualised via the appropriate dye, and internalisation of compounds such as in this project can be achieved.

Confocal microscopy was therefore used throughout this project to asses the cell uptake of polymers conjugated with fluorophores in either the naked or folic acid conjugated form. It was used as oppose to fluorescent microscopy due to the

advantages that pinholes produce in the reduction of halos and better image resolution.

2.2.6 Mass Spectrometry

Mass spectrometry is a technique that utilised the mass to charge ratio of ions in order to characterise both pure compounds and complex mixtures, such as DNA or cell extracts. Hence, spectra obtained from this technique is related not to the mass of the compound as the name suggests but the m/z (mass to charge) ratio, therefore, it is imperative that the charge is accounted for when elucidating and characterising the mass of compounds and elemental isotopes found within. In general mass spectrometry machines consist of a sample inlet, ion source, a mass analyser/sorter, a detector and finally a data output system (**Figure 2-10)**.

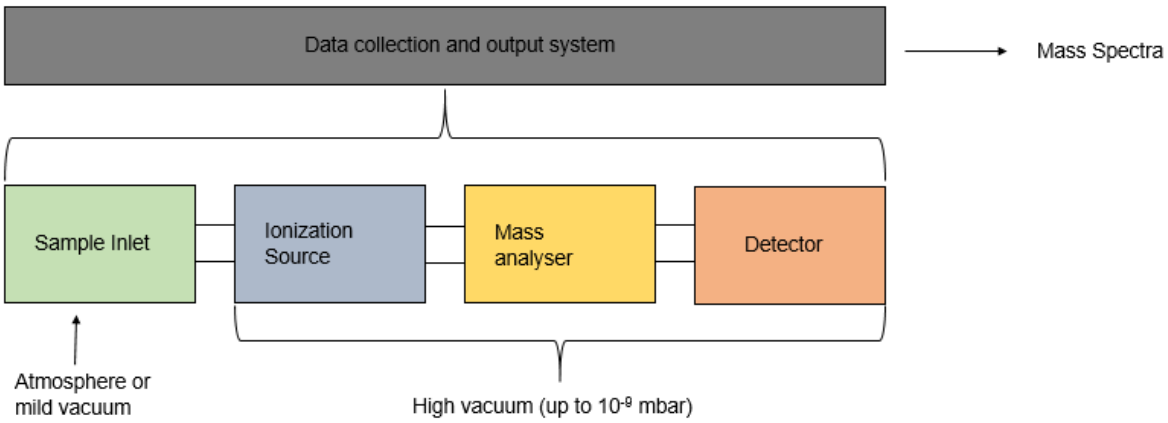

Figure 2- 10: Set-up of Mass Spectrometry systems

In order to perform mass spectrometry on a sample, crude or otherwise, firstly there needs to be either positive or negative ionization. Traditionally mass spectrometers would perform ionisation via one of the following methods: Electron Impact (EI) ionisation, in which a beam of electrons is used in order to remove an

electron from the sample inducing cationic character and a subsequent radical, or Fast Atom Bombardment (FAB) ionisation, where, samples are initially dissolved in a matrix such as glycerol and were, as the name suggests, bombarded with inert atoms (e.g. Ar, Xe). The subsequent ions formed were then adducts of the initial sample. These adducts can range from proton addition to Li or ammonia based adducts.

EI, unlike FAB, is considered a “hard” ionisation technique however, and this is due to the tendency of this technique to cause ions to fragment. Hence, spectra gained with the use of this ionisation method may require further analysis than “soft” techniques as the analyst is required to piece together individual fragment ions in order to deduce whether the desired compound is present within the sample provided. Furthermore, another factor to consider in fragmentation techniques is that there is scope for internal rearrangement, it is possible that protons may be transferred from one region of the molecule to another and it is not unusual to see notation in mass spectroscopy analysis indicating ion “X” with m/z “Y” as either “X+H” or “X+2H” indicating whether the ion was formed as a result of a single or double rearrangement.

As technology has advanced different ionisation methods have become widely used, although the principal behind them is the same. For instance in the case of volatile samples either the aforementioned EI technique can be used or the analyst may use Chemical Ionisation (CI). CI is termed a soft ionisation technique and thus has some differences to EI with the key difference being that reagent gas is added into the chamber in an excess to the sample to be analysed. The ionised reagent gas then protonates samples producing neutral gas species and an ionised sample. The benefit of CI is that it can be used in both positive and negative mode. For instance in the positive mode gases such as methane or ammonia are used as the reagent gas whereas in the negative mode it is common to use methane with an electron capture.

For compounds that do not display volatility however, FAB may be used but there is also an array of other techniques such as: matrix assisted laser desorption ionisation (MALDI), electrospray ionisation (ESI) and atmospheric pressure CI (APCI). MALDI is unique as an ionisation technique as it allows a high range of masses to be analysed, such as polymers [30,31], where other ionisation techniques may not be capable. Similarly to FAB, MALDI involves dissolving the sample in a suitable matrix such as Sinapinic Acid. The matrix is then bombarded by laser generated light which is absorbed subsequently ionising the sample, which is then extracted toward the

mass analysis chamber. Unlike other ionisation techniques MALDI is exclusively used alongside time of flight analysers which use the time taken to reach the detector as a measure of the sample's m/z ratio.

ESI has widely become a technique used coupled to LC-MS systems [32,33]. In the electrospray technique the sample is passed through an electrospray probe with a potential of around +3 kV. The sample alongside solvent is directed upon a heated capillary with a much higher potential (up to around +190 kV). This potential difference creates an electrostatic spray of droplets which are multiply charged, and as a consequence of the electronic field generated the solvent is instantly evaporated. As technology has advanced electrospray has seen advancements such as nanospray ionisation, which can analyse samples at a flow rate of nl/min whereas conventional electrospray generally analyses samples at a flow rate of µl/min [34,35].

Whilst the source of ionisation is of great importance to any mass spectroscopy analysis it is just as important to ensure that the mass analyser and detector is appropriate for the samples to be analysed. Therefore, a variety of different mass analysers are commercially available such as: quadrupole analyser or the quadrupole ion trap analyser, time of flight analyser, electrostatic analyser, magnetic sector analyser and ion cyclotron analyser.

The quadrupole mass analyser consists of four cylinder shaped rods set parallel to one another and the ions are filtered throughout based on the trajectories they exhibit when passing through with an oscillating external electrical field applied. Nowadays, it is common to see "triple-quad" (TQ) set ups, as standalone instrumentation, whilst this affords high sensitivity there is a drawback of a lower mass range. However, this allows an analyst to produce much more robust analysis on sample, especially crude. Experiments can be set so that a product of known m/z can be filtered through Q_1, fragmented in Q_2 and then the entire m/z range can be scanned in Q_3 **(Figure 2-11).**

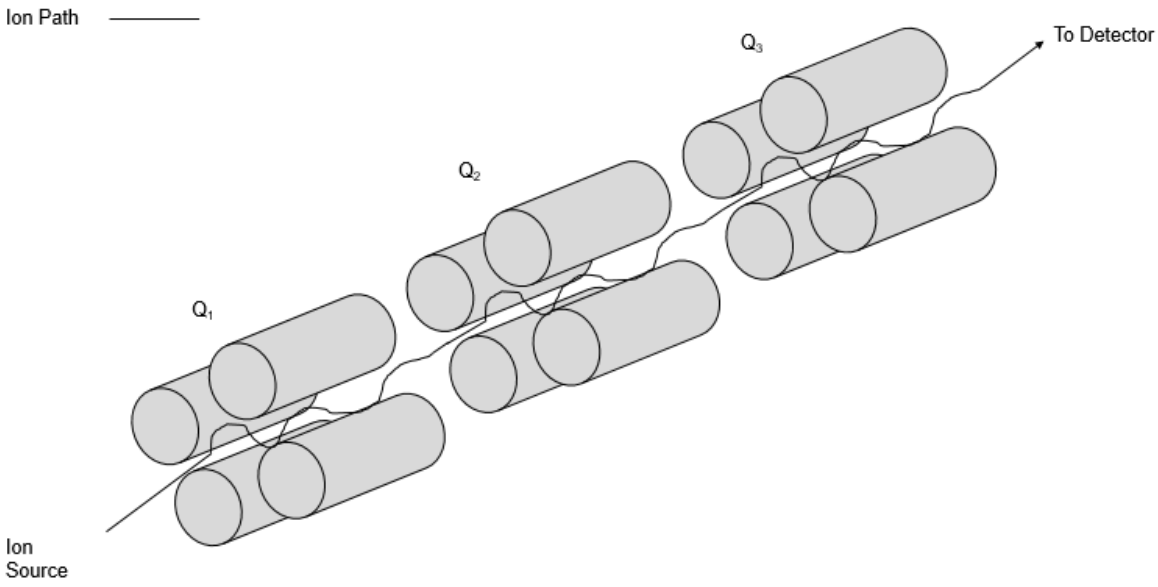

Figure 2- 11: A Triple-Quadrupole (TQ) mass analyzer

Time of Flight (ToF) analysers, as the name implies, calculate the m/z of a compound based on the time they take to reach the detector. Once ionised the samples are then accelerated via an electronic field kinetic energy applied is constant. Hence, the velocity of each ion is dependent on its mass via the following equation (eq. 2-11).

(eq. 2-11)

$$v = \sqrt{\frac{2KE}{m}}$$

Where KE is the kinetic energy of the particle m is the mass of the particle and v is the velocity. In this way once the ions reach the detector the data management is able to convert the time taken into mass, wherein the lighter ions reach the detector faster than those that are heavier. However, as ions reach heavier mass there is not a homogenous velocity of all particles at identical m/z. In order to combat this a reflectron can be added into the ToF analyser. The reflectron consists of high voltage electrodes at the end of the ToF pathway. Upon reaching the reflectron, ions are reflected in the opposite direction, in turn this allows a much greater resolution in

obtained spectra as there is a more homogeneous distribution of velocity within particles of the same m/z value.

Similar to ToF analyzers magnetic sector analysers accelerate ions through a defined flight tube and as such the ions are separated via their respected m/z ratios. Although as the name implies a magnetic field is applied in order to perform the separation. In essence, upon application of the external magnetic field ions are projected upon different trajectories. If both the magnitude of the magnetic field and the voltage applied are kept constant then the m/z can be calculated via the following equation (2-12)

$$m/z = \frac{B^2 r^2}{2V} \qquad \text{(eq. 2-12)}$$

Where B is the magnitude of the applied magnetic field, r is the radius of trajectory and V is the potential difference (Voltage difference). Magnetic sector analysers therefore can be programmed so that only ions of a specific m/z are allowed to reach the detector leading them to become a good choice when crude samples are being tested for a specific analyte. Electrostatic mass analysers are closely related to magnetic sector analysers with the key difference being that electric fields are used in lieu of magnetic fields. The consist of two plates of equal and opposite potential and as the ion passes through the electric field it is deflected and ions of a specific kinetic energy are focused on and allowed to pass through to the detector. In the same way as magnetic sector analysers they can be used to pinpoint specific compounds within a crude sample.

Finally, ion cyclotron analysers, which act as an ion trap for specific particles of a defined m/z. No separation occurs within this analyser, in fact only those ions that meet the defined criteria dictated beforehand will be trapped. A magnetic field is applied in order to trap ions focusing them into a cylindrical orbit, with an external

electrical field applied in order to enhance the signal. It is then that the angular velocity is used in order to determine the m/z ratio via the following equation (2-13).

$$\omega_c = \frac{zB}{m} \qquad \text{(eq. 2-13)}$$

Where $\omega_c$the angular velocity z is is the charge B is the magnitude of the applied magnetic field and m is the mass. In order then to ascertain the number of ions trapped a varied electric field is applied to the trap (eq. 2-14).

$$E = E_0 \cos(\omega_c t) \qquad \text{(eq. 2-14)}$$

Essentially, when the angular velocity of the electric field is homogenous with angular velocity of ions the energy is absorbed and velocity is increased. Oscillation then between the two plates causes electron accumulation inducing current that is converted into ion density.

After mass analysis and sorting the “accepted” ions are sent to a detector. The detector is simply put a plate that measures the number of ions passing through electrically in the form of current. This allows a detector to be versatile in the sense that it can detect a +ve current (for cations) and –ve current (for anions) and hence can be used in both positive and negative mode within the instrument without the need to change depending on ionisation method. The data output is then given to the analyst in the form of peak intensities, all normalised to one another.

In this project mass spectrometry was used in order to detect gemcitabine in cell extracts.

Gemcitabine (dFdC) was purchased from Discovery Fine Chemicals. Water, methanol and formic acid, all Optima LC/MS grade, were purchased from Fisher Scientific UK. UPLC-MS/MS experiments were performed on a Waters Acquity UPLC system coupled to a Waters Xevo TQ-XS Tripe Quadrupole. The weak needle wash solution was mobile phase A, the strong needle wash solution was mobile phase B. Sample preparation: freeze dried cell extract was reconstituted in 120 µl of water, centrifuged at 20’000g for 10 minutes at 4°C in an Eppendorf 5430R bench top centrifuge, and 50ul supernatant was mixed with 50 µl of a solution consisting of 20% methanol and 0.2% formic acid. The samples were kept at 10°C in the autosampler. The injection volume was 5 µl. Chromatographic separation was carried out on a Hypersil Gold C18 column (100x2.1mm, 1.9 µm particle size, Thermo Scientific), kept at 40°C in the column oven. Mobile phase A consisted of 10% methanol and 0.1%

formic acid. Mobile phase B consisted of 95% methanol and 0.2% formic acid. The gradient was: 0-1 min, 0%-100% B; 1-3 min, 100%B, 3-3.5 min, 100%-0%B, 3.5-7.5 min, 0%B. The flow rate was 0.2 ml/min throughout the experiment. The mass spectrometer was fitted with a heated electrospray ionisation Waters Zspray^{TM} probe operated in positive ionization mode. The source parameters were: capillary voltage, 3kV; cone voltage, 2V; desolvation temperature, 450°C, desolvation gas flow, 600l/h, cone gas flow, 150l/h, nebuliser gas, 7bar. The analyser parameters were: LM resolution 1, 2.75; HM resolution 1, 15.39; ion energy 1, -0.3; LM resolution 2, 2.68; HM resolution 2, 15.94; ion energy 2, 0.5; collision gas flow, 0.15ml/min. The following mass-to-charge (m/z) transitions was monitored: dFdC: 264.1 to 112.1 at a collision energy of 15eV and a dwell time of 0.33 seconds.

The amount of dFdC in the HeLa samples was quantified with TargetLynx (Waters), using the linear range of a calibration curve obtained with dFdC as external standard.

Additionally, gemcitabine metabolites were analysed via the following method. Gemcitabine monophosphate (dFdCMP) was purchased from Toronto Research Chemicals Inc. Gemcitabine diphosphate (dFdCDP) and Gemcitabine triphosphate (dFdCTP) were purchased from Jena Bioscience. Water, acetonitrile and acetic acid, all Optima LC/MS grade, were purchased from Fisher Scientific UK. UPLC-MS/MS experiments were performed on a Waters Acquity UPLC system coupled to a Waters Xevo TQ-XS Tripe Quadrupole. The weak needle wash solution was mobile phase A, the strong needle wash solution was mobile phase B. Sample preparation: freeze dried cell extract was reconstituted in 120 µl of water, centrifuged at 20’000g for 10 minutes at 4°C in an Eppendorf 5430R bench top centrifuge, and 50 µl supernatant was mixed with 50 µl mobile phase A. The samples were kept at 10°C in the autosampler. The injection volume was 5 µl. Chromatographic separation was carried out on a Hypercarb column (150x2.1mm, 5 µm particle size, Thermo Scientific), kept at 30°C in the column oven. Mobile phase A consisted of 0.1% ammonium hydroxide, pH 10.0 adjusted with acetic acid. Mobile phase B consisted of 0.1% ammonium hydroxide, 80% acetonitrile, pH 10.0 adjusted with acetic acid. The gradient was: 0-8 min, 10%-95% B; 8-9 min, 95%B, 9-9.2 min, 95%-10%B, 9.2-11 min, 10%B. The flow rate was 0.4 ml/min throughout the experiment. The mass spectrometer was fitted with a heated electrospray ionisation Waters Zspray^{TM} probe operated in positive ionization mode.

The source parameters were: capillary voltage, 3kV; cone voltage was set at 2V; desolvation temperature, 600°C, desolvation gas flow, 600l/h, cone gas flow, 150l/h, nebuliser gas, 7bar. The analyser parameters were: LM resolution 1, 2.75; HM resolution 1, 15.39; ion energy 1, -0.3; LM resolution 2, 2.68; HM resolution 2, 15.94; ion energy 2, 0.5; collision gas flow, 0.15ml/min. The following mass-to-charge (m/z) transitions were monitored: dFdCMP: 344.0 to 112.1 at a collision energy of 20eV, 344.0 to 246.1 at a collision energy of 20eV; dFdCDP: 424.0 to 112.1 at a collision energy of 35eV, 424.0 to 326.0 at a collision energy of 20eV; dFdCTP: 504.0 to 112.1 at a collision energy of 35eV, 504.0 to 326.0 at a collision energy of 20eV. The dwell time was 0.052 seconds for all m/z transitions.

Finally, analysis of the CTC linker was performed via the following methodology. LC-MS/MS experiments were performed on a Thermo Scientific Vanquish UHPLC system coupled to a Thermo Scientific Q Exactive Plus.

Sample preparation: freeze-dried cell extract and freeze-dried synthesised CTC-Gemzar was reconstituted in 120 µl of water, centrifuged at 20’000g for 10 minutes at 4°C in an Eppendorf 5430R bench top centrifuge, and 50ul supernatant was mixed with 50 µl mobile phase A.

The samples were kept at 10°C in the autosampler. The needle wash solution was 10% Methanol in water. The injection volume was 5 µl. Chromatographic separation was carried out on a Hypersil Gold C18 column (100x2.1mm, 1.9 µm particle size, Thermo Scientific), kept at 40°C in the column oven.

Three different mobile phase systems and gradients were used: 1) Mobile phase A consisted of 10% methanol and 0.1% formic acid. Mobile phase B consisted of 95% methanol and 0.2% formic acid. The gradient was: 0-1 min, 0%-100% B; 1-3 min, 100%B; 3-3.5 min, 100%-0%B, 3.5-7.5 min, 0%B. The flow rate was 0.4 ml/min throughout the experiment. 2) Mobile phase A consisted of water and 0.1% formic acid. Mobile phase B consisted of 100% acetonitrile and 0.1% formic acid. The gradient was: 0-1 min, 10%-98% B; 1-3 min, 98%B; 3-3.5 min, 98%-10%B, 3.5-7.5 min, 10%B. The flow rate was 0.4 ml/min throughout the experiment. 3) Mobile phase A consisted of water and 0.1% formic acid. Mobile phase B consisted of 100%

acetonitrile and 0.1% formic acid. The gradient was: 0-20 min, 10%-99% B; 20-24 min, 99%B; 24-25 min, 99%-10%B, 25-30 min, 10%B. The flow rate was 0.4 ml/min throughout the experiment.

The mass spectrometer was fitted with a heated electrospray ionisation (HESI-II) probe operated in positive ionization mode. The source parameters for mobile phase and gradient combinations 1) and 2), see above, were: sheath gas flow rate, 40; auxiliary gas flow rate, 15; sweep gas flow rate, 1; spray voltage, 3kV; capillary temperature, 300°C; S-lens RF level, 50; auxiliary gas heater temperature, 300°C. Full MS-SIM scans were carried out with the following parameters: in-source CID, 0 eV; microscans, 1; resolution, 70’000; AGC target, 1e6; maximum IT, 240ms; scan range, 100-800 m/z, spectrum data type, profile. The source parameters for mobile phase and gradient combination 3), see above, were: sheath gas flow rate, 40; auxiliary gas flow rate, 15; sweep gas flow rate, 1; spray voltage, 3kV; capillary temperature, 300°C; S-lens RF level, 50; auxiliary gas heater temperature, 300°C. Full MS-SIM scans were carried out with the following parameters: in-source CID, 0 eV; microscans, 1; resolution, 140’000; AGC target, 1e6; maximum IT, 500ms; scan range, 100-1200 m/z, spectrum data type, profile.

Mass spectrometry, as discussed was therefore used to detect gemcitabine extracts within cells. This section therefore focused on the foundations of mass spectrometry in brief so that the reader can understand why this technique was chosen as to oppose to NMR or FTIR for example. Mass spectrometry can take many forms however, signposting to literature within the Hartsuiker group at Bangor University, it is a useful method of gemcitabine quantification, with a former PhD student of his Lennart Bockemeier producing a plethora of results regarding this [36]. As my co-supervisor I collaborated with Dr. Hartsuiker on using this work as a springboard for detection of gemcitabine delivery towards cells within my own project, drawing on expertise and previous results to garner preliminary results, that are discussed in chapter 4.

2.2.7 Dynamic Light Scattering (DLS) for particle size analysis

Dynamic Light Scattering (DLS) is one of the primary techniques for the analysis of particles in solution with respect to their size distribution. In principle the technique works due to the Rayleigh scattering phenomenon. In essence, Rayleigh scattering, named after the British physicist Lord Rayleigh, explains the elastic scattering of electromagnetic radiation by particles (where the particle inducing the scattering is smaller than the wavelength of radiation being scattered) due to induced dipole moments [37].

In general the instrument is similar in appearance to a UV-Vis machine, with a light source, a single cuvette holder (whereas UV-Vis has two) and a detector. In operation a laser is shone through a polarizer before reaching the sample. Upon scattering of light by the particles in solution the scattered light is passed through a second polarizer and a speckle pattern is generated (**Figure 2-12)**. The nature of the scattered light means interference can occur both constructively and destructively, either scattered light amplifies other scattered light or nullify it. Therefore, speckle patterns consist of both light and dark regions respectively.

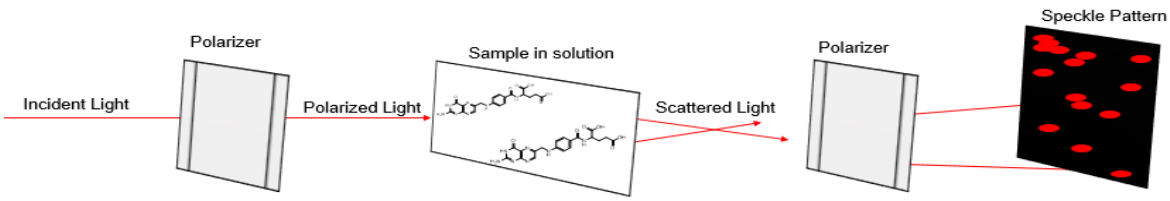

Figure 2- 12: Speckle pattern generation utilising a Vertical-Vertical polarizer set-up.

In order to reduce the effects of interference, multiple repeats of the experiment are performed and an autocorrelation calculation ensures that the light and dark regions of the speckle pattern are analysed over time. In terms of the polarizers they can be set in two geometric positions either Vertical-Vertical or Vertical-Horizontal. Of course, in the latter as the second polarizer is set to a different geometric position

incident light cannot be mistaken for refracted light and thus light passing straight through samples is not recorded.

An important fact to consider when performing any DLS measurement is the effect of convection currents on the path of light. Therefore, as many modern instruments contain an oven it is advisable that the sample to be measure is left in the machine for at least 10-15 minutes in order to negate the effects of such currents. By performing this action beforehand particle collisions and movement will be much more randomised and exhibit Brownian motion behaviour as oppose to collisions and movement due to the effects of eddies and convection [38].

As previously mentioned, samples are measured over a number of times and then an autocorrelation technique ensures that speckle patterns generated are a true indication of refracted light and interference is accounted for. (eq. 2-15) Therefore, the autocorrelation function must take into account a variety of different factors but by far the simplest form of the function in the first order can be written as such (eq. 2-15):

(eq. 2-15)

$$g^1(q;t) = \exp\left(-\Gamma\tau\right)$$

Where $g^1(q;t)$ is the autocorrelation function at a specific wave vector (q) at time (t). Hence this is directly related to the exponent of the decay time (Γ). Therefore, for monodisperse population the first order autocorrelation is appropriate. However, whilst this may be for pure samples of small molecules more disperse systems such as polymers or proteins cannot be accurately represented by this equation. Therefore, the autocorrelation for these systems must consist as a sum of the exponential decays of all species within the sample, as to account for each one individually (eq. 2-16).

$$g^1(q;\tau) = \sum_{i=1}^{n} G_i(\Gamma_i)\exp(-\Gamma_i\tau) = \int G(\Gamma)\exp(-\Gamma\tau)d\Gamma \qquad \text{(eq. 2-16)}$$

Through this formula therefore it is possible to solve and extract $G(\Gamma)$ which is directly proportional to the distribution of sizes with the sample. However, when taking into account Jacques Hadamard's description of mathematical formula that represent phenomena in the physical world extracting $G(\Gamma)$ is not well-posed, as data would be required for $g^1(q;\tau)$ and an inversion would need to take place. Therefore, further

analysis of the results obtained via the autocorrelation function are required before size distributions can be truthfully represented.

There are various mathematical formula in order to analyse the autocorrelation function and thus provide the analyst with the data required however two methods: the Cumulant fitting method and the CONTIN regularization method are the most widely used.

The Cumulant fitting method utilises the theory in statistics that probability distributions (in this case the size distributions) have a set of quantifiable properties (cumulants) that determine the moment (i.e. the physical density representation). The cumulant method is used to derive information on the variance of the system using both the average decay rate and the second order dispersity value. However, is limited to the fact that samples have both a small τ value and a narrow $G(\Gamma)$. Hence, for samples that have a large dispersity such as synthetic polymers the CONTIN regularization method is used. The CONTIN method developed by Steven Provencher utilises inverse laplace transformation and is ideal for diverse mixtures [39]. Using this method the analyst can gather a much higher resolution between different size populations, whereas via the cumulant method they have merged and been difficult to separate.

In this project DLS was used to size materials both labelled and unlabelled with targeting ligand at different pH values so that the size of the material and the stimuli response can be observed. Analysis was performed in Wrexham Glyndwr University with the kind supervision of Dr. Ian Ratcliffe and Dr. Chandra Senan. A Malvern Zetasizer 1000Hsa at 25°C with a 90° front scatter laser (633 nm) was used for particle sizing experiments. The results were analysed via use of the CONTIN regularization method using PCS software v1.61. Materials were dissolved in distilled water at either pH 7.4, 6.8 or 5.4 at a final concentration of 0.1% (w/v). Measurements were then performed in a 10 mm polystyrene cuvette with 99% transparency and were blown with compressed air before sample addition to avoid dust contamination. Cuvettes were then allowed to equilibrate inside the machine for 15 minutes before analysis was performed.

References

[1] I. Rabi, R. Zacharias, S. Millman, P. Kusch, A new method of measuring Nuclear Magnetic Moment, Phys. Rev. 53 (1938) 318. https://doi.org/10.1016/S0031-8914(39)80004-0.

[2] R. Harris, E. Becker, S. Cabral De Menezes, R. Goodfellow, P. Granger, NMR Nomenclenture. Nuclear Spin Properties and Conventions for Chemical Shifts, Pure Appl. Chem. 73 (2001) 1795–1818.

[3] Recommendations for the Presentation of NMR Data for Publication in Chemical Journals, Pure Appl. Chem. 29 (2008) 625–628. https://doi.org/10.1351/pac197229040625.

[4] T. Hoye, P. Hanson, J. Vyvyanlb, A Practical Guide to First-Order Multiplet Analysis in 1H NMR Spectroscopy, J. Org. Chem. 59 (1994) 4096–4103.

[5] H.E. Gottlieb, V. Kotlyar, A. Nudelman, NMR chemical shifts of common laboratory solvents as trace impurities, J. Org. Chem. 62 (1997) 7512–7515. https://doi.org/10.1021/jo971176v.

[6] R.D. Armstrong, J. Hirayama, D.W. Knight, G.J. Hutchings, Quantitative determination of Pt-catalyzed D-glucose oxidation products using 2D NMR, ACS Catal. 9 (2018) 325–335.

[7] J. Nath, T. Smith, A. Hollis, S. Ebbs, S.W. Canbilen, D.A. Tennant, A.R. Ready, C. Ludwig, 13 C glucose labelling studies using 2D NMR are a useful tool for determining ex vivo whole organ metabolism during hypothermic machine perfusion of kidneys, Transplant. Res. 5 (2016) 1–8.

[8] A.A. de Graaf, A. Maathuis, P. de Waard, N.E.P. Deutz, C. Dijkema, W.M. de Vos, K. Venema, Profiling human gut bacterial metabolism and its kinetics using [U-13C] glucose and NMR, NMR Biomed. An Int. J. Devoted to Dev. Appl. Magn. Reson. Vivo. 23 (2010) 2–12.

[9] A. Tochwin, A. El-Betany, H. Tai, K.Y. Chan, C. Blackburn, W. Wang, Thermoresponsive and reducible hyperbranched polymers synthesized by RAFT polymerisation, Polymers (Basel). 9 (2017) 1–15. https://doi.org/10.3390/polym9090443.

[10] J. Martin, J. Johnson, R. Cooper, Properties of Polymers : The Influence of

Molecular Weight and Molecular Weight Distribution, J. Macromol. Sci. Part C. 8 (2006) 57–199.

[11] B.H. Bersted, T.G. Anderson, Influence of molecular weight and molecular weight distribution on the tensile properties of amorphous polymers, J. Appl. Polym. Sci. 39 (1990) 499–514. https://doi.org/10.1002/app.1990.070390302.

[12] H.W. Mccormick, F.R.T. Brower, L.E.O. Kik, The Effect of Molecular Weight Distribution on the Physical Properties of Polystyrene, X (1959) 87–100.

[13] L.H. Judovits, R.C. Bopp, U. Gaur, B. Wunderlich, The heat capacity of solid and liquid polystyrene, p-substituted polystyrenes, and crosslinked polystyrenes, J. Polym. Sci. Part B Polym. Phys. 24 (1986) 2725–2741. https://doi.org/10.1002/polb.1986.090241209.

[14] M. Rogošić, H.J. Mencer, Z. Gomzi, Polydispersity index and molecular weight distributions of polymers, Eur. Polym. J. 32 (1996) 1337–1344. https://doi.org/10.1016/S0014-3057(96)00091-2.

[15] D. Bontempo, R.C. Li, T. Ly, C.E. Brubaker, H.D. Maynard, One-step synthesis of low polydispersity, biotinylated poly(N- isopropylacrylamide) by ATRP, Chem. Commun. (2005) 4702–4704. https://doi.org/10.1039/b507912h.

[16] H. Gao, S. Ohno, K. Matyjaszewski, Low polydispersity star polymers via cross-linking macromonomers by ATRP, J. Am. Chem. Soc. 128 (2006) 15111–15113. https://doi.org/10.1021/ja066964t.

[17] A. Goto, T. Fukuda, Effects of radical initiator on polymerization rate and polydispersity in nitroxide-controlled free radical polymerization, Macromolecules. 30 (1997) 4272–4277. https://doi.org/10.1021/ma9702152.

[18] H. Okamura, Y. Takatori, M. Tsunooka, M. Shirai, Synthesis of random and block copolymers of styrene and styrenesulfonic acid with low polydispersity using nitroxide-mediated living radical polymerization technique, Polymer (Guildf). 43 (2002) 3155–3162. https://doi.org/10.1016/S0032-3861(02)00162-3.

[19] G. Moad, T. Mayadunne, E. Rizzardo, M. Skidmore, S. Thang, Kinetics and Mechanism of RAFT Polymerization, in: K. Matyjaszewski (Ed.), Adv. Control. Radic. Polym., American Chemical Society, Washington, DC, 2003: pp. 520–535. https://doi.org/10.1002/anie.197407811.

[20] J. Ferreira, J. Syrett, M. Whittaker, D. Haddleton, T.P. Davis, C. Boyer,

Optimizing the generation of narrow polydispersity “arm-first” star polymers made using RAFT polymerization, Polym. Chem. 2 (2011) 1671–1677. https://doi.org/10.1039/c1py00102g.

[21] O. Faix, Fourier Transform Infra-Red Spectroscopy, in: Methods Lignin Chem., Springer Berlin Heidelberg, 1992: pp. 83–109. https://doi.org/10.1007/978-3-642-74065-7_7.

[22] M. Parsian, P. Mutlu, S. Yalcin, U. Gunduz, Characterization of Gemcitabine Loaded Polyhydroxybutyrate Coated Magnetic Nanoparticles for Targeted Drug Delivery, Anti-Cancer Agents Med. Chem. (Formerly Curr. Med. Chem. Agents). 20 (2020) 1233–1240.

[23] A. Belay, K. Ture, M. Redi, A. Asfaw, Measurement of caffeine in coffee beans with UV/vis spectrometer, Food Chem. 108 (2008) 310–315. https://doi.org/10.1016/j.foodchem.2007.10.024.

[24] W. Haiss, N. Thanh, J. Aveyard, D. Fernig, Determination of Size and Concentration of Gold Nanoparticles from UV-Vis Spectra, Anal. Chem. 79 (2007) 4215–4221. https://doi.org/10.1021/ac0702084.

[25] R. Tsien, A. Waggoner, Flourophores for Confocal Microscopy, in: Handb. Biol. Confocal Microsc., Springer, Boston, MA, 1995: pp. 267–279. https://doi.org/10.1007/978-1-4757-5348-6_16.

[26] LSM 710 Confocal Microscope : Internal Diagram, (2019). http://nisms.stanford.edu/Equipment/LSM710Scanhead01v01.html (accessed November 7, 2019).

[27] K. Yin Win, S.S. Feng, Effects of particle size and surface coating on cellular uptake of polymeric nanoparticles for oral delivery of anticancer drugs, Biomaterials. 26 (2005) 2713–2722. https://doi.org/10.1016/j.biomaterials.2004.07.050.

[28] U.O. Häfeli, J.S. Riffle, L. Harris-Shekhawat, A. Carmichael-Baranauskas, F. Mark, J.P. Dailey, D. Bardenstein, Cell uptake and in vitro toxicity of magnetic nanoparticles suitable for drug delivery, Mol. Pharm. 6 (2009) 1417–1428. https://doi.org/10.1021/mp900083m.

[29] J.E. Schroeder, I. Shweky, H. Shmeeda, U. Banin, A. Gabizon, Folate-mediated tumor cell uptake of quantum dots entrapped in lipid nanoparticles, J. Control. Release. 124 (2007) 28–34.

https://doi.org/10.1016/j.jconrel.2007.08.028.

[30] M.W.F. Nielen, Polymer Analysis by Micro-Scale Size-Exclusion Chromatography/MALDI Time-of-Flight Mass Spectrometry with a Robotic Interface, Anal. Chem. 70 (1998) 1563–1568. https://doi.org/10.1021/ac9712409.

[31] H.J. Räder, I.K. Sclirepp, MALDI-TOF mass spectrometry in the analysis of synthetic polymers, Acta Polym. 49 (1998) 272–293. https://doi.org/10.1002/(sici)1521-4044(199806)49:6<272::aid-apol272>3.3.co;2-t.

[32] J.F. Banks, S. Shen, C.M. Whitehouse, J.B. Fenn, Ultrasonically Assisted Electrospray Ionization for LC/MS Determination of Nucleosides from a Transfer RNA Digest, Anal. Chem. 66 (1994) 406–414. https://doi.org/10.1021/ac00075a015.

[33] M.J. Huddleston, M.F. Bean, S.A. Carr, Collisional Fragmentation of Glycopeptides by Electrospray Ionization LC/MS and LC/MS/MS: Methods for Selective Detection of Glycopeptides in Protein Digests, Anal. Chem. 65 (1993) 877–884. https://doi.org/10.1021/ac00055a009.

[34] R. Juraschek, T. Dülcks, M. Karas, Nanoelectrospray - More than just a minimized-flow electrospray ionization source, J. Am. Soc. Mass Spectrom. 10 (1999) 300–308. https://doi.org/10.1016/S1044-0305(98)00157-3.

[35] M. Wilm, A. Shevchenko, T. Houthaeve, S. Breit, L. Schweigerer, T. Fotsis, M. Mann, Femtomole sequencing of proteins from polyacrylamide gels by nano-electrospray mass spectrometry, Nature. 379 (1996) 466–469. https://doi.org/10.1038/379466a0.

[36] L. Böckemeier, The role of DNA repair in resisting treatment with gemcitabine and other nucleoside analogues, (2020).

[37] H. Moosmüller, W.P. Arnott, Particle optics in the rayleigh regime, J. Air Waste Manag. Assoc. 59 (2009) 1028–1031. https://doi.org/10.3155/1047-3289.59.9.1028.

[38] A. Einstein, On the Motion of Small Particles Suspended in a Stationary Liquid, as Required by the Molecular Kinetic Theory of Heat, Ann. Phys. 322 (1905) 549–560. https://doi.org/10.1002/andp.19053220806.

[39] S.W. Provencher, CONTIN: A general purpose constrained regularization

program for inverting noisy linear algebraic and integral equations, Comput. Phys. Commun. 27 (1982) 229–242. https://doi.org/10.1016/0010-4655(82)90174-6.

Chapter Three – RAFT Synthesis of Hyperbranched Polymers

Parts of this chapter have been published in

C. Blackburn, H. Tai, M. Salerno, X. Wang, E. Hartsuiker, W. Wang, Folic acid and rhodamine labelled pH responsive hyperbranched polymers : Synthesis , characterization and cell uptake studies, Eur. Polym. J. 120 (2019) 109259. doi:10.1016/j.eurpolymj.2019.109259.

C. Blackburn, H. Tai, M. Salerno, X. Wang, C. Senan, I. Ratcliffe, E. Hartsuiker, W. Wang, Data presenting the synthesis of three novel stimuli responsive hyperbranched polymers synthesised via RAFT polymerisation and the bio conjugation of folic acid, Data Br. 28 (2020) 104861 doi:10.1016/j.dib.2019.104861

3.1 Introduction

This chapter focuses on the experimental results and methodology for the synthesis of the stimuli responsive hyperbranched polymers used throughout this project. Polymerisation reactions were conducted with the well-known Reversible Addition Fragmentation chain Transfer (RAFT) polymerisation technique, in order to better control molecular weight, particle size and poly dispersity index as oppose to traditional free radical polymerisation methods. Initial synthetic routes aimed to synthesise polymers of hyperbranched topology via the use of 2-Propyl Acrylic Acid (PAA) and Disulfanediylbis(ethane-2,1-diyl) diacrylate (DSDA) to little success, with synthetic routes towards monomer production discussed. Later modifications of reaction procedures introduced 2-(Dimethylamino)ethyl methacrylate (DMAEMA) monomer into synthetic routes in order to synthesise a tri-monomeric based hyperbranched co-polymer with differing monomeric and RAFT agent feed ratios, all of which is discussed in detail in this chapter. Characterisation of hyperbranched polymers including Nuclear Magnetic Resonance spectroscopy, Dynamic Light Scattering and Size Exclusion Chromotography is presented within this chapter also.

3.2 Experiemental

3.2.1 Materials

All solvents were purchased from Fisher Scientific as analytical grade and used as received. Diethyl propyl malonate (Alfa Aesar 99%), 2-2'disulfanediylbis(ethan-1-ol) (90% technical grade), Acryloyl Chloride (Alfa Aesar 96%. Stab. With 400 ppm phenothiazine), Methacryloyl chloride (95%. Stab. With 200 ppm MEHQ), trimethylamine (Alfa Aesar 99%), KOH pellets, HCl (37%), Na_2CO_3 (99%) and $CDCl_3$ (Acros Organics 99.8% atom D) were purchased from Fisher Scientific and used as received.

2-(Dimethylamino) ethyl methacrylate (98%) (DMAEMA), 4-4'-Azobis(4-cyano-valeric acid) (ACVA) (98%) were purchased from Sigma Aldrich and used as received.

2-2'-Azobis(2-methylpropionitrile) (AIBN) (98%) was purchased from Sigma Aldrich and was freshly recrystallized in methanol before use in any experiments.

4-cyano-4-(((dodecylthio)carbonothioyl)thio)pentanoic acid (CDCTPA) was synthesised previously [1] and was used without any further purification.

3.2.2 ^{1}H Nuclear Magnetic Resonance (^{1}H NMR)

^{1}H NMR were run on a Bruker Ultra-shield 400 MHz NMR machine loaded with topspin software for 16 scans. Corresponding NMR spectra for the following compounds can be found in the appendix of this thesis as data files: PAA (**Figure S3-1**), DSDA (**Figure S3-2**), DSDMA (**Figure S3-3**) Poly(PAA-*co*-DSDA) (**Figure S3-4**), HBP3070 (**Figure S3-5**), HBP5050 (**Figure S3-6**), HBP4060 (**Figure S3-7**),

HBP4060_2 (**Figure S3-8**), HBP4060_3 (**Figure S3-9**) and HBP4060_4 (**Figure S3-10**).

3.2.3 Synthesis of 2-Propyl Acrylic Acid (PAA)

PAA was synthesised via the reported method from Ferritto and Tirrell [2] and characterised by ^{1}H NMR. Diethyllpropylmalonate (50g, 0.24mol) was added to a r.b.f. alongside 300ml of 1M KOH solution (IMS) and left to stir at room temperature overnight. The solid precipitate was filtered and placed into a 1L conical flask. The solution was then concentrated *in vaccuo* and the resultant oil was added and to the solid. The contents of the conical flask were then dissolved in 7ml deionised water and further acidified to pH 2 by addition of dilute HCl, once this pH had been reached an oil separated from the solution. The resultant oil was taken into diethyl ether and the aqueous layer was extracted thrice with 200ml of ether. The organics were then dried with magnesium sulfate, filtered and concentrated to yield quantitatively 2-(ethoxycarbonyl)pentoic acid (42g 0.24mol). FTIR (neat cm^{-1}) 3500-3000, 1710. The synthesized 2-(ethoxycarbonyl) pentanoic acid (42 g 0.24 mol) was placed into a round bottom flask equipped with a reflux condenser and cooled in an ice bath before addition of diethyl amine (12.5 ml 0.24 mol). An addition funnel is equipped to the reflux condenser and charged with formalin solution (37% formaldehyde in water) (0.24 mol 19.3 g) the contents of the addition funnel were then added dropwise to the cooled reaction vessel and then allowed to warm to room temperature and allowed to stir for 24hrs. The reaction mixture was then heated to 60°C and allowed to stir for a further 8hrs. The reaction now consisted of two distinct layers. The mixture was again cooled with an ice bath and concentrated sulfuric acid was added until the evolution of gas was no longer present and the mixture was extracted thrice with 200 ml of diethyl ether. The organic extracts were combined and dried with magnesium sulfate, filtered and concentrated *in vaccuo* to yield crude ethyl 2-methylenepentanoate (91% yield). Finally, crude ethyl 2-methylenepenatanoate (0.22 mol) was added to a round bottom flask equipped with a reflux condenser alongside 400 ml of 1 M KOH (aq) and was heated to reflux for 20hrs. The solution was then allowed to cool to room temperature and was acidified to pH 2 with dilute

HCl. An oil then separated from the solution. Extraction was performed 4 times with 200 ml of diethyl ether and the organics were dried with magnesium sulfate filtered and concentrated to obtain as an oil 2-propyl acrylic acid (81% yield). ^{1}H NMR (400 MHz $CDCl_3$) δ 11.67 (s, 1H CO**OH**) 6.23 (s, 1H vinyl H) 5.58 (s, 1H vinyl H) 2.21 (t, 2H, CH_2-**CH_2**) 1.51-1.39 (m, 2H CH_3-**CH_2**) 0.87 (t, 3H, CH_2-**CH_3)**

3.2.4 Synthesis of DSDA (Disulfanediylbis(ethane-2,1-diyl) diacrylate) and DSDMA ((Disulfanediylbis(ethane-2,1-diyl) dimethacrylate

Disulfanediylbis(ethane-2,1-diyl) diacrylate (DSDA) was synthesized via the reported method reported by Huang et al. [3] from starting material 2-2'-disulfanediylbis(ethan-1-ol). Briefly, 2-2'-disulfanediylbis(ethan-1-ol) (9.8 ml 0.08 mol) was dissolved in 200ml chloroform and placed into a 2-neck round bottom flask submerged into an ice bath whilst also being bubbled with nitrogen. Trimethylamine (44.5 ml 0.32 mol) was added to the reaction flask and the mixture was left to stir for 20 mins. Whilst still cool and bubbling acryloyl chloride (25.8 ml 0.32 mol) was added dropwise for 30 mins. The flask was then sealed with a nitrogen balloon and the nitrogen pipe was removed. The mixture was then left to stir for 36 hrs at room temperature. The solution was then filtered to remove solid precipitate and washed twice with 150 ml of de-ionized water and 150 ml of 0.1 M Na_2CO_3 (aq) solution six times before two final washes with NaCl brine. The organics were then dried with magnesium sulfate, filtered and concentrated to yield a brown oil of crude DSDA. Purification was afforded via column chromatography. The crude oil was passed through an aluminum oxide column washed with dichloromethane and the product fractions were concentrated to yield a dark brown oil of DSDA (Yield 45%). ^{1}H NMR (400 MHz $CDCl_3$) δ 6.54-6.27 (m, 2H 2x vinyl H) 6.18-5.95 (m, 2H 2x vinyl H) 5.79 (m, 2H 2x vinyl H) 4.45-4.28 (t, 4H 2x **CH_2-**O) 2.29 (t, 4H 2x S-**CH_2**)

For the synthesis of DSDMA the same procedure as the above was used, acryloyl chloride was substituted for methacryloyl chloride (Yield 63%) ^{1}H NMR (400 MHz

$CDCl_3$) δ 6.25 – 5.91 (m, 2H, 2x vinyl H), 5.59 (m 2H 2x Vinyl H), 4.45 – 4.15 (m, 4H, O=C-O-**CH_2**), 2.97 – 2.82 (m, 4H, **H_2C-**S-S-**CH_2**), 1.88 (s, 6H **CH_3**-C=C).

3.2.5 PAA and DSDA homopolymerization reactions

All reagents were added into a 10 ml reaction vial according to reactions presented in **Table 3-1** equipped with a open top cap sealed with a PTFE septa. Stirring speed was set to 300rpm and the reaction vials were purged with nitrogen for 20 minutes before attachment of nitrogen balloon to ensure a nitrogen rich environment. Reactions were heated and left to polymerize as specified. Reactions were then quenched and purification was afforded via precipitation into diethyl ether thrice and drying was performed at 37.5°C in a vacuum oven for 24hrs.

Table 3- 1: PAA and DSDA homopolymerization experimental conditions

Entry	Polymer Sample	F[A]	RT[B] (hrs)	Temp (°C)	Solvent	Yield (wt. %)
1	$P(PAA)_{FRP1}$	1:1:0[C]	39	60	BULK	9
2	$P(PAA)_{FRP2}$	1:1:0[D]	20	65	BULK	5
3	$P(PAA)_{RAFT}$	1:1:1[D]	20	65	BULK	3
4	$P(DSDA)_{RAFT}$	1:1:1[C]	<1hr	60	BULK	100

A: Feed molar ratio of [Monomer]:[I];[CDCTPA] B: Reaction Time C Initiator used was AIBN D Initiator used was ACVA

3.2.6 PAA-DSDA and PAA-DSDMA RAFT co-polymerisations

All reagents were added into a 10 ml reaction vial according to reactions presented in **Table 3-2** equipped with an open top cap sealed with a PTFE septum. Stirring speed was set to 300rpm and the reaction vials were purged with nitrogen for 20 minutes before attachment of nitrogen balloon to ensure a nitrogen rich environment. Reactions were heated to 65°C and left to polymerize for the time specified. Reactions were then quenched and purification was afforded via precipitation into diethyl ether thrice and drying was performed at 37.5°C in a vacuum oven for 24hrs.

Table 3- 2: PAA-DSDA and PAA-DSDMA RAFT co-polymerisation experiemental conditions

Entry	Polymer Sample	F[A]	RT[B] (hrs)	Temp (°C)	Solvent	Yield (wt. %)
1	$HBP991_{DSDA}$	99:1:0:1:1	20	65	BULK	4 (crude)
1-repeat	$HBP991_{DSDA*}$	99:1:0:1:1	20	65	BULK	6 (crude)
3	$HBP991_{DSDMA}$	99:0:1:1:1	20	65	BULK	3 (crude)

A: Feed molar ratio of [PAA]:[DSDA]:[DSDMA]:[AIBN];[CDCTPA] B: Reaction Time

3.2.7 Hyperbranched Polymer Synthesis via RAFT co-polymerization reactions

All reagents were added into a 10 ml reaction vial according to reactions presented in **Table 3-3** equipped with an open top cap sealed with a PTFE septum. Stirring speed was set to 300rpm and the reaction vials were purged with nitrogen for 20 minutes before attachment of nitrogen balloon to ensure a nitrogen rich environment. Reactions were heated to 65°C and left to polymerize for the time

specified. Reactions were then quenched and purification for HBP3070, HBP4060 and HBP5050 was afforded via precipitation into 8:2 hexane: diethyl ether once before precipitation into pure ether a further two times and drying was performed at 37.5°C in a vacuum oven for 24hrs. Whilst in the case of HBP4060_2 HBP4060_3 and HBP4060_4 purification was employed via the use of dialysis (regenerated cellulose membrane MwCO: 2000Da) in a 80:20 water:THF solvent system for 2 days, with solvent changes every 12hrs. Before a further 3 days in water, with solvent changes every 12hrs. Drying was afforded by freeze drying the liquid that remained in the membrane after the specified time.

Table 3- 3: Hyperbranched co-polymer synthesis experimental conditions

Entry	Polymer Sample	F[A]	RT[B] (hrs)	Temp (°C)	Solvent[C]	Yield (wt. %)
1	HBP3070	30:70:1:1:1	18	65	THF	63
2	HBP4060	40:60:1:1:1	18	65	THF	67
3	HBP5050	50:50:1:1:1	18	65	THF	60
4	HBP4060_2	40:60:1:1:2	18	65	THF	20
5	HBP4060_3	40:60:1:1:3	18	65	THF	11
6	HBP4060_4	40:60:1:1:4	18	65	THF	25

A: molar feed ratio of [PAA]:[DMAEMA}:[DSDA}:[ACVA]:[CDCTPA] B: Reaction Time C: [Monomer]:[Solvent] ratio is 1:1 *v:v*

3.3 Results and Discussion

3.3.1 PAA and DSDA hyperbranched polymer synthesis

2-Propyl Acrylic Acid (PAA) was initially chosen as a core building block due to the unique and desirable pH responsive properties displayed once polymerization has taken place. Previous studies by the Hofmann group have utilized the pH responsive properties of this monomer to produce a plethora of studies for the suitability of this

building block for pH responsive drug delivery purposes [4–6]. Utilizing pH as a stimulus in “smart” stimuli responsive mechanisms therefore, would allow drug delivery to sites particularly effected by acidosis. For instance, it is known that within neoplasms and increase in lactic acid formation is seen, attributed to the “Warburg effect”, in which neoplasia favors anaerobic respiration mechanisms in order to propagate growth [7,8]. Utilizing “smart” macromolecules that respond sharply to the acidic conditions shown within the tumorous microenvironment would facilitate a transition change from hydrophilic to lipophilic conformations allowing interactions with cell membranes and drug release [9–11]. Furthermore, the decision to utilize DSDA as the branching agent as oppose to other multi-vinyl monomers such as Poly(ethyleneglycoldiacrylate) (PEGDA) was due to the disulfide divalent bond presented in this molecule. The disulfide bond is known for being readily reducible, indeed, Zhao et al. displayed that their hyperbranched DMAEMA-DSDA hyperbranched co-polymer presented itself with a much higher degree of degradation when the protein glutathione was introduced [12]. Furthermore, within the Tai group, at Bangor University, DSDA has been studied for degradability properties via redox reactions [13]. It is known that glutathione within the human body is one of the most abundant proteins belonging to the anti-oxidant class [14,15]. In a variety of studies, it has been shown that there is a significant link between the role of glutathione and cancer metathesis [16–19]. Furthermore, the increased concentration of glutathione within neoplasia facilitates exploitation of this protein for degradability of delivery devices via redox facilitated bond breakage [18,20]. There are major concerns associated with the drug delivery process such as degradability and the excretion of vehicles once the payload has been delivered. Therefore, Disulfanediylbis(ethane-2,1-diyl) diacrylate) (DSDA) was not only chosen for its multi-vinyl properties, but as previous studies have shown degradability of this repeating unit with glutathione. Pairing this property with various reports correlating glutathione concentration and tumor metathesis this monomer can facilitate both hyperbranching and biodegradable properties within the synthesized macromolecule.

With all this in mind, the design of a PAA and DSDA hyperbranched co-polymer was formed, in order to exploit the benefits of each degradability and hyperbranched topology. Initial trials aimed to produce a polymer with 99:1 PAA:DSDA ratio, termed “HBP991”. Unfortunately, however, after numerous attempts purification led to excep-

tionally low yield of polymeric species, that could also not be conclusively characterized as the desired compound, due to a large amount of monomeric PAA residue as seen in the ^{1}H NMR spectrum (**Figure 3-1**), whilst high insolubility of precipitated solid was also observed.

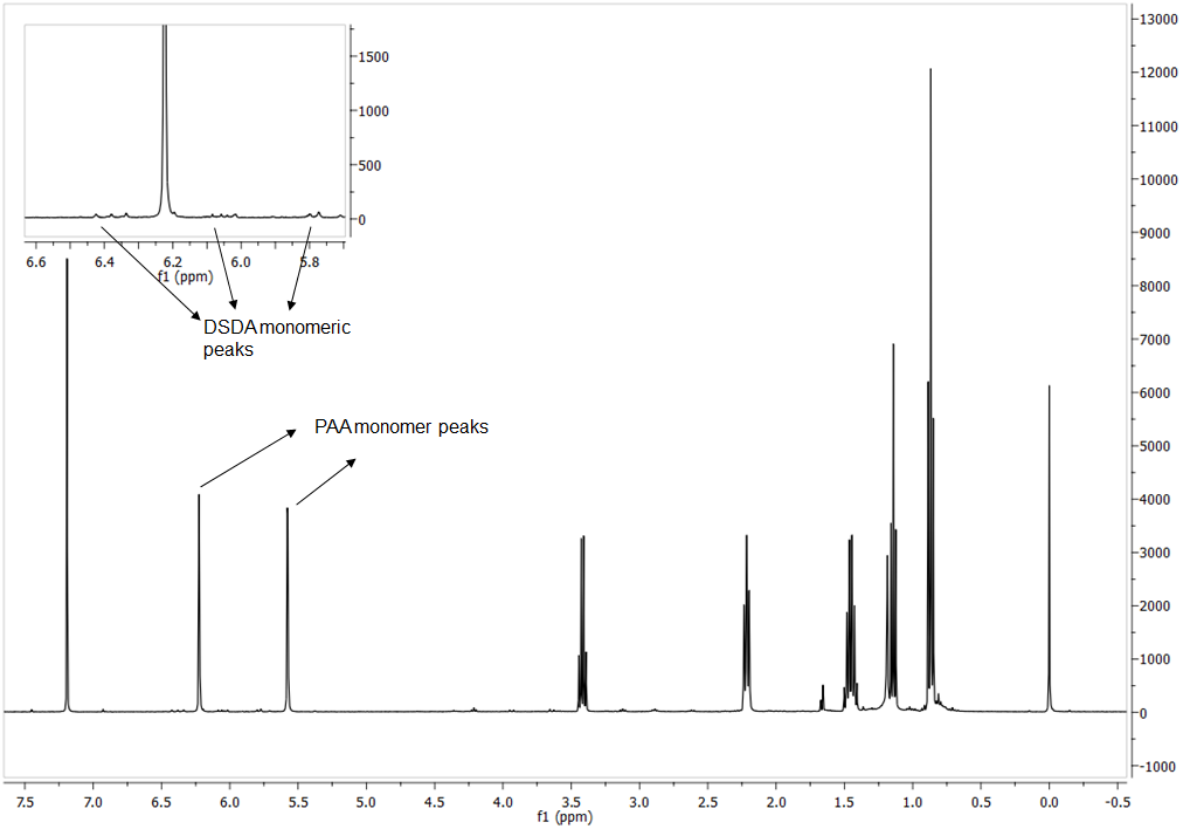

Figure 3- 1: ^{1}H NMR of PAA:DSDA 99:1 solid precipitate performed in CDCl3

From the ^{1}H NMR spectrum monomeric vinyl peaks of both PAA and DSDA can be seen between 6.5 and 5.5 ppm. Furthermore, there is a large observed intensity between the peaks associated between each monomer, this is as expected due to the initial experimental feed ratio of 99:1 between PAA and DSDA. Between 0.5 and 1.5 ppm PAA peaks can be observed (0.87 and 1.45) sandwiching one of two diethyl ether peaks seen at 1.15 and 3.4. Further peaks can be seen at low intensity, such as the DSDA vinylic groups, however, the obtained spectra were enough evidence to suggest that co-polymerisation of these monomers would incur some difficulties.

It is suggested that this could be due to incompatibility between the two monomers, in terms of their reaction rate and therefore, homopolymerizations of both PAA and DSDA were conducted to assess their reaction rates. It is worth noting that previous studies have shown PAA to be a highly unreactive monomer, due to the presence of the carboxyl group and propyl chain on the propagating terminus, leading to steric hindrance[4–6].

It was seen that within 45 minutes the DSDA homopolymerization reaction had formed an overexpressed gel and a brittle solid product was obtained, which was insoluble in all common solvents tested (Water, Methanol, DMF, DMSO, Chloroform). On the other hand, however, homopolymerization of PAA lead to exceptionally small yield after precipitation (3% wt.), adding weight to the argument that these two monomers within the reaction conditions were incompatible. Therefore, the methacrylated derivative of DSDA, disulfanediylbis(ethane-2,1-diyl) bis(2-methacrylate) (DSDMA), was chosen as an alternative monomer for co-polymerization with PAA in order to attempt to provide compatibility, and a lowered reaction rate due to additional steric hinderance on both vinyl groups, and hence a successful polymerization. However, as in previous reactions with DSDA, low yield was obtained and NMR results provided inconclusive as to the success of the reaction, with again most of the precipitated material containing monomeric PAA, as characterized by the presence of vinylic peaks.

The incompatibility issue therefore was becoming a huge stumbling block in the synthesis of the desired polymer, the initiator 2-2’-Azobis(2-methylpropionitrile) (AIBN) was substituted for 4-4’-azobis(4-cyano-valeric acid) (ACVA) (the initiator used for the synthesis of the RAFT agent 4-cyano-4-(((dodecylthio)carbonothioyl)thio)pentanoic acid (CDCTPA) itself, in an attempt to further increase compatibility of all reagents within the reaction vial, although this again gave no promising results. Interestingly, previous studies on the co-polymerization of DMAEMA-DSDA based hyperbranched polymers were published by Zhao and co-workers [12], demonstrating compatibility between the two monomers. It was then hypothesized that the introduction of this monomer, at differing feed ratios alongside PAA and DSDA could allow a successful co-polymerization to occur, although achieving enough PAA incorporation into the final product, to facilitate the desirable pH responsive properties could still lend the design to be cumbersome in synthesis.

3.3.2 Overcoming incompatibility – DMAEMA introduction into hyperbranched polymers - synthesis and characterization

As previously discussed, the incompatibility between DSDA and PAA led to undesirable results with low yield and exceptionally poor purity. Therefore, 2-(Dimethylamino)ethyl methacrylate (DMAEMA) was introduced into the reaction as to attempt a successful full co-polymerization of all three monomers. This monomer has previously been described as having synthetic compatibility alongside DSDA [12] and therefore, critically it was hypothesized that this would lead to a successful co-polymerisation of all three units. This was done in three feed ratios namely a 50:50:1, a 40:60:1 and a 30:70:1 (PAA:DMAEMA:DSDA) in order to assess the most efficient amount of DMEAMA addition to allow co-polymerization resulting in an easy to purify polymer with a high yield, purity and low dispersity (**Table 3-4**).

Table 3- 4: HBPs synthesized via RAFT co-polymerization of PAA DMAEMA and DSDA

Entry	Polymer Sample	F[A]	RT[B] (Hrs.)	Yield (wt. %)
1	HBP3070	30:70:1:1:1	18	63
2	HBP4060	40:60:1:1:1	18	67
3	HBP5050	50:50:1:1:1	18	60

[A:]Feed molar ratio of [PAA]:[DMAEMA]:[DSDA]:[ACVA]:[CDCTPA] [B:]Reaction Time

In addition, ACVA was chosen as the sole initiator in these reactions as to provide further compatibility with the RAFT agent, whilst reactions were now performed within the THF solvent system, to further slow the reaction rates and provide more control over the reaction (**Scheme 3-1**).

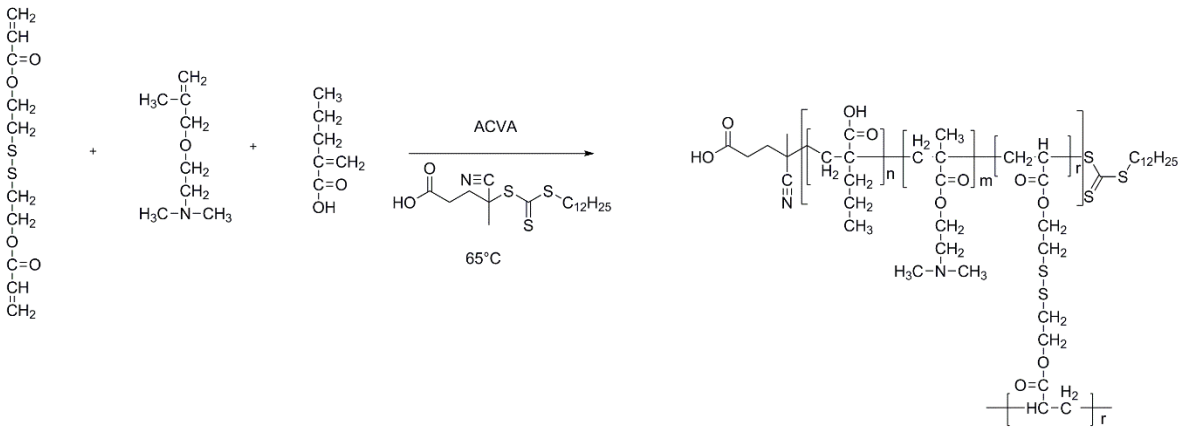

Scheme 3- 1: Synthesis of hyperbranched polymers via Reversible Addition Fragmentation Chain Transfer (RAFT) polymerization.

It was found that the use of DMAEMA allowed for successful co-polymerization of all three monomers, as calculated via ^{1}H NMR spectroscopy post precipitation (**Table 3-5**) using the following method.

Table 3- 5: Monomeric feed ratio and resulting co-polymer composition of Poly(PAA-co-DMAEMA-co-DSDA) HBPs as determined via 1H NMR

Sample	F^{A} PAA:DMAEMA:DSDA	F^{B} PAA:DMAEMA:DSDA
HBP3070	30:70:1	46:52:2
HBP4060	40:60:1	54:43:3
HBP5050	50:50:1	55:42:3

A. Molar feed ratio for polymerization reactions. **B.** Co-polymer composition determined by ^{1}H NMR analysis.

Using HBP4060 as an example throughout the following calculations firstly, the integration value per proton is calculated. This is performed via the sum of integrations per repeat unit where A = PAA K = DMAEMA and Q = DSDA and the value is divided by the total number of hydrogens within the repeat unit. (eq. 3-1)

$$\int per\ H = \frac{\int A}{3x} = \frac{\int K}{6y} = \frac{\int Q}{4z} \qquad \text{(eq. 3-1)}$$

Afterwards, the ratio of A, K, and Q from eq. 3-1 is used to calculate the ratio of repeat units in the polymer (eq. 3-2).

$$\frac{1}{3}:\frac{1.62}{6}:\frac{0.06}{4} = 0.33:0.27:0.015 = 33:27:1.5 = 66:54:3 \qquad \text{(eq. 3-2)}$$

The sum of the ratio repeat units is then used to calculate the overall polymer composition as a percentage by the following (eq. 3-3)

$$\%\,Polymer\ Composition = \frac{66}{123}:\frac{54}{123};\frac{3}{123} * 100\% = 54:43:3 \qquad \text{(eq. 3-3)}$$

One interesting note is that in all three polymerization reactions the yielded compound contained more PAA than the initial feed, contrary to initial co-polymerizations with DSDA alone, which yielded highly insoluble material and significant amounts of the PAA monomeric species, as characterized by the presence of vinylic peaks. The spectra of HBP3070, HBP4060 and HBP5050 display purified compounds with all three monomeric units incorporated and easily recognizable, with a huge decrease of vinylic peaks present, although a small residue of PAA vinyl groups remain. It was by association of the characteristic peaks of each monomeric repeating unit that the composition analysis was performed, with repeat unit characteristic peaks for PAA, DMAEMA and DSDA (A, K and Q respectively) integrations used for this purpose (**Figure 3-2**). Spectra for HBP3070, HBP4060 and HBP5050 complete with integrations can be found in the appendix of this thesis (**Appendix Figures S3-5 – S3-7**).

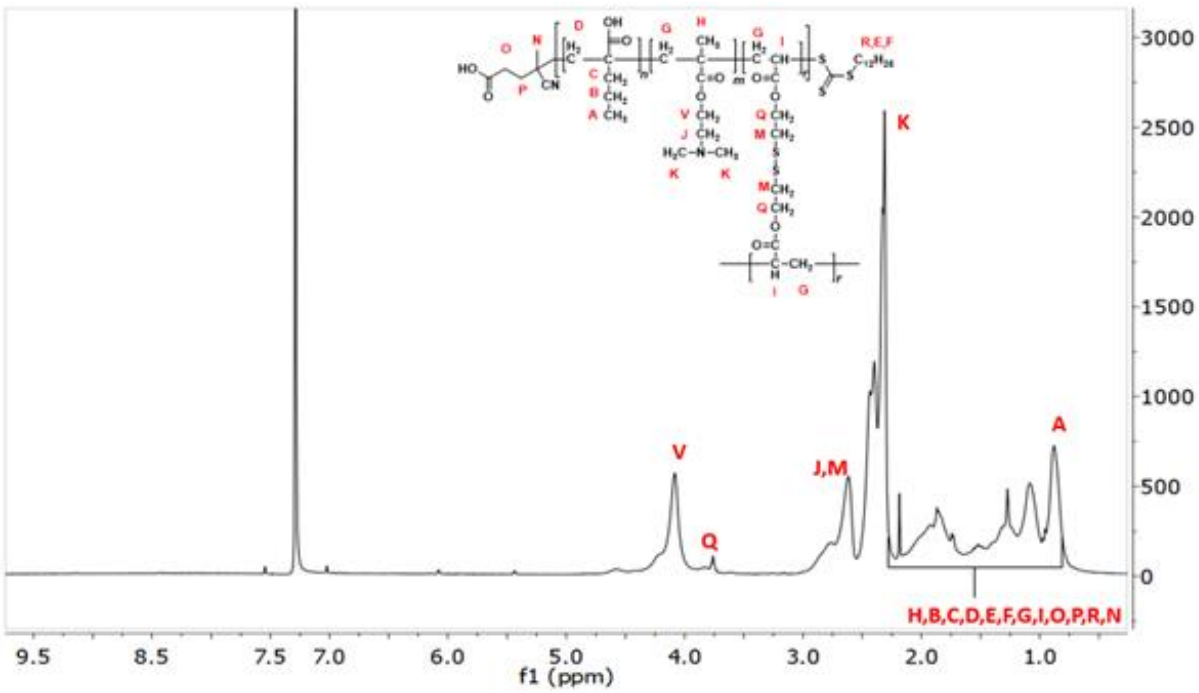

Figure 3- 2: 400 MHz 1H NMR spectrum for HBP4060 in CDCl3 co-polymer composition (n, m, r) can be calculated from integral data

Additional PAA observed within the macromolecular structure could be due to a variety of reasons, however, the addition of DMAEMA into the reaction mixture seems the most likely culprit. DMAEMA's role in facilitating successful polymerization it is suggested is due to the high compatibility to polymerize alongside DSDA. Previously, it was stated that when homopolymerizations were performed DSDA had over-expressed gelation within the first 45 minutes. DMAEMA therefore, as it polymerizes alongside DSDA, may be retarding the rate at which the gelation process is accomplished and subsequently overexpressed. In this hypothesis, DMAEMA-DSDA type polymers would initially form and in turn PAA can then polymerize easier with this structure than DSDA alone for example. Although, taking this into account it would then be expected that there would be a much higher DMAEMA composition in the final product. It is also completely plausible that the introduction of THF into the reaction mixture facilitated this finding. It is well known within polymerizations that are conducted in solvent that there are solvent induced effects on the kinetic profile of the reaction consequently. For instance, the "solvent cage" effect, in which molecules in solvated reaction systems behave as if they are encapsulated and must first diffuse outwards of their solvent cage in order to interact with other molecules (**Figure 3-3**).

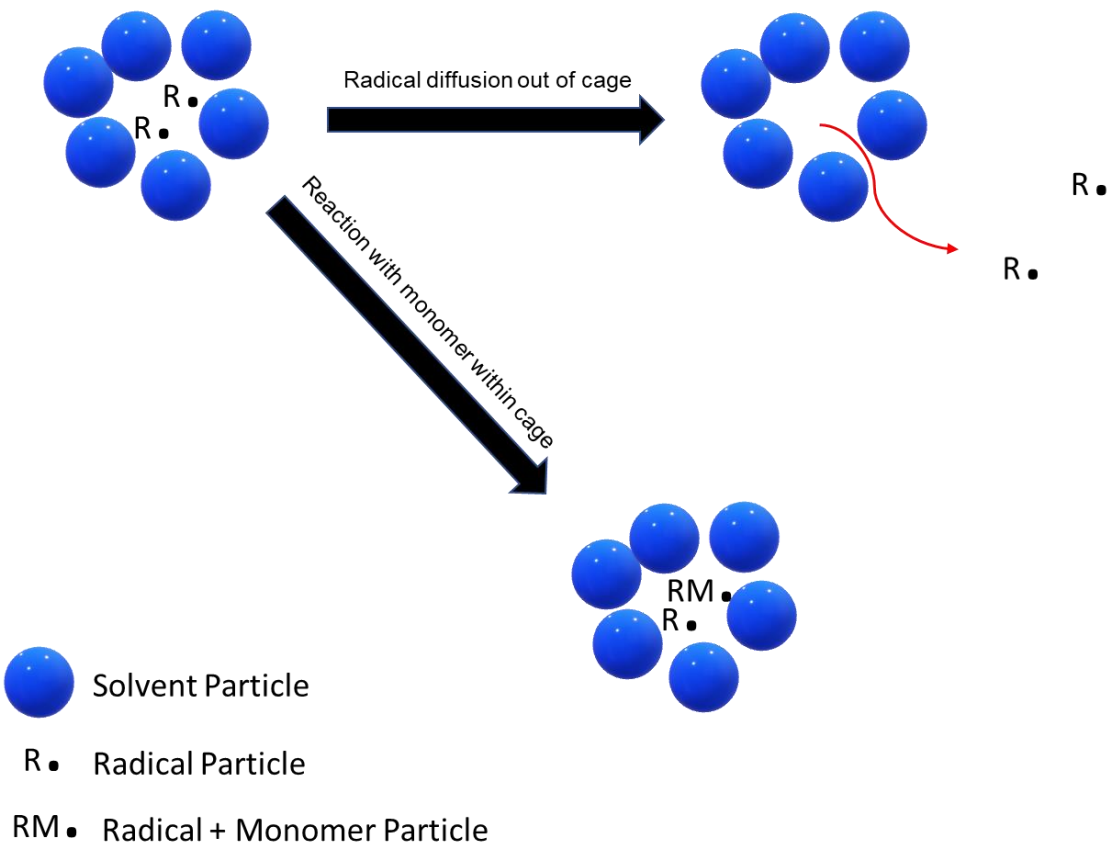

Figure 3- 3: Diagram depicting the cage effect as seen in Radical polymerization mechanisms

The cage effect was first theorized in the mid-1930s by Franck and Rabinowich as a description of the effect of free radicals and their collisions with other particles with respect to this relationship altering the photochemistry of solutions [21,22]. Essentially, as described by Denisov molecules dissolved within a solvent behave not as individual particles but instead as particles encapsulated within the solvent itself [23]. Therefore, for interaction to occur molecules must first diffuse outwards of their cage and trend towards diffusion into a secondary cage in which collisions with a non-identical molecule can occur i.e. for X to collide with Y it must first diffuse outwards and subsequently diffuse into a cage containing Y. Of course, it is also completely reasonable that radicals formed from decomposition may be encapsulated with their target molecule. Monomers (M•) can be encapsulated alongside initiator radicals (R•) in the first instance negating the need for outward diffusion and then diffusion into a cage with the target molecule for interaction (assuming a RM target molecule).The effect

therefore of the so-called cage effect would be observed as retardation of the reaction rates for the whole system, when compared to a bulk system for instance. More time can be therefore be afforded to the reaction before the gelation of DSDA occurs within the reaction vial.

Additionally, solvents within polymerization reactions are known to interfere with the chain transfer or propagation step, monomeric or initiator radicals can abstract hydrogen from the solvent and thus form radicals of the solvent, whilst “de-activating” their radical behavior (**Scheme 3-2**).

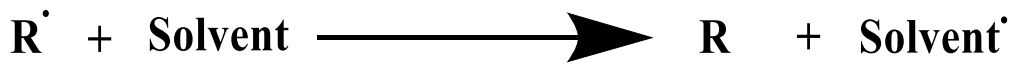

Scheme 3- 2: Initiator radical abstracting hydrogen from solvent particles “de-activating” the initiator

This solvent behavior is also just as plausible as a mechanism for initially slowing the reaction rate of DSDA as the cage effect previously described. However, extensive kinetic studies must be performed on this reaction in order to ascertain the mechanism in which PAA has allowed itself to be introduced into the final macromolecule at higher than feed compositions. In truth, there would be no “one reason” behind this and indeed a combination of all the above hypotheses is a likely scenario.

The three synthesized polymers were then subject to Size Exclusion Chromatography (SEC) in order to assess their molecular weight and dispersity (**Table 3-6**).

Table 3- 6: SEC results for HBPs synthesized with varying DMAEMA composition

Entry	Sample	Retention Time (mins)	GPC Refractive Index		
			M_w (KDa)	M_n (KDa)	Dispersity
1	HBP5050	Peak 1 (11.83 - 13.85) Peak 2 (13.85 - 17.71)	84.5 19.3	73.5 10.4	1.149 1.855
2	HBP4060	12.1 - 18	24.2	9	2.67
3	HBP3070	Peak 1 (11.25 - 13.78) Peak 2 (13.78 - 17.18)	102.4 24.3	83.4 15.3	1.22 1.59

As a vital property of any drug delivery system, there is a constant battle for space within a nano-sized limit and therefore for the purpose of this project the upper limit was set as a hard 200 nm as this has been shown to be the upper limit for receptor mediated endocytosis pathways [24,25]. Within this diameter, particles can also exploit the Enhanced Permeation and Retention (EPR) effect [26]. The EPR effect itself is a consequence of the malignant cells vast reproductive speed. This is due to the Vascular Epithelial Growth Factor (VEGF). VEGF is known to stimulate the production of the blood vessels needed for the delivery of resources required [27]. The result of the abnormally high levels of VEGF is the EPR effect itself, which allows for the passive accumulation of macromolecules into the tumor tissue as the vasculature has developed porous and “leaky” properties [28]. This property unique to the cancerous environment has allowed for nanoparticles [29], liposomes [30] and macromolecular drugs [31] to accumulate within cancerous tissues as oppose to their healthy counterparts.

The synthesized polymers were then subject to SEC analysis in order to obtain molecular weight information. From the SEC results obtained there was a clear indication that within HBP3070 and HBP5050 there were two distinct polymer populations, due to the presence of large shouldering in HBP3070 whilst HBP5050 displayed two peaks, which can be seen in the chromatogram (**Figure 3-4**).

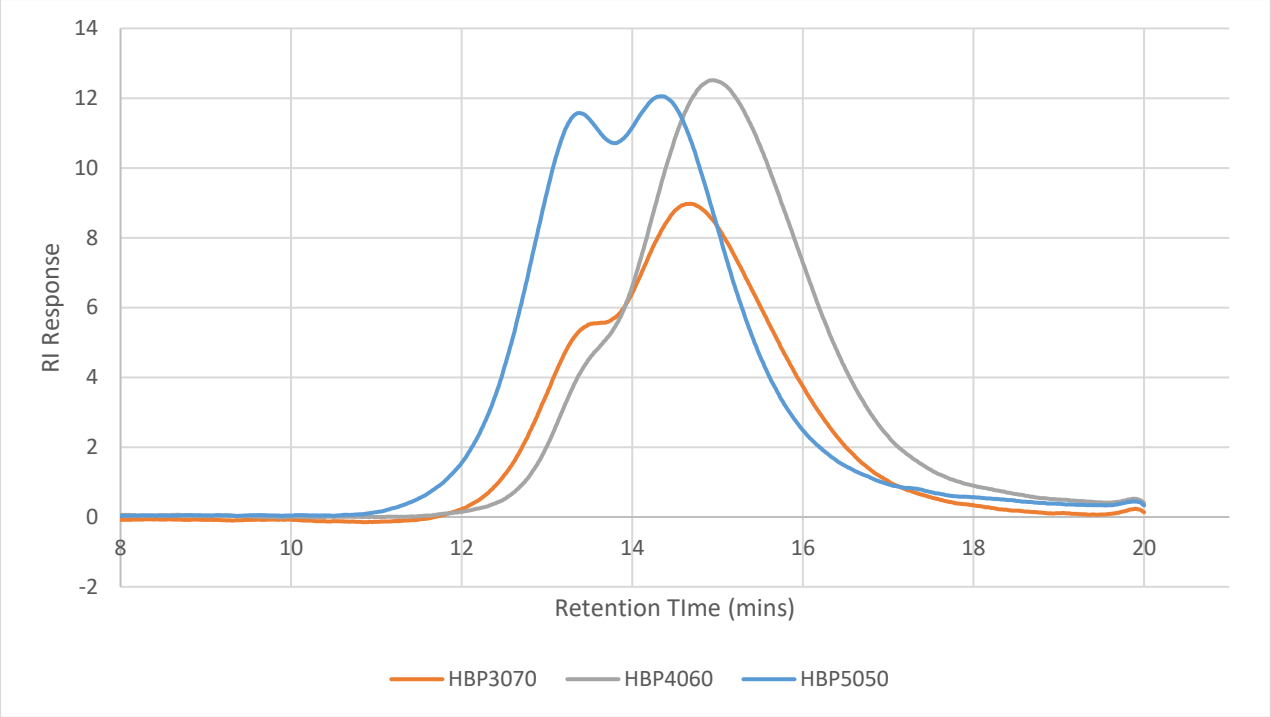

Figure 3- 4: SEC chromatogram for HBPs synthesized with varying DMAEMA composition

Within HBP4060 there was a lack of a pronounced shoulder as seen in the other samples (although mild shouldering did occur) leading to a much higher than expected dispersity value for all three polymers; uncharacteristic of the RAFT approach. In the case of HBP3070 and HBP5050 however, populations with a larger molecular weight did trend towards a value of 1. When the feed of initiator and RAFT agent is taken into consideration however ([I]:[CTA] = 1:1) this lack of control with respect to the dispersity values obtained could be explained as control afforded by the technique was not exploited to the full potential as initiator and RAFT agent concentrations are equal. Normally within a RAFT experiment it is generally accepted that a higher amount of RAFT agent gives a much larger control over the reaction at the expense of the reactivity. i.e. there would be a decrease in molecular weight with respect to a larger molar feed of RAFT agent used, comparative to monomer and initiator molar feed. For instance, a twofold increase of RAFT agent would give a larger molecular weight product when compared to reactions that include a fourfold increase for example if reaction times, temperatures, solvent volume and purification methods remain constant between the two experiments. Furthermore, increasing the amount of

RAFT agent would in turn lower the dispersity value trending towards 1, as greater control is afforded over the reaction as displayed by the mechanism [32] (**Scheme 3-3**).

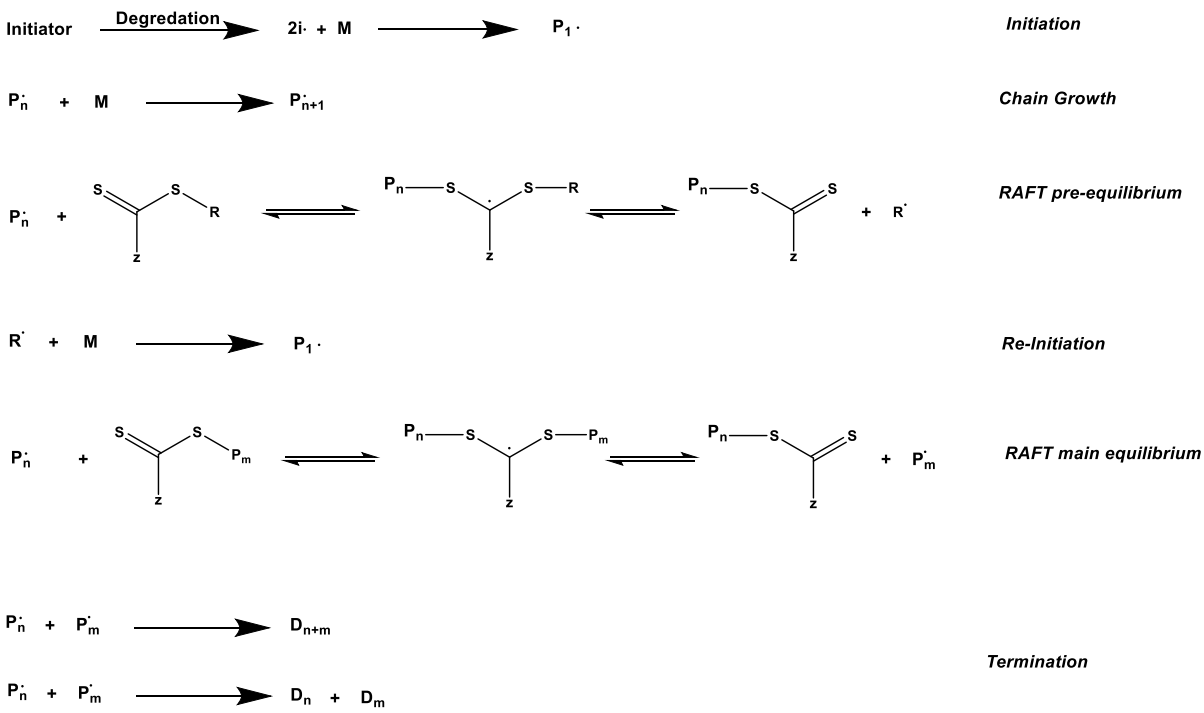

Scheme 3- 3: RAFT polymerization mechanism

It is through the "*living/controlled"* characteristics of the RAFT technique that the reaction can be controlled. Within the main equilibrium of the mechanism that the RAFT adducts are formed and the subsequent RAFT intermediates. This transfer step that is absent from free radical polymerization reactions allows for a much greater control of the reaction. Hence, as previously described an elevated molar amount of RAFT agent when compared to initiator would see a retarding of the propagation rate and a greater concentration of RAFT intermediates.

Despite this, it is interesting to see the effect that composition itself had upon the polymers obtained. For instance, HBP4060 displays a lower molecular weight with less shoulder than the sister polymers, suggesting a mildly different reaction pathway when compared to the other two samples. Although within all three samples there was a distinct polymer population ranging between 19 KDa – 24.3 KDa, only in HBP4060 was it observed that there was no distinction between polymer populations. HBP5050,

from the results obtained, stands out as having two identifiable distinct polymer populations due to the doublet peak observed. Whilst it could be argued that HBP3070 if left longer to react would trend also towards a doublet peak. The same could be said regarding HBP4060 although within the results obtained the polymer population is more homogenous in nature as observed with the current SEC set-up the resolution of the peaks was not adequate to provide distinction between them. Another key point of analysis is the “head” of each peak. For instance, HBP5050 both peaks elute with the highest response alongside HBP3070, whereas HBP4060 stands out as although all peaks overlap in some capacity the greatest response can be seen at a larger retention time than the other samples. As a result of a more homogenous peak and a lower relative molecular weight, when compared to the other samples, HBP4060 was chosen as the material move forward throughout the rest of project as a foundation for further studies.

In order to confirm that the synthesized structure had indeed allowed for the retention of the desirable stimuli responsive properties that the inclusion of PAA was designed upon, HBP4060 was subject to Dynamic Light Scattering (DLS) particle sizing experiments in aqueous media ranging in pH values to assess the effect of pH on the overall polymer behavior. It is imperative to the study that this structure retains the pH responsive characteristics of PAA in order to facilitate endosomal escape. Previous studies have demonstrated this via hemolysis studies. Within physiological conditions (pH 7.4) no activity was observed however, when the pH was dropped to 5.8 90% activity was observed [5]. This activity was attributed to the PAA moieties within the structure. Furthermore, PAA is known to form a compact hypercoiled structure at pH below 6, whereas as pH is increased the opposite is true and solvation can occur [33,34]. Therefore, using DLS this sharp pH response can be observed.

In addition, endocytosis, facilitated by folic acid for example, materials are trafficked into the cells via the folate receptor protein as first described by Bart Kamen [35]. Upon internalization early endosomes display a pH within the range of 6.8-6.1 whilst late endosomes drop to between 6.0-4.8. Therefore, the regulation of pH in endocytic organelles is an important part of their maturation process [36]. It is therefore hypothesized that PAA moieties would facilitate a switch from hydrophilic to lipophilic characteristics which would then allow escape of the drug carrier and the subsequent delivery of drugs, within the intracellular environment.

Therefore, as a relatively inexpensive and brisk measurement technique DLS was chosen in order to identify change in particle size and possible aggregate formation within HBP4060 as a result of pH change. The particle sizing technique relies on a laser beam bombarding particle and the resultant scatter of the beam is used to calculate particle size. Kinetic laws are therefore paramount in understanding and interpretation of the data. Einstein first theorized the idea of Brownian motion in 1905 [37]. Therefore, to observe a true representation of the particle diameter the effects of convection must be negated and the “multiple scatter” phenomena, in which the laser beam can incur interference from the solvent whilst also being scattered by multiple particles on route to the detector, must be taken into consideration.

Initially, the material was dissolved at a 0.1% (w/v) concentration within distilled water adjusted to pH values 7.4, 6.8 and 5.4 with HCl and NaOH in order to mimic pH values pertaining to physiological pH, neoplasia pH and late endosomal pH respectively. Additionally, Dulbecco’s Phosphate Buffered Saline (PBS) was used with material again dissolved at a 0.1% (w/v) concentration. However, by use of the naked eye no clouding of any of the solutions was observed.

This suggested that at the very least there were no solubility issues as a result of fluctuations in the pH of the media. However, whilst solubility was no issue within this range there was no clear indication of the polymer size and self-assembly mechanisms leading to DLS measurements being conducted in order to elucidate any change in particle size as a result of fluctuations in pH within the chosen media.

As seen from the below table (**Table 3-7**) there is a distinct change in size between the differing pH values at a concentration of 0.1% (w/v).

Table 3- 7: DLS results for HBP4060

pH value	Particle diameter Z_{ave}^{ab} (nm)
7.4	100
6.8	75
5.4	337
Dulbecco's PBS	109

a: Harmonic intensity averaged hydrodynamic particle diameter b: measurements showed a neglible error of ± 0.0005 nm and therefore are omitted.

The decrease in particle size initially observed from pH 7.4 to 6.8 could be attributed to the PAA within the sample. As previously mentioned, even mildly acidic environments this building block has been seen to display cationic behavior on the carboxylic acid group and consequentially PAA repeat units coil resulting in a compact structure as a result of induced hydrophobic interactions [33,34]. In addition to this, a larger particle size is found within the lowest pH solution. This could be due to DMAEMA acting as a proton acceptor and inducing solvation within hydrophilic pockets. Interestingly, it is suggested by the data output formation of aggregates (as exemplified by the multiple peak character) is observed in all solutions apart from the solution where the pH is the lowest.

This was interesting as it points to the idea that aggregation formation in HBP4060 is not necessarily a net result from acidification of the pH of the media. It was observed that in both Dulbecco's PBS and media of 7.4 pH the polymer in solution exhibits similar behavior. In both solutions the smallest particle diameters are seen around 10 nm whilst populations of larger particle diameter are observed around 50 – 80 nm. A point of further intrigue is that particles suspended in a solution of pH 7.4 have their largest population between 150-300 nm whereas in PBS solution the reverse is true (highest intensity population is observed at the lowest values). What can be seen from the outputted data is that despite a lower Zave particle diameter polymers suspended in the pH 6.8 solution do not assemble in any sense around the 10 nm mark. Observations indicated that around 20 nm populations assemble with the

smallest diameter, with a distinct population assembling around 100-175 nm in diameter. Whilst the particles displaying this larger diameter are expected to be the result of aggregation the lack of a third distinct population has overall lead to an observed particle diameter lower than that of any other solution.

The Zave was chosen for the reporting as the particle diameter as oppose to the number-average or the volume-average mean size for various reasons. Most importantly, the intensity averaged particle diameter is the most sensitive method for sizing measurements. Even small amounts of aggregation can be detected using this technique. For example, the use of the volume or number averaged particle sizing methodology there are two assumptions that must be taken into account for the results to be accepted as true: the data correlation functions must be repeatable and therefore the data must be of good quality and secondly, the transformation of the data assumes that the spherical, homogeneity and the optical properties of the substance is known. It is widely accepted that the intensity averaged particle size therefore, is the truest representation of the data, especially when particles are known to aggregate. For example, it has been known that through transformations peaks of low intensity can be “lost” and discounted. For example, transforming from intensity to number averaged diameters contributions of peaks may be insignificant to the transformation. This can lead to misunderstanding of results. In fact, it can be all too appealing to transform to the number averaged diameter as this generally gives results of a smaller diameter, as was observed in the data set for HBP4060. Transforming the above data into both the volume and number averaged variants therefore gives the following outputs (**Table 3-8**).

Table 3- 8: Comparison of DLS data via data transformations

Entry	pH value	Particle diameter Z_{ave}[a] (nm)	Volume Averaged Diameter	Number Averaged Diameter
1	7.4	100	10	9
2	6.8	75	21	21
3	5.4	337	428	413
4	Dulbecco's PBS	109	10	10

As displayed by both the number and volume averaged data sets there is firstly the loss of shrinkage of the polymer and the reverse is observed, although the huge increase in diameter is consistently seen throughout all transformations upon stimulation with a media of highest acidity. As previously mentioned, these values seem to neglect the presence of aggregates even at a neutral pH, distorting the data to give the lower diameter value with a gradual increase as pH is dropped to 6.8. What can be obtained from these transformations however is that as pH is dropped to the lowest acidity particle size drastically increases, suggesting solvation of the particle in hydrophilic pockets, as opposed to just a net result of aggregation.

In addition to possible solvation, the polyelectrolyte nature of the HBP cannot be neglected, as both COOH group due to the high pKa value and the tertiary amine by nature can both accept protons there is a rationale that there can be a transfer of charges between these repeat units. In addition to this a zwitterionic character could be displayed with DMAEMA accepting protons from the COOH group in PAA resulting in net charge zero, thus disrupting any pH response. However, this character was not observed and DLS results suggest that there is the expected sharp pH response when this polymer is subjected to acidic media.

In order to fully assess therefore the morphology of these polymers to accurately explain this change in size as a result of morphology and self-assembly changes it would be desirable to perform either Scanning Electron Microscopy (SEM) or Atomic

Force Spectroscopy (AFM). However, sample preparation for these techniques rely on samples being prepared in the solid state and particularly with SEM conductivity is required (normally as a gold-plated sample). The preparation of samples within the desired media and subsequent evaporation of media, not to mention the need for possible modifications such as gold coating would interfere with the particle's true morphology and behavior. Hence, a true indication of their behavior in these media would not be observed via these experimental methods. Additionally, the heat required to evaporate the solvent in question could induce aggregation within the polymer molecules, which would give a false reading for the formation of such and therefore the use of these techniques was discounted.

3.3.4 Utilization of RAFT for controllability of Hyberbranched polymers

After the previous experiments allowed for the composition of the HBP to be tailored to allow full co-polymerizations the focus was on reducing the size and molecular weight of synthesized molecules, with reaction conditions unchanged. Therefore, the controllability of the RAFT approach was exploited leaving reaction feed and temperature and reaction time unchanged, with the exception, of course, of RAFT agent which was increased, in three subsequent reactions. Namely HBP4060_2,3 and 4 (**Table 3-9**) in order to attempt to reduce molecular weight of the compounds without adversely affecting their reaction conditions.

Table 3- 9: HBP4060 sister polymers synthesized via RAFT co-polymerization of PAA DMAEMA and DSDA with variable RAFT agent feed ratio

Entry	Polymer Sample	F[A]	RT[B] (Hrs.)	Yield (wt. %)
1	HBP4060_2	40:60:1:1:2	18	20
2	HBP4060_3	40:60:1:1:3	18	11
3	HBP4060_4	40:60:1:1:4	18	25

[A:]Feed molar ratio of [PAA]:[DMAEMA]:[DSDA]:[ACVA]:[RAFT] [B:]Reaction Time

Further composition analysis was performed as before via ^{1}H NMR spectroscopy. It was seen that in HBP4060_3 and HBP4060_4 there was a comparable similarity towards the initial HBP4060 polymer in terms of composition suggesting a 3% and 4% feed ratio of RAFT agent had no effect on the reaction however, within HBP4060_2 there was a much-increased amount of DMAEMA and DSDA when compared to PAA (**Table 3-10**).

Table 3- 10: HBP4060 sister polymer compositions calculated via 1H NMR

En-try	Sample	F^{A} PAA:DMAEMA:DSDA	F^{B} PAA:DMAEMA:DSDA
1	HBP4060_2	40:60:1	33:62:5
2	HBP4060_3	40:60:1	62:37.5:0.5
3	HBP4060_4	40:60:1	51:46:2

[A.] Molar feed ratio for polymerization reactions. [B.] Co-polymer composition determined by ^{1}H NMR analysis.

With respect to HBP4060_2 there is an argument that the composition obtained is an anomaly as it diverts from the overall trend observed, however, from the composition obtained this variant more truly reflects the initial feed ratio of monomers inserted into the mixture. Therefore, on the flip side it could be argued that with this amount of RAFT agent within the feed this polymer can be obtained with composition closer to the desired feed than is seen with other reactions. One could argue that as the reaction rates of the monomers decrease due to the increased influence of the RAFT agent within the kinetic mechanism the probability of incorporation of all three to match the initial feed has increased. Whilst this is plausible it cannot account for the higher PAA composition seen in HBP4060_3 and HBP4060_4. This could be due to a further slowing of propagation rates negating the notoriously slow rate of growth of PAA chains.

Therefore, in order to fully understand this phenomenon further work on the reaction profile of this co-polymerisation is needed, both computationally and with traditional lab-based work. With a better understanding of the specific reaction profile associated with this reaction, a greater understanding not only of precise amounts of RAFT agent feed to introduce into reaction feeds to give a desired molecular weight can be obtained but in reference to HBP3070 HBP4060 and HBP5050 a much

clearer view of the reasoning behind, at least in the case of HBP5050, doublet peaks and large shouldering when characterisation was performed via SEC analysis.

As with the previous three HBPs HBP4060_2,3 and 4 were subject to SEC analysis and in all cases, it was found that there was relationship between the amount of RAFT agent with respect to the initiator and the overall molecular weight of the polymer. As expected, as RAFT agent feed increased the molecular weight of the polymer decreased. The original HBP4060 was also ran alongside the sister polymers so that an objective view could be taken regarding the increase in RAFT agent and the relationship with molecular weight and dispersity observed, without difference in calibration curves, solvent batch etc. varying throughout. (**Figure 3-5** and **Table 3-11**).

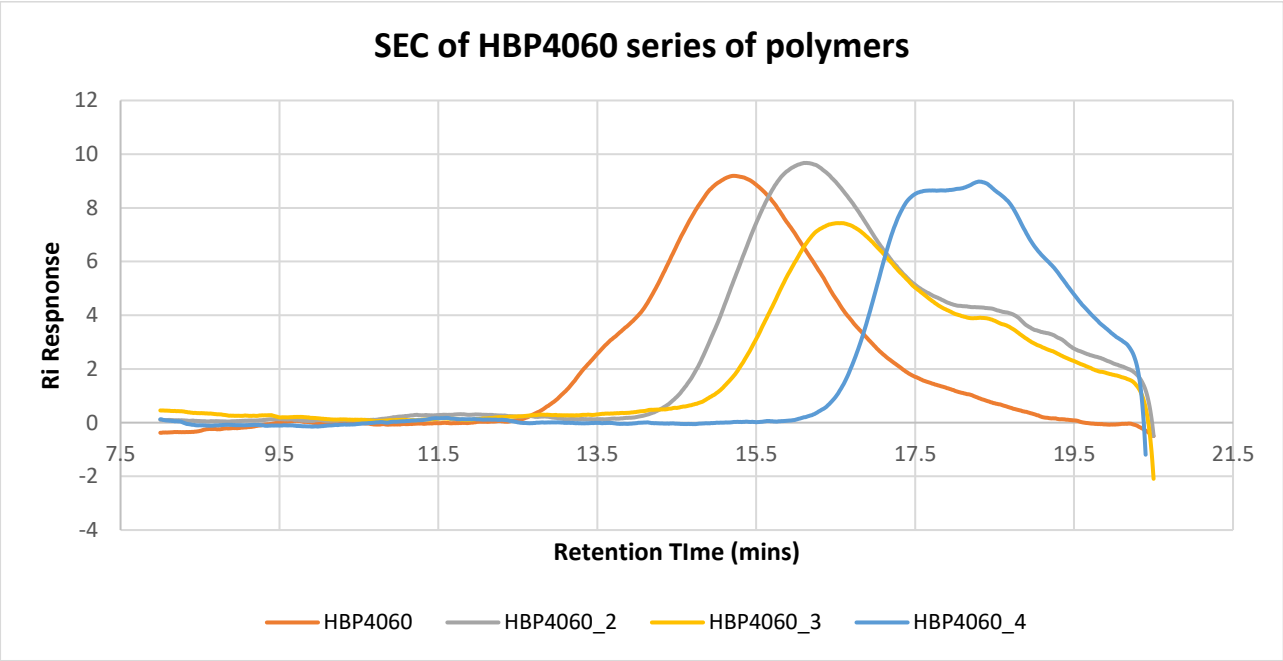

Figure 3- 5: SEC results for HBP4060 and all sister polymers

Table 3- 11: SEC results for HBP4060 and all sister polymers

Entry	Sample	Retention Time (mins)	GPC Refractive Index		
			Mw (Kda)	Mn (Kda)	Dispersity
1	HBP4060	19.13	24.3	6.6	3.7
2	HBP4060_2	Peak 1 (13.85-17.83)	8.1	4.8	1.7
		Peak 2 (17.83-19.78)	0.7	0.6	1.3
3	HBP4060_3	Peak 1 (14.36-18.13)	5.7	3.4	1.7
		Peak 2 (18.13-19.66)	0.6	0.5	1.2
4	HBP4060_4	15.66-19.68	1.4	0.8	1.7

It was interesting to see indeed again there was shouldering in all three cases, however, whereas before the shouldering suggested larger molecular weight molecules eluting faster than the main peak these three polymers all shouldered post elution of the majority population. This leads to the suggestion of the presence of oligomers as molecular weight ranges for the observed shoulders were obtained below 1 KDa for both the M_n and M_w and were broad in character. In the case of HBP4060_4 there appeared to be two peaks merging to create a large broad peak with a tailing shoulder suggesting that despite the low molecular weight obtained there were various population of this polymer, although accurate analysis of this shoulder was not possible due to the broad nature of the peak itself. Positively, however, when assessed for dispersity all polymers with an increase in RAFT agent displayed much lower dispersity than their sister HBP4060. Compared to the initial analysis the dispersity of this polymer increased by a single integer from 2.7 to 3.7. Despite this the molecular weight and shape of the peak of itself remained consistent. This large discrepancy in the measured M_n of this polymer could be due to firstly a different calibration curve and hence a different standard set being used. Whilst the chemical standard remained the same in the fact Poly(methylmethacylate) standards were used in both cases one cannot conclusively state that the calibrations performed on different days will be identical. Interestingly, there was, in the case of the measured M_w, no real discrepancy between the previously observed value and the value observed in the second instance (an increase of 0.1 KDa was observed). It is theorised that this discrepancy is down to degradation of the

individual polymer chains over time. The disulfide bond present in the DSDA hyperbranching agent can be readily reduced to the thiol form and has been presented to do such in numerous literature studies. It is hypothesised that over time and storage this bond has broken down naturally to form thiol end groups and thus chain breakage. This breakage could therefore account for the reduction observed in M_n whilst also the large increase in dispersity seen throughout the sample.

Focusing on dispersity values, HBP4060_2 HBP4060_3 and HBP4060_4 displayed similar dispersity values to one another. Whilst on composition alone it cannot be argued comprehensively that increasing the amount of RAFT agent has led to greater control for any of the newly synthesised polymers than the first sample HBP4060. As from this data alone it would appear that different reaction kinetics have taken place with respect to the growth of the polymer chains, especially in the case of HBP4060_2 regarding DMAEMA incorporation or the diminished DSDA incorporation in HBP4060_3. When comparing HBP4060_2,3 and 4 it can be seen from the observed SEC data that there is a decrease in the dispersity trending towards 1, with all three samples displaying a dispersity value of 1.7 with their associated oligomers trending further towards 1. These observations therefore suggest that greater control has indeed been afforded over the reaction as a result of the increase of RAFT agent in the feed ratio with a much more uniformed distribution of chains calculated than in the original HBP4060.

With this reduction in molecular weight in mind there is an expectation that there should be a reduction in the overall particle size. In addition to this, except for HBP4060_2 it can be theorized that there should be a similar pH response, as a result of their comparable composition when comparing HBP4060 to HBP4060_3 and 4. Previously, it was hypothesised the role DMAEMA may have to play in the self-assembly of these particles in media varying in pH values. Therefore, it will be interesting to see if there is an increase in the particle size as pH drops confirming the suspicion that DMAEMA is facilitating solvation of the overall particle.

Therefore, as previously, all three polymers were subject to DLS in aqueous media varying in pH value, as well as the Dulbecco’s PBS. From the observed data (**Table 3-12**) it was observed that as molecular weight decreases there is also a reduction in the overall particle size.

Table 3- 12: DLS data HBP4060 sister polymers

Entry	Sample	pH	Zave Particle Diameter (nm)
1	HBP4060_2	7.4	135
		6.8	150
		5.4	146
		Dulbecco's PBS	150
2	HBP4060_3	7.4	144
		6.8	194
		5.4	291
		Dulbecco's PBS	80
3	HBP4060_4	7.4	9
		6.8	17
		5.4	26
		Dulbecco's PBS	31

In addition to this, as expected there is a similar pH response between the samples HBP4060_3 and HBP4060_4 with HBP4060_2 displaying slightly different characteristics. Although, unlike HBP4060 there was no shrinkage seen as pH was lowered from 7.4 to 6.8. However, overall the trend of reducing pH to 5.4 increases the particle size greatly in these two samples. Interestingly, as seen in HBP4060_2 the size of particles between pH 6.8 and 5.4 are very similar with only a 4 nm difference between the two. This is most likely due to the heightened presence and influence of DMAEMA within the overall structure, allowing stabilisation of the structure and hence self-assembly mechanisms of this sample within the pH ranges studied is similar, as oppose to HBP4060-3 and 4 in which it can be argued the increase of pH alters this mechanism. HBP4060_2 can therefore give a better indication of the influence DMAEMA has on “masking” the pH response of PAA particles within aqueous media through the observed DLS results. For instance, as previously stated when media is lowered even slightly to a lower pH there is a sharp response resulting from PAA’s tendency to coil and form compact topologies in these conditions. Although in HBP4060_3 and HBP4060_4 this was not seen. This could be due to the number of repeat units of PAA within these particles. Of course, with a reduction in molecular weight there is a trade-off with the number of repeating units incorporated within the structure. Taking HBP4060 as an example for the calculations the following applies:

Firstly, the molecular weight of each repeat unit in the polymer is found by a multiplication of the M_w of the polymer obtained via SEC and the composition % obtained via ^{1}H NMR spectroscopy (eq. 3-4).

$$\begin{aligned} Molecular\ weight\ of\ total\ repeat\ units\ PAA{:}\,DMAEMA{:}\,DSDA \\ = (24200 * 0.54){:}\,(24200 * 0.43){:}\,(24200 * 0.03) \\ = 13068\ Da{:}\,10406\ Da{:}\,726 Da \end{aligned} \quad \text{(eq. 3-4)}$$

Secondly, from the calculated total weight of repeating units the number of repeating units is calculated by division of the calculated values by the molecular weight of the monomeric units (eq. 3-5).

$$\begin{aligned} no.of\ repeat\ units\ PAA{:}\,DMEAMA{:}\,DSDA = \frac{13068}{114}{:}\,\frac{10406}{157}{:}\,\frac{726}{262} \\ = 115{:}\,66{:}\,3 \end{aligned} \quad \text{(eq. 3-5)}$$

Using this methodology, the number of repeat units for each polymer synthesised can be calculated and are presented in **Table 3-13**. For HBP4060_2, HBP4060_3 and HBP4060_4 M_w as characterised via SEC was assumed to be the larger value, as this pertained to the main polymer chains and not to oligomers, dimers or trimers that were found to be present.

Table 3- 13: Calculated no. of repeating units in HBPs

Entry	Polymer Sample	Mw via SEC	% composition via NMR	No. of Repeat Units
1	HBP4060	24.3	54:43:3	115:66:3
2	HBP4060_2	8.1	33:62:5	23:32:15
3	HBP4060_3	5.7	62:37.5:0.5	31:14:0.1
4	HBP4060_4	1.4	51:46:2	6:4:0.1

From the calculated values for the numbers of repeating unit per polymer sample there is reason to suspect that the difference in pH responsive character shown between HBP4060 and HBP4060_3 and HBP4060_4 despite similar composition values. This could be due in part to the limited DSDA repeating units within the samples. Due to the much lower molecular weight of these samples and

the limited amount of DSDA introduced through the feed, there is a distinct lack of DSDA repeating units in the polymer chains. In this respect utilising the composition alone for predictions and interpretations of the DLS data can lead to slightly misleading propositions. For instance, by composition alone it would be reasonable to suggest that there is a limited amount of DSDA in the polymers leading to slight hyperbranching in all samples. Considering HBP4060_3 and HBP4060_4 there is such a limited amount of DSDA within samples of low molecular weight that the majority of the sample may indeed be linear in topology, although hyperbranching will occur in some chains but not all; as proposed by the repeat unit calculations. This scenario could be one reason for the difference in responsive behaviour these two polymers display compared to HBP4060. In a more linear topology, there is not the benefits of a hyperbranching structure, such as a compact structure with a vast amount of functionality [13,38–40]. This therefore, could hinder the pH response and lead to exaggerated solvation through DMAEMA moieties. Another point to consider is that there is a fourfold decrease of PAA units in HBP4060_3 and almost a twentyfold decrease of PAA units in HBP4060_4 when compared to the largest HBP4060. This fact alone could go some way to understanding the lack of shrinkage expected from PAA moieties as there is an insufficient amount of such units presented within the samples themselves to induce a measurable change.

As with the initial HBP4060 transformations of the data to both the volume averaged and number averaged particle diameter was performed, and the results are summarised in **Table 3-14**

Table 3- 14: Comparison of DLS data via data transformations for HBP4060 sister polymers

Entry	Sample	pH	Zave Particle Diameter (nm)	Volume Averaged Diameter (nm)	Number Averaged Diameter (nm)
1	HBP4060_2	7.4	135	132	112
		6.8	150	198	146
		5.4	146	156	151
		Dulbecco's PBS	150	16	14
2	HBP4060_3	7.4	144	126	118
		6.8	194	126	121
		5.4	291	43	26
		Dulbecco's PBS	80	8	8
3	HBP4060_4	7.4	9	8	8
		6.8	17	7	7
		5.4	26	5	4
		Dulbecco's PBS	31	7	6

As before it can be observed that in general the volume and number averaged diameters neglect the effect of aggregation and the smallest observed particle diameters are reported. Interestingly for both HBP4060_3 and HBP4060_4 there is a noticeable shrinkage in size from pH 6-8 – 5.4 after an initial increase, which is to the contrary of the transformations performed on HBP4060, whilst HBP4060_2 transformations seem to reflect the Zave reported data.

This shrinkage observed in HBP4060_3 and 4 via the transformations could be evidence of PAA pH response, which has been masked by the aggregation formed due to the hydrophobic character displayed upon PAA coiling. Again, it is unfortunate that SEM, TEM or AFM could not be performed on these particles in solution to confirm this theory, however, these data present themselves as a foundation for further work to be performed on assessing further in depth how both

the molecular weight and polymer composition influence the behaviour of PAA based co-polymers in solution.

3.4 Concluding Remarks

The aim of this project was to synthesise a novel stimulus responsive hyperbranched structure for the use in targeted chemotherapeutics via the exploitation of the folate receptor via the use of the RAFT polymerisation technique. Initially, two monomers were chosen for this role PAA, due to its well observed stimuli responsive nature, and DSDA, due to the attractive properties of having a readily reducible disulfide bond alongside multi vinyl properties and reactions were conducted in a 99:1 (PAA:DSDA) monomer molar reaction feed, with initiators and RAFT agent used a 1% compared to the overall monomer molar amount. However, incompatibility between the two monomers was observed due to vastly differing reaction rates with initial experiments yielding a small amount of polymer with highly insoluble particulates contained within. Therefore, logically the next step was the introduction of a further monomer that had previously displayed compatibility with DSDA, it was in this vein that DMAEMA was introduced to form a three monomer reaction mixture, aiming to produce a macromolecule that indeed incorporated all three monomers into the overall structure. Therefore, polymer synthesis reactions were performed with a 50:50:1, 40:60:1 and 30:70:1 (PAA:DMAEMA:DSDA) reaction molar feed ratio, with a 1% RAFT agent and initiator ACVA feed ratio (when compared to overall monomer molarity). Indeed, the hypothesis was proven to be correct with successful synthesis of the desired compounds which were characterised using ^{1}H NMR, GPC-SEC, FTIR and DLS. Further work then aimed to further control the reaction as GPC analysis lead to the conclusions that multiple polymer populations were present within HBP5050, HBP4060 and HBP3070, however, it was HBP4060 that displayed the most desirable characteristics in terms of macromolecule homogeneity. Additionally, DLS confirmed the initial hypothesis of stimuli responsive characteristics being induced by the inclusion of PAA, when tested at pH 5.4, 6.8 and 7.4. However, in all cases macromolecules displayed undesirable particle sizing characteristics, with the indication that further conjugation

onto these polymers would result in a drug delivery device that will surpass the 200 nm radius cut off for endocytosis to occur. Therefore, RAFT agent molar feed amounts were increased to 2%, 3% and 4% in subsequent reactions in order to assert further control over the polymerization process to form HBP4060_2,3 and 4, which again were characterised by the use of ^{1}H NMR, GPC-SEC, FTIR and DLS. GPC analysis confirmed that greater control was afforded over the reaction with a decrease in molecular weight of polymers and decrease in PDI. DLS analysis also substantiated the claims of higher reaction control, with stimuli responsive characteristics maintained, and a much lower and acceptable particle radius observed. However, there was still the presence of multiple polymer populations presented suggesting a complex mechanism of polymerization in which two initial chains are formed, perhaps of different monomer composition. Therefore, an assessment of the research conducted and summary of the conclusions is that A. due to a retarded reaction rate the monomer PAA requires polymerisation in bulk, in terms of reactions with DSDA or the methacrylate sister DSDMA bulk reactions result in intensive overexpressed gelation of the disulfide containing monomers. B. The introduction of DMAEMA into the polymerization reaction feed allowed for full polymerization of all three monomers allowing for the synthesis of stimuli responsive hyperbranched polymers and C. increasing RAFT agent ratio within the reaction allowed for greater control over molecular weight and particle size at the expense of product yield.

Work on computational chemistry was conducted in order to attempt to resolve some of the conclusions stated within using the MCPolymer program, which utilises the Monte Carlo simulation method for polymer simulations and was designed by Drache and Drache. Experiments were conducted initially on the *in-situ* RAFT polymerisation of methyl methacrylate (MMA) and were correlated against wet chemistry GPC kinetic studies. It was observed that there was some correlation between computational and experimental results, in terms of PDI and molecular weight of the polymers synthesised, however the results obtained were crude and deemed inappropriate for reporting. Therefore, it would be suggested further work in this area would have eliminated the trial and error of the initial polymer synthesis, and thus kinetic studies need to be performed on each constituent of a proposed polymeric structure (monomers, initiators etc) in order to obtain accurate kinetic

profiles and rate constants to program. This was proposed to be performed, however, technical difficulties in obtaining GPC results in house limited these experiments with ^{1}HNMR the only method for kinetic profiling. Thus, it is suggested that more focus is paid to the computational chemistry behind the RAFT polymerisation of these polymers so that the molecule can be synthesised with the desired characteristics.

References

[1] A. Tochwin, Hydrophilic Copolymers from Multivinyl Monomers via Reversible Addition-Fragmentation Chain Transfer Polymerisation (RAFT) for Hydrogel Applications, PHD Thesis. (2016).

[2] M. Ferritto, D.A. Tirrell, Poly(2-ethylacrylic acid), Volume 11, Wiley 1992, 1992.

[3] Y. Huang, R. Sun, Q. Luo, Y. Wang, K. Zhang, X. Deng, W. Zhu, X. Li, Z. Shen, In situ fabrication of paclitaxel-loaded core-crosslinked micelles via thiol-ene “click” chemistry for reduction-responsive drug release, J. Polym. Sci. Part A Polym. Chem. 54 (2015) 99–107. https://doi.org/10.1002/pola.27778.

[4] X. Yin, A.S. Hoffman, P.S. Stayton, Poly(N -isopropylacrylamide- c o -propylacrylic acid) Copolymers That Respond Sharply to Temperature and pH, Biomacromolecules. 7 (2006) 1381–1385. https://doi.org/10.1021/bm0507812.

[5] H. Tai, C.L. Duvall, P.S. Stayton, A.S. Hoffman, W. Wang, pH-Responsive Hyperbranched Copolymers from One-pot RAFT Copolymerization of Propylacrylic Acid and Poly (Ethylene Glycol Diacrylate), Adv. Sci. Technol. 77 (2013) 333–342. https://doi.org/10.4028/www.scientific.net/AST.77.333.

[6] N. Murthy, J.R. Robichaud, D.A. Tirrell, P.S. Stayton, A.S. Hoffman, The design and synthesis of polymers for eukaryotic membrane disruption, J. Control. Release. 61 (1999) 137–143. https://doi.org/10.1016/S0168-3659(99)00114-5.

[7] O. Warburg, Injuring of Respiration the Origin of Cancer Cells, Science (80-.). 123 (1956) 309–14. https://doi.org/10.1126/science.123.3191.309.

[8] M.G. Vander Heiden, L.C. Cantley, C.B. Thompson, P. Mammalian, C. Exhibit, A. Metabolism, Understanding the Warburg Effect : Cell Proliferation, Science (80-.). 324 (2009) 1029–1034. https://doi.org/10.1126/science.1160809.

[9] M.A. Ward, T.K. Georgiou, Thermoresponsive polymers for biomedical applications, Polymers (Basel). 3 (2011) 1215–1242. https://doi.org/10.3390/polym3031215.

[10] M.E.H. El-Sayed, A.S. Hoffman, P.S. Stayton, Rational design of composition and activity correlations for pH-responsive and glutathione-reactive polymer therapeutics, J. Control. Release. 104 (2005) 417–427. https://doi.org/10.1016/j.jconrel.2005.01.009.

[11] S. Lv, Z. Tang, D. Zhang, W. Song, M. Li, J. Lin, H. Liu, X. Chen, Well-defined polymer-drug conjugate engineered with redox and pH-sensitive release mechanism for efficient delivery of paclitaxel, J. Control. Release. 194 (2014) 220–227. https://doi.org/10.1016/j.jconrel.2014.09.009.

[12] T. Zhao, H. Zhang, B. Newland, A. Aied, D. Zhou, W. Wang, Significance of branching for transfection: Synthesis of highly branched degradable functional poly(dimethylaminoethyl methacrylate) by vinyl oligomer combination, Angew. Chemie - Int. Ed. 53 (2014) 6095–6100. https://doi.org/10.1002/anie.201402341.

[13] A. Tochwin, A. El-Betany, H. Tai, K.Y. Chan, C. Blackburn, W. Wang, Thermoresponsive and reducible hyperbranched polymers synthesized by RAFT polymerisation, Polymers (Basel). 9 (2017) 1–15. https://doi.org/10.3390/polym9090443.

[14] R. Masella, R. Di Benedetto, R. Varì, C. Filesi, C. Giovannini, Novel mechanisms of natural antioxidant compounds in biological systems: Involvement of glutathione and glutathione-related enzymes, J. Nutr. Biochem. 16 (2005) 577–586. https://doi.org/10.1016/j.jnutbio.2005.05.013.

[15] M. Mari, A. Morales, A. Colell, C. Garcia-Ruiz, J.C. Fernandez-Checa, Mitochodrial Glutathione, a Key Survival Antioxidant, Antioxid. Redox Signal. 11 (2014) 2685–2700. https://doi.org/10.1089/ars.2013.5179.

[16] C.C. Yeh, M.F. Hou, S.H. Wu, S.M. Tsai, S.K. Lin, L.A. Hou, M. Hsu, L.Y. Tsai, A study of glutathione status in the blood and tissues of patients with breast cancer, Cell Biochem. Funct. 24 (2006) 555–559. https://doi.org/10.1002/cbf.1275.

[17] T. Schnelldorfer, S. Gansauge, F. Gansauge, S. Schlosser, H.G. Beger, A.K. Nussler, Glutathione depletion causes cell growth inhibition and enhanced apoptosis in pancreatic cancer cells, Cancer. 89 (2000) 1440–1447. https://doi.org/10.1002/1097-0142(20001001)89:7<1440::AID-CNCR5>3.0.CO;2-0.

[18] J.M. Estrela, A. Ortega, E. Obrador, Glutathione in cancer biology and therapy., 2006. https://doi.org/10.1080/10408360500523878.

[19] G.K. Balendiran, R. Dabur, D. Fraser, The role of glutathione in cancer, Cell Biochem. Funct. 22 (2004) 343–352. https://doi.org/10.1002/cbf.1149.

[20] P. Calvert, K.S. Yao, T.C. Hamilton, P.J. O'Dwyer, Clinical studies of reversal of drug resistance based on glutathione, Chem. Biol. Interact. 111–112 (1998) 213–224. https://doi.org/10.1016/S0009-2797(98)00008-8.

[21] J. Franck, E. Rabinowitch, Some Remarks About Free Radicals and, Trans. Faraday Soc. 30 (1934) 120–130.

[22] E. Rabinowitch, W.C. Wood, The collison mechanism and the primary photochemical process in solutions, Trans. Faraday Soc. 32 (1936) 1381–1387. https://doi.org/10.1039/TF9363201381.

[23] E.T. Denisov, Cage effects in a polymer matrix, Die Makromol. Chemie. 8 (1984) 63–78. https://doi.org/10.1002/macp.1984.020081984106.

[24] J. Rejman, V. Oberle, I.S. Zuhorn, D. Hoekstra, Size-dependent internalization of particles via the pathways of clathrin- and caveolae-mediated endocytosis, Biochem. J. 377 (2004) 159–169. https://doi.org/10.1042/BJ20031253.

[25] J.M. Oh, S.J. Choi, G.E. Lee, J.E. Kim, J.H. Choy, Inorganic metal hydroxide nanoparticles for targeted cellular uptake through clathrin-mediated endocytosis, Chem. - An Asian J. 4 (2009) 67–73. https://doi.org/10.1002/asia.200800290.

[26] J. Fang, H. Nakamura, H. Maeda, The EPR effect: Unique features of tumor blood vessels for drug delivery, factors involved, and limitations and augmentation of the effect, Adv. Drug Deliv. Rev. 63 (2011) 136–151. https://doi.org/10.1016/j.addr.2010.04.009.

[27] H.L. Goel, A.M. Mercurio, VEGF targets the tumour cell, Nat. Rev. Cancer. 13 (2013) 871. https://doi.org/10.1038/nrc3627.

[28] V. Torchilin, Tumor delivery of macromolecular drugs based on the EPR effect, Adv. Drug Deliv. Rev. 63 (2011) 131–135. https://doi.org/10.1016/j.addr.2010.03.011.

[29] S. Acharya, S.K. Sahoo, PLGA nanoparticles containing various anticancer agents and tumour delivery by EPR effect, Adv. Drug Deliv. Rev. 63 (2011) 170–183. https://doi.org/10.1016/j.addr.2010.10.008.

[30] K. Maruyama, Intracellular targeting delivery of liposomal drugs to solid tumors based on EPR effects, Adv. Drug Deliv. Rev. 63 (2011) 161–169. https://doi.org/10.1016/j.addr.2010.09.003.

[31] R. Duncan, Polymer conjugates as anticancer nanomedicines., Nat. Rev. Cancer. 6 (2006) 688–701. https://doi.org/10.1038/nrc1958.

[32] C. Barner-Kowollik, M. Buback, B. Charleux, M. Coote, M. Drache, T. Fukuda, A. Goto, B. Klumperman, A.B. Lowe, J. Mcleary, G. Moad, M. Monteiro, R. Sanderson, M. Tonge, P. Vana, Mechanism and Kinetics of Dithiobenzoate-Mediated RAFTPolymerization. I. The Current Situation, Polymer (Guildf). 48 (2010) 1973–1978. https://doi.org/10.1002/POLA.

[33] A. Katchalsky, H. Eisenberg, Molecular weight of polyacrylic and polymethacrylic acid, J. Polym. Sci. 6 (1951) 145–154. https://doi.org/10.1002/pol.1951.120060202.

[34] T. Swift, L. Swanson, M. Geoghegan, S. Rimmer, The pH-responsive behaviour of poly(acrylic acid) in aqueous solution is dependent on molar mass, Soft Matter. 12 (2016) 2542–2549. https://doi.org/10.1039/c5sm02693h.

[35] B. a Kamen, a Capdevila, Receptor-mediated folate accumulation is regulated by the cellular folate content., Proc. Natl. Acad. Sci. U. S. A. 83 (1986) 5983–7. https://doi.org/10.1073/pnas.83.16.5983.

[36] F.R. Maxfield, D.J. Yamashiro, Endosome acidification and the pathways of receptor-mediated endocytosis., in: Atassi M.Z. Immunobiol. Proteins Pept. IV. Adv. Exp. Med. Biol., Springer, Boston, MA, 1987: pp. 189–198. https://doi.org/10.1007/978-1-4684-5442-0_16.

[37] A. Einstein, On the Motion of Small Particles Suspended in a Stationary Liquid, as Required by the Molecular Kinetic Theory of Heat, Ann. Phys. 322 (1905) 549–560. https://doi.org/10.1002/andp.19053220806.

[38] B.I. Voit, A. Lederer, Hyperbranched and Highly Branched Polymer Architectures — Synthetic Strategies and Major Characterization Aspects Hyperbranched and Highly Branched Polymer Architectures s Synthetic Strategies and Major Characterization Aspects, Chem. Rev. 109 (2009) 5924–5973. https://doi.org/10.1021/cr900068q.

[39] D. Wang, T. Zhao, X. Zhu, D. Yan, W. Wang, Bioapplications of hyperbranched polymers, Chem. Soc. Rev. 44 (2015) 4023–4071. https://doi.org/10.1039/c4cs00229f.

[40] D.A. Tomalia, J.M.J. Fréchet, Discovery of dendrimers and dendritic polymers: A brief historical perspective, J. Polym. Sci. Part A Polym. Chem. 40 (2002)

2719–2728. https://doi.org/10.1002/pola.10301.

[41] M. Drache, G. Drache, Simulating controlled radical polymerizations with mcpolymer-a monte carlo approach, Polymers (Basel). 4 (2012) 1416–1442. https://doi.org/10.3390/polym4031416.

Chapter Four – Bio-conjugation of Hyperbranched Polymers and assessment of their in vitro bioactivity

---

Parts of this chapter have been published in

C. Blackburn, H. Tai, M. Salerno, X. Wang, E. Hartsuiker, W. Wang, Folic acid and rhodamine labelled pH responsive hyperbranched polymers : Synthesis , characterization and cell uptake studies, Eur. Polym. J. 120 (2019) 109259. doi:10.1016/j.eurpolymj.2019.109259.

C. Blackburn, H. Tai, M. Salerno, X. Wang, C. Senan, I. Ratcliffe, E. Hartsuiker, W. Wang, Data presenting the synthesis of three novel stimuli responsive hyperbranched polymers synthesised via RAFT polymerisation and the bio conjugation of folic acid, Data Br. 28 (2020) 104861 doi:10.1016/j.dib.2019.104861

4.1 Introduction

This chapter discusses mainly the bio-conjugation work and analysis of polymer bioactivities with respect to the polymers discussed in chapter three. Bio-conjugation work was utilised using the well-known Steglich esterification technique in order to form amide bonds with the carboxylic acid group present on either the polymer functional groups or the target ligand itself (folic acid or fluorophores) and a 1° amine group. Three main linkers were used throughout the project namely two PEG-diamines and an ethylene diamine and the suitability of each is discussed throughout this chapter, with attention paid to their synthetic route and cytotoxicity. Whilst drug loading of gemcitabine was performed via the use of a disulfide bridging amino acid, with further cytotoxicity and therapeutic uptake studies performed. Particular attention is paid in towards the end of this chapter towards the suitability of the structure for the role and whether proof of concept can be achieved to continue with this structure further or if further modifications are needed in order to optimise bio-activity.

4.2 Experimental

4.2.1 Materials

All solvents (hydrous and anhydrous) were bought from Fisher Scientific at the highest possible grade unless specified otherwise. PEG (Mw 400 and Mw 200), Phthalimide (99%), N-Hydroxysuccinimide (98%), dicyclohexylcarbodiimide (99%), Triflouroacetic acid (99%), ethylene diamine (99%), Boc anhydride (97%), thioglycolic acid (98%), Fluorescein sodium salt, Rhodamine B and cysteamine (ca. 95%) were all purchased from sigma Aldrich.

Diisopropylazodicarboxylate (DIAD) (alfaaesar 94%), triphenylphosphine (ACROS Organics 99%), hydrazine hydrate 55% (35% hydrazine) (ACROS Organics) folic acid (Fisher bioreagents), hydrogen peroxide (Honeywell Fluka 30%) and Ferrous Sulphate were all purchased from Fisher Scientific

Dialysis tubing (regenerated cellulose)2KDa cut off was purchased from Spectrum Labs and were stored in water in the fridge before use.

Dulbecco's minimum essential medium, Dulbecco's phosphate buffered saline (DPBS),penicillin, streptomycin, L-glutamine, fetal bovine serum (FBS), DAPI (4′,6-diamidino-2-phenylindole), bovine serum albumin (BSA) and were all purchased from Sigma Aldrich at the highest possible grade (suitable for cell culture).

Folate deficient DMEM (high glucose w/ 4.5 g glucose /L L-glutamine, sodium bicarbonate and sodium pyruvate) was purchased from Trafalgar Scientific LTD.

HeLa cell line was kindly donated by Dr Chris Staples at the North West Cancer Research Institute at Bangor University.

Gemcitabine (98%) was purchased from discovery fine chemicals.

4.2.2 Synthesis of PEG linker

10 g of PEG_8 (Mw400) (25 mmol PEG, 50 mmol OH groups) was dissolved in 150 mL of 1, 4-Dioxane (anhydrous) and purged with argon for 20 minutes. Separately, a solution of Diisopropylazodicarboxylate (DIAD) (17.7 g, 87.5 mmol, 1.75 eq) in 10 mL 1,4-dioxane (anhydrous) was added dropwise under argon to an ice cooled solution of PPh_3 (22.95 g, 87.5 mmol, 1.75 eq) under a continuous stirring of the solution for a further 30 mins. PEG solution was then transferred under argon by use of a double-ended needle and the solution could stir for a further 30 mins at ambient temperature. As a powder, phthalimide was added (12.9 g, 87.5 mmol, 1.75 eq) and the resultant mixture was allowed to stir at ambient temperature for a further 1 hr. afterwards, the mixture was heated to 50C and allowed to react overnight. Extraction of the desired compound was afforded by firstly removing 1, 4-dioxane in vacuo and suspending the orange oil in 200 mL of water, washed with 50 mL ethyl acetate twice and diethyl ether once and IMS was used to break down emulsions that had formed (ca.2 mL). Extraction of the desired compound was then performed thrice upon the aqueous layer via 75 mL DCM. The latter was then dried over magnesium sulfate for 1 hr, filtered and volatiles were removed in vacuo. Precipitation of the product was then performed in ice cold diethyl ether to produce a slightly yellow oil of PEGdiPHT (12.34 g,18 mmol, 75% yield). ^{1}H NMR (400 MHz $CDCl_3$),7.8-7.52 (m, 4H aromatic H on phthalimide), 3.91 (t, 4H **CH_2-CH_2**-Phthalimide), 3.75 (t, 4H-**CH_2-CH_2**-Phthalimide), 3.7-3.51 (m, 4H **-[CH_2]$_2$**-O). PEGdiPHT (12.34 g, 18 mmol of PEG, 36 mmol of PHT) was dissolved in 125 mL of absolute ethanol in a round bottom flask. To the flask 10 equivalents of hydrazine hydrate (35%) was added and the mixture was left to reflux for 6 hrs. The mixture was then allowed to cool and thereafter filtered to remove the white precipitate that had formed. The solution was then concentrated in vacuo and dissolved in 150 mL of DCM, filtered again and extracted with 2 mL 1 M NaOH (aq). The aqueous layer was then back extracted with 25 mL DCM and the combined organics were dried over magnesium sulfate and concentrated in vacuo. The resultant brown oil yielded PEG diamine, this was stored in the fridge and any free phthalamide could crystallize before being filtered, and a further precipitation into ice cold diethyl ether. (33% yield).^{1}H NMR (400 MHz $CDCl_3$) 3.63-3.57 (m, - **[CH_2]$_2$**-O), 3.48 (t, 4H-C**H_2**-C**H_2**-

NH_2), 2.82 (t, 4H-CH_2-CH_2-**NH_2**). For the synthesis of PEG_4 diamine linker the same procedure was followed however PEG_8 was substituted (5% yield). ^{1}H NMR crude (400 MHz $CDCl_3$) 3.7-3.57 (m, - **[CH_2]$_2$**-O and 4H-C**H_2**-C**H_2**-NH_2), 2.87-2.95 (CH_2-CH_2-**NH_2**).

4.2.2 Mono Boc protection of diamine linkers

For the Boc protection of ethylene diamine 0.5 eq. of Boc anhydride was dissolved in 100 mL chloroform and added dropwise to an ice-cold solution of ethylene diamine over a period of 3 hrs. The mixture was stirred overnight and washed eight times with 150 mL of distilled water. The organic phase was then dried with magnesium sulfate, filtered and dried via rotary evaporation, and a clear slightly yellow oil was obtained in quantitative yield w.r.t Boc.1H NMR (400 MHz CDCl3d), 5.21 (s, 1H CH_2-N**H**), 3.1 (s, 2H C**H_2**-NH), 2.74 (s, 2H H_2N-C**H_2**), 1.36 (m, 9H BOC methyl groups), 1.12 (s, **H_2**N-CH_2) For the Boc protection of PEG Diamines, Boc anhydride (110 mg, 0.5 mmol) was dissolved in 10 mL chloroform andt he mixture was added dropwise to an ice-cold solution of a PEG diamine (500 mg, 1.25 mmol) over a period of 2 hrs. The mixture was stirred overnight and washed 5 times with 100 mL distilled water. The organic phase was dried under magnesium sulfate, filtered and concentrated before precipitation in ice cold diethyl ether to yield a brown oil (250 mg PEG_8 diamine 80% yield w.r.t Boc and 193 mg PEG_4 diamine quantitative yield w.r.t Boc).1H NMR (400 MHz CDCl3d), 3.58 (s,-[C**H_2**]$_2$-O), 3.46 (t, 4H C**H_2**-C**H_2**-NH2), 2.80 (t, 4H C**H_2-** C**H_2**-NH_2),1.37 (s, 9H BOC methyl groups).

4.2.3 Synthesis of Boc-PEG-Folate

Folic acid (264 mg, 0.6 mmol) was dissolved in 10 mL DMF alongside N-hydroxysuccinimide (115 mg,1 mmol) and dicyclohexylurea (206 mg,1 mmol) and left to stir at ambient temperature in the dark for 2 hrs. After this time, BOC-PEG_8-NH_2

(200 mg, 0.3 mmol) was dissolved in 1 mL of DMF and added into the reaction mixture and left to stir overnight in the dark. The mixture was then filtered, water (2 mL) was added and the product was freeze dried to remove DMF to yield 250 mg (yield 87%) crude material as a brown/orange powder that was used without further purification for the next step. For the synthesis of Boc-PEG$_4$-Folate (193 mg 0.6 mmol) 264 mg of folic acid (0.6 mmol) was dissolved alongside N-hydroxysuccinimide (69 mg,0.6 mmol) and dicyclohexylurea (123 mg 0.6 mmol) in 15 mL DMF and left to stir overnight in the dark. The mixture was then filtered, water (2 mL) was added and the product was freeze dried to remove DMF to yield 250 mg (yield 98%) crude material as a brown/orange powder that was used without further purification for the next step.

4.2.4 Deprotection of BOC-PEG-Folate

Boc-PEG$_8$-Folate (250 mg, 0.26 mmol) was suspended in 2 mL of chloroform before the addition of trifluoroacetic acid (20 µL, 0.32 mmol) into a 10 mL reaction vial and submerged in a sand bath protected from light and left to stir at 30°C for 3 hrs. Subsequently, the suspension had formed a dark orange solution. Volatiles were removed via rotary evaporation to yield an orange powder of NH$_2$-PEG$_8$-Folate (217 mg, 0.25 mmol, 96% yield).1H NMR (400 MHz DMF-d7) 10.76 (s, 1H,a-COOH) 10.50 (s, 1H, N**H**; guanidine on folate) 8.82 (s, 1H, N=C**H**) 8.71 (d, 1H, O=C-N**H**; folate) 8.39 (s) 8.33 (d) 7.85(m, 2H, arH-C-C=O) 6.80 (dd, 2H, (NH-ar**H**) 4.71-4.66 (t, 1H NH-C**H**) 4.66 (s, 2H, N=C-C**H$_2$**) 3.58(s,-[**CH$_2$]$_2$**-O), 3.48 (t, 4H C**H$_2$**-C**H$_2$**-NH2).

For Boc-PEG$_4$-Folate (457 mg 0.59 mmol) the same procedure was applied to yield a dark orange powder of NH$_2$-PEG-Folate in quantitative yield that was used without further characterisation or purification.

4.2.5 Conjugation of Folic acid onto polymers

The amount of COOH on HBP4060 Polymer was determined via ^{1}HNMR. For folic acid conjugation, 0.3 g of polymer (containing 2.5 mmol of COOH groups) was dissolved in 5ml DMF and DCC (3.2mmol,0.65g, 1.5eq) and NHS (3.2mmol, 0.36g, 1.5eq) was added and the reaction was left to stir for 2 hrs in the dark at 30°.Simultaneously,folic acid (0.65g, 1.49mmol) was dissolved in 5ml DMF and DCC (0.6g,2.9mmol) and NHS (0.34g, 2.9mmol) were added and the reaction was left to stir in the dark at 30°C. Upon formation of the dicyclohexylurea precipitate the two mixtures were added together and ethylenediamine added (0.36g, 6mmol) allowed to stir in the dark overnight. In the case of PEG_8 linked folate, folic acid was substituted for folate-PEG_8-NH2(0.2g 0.2mmol) and this was dissolved in 5ml DMF and left to stir alongside DCC (0.06g, 0.3mmol) and NHS (0.03g,0.3mmol). Purification was performed using dialysis (regenerated cellulose 2 KDa cut off Spectrum Labs) over 4 days in a 5:95 DMF: H2Osystem (v/v)with system changes every 24 hrs.The resultant liquid was then freeze-dried to yield polymer folate conjugate of either $HBP4060_{ethylf}$ as a yellow powder(30%wt.yield) or $HBP4060_{pegf}$ as a dark orange/brown powder (80% wt. yield).

For sister polymers HBP4060_2,3 and 4 150 mg of either naked polymer or polymer linked with FITC was used (HBP4060_2_{fitc},3_{fitc} or 4_{fitc}) (equating to 0.26 mmol of COOH in each case) in a 50:1 molar ratio (polymer to reagent) and the same procedure was applied to yield folate linked polymers (% wt.) HBP4060_2_{pegf} (43%) HBP4060_3_{pegf} (56%) HBP4060_4_{pegf} (86%) HBP4060_2_{fitc_pegf} (53%) HBP4060_3_{fitc_pegf} (66%) and HBP4060_4_{fitc_pegf} (69%)

4.2.6 MTT assay of polymeric compounds

Polymeric samples were dissolved into appropriate concentrations overnight using Dulbecco's phosphate buffered saline as solvent. Samples were then filtered through a 0.2um membrane filter for sterilization.

HeLa cells were cultured in Dulbecco's Minimum Essential Medium (DMEM) with 10% FBS 2mM glutamine and 100U Penicillin with 0.1mg/ml streptomycin until they reached 70-80% confluency and were plated at roughly 5K cells per well in a 96 well plate of 100ul volume, and were placed into 37 degree 5% CO2 incubator for 4

hours. After the specified time period polymer stimulus of unlabeled ethylene diamine linked folate and PEG400 diamine linked folate polymers were added to cells to achieve the desired concentrations (1mg/ml-10ug/ml), alongside positive controls of DPBS. The cells were then placed back into the incubator and were allowed to proliferate for 72 hours with polymer stimulus.

After the specified time period, 25 µl of MTT reagent was added to the wells and the 96 well plate was placed in the incubator for a further 2 hours. The solution was then aspirated, and the resultant purple crystals were dissolved in DMSO and absorption was read at 560nm using a Wallac 1420 UV plate reader. Standard deviations were calculated (n=3) and compared against controls, which were assumed as 100% viability and overall cell viability for the polymer samples was calculated from these values.

4.2.8 Synthesis of Rhodamine B ethylene diamine

Mono-boc protected ethylene diamine was synthesised using the same method described in 4.2.2 Rhodamine B (887 mg, 2 mmol) was dissolved in 10 mL DMF alongside NHS (287 mg, 2.5 mmol) DCC (516 mg, 2.5 mmol) and mono-BOC protected ethylene diamine (400 mg, 2.5 mmol) and left to react overnight at ambient temperature in the dark. Solids were filtered and the resultant solution was concentrated via rotary evaporation. The resultant oil was then dissolved in 3 mL of water and then freeze dried to yield a dark red solid which was used crude (700 mg, 1.2 mmol 60% yield).The resultant compound was taken and dissolved in 4 mL DCM in a 10 mL reaction vial alongside TFA (400 µL) and submerged in a sand bath protected from light and heated to 30°C for 3 hrs. Volatiles were removed via rotary evaporation to yield an dark red powder of Rhodamine B ethylene diamine (291 mg 0.6 mmol 50%)

4.2.9 Synthesis of Rhodamine conjugated polymers

For HBP4060, 30mg of HBP4060 (ca 0.25mmol COOH) was dissolved in 2 ml DMF in a10 ml reaction vial. To this solution, NHS (4mg,0.03mmol) and DCC (6mg, 0.03mmol) were added and the solution was stirred in the dark at ambient temperature for 2 hrs. Following the above procedures, rhodamine B ethylene diamine (10mg, 0.002 mmol) was added to each solution containing either HBP4060 or $HBP4060_{pegf}$. Then the vial was submerged into a sand bath protected from light and heated to 30°C and left to react overnight. The solution was then subjected to dialysis (regeneratedcellulose2KDa cut off Spectrum Labs) in a 5:95 DMF:H2O system (v/v) with system changes every 24h, until the solvent system was colourless (4days for HBP4060pegfand 5days for HBP4060). After freeze drying, the products appeared as an orange powder ($HBP4060_{pegfR}$ yield 33%wt.) and a red powder ($HBP4060_{R}$ yield 60%wt.). Characterization was performed via UV–Vis absorption spectroscopy in DMF at 554 nm.

4.2.10 Synthesis of Fluorescein (FITC) conjugated polymers

1 g of Fluorescein sodium salt (2.6 mmol) was dissolved in 5 ml of deionised water in a conical flask and HCl was added dropwise to precipitate fluorescein in the free acid form alongside constant stirring of the solution. Afterwards, the mixture was filtered via vacuum filtration and the solid subsequently freeze dried to yield fluorescein as a $FITC_{freeacid}$ (573 mg 1.7mmol 61% yield). The free acid was then subject to conjugation to an ethylene diamine linker. $FITC_{freeacid}$ (573 mg 1.7 mol) was dissolved in the minimum amount of THF required alongside NHS and DCC in a RBF equipped with a stirrer bar and protected from light. The solution was allowed to stir at room temperature (approx. 20°C) for 3 hrs before the addition of ethylene diamine mono boc (320 mg 2 mol 1.2 eq) also dissolved in THF. The solution was then allowed to react overnight before filtration of the DDCu side product and removal of THF via rotary evaporator to yield BOC-ethylene-FITC (700 mg 85% yield). Deprotection of the BOC group was then afforded by the dissolution of x mg of

BOC-ethylene-FITC in chloroform before addition to a 10 ml reaction vial equipped with rubber septa and stirrer bar. The solution was then protected from light via submerging into a sand bath and heated to 30°C. x ml (1.7 mmol) of TFA was then added and the solution stirred and left to react for 3 hrs. Upon completion the mixture was transferred to a 25 ml RBF and rotary evaporation was performed to remove the volatiles to yield as a yellow/orange powder NH_2-ethylene-FITC (550 mg 1.4 mmol 100% yield)

FITC was then conjugated to either HBP4060_2, HBP4060_3 or HBP4060_4. Briefly, polymer was dissolved in DMF in a 10 ml reaction vial equipped with PTFE septa and stirrer bar and submerged into a sand bath to protect from light. NHS and DCC dissolved in DMF were then added and the mixture was allowed to stir for 3 hrs. Afterwards, NH_2-ethylene-FITC dissolved in DMF was added and the mixture was allowed to stir overnight in a 50:1molar ratio of polymer to reagents. The solution was then subjected to dialysis(regeneratedcellulose2KDa cut off Spectrum Labs) in a 5:95 DMF:H2O system (v/v) withsystem changes every 24h, until the solvent system was colourless (8 days) and the resultant solution was freeze dried to yield a dark orange powder of FITC conjugated polymers. HBP4060_2_{fitc} (30% wt.), HBP4060_3_{fitc} (56% wt.) and HBP4060_2_{fitc} (58% wt.). Characterisation was performed via UV-Vis at 486 nm.

4.2.11 S-Carboxymethylthiocysteamine (CTC) linker synthesis

Briefly, cysteamine (1.2 g 15.6 mmol) was dissolved in 50 ml of deionised water alongside 4 eq. of thioglycolic acid (5.73 g 62 mmol) in a 250 ml RBF and submerged into an ice bath. Neutralisation of the solution was then afforded by the dropwise addition of 2 M NaOH and tested with universal indicator paper. To this solution ferrous sulphate was added (a shallow spatula will suffice) as an indicator. $H_2O_{2(aq)}$ (16%) was then added dropwise to the solution until the rose solution turned yellow. Upon the colour change TLC was performed with a Ethyl acetate:Acetic Acid:Water (8:2:1) mobile phase and ninhydrin stain was employed to monitor the products of the reaction, leaving only one visible spot from the reaction mixture (R_f

0.24). Acidification was then performed by the use of 2 M HCl added dropwise until the pH of the solution reached 2 and then purification was performed on a Dowex 50 column with a gradient mobile phase of 0.05 M pyridine-Acetic Acid (pH values 3.1 - 5) with an increase of pH by 0.5 every 200 ml and fraction elution of 10 ml. TLC was performed on the fractions utilising Ethyl acetate:Acetic Acid:Water (8:2:1) mobile phase and ninhydrin stain with R_f values for the product ranging from 0.2 - 0.3. Fractions containing the product were then taken and diluted with 50 ml of deionised water and freeze dried to yield the product as a very pale yellow oil (1.2 g 7.2 mmol 46%)

4.2.12 CTC gemcitabine linker synthesis

Boc protection of CTC was performed by first dissolution of 200 mg of CTC (eq. to 1 mmol of NH_2 groups) within 1 ml of deionised water and placed within a 10 ml reaction vial equipped with stirrer bar and PTFE septa. 370 mg of Boc anhydride (1.6 mmol) was added as a solid into the reaction vessel. Initially the Boc solid did not dissolve leaving clear solid particulates within the reaction vessel, as a heterogenous mixture. The mixture was then stirred at room temperature (approx. 20°C) for 3 hrs. After this time the reaction was deemed to have been completed as the solution now existed as a homogenous mixture. The solution was then freeze dried to yield 100 mg of BOC-CTC (0.3 mmol 71%).

100 mg of BOC-CTC was then dissolved in 1 ml DMF alongside NHS and DCC and left to stir for 3 hrs before the addition of gemcitabine dissolved in 2 ml DMF. The reaction was then left to stir overnight and was filtered to remove DCCu precipitate, diluted with 5 ml of water and freeze dried to yield 40 mg BOC-CTC-Gemzar (0.07 mmol 50% yield) as a white viscous solid, that was used without further characterisation and purification.

Boc deprotection of the linker was then afforded via dissolution of the linker in 1 ml of chloroform, which was added into a 10 ml reaction vial equipped with PTFE septa and stirrer bar. 6 µl (0.09 mmol) of TFA was then added and the reaction vessel was submerged into a sand bath heated to 30°C and stirred for 3 hrs. The

solution was then transferred to a 25 ml RBF and volatiles were removed via use of a rotary evaporator to yield 15 mg of CTC-Gemzar (0.035 mmol 50% yield).

4.2.13 Polymeric drug loading with CTC gemcitabine

CTC-Gemzar was conjugated onto HBP4060_4_{pegf} exclusively in a aimed ratio of 15 µg gemcitabine per 100 µg of polymer. Briefly, 20mg HBP4060_4_{pegf} was dissolved in 1 ml DMF (0.26 mmol of COOH) alongside 1.2 molar eq of NHS (0.8 mg) and DCC (1.5 mg) in a 10 ml reaction vial equipped with PTFE septa and stirrer bar and submerged in a sand bath to protect from light. The reaction was then stirred at room temperature (approx. 20°C) for 3 hrs. Afterwards, 1.4 mg of CTC-Gemzar (326 nmol), dissolved in 1 ml of DMF, was added to the vial and the reaction was left to stir overnight. Purification of the solution was then afforded by dialysis (regeneratedcellulose2KDa cut off Spectrum Labs) in a 5:95 DMF:H2O system (v/v) with system changes every 24h. Samples of the system were taken every water change and were tested via UV-Vis spectroscopy for the presence of gemcitabine. This was performed by retaining 10 % of the system (100 ml) and freeze drying. Any residue was then dissolved in 1 ml of deionised water and measured at a λ_{max} 267 nm, with any signal peaks therefore elucidating the removal of gemcitabine from the dialysis tubing. Dialysis was performed for 4 days and afterwards the solution within the tubing was subject to freeze drying to yield 5 mg of HBP4060_$4_{pegfCTCgemzar}$ (20% yield % wt.)

4.2.14 Methanol based Cell extraction of nucleotides

Briefly, polymer samples (HBP4060_4, HBP4060_4_{pegf} and HBP4060_$4_{pegfCTCgemzar}$) and free gemcitabine were dissolved into appropriate concentrations overnight in Dulbecco's phosphate buffered saline. Samples were then filtered through a 0.2µm membrane filter for sterilization. HeLa cells were cultured in 10 cm tissue culture dishes with Dulbecco's Minimum Essential Medium (DMEM)

with 10% FBS 2mM glutamine and 100 U penicillin with 0.1mg/ml streptomycin until they reached 70–80% confluency (approx. 1 million cells per plate). Afterwards, treatments of either polymer or free drug were dosed at cells and they were incubated at 37.5°C with 5 % CO_2 for 30 minutes. After this time had passed, the media was aspirated and replaced with 10 ml of methanol pre-cooled to -20°C and placed into a -20°C freezer for 30 minutes. Afterwards, the methanol was centrifuged (15,000 x g for 5 mins) to remove the protein precipitate as a pellet. The methanol solution was then taken and freeze dried before MS analysis.

4.3 Bio-conjugation of folic acid – synthetic techniques, purification and characterisation

4.3.1 – Folate conjugated linker synthesis

There are numerous bio-conjugation techniques that the chemist may employ in order to successfully link molecules together, such as benzyl fluoride, isocyantes and isothiocyanates for lysine conjugation. However, one of the most widely used and well-known techniques, the Steglich esterification, allows for quick esterification and formation of an amide bond between two target molecules with relative ease; as long as both a 1° amine and carboxylic acid are present [1], whilst esterification of alcohols and carboxylic acids is also possible [2,3], with thiols also reported [4]. Due to the high functionality of carboxylic acid groups within all synthesised hyperbranched polymers this technique is ideal for quick and easy conjugation of polymers to ligands, through first activation of carboxylic acid via DCC/NHS addition and then addition of amine containing ligands in order to produce polymer-ligand conjugates (P-L-Cs). However, limitations with the technique can arise when neither molecules needed to form P-L-Cs contain either carboxylic acid or amine functionality, as seen in the case of HBP4060 and folic acid. Therefore, in order to suitably address the limitations with the desired reagents a diamine linker can be introduced in order to bridge both ligand and polymer together negating the need for both functionalities required for amide bond formation.

However, with the introduction of a diamine linker there are concerns regarding the control of the reaction, and negating the cross-linking effect forming ligand-ligand conjugates (L-L-Cs) or polymer-polymer conjugates (P-P-Cs) therefore, both controlled and uncontrolled conjugations were assessed in this project in order to suitably determine the most efficient method to form P-L-Cs with the greatest purity and yield, as key indicators for success of the reaction rather than the cost and time associated with multi-step syntheses and linker formation.

Folic acid was chosen as the ligand of choice for targeted drug delivery for a variety of reasons and these include: it is known to be generally benign to the human body [5–7], folate receptors (FR) are overexpressed within cancerous cells and tumours and there has been a vast amount of research in this field suggesting the suitability of the folic acid ligand for the role in question [8–11]. With respect to the overexpression of FR within cancerous cells and confirmed biomarker status this has been shown to occur in many human cancers [12–16].

First and foremost, due to the lack of suitable amines for conjugation situated on either the polymer or folic acid ligand the synthesis of a diamine linker was required. One of the main issues when introducing a linker to facilitate conjugation is how the linker will affect the final size of the molecule upon self-assembly in the dissolving media. Previously, in chapter three, it was stated that the upper limit for endocytosis is around 200 nm and therefore, the linker needs to reflect the need to keep particle size down to a minimum. Hence, two initial linkers were chosen to be tested for their suitability as a conjugation linker with HBP4060 namely ethylene diamine and a PEG_8-diamine. HBP4060 was chosen as oppose to other polymers for this purpose firstly because HBP3070 and HBP5050 had a much higher molecular weight and two distinct polymer populations and therefore reproducibility of experiments could be an issue. Secondly, HBP4060_2,3 and 4 were synthesised with a much lower yield than HBP4060, by using the sister polymer HBP4060 the effects of the linkers and reaction conditions with respect to control over conjugation can be studied with less risk of complete consumption of polymer. If a new batch of polymer would need to be synthesised this would warrant a unnecessary waste of time and resources that could otherwise be avoided.

Ethylene diamine is a readily available chemical from the common retailers (Sigma Aldrich, Fisher Scientific) at a low cost and therefore no synthesis was

required. However, PEG-diamines are not commonly found and thus a two-step synthetic route was required for the synthesis of the linker.

Firstly, the Mitsunobu reaction is used utilising a phthalamide nucleophile to form a very pale yellow PEG-diphthalamide (PEG-diPHT) before reductive amination with hydrazine hydrate to form the final dark brown PEG-diamine. Like the Gabriel synthesis in which the addition of the same nucleophile is performed on alkyl halide systems before amination [17]. However, using this technique although reliable encountered two main issues after amination: low yield and cumbersome phthalamide removal. Free phthalamide will crystalize out within the newly formed brown oil upon concentration of the product, leading to a need for the product to be dissolved in absolute ethanol and filtering before concentration, this process may need repeating numerous times before complete removal of the free pthalamide, upon which the brown oil can be precipitated within ether. The use of column chromatography was considered instead of this process however, due to the exceptionally low yield of product formed this was decided against due to the risk of losing much of the product through the column. An alternative method for release of PEG-diamine from the PEG-diPHT would be the use of a KOH solution and boiling, due to the relatively acidic nature of the phthalimide conjugate, this method though was not trialled for the purpose of this project. A crude ^{1}H NMR of the product is shown within the appendix (**Appendix 4-S1**) of this thesis displaying remaining free phthalamide within the product.

The formed PEG-diamine was then taken for mono-boc protection. In order to exhibit control over the conjugation reaction it is the most logical course of action to synthesise a folated form of the linker. Hence, by first underreacting the boc group towards the amines present and subsequent folate addition deprotection can be afforded via the use of tri-fluoroacetic acid and conjugation towards polymeric species can be obtained. Comparative spectra of protected and unprotected folate conjugated linkers can be seen in **Appendix 4-S2**.

4.3.2 – Conjugation of HBP4060 to folic acid – random and controlled methods

Upon synthesis of a folate containing PEG linker the means for the analysis of a controlled vs random conjugation reaction were achieved and thus the two techniques were studied and the final product of uncontrolled conjugation **A: HBP4060$_{ethyf}$** and **B: HBP4060$_{pegf}$** are displayed in **Scheme 4-1**.

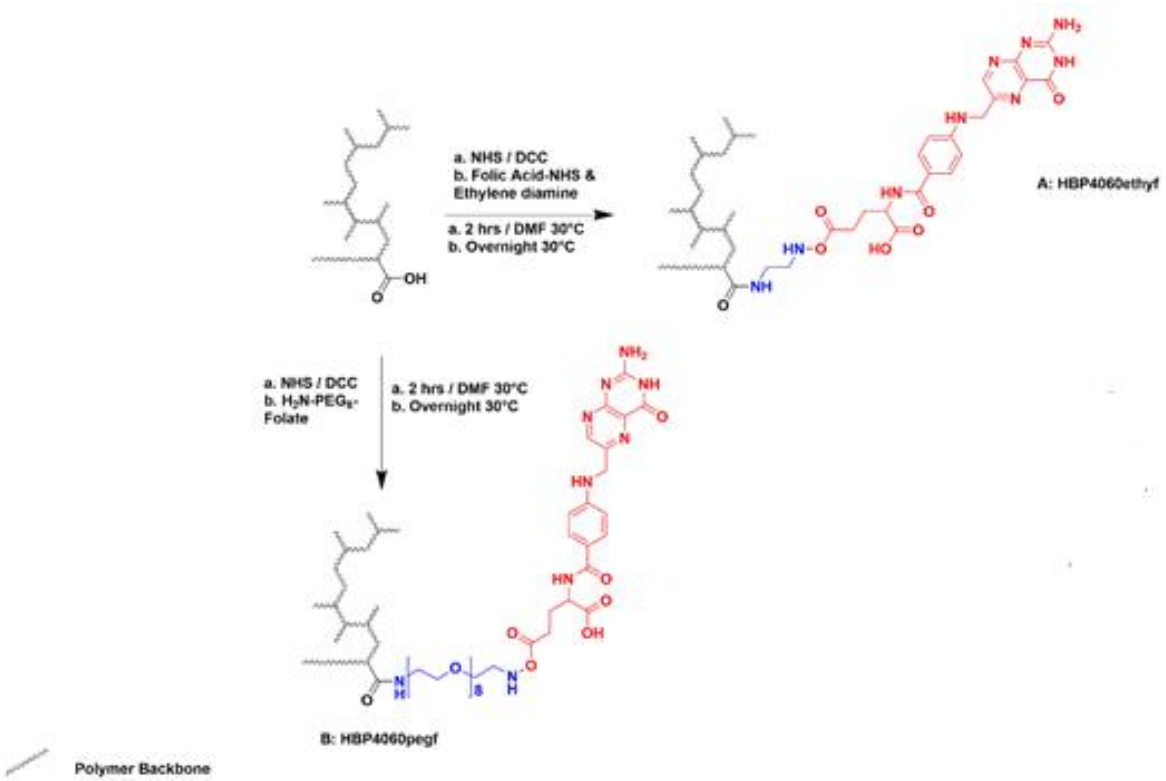

Scheme 4- 1: Reaction conditions for both uncontrolled and controlled folate bio-conjugations.

Firstly, conjugation was performed via the use of ethylene diamine in a random manner. There was no way to control the selectivity of the reaction and therefore it was difficult to accurately predict beforehand the amount of cross-linked polymer, cross-linked folate molecules and desired product. This method provided a low yield of final product with a low amount of folate conjugated onto the polymer when assessed via UV-Vis. There are two possible scenarios that are suspected to lead to the low conjugation seen in this reaction, namely: the lack of control over the reaction due to the random nature and aminolysis of the trithiocarbonate containing RAFT agent end groups [18]. In terms of the lack of control over the reaction the principle behind the Steglich esterification is that the COOH groups are “activated” ready for nucleophilic attack, in this case via amine lone pair of electrons. Therefore, taking into account both the structure of the polymer and folic acid there are

numerous different carboxylic acid groups that are ripe for activation. Both PAA and RAFT agent end group functionality within the HBP4060 sample itself contain COOH whilst also there are two present on folic acid. Therefore, a number of different combinations of conjugates can occur such as: polymer-polymer conjugate (either through RAFT-PAA, PAA-PAA or RAFT-RAFT) folate-folate or the desired polymer-folic acid conjugate. Secondly, aminolysis of the trithiocarbonate end group is completely plausible. Previous studies by Qiu and Winnick displayed that the introduction of a free amine to their trithiocarbonate RAFT agent allowed transformation of the RAFT agent end groups [18]. Furthermore, due to the diamine nature of the linker, any transformations of raft agent end groups would lend themselves completely free to contribute to unwanted cross linking.

Therefore, in order to assert control over the reaction mono-boc protection of a PEG-diamine linker was first performed via the method published by Muller et al. [19] and then subsequent linking to folic acid and de-protection to synthesise a folate conjugated PEG linker.

Purification was performed via dialysis. Dialysis has been shown to be a robust and benign method of purification of large molecules and is based on the principles of osmosis and diffusion. By use the of the correct membrane (material, cut-off weight) and solvent system (either pure water, water/organics mixture, organic/organic mixture or pure organic) smaller molecules are able to escape the membrane and the larger desired products are trapped inside which then can be concentrated and purified via rotary evaporation or more commonly freeze drying techniques. For the purification of all polymer-folic acid conjugates dialysis was performed utilising a regenerated cellulose membrane with a 2KDa cut off. This cut off was chosen for a number of reasons: it would allow any carry through impurities (such as free phthalimide, solvent residues, NHS and DCC by-products etc.) to be removed from the sample alongside any unconjugated linkers; the polymer itself retains a molecular weight (unconjugated) of approx. 24KDa and hence would be entirely trapped by the membrane and finally the use of regenerated cellulose tubing lends itself to a variety of different solvent systems as oppose to using snake skin for example and thus a water:DMF based solvent system can be employed without risk of damaging the membrane. Indeed, for the solvent system a water:DMF 95:5 system was used. This was used to ensure that organic molecules such as folic acid,

DCC and NHS that would otherwise precipitate out in water would be able to diffuse through the membranes. Folic acid, for example although soluble in water at mg/L levels, lends itself to more acidic or aprotic media, whilst a large amount of time is required for dissolution [20]. Since DMSO or acetic acid were not compatible with polymeric systems due to either risk of bond breakage or general insolubility DMF was used in small amounts throughout the dialysis process. Dialysis was performed over the course of 4 days (until the solvent system became colourless) with solvent changes every 24 hrs. Despite attempts to remove all impurities it was found that within the membrane insoluble white powder had formed. This was initially thought to be either residue phthalimide crystals that were not fully removed in the linker synthesis or DCCu (the urea form of DCC) or NHS. Filtration of the now pale orange liquids allowed for extraction of the white solid which was subject to ^{1}H NMR analysis to ascertain whether this procedure was unable to fully remove carry through impurities from linker synthesis or was a result of Steglich bi-products. It was found to be the latter, and therefore, further conjugation reactions utilising this technique would require pre-filteration before dialysis in an attempt to remove these bi-products before dialysis as to ensure a much more streamlined dialysis process and less risk of loss of compound.

Upon filtration products were filtered to yield an orange solid in the case of $HBP4060_{pegf}$ and a pale yellow solid ($HBP4060_{ethyf}$).

Quantification of folate on each polymer was first attempted via ^{1}H NMR analysis although this was found to be cumbersome and the results garnered were not deemed to be accurate. For instance, there was trouble dissolving both compounds in common NMR solvent and hence DMF-D_7 was used as D_2O overpowered the spectrum relegating aromatic folate peaks to just noise. This however led to complications within analysis due to the peak around 8 ppm resulting from DMF. Furthermore, no aromatic peaks were found within $HBP4060_{ethyf}$ (**Figure 4-1**).

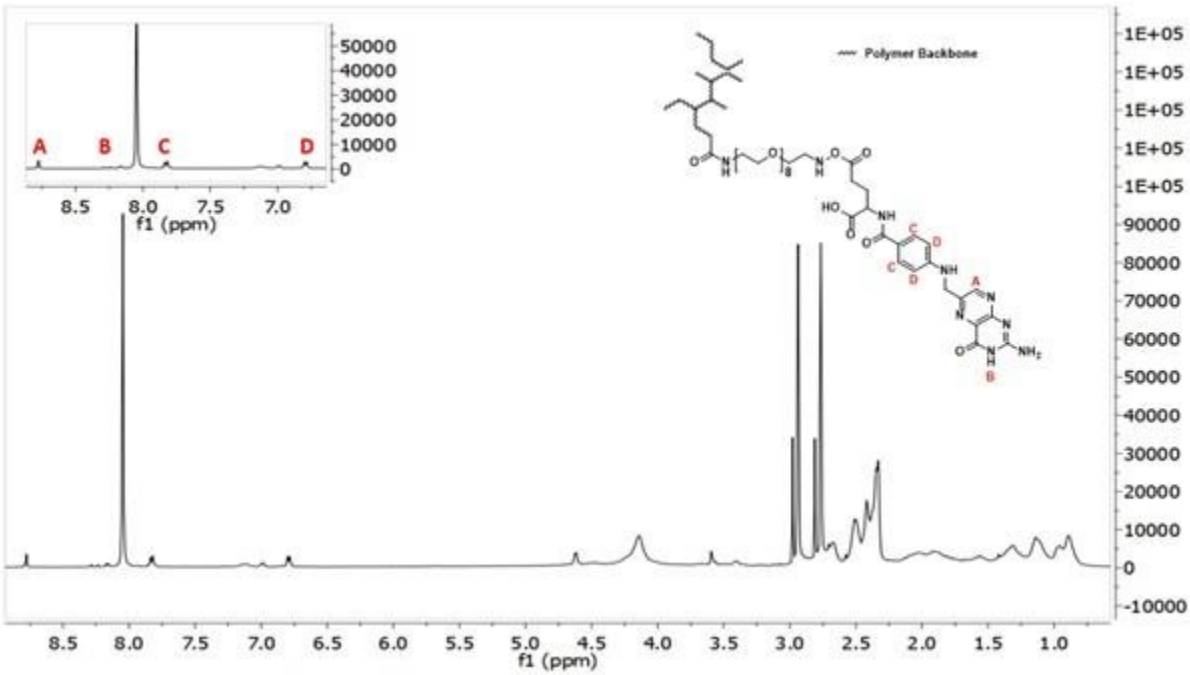

Figure 4- 1: 500MHz 1H NMR HBP4060pegf (DMF-d7) post dialysis indicating conjugation of folic acid through the presence of aromatic peaks between 7-9ppm, with DMF peaks at 2.7, 3 and 8 ppm. Full polymer peak assignments can be found in Chapter 3.

UV-Vis quantification was used in order to assess folate conjugation. Folic acid is a well-known to be UV active and industries such as the food industry use this method of quantification to assess the content of folate within products to be sold to the public [21], amongst other industrial applications [22,23]. Folic acid has been shown to have λ_{max} values of 282 and 377 nm [24]. In terms of the polymeric molecule itself RAFT agent end groups are expected to produce UV-active properties, and this was observed within 280-320 nm excluding the common λ_{max} of 282 nm for analysis [25]. Sweeping of folate spectra was performed in order to ascertain the precise λ_{max} value exhibited on the hardware and 362 nm was then chosen as the point of quantification (**Figures 4-2 and 4-3**).

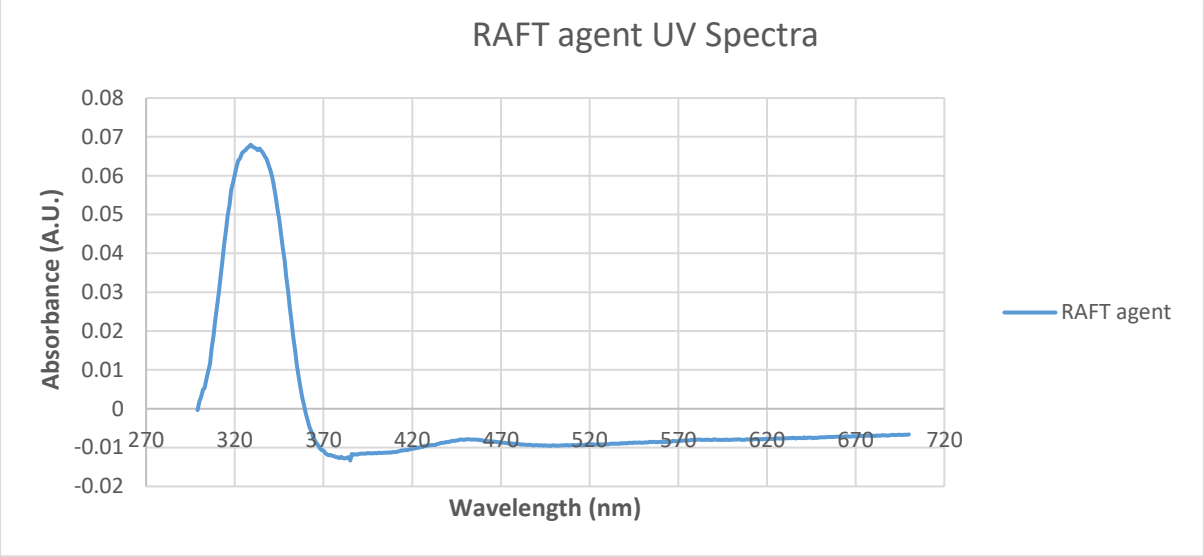

Figure 4- 2: UV-Vis Spectra of RAFT agent used for polymer synthesis in DMF

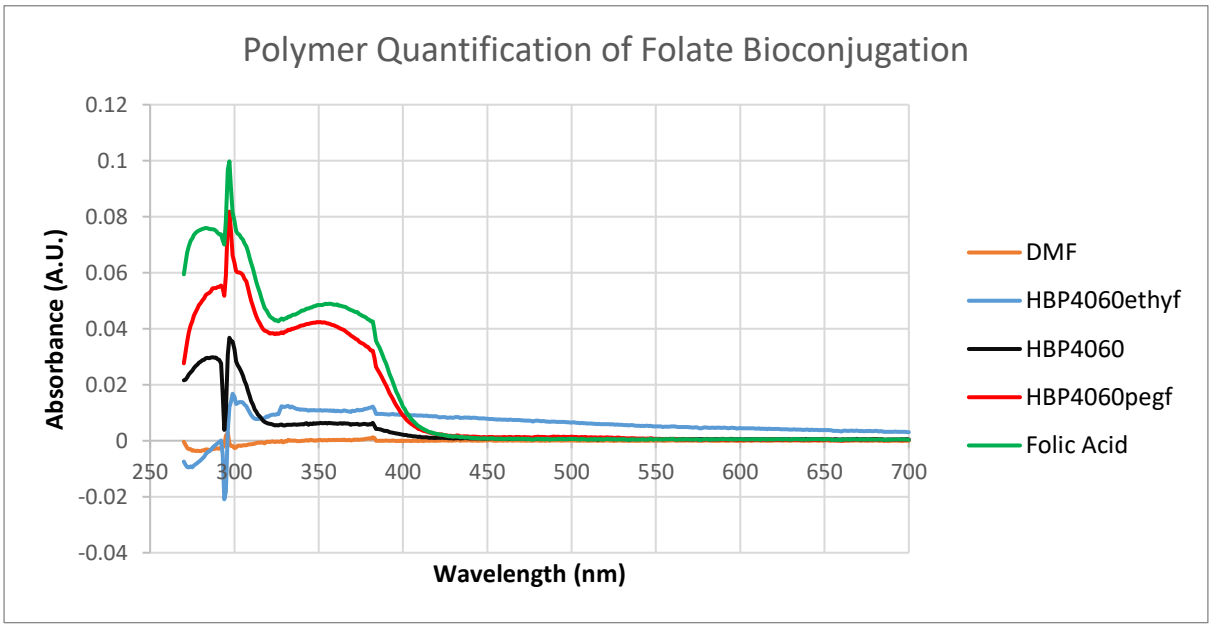

Figure 4- 3: UV-Vis spectra for the quantification of folic acid conjugation

Whilst it could be argued that RAFT agent removal from polymer would remove interference from the UV spectra there were three further points of consideration that outweighed the benefits of RAFT removal. Firstly, carboxyl groups on the polymer chain itself would induce π → π* excitations and thus absorbance at around 280 nm as seen in acetone for example [26]. Furthermore, as previously discussed it is completely plausible that RAFT end group transformations as a result of amine addition could occur, however this would likely be a minimal cause of

conjugation due to favourable conditions for carboxylic acid based addition due to Steglich additions performed, and thus removal of RAFT end groups could remove either carboxylic acid based RAFT conjugations and the aforementioned transformation additions, leading to a quantification that is not truly representative of the amount of folate conjugated. Finally, removal of RAFT groups would require reduction-based chemistry to replace trithiocarbonates with thiol groups, this could lead to unwanted side reactions such as amide breakage back to amine and carboxylic acid groups and breakage of DSDA hyperbranching agent. The possible breakage of the hyperbranched structure would then lead to complications within purification. Dialysis would be required in order to again purify samples before quantification as to ensure that only polymeric species would be analysed. However, one cannot truly say that the polymer obtained from such a method would be truly representative of the weight of polymer initially subjected to the method. There is a large possibility that with breakage of hyperbranching structure there will be losses within dialysis as reduction would break down polymer structure and in turn the lower molecular weight of the macromolecular chains themselves. Due to the random nature of branching it is plausible that PAA end groups conjugated to folate would be lost through dialysis and in turn results obtained would not be truly representative of folate added onto polymer. Furthermore, however unlikely it may seem, the chance that PAA end groups are present only on branched chains (that upon degradation are <2KDa) could lead to no folate being present on the freeze-dried purified product. With all three factors in mind it was decided that the polymer would be quantified for folate in the complete form i.e. as would be used for the intended end use, as to ensure a true reflection of folate content presently conjugated with the use of the less commonly used, but reported none the less, $\lambda_{max.}$

As expected, the controlled method of conjugation yielded more product with a higher amount of folate present on the overall polymer, with a tenfold decrease in folate to polymer ratio used for conjugation **(Table 4-1).**

Table 4- 1: Yield and UV-Vis quantification for folate conjugated HBP4060

Sample	Folic acid molar eq. to polymer (Steglich Esterfication)	Yield (wt. %)	A.U. 362 nm	µmol/mg (folate/polymer) conjugated
HBP4060$_{ethyf}$	1.3	30	0.0062	0.17
HBP4060$_{pegf}$	0.1	80	0.0500	1.12

In order to further asses completeness of reactions the ninhydrin test (sometimes termed the Kaiser test) was performed on both HBP4060$_{ethyf}$ and HBP4060$_{pegf}$ to ascertain whether free amine groups are present on the polymer as the result of incomplete conjugation (stemming from the diamine linker). The amino acid glycine and HBP4060 were used as a control for the experiment. Upon treatment with the Ninhydrin solid all samples that contained polymer (HBP4060, HBP4060$_{ethyf}$ and HBP4060$_{pegf}$) turned from a colourless to a yellow solution indicative of the presence of a 2° or 3° amine present (DMAEMA and folic acid) whilst only the glycine solution turned purple, indicative of a positive test for 1° amine. With respect to these results and the results obtained spectrally the samples were deemed “fit for purpose”. Adequate satisfaction was gathered that folate had been conjugated onto the polymers at the recorded amounts and that it wasn’t a result of free folate/ folate containing linkers trapped within the polymer.

4.4 Biological screening of HBP4060

4.4.1 – Do or die: initial cytotoxicity screening of HBP4060

Before further work was carried forward it is imperative that the polymer displays characteristics of a benign molecule and doesn’t induce cytotoxicity to a high degree. This was defined as the following “*HBP toxicity should not induce a toxicity at x dose significantly higher than the therapeutic dose of the drug in*

question". Essentially, the key to measuring HBP toxicity was to identify whether there was a significant difference in toxicity between toxic doses of the polymer and the therapeutic doses of the drug itself. Therefore, an initial screen of polymeric toxicity was performed, in order to gather information on general polymer toxicity so that appropriate ranges of concentration can be utilised in further studies. Furthermore, as two different linkers were used for the conjugation of folic acid, information on the toxicity of these linkers can be assessed for further work. It is expected that the ethylene diamine linker would produce a much higher level of toxicity than the PEG based linker. Ethylene diamine has been shown to react with moisture in air to produce a corrosive and toxic mist that can produce harm to health, such as nitrogen oxides or ammonia gas. Hence, should breakdown occur resulting in these hazardous compounds within the body it would deem the ethylene diamine linker unsuitable for further use.

A well-established method for the analysis of compound cytotoxicity is using the so-called MTT method. The MTT assay is a colorimetric method for the analysis of metabolic activity of cells that have been cultured and exposed to external stimuli, such as drugs, vitamins, minerals etc. In essence the cells are cultured alongside the stimuli for a period of three cell cycles and the tetrazole compound (3-(4,5-dimethylthiozol-yl)-2,5-diphenyltetrazolium bromide) used for analysis added into the mixture at a specified time point is converted by NAD(P)H dependent enzymes to the formazan equivalent [27,28] **(Scheme 4-2)**.

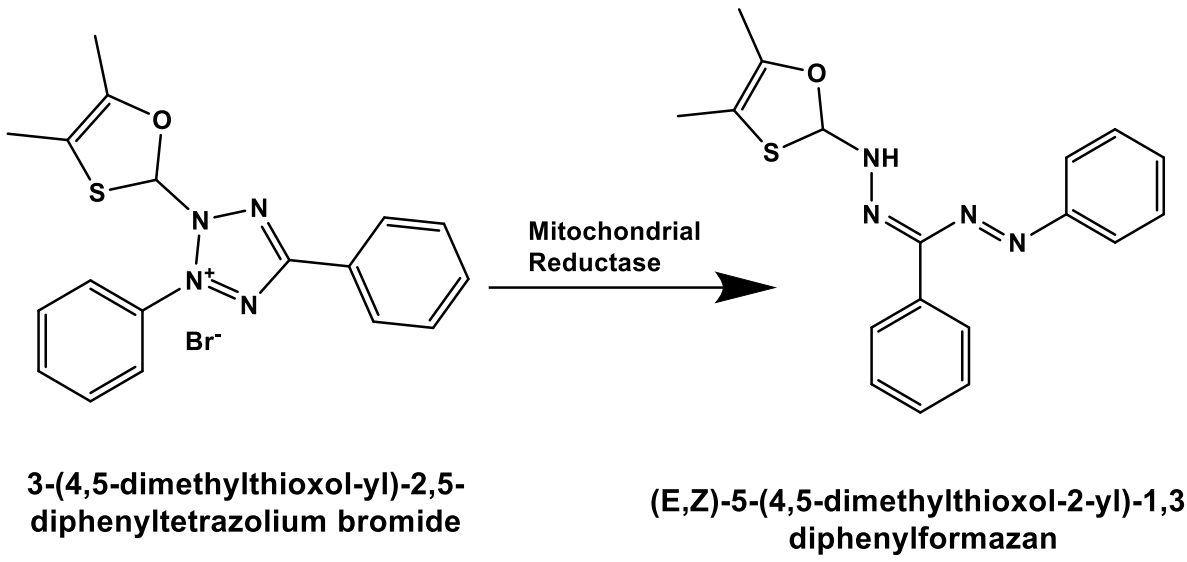

Scheme 4- 2: MTT conversion to the formazan equivalent as a direct result of cell metabolic activity

Analysis of the metabolic activity is then performed by aspiration of culturing media, containing any leftover external stimuli and leftover MTT solution, leaving the solid formazan crystals at the bottom of the well. Dissolution in DMSO is then performed before analysis via UV-Vis on an appropriate plate reader at 570 nm.

For the analysis of cytotoxicity using the MTT assay the HeLa cell line was chosen as the most appropriate cell line for initial screening. HeLa cells have been used since 1950s with research as early as 1951 for the purpose of studying viral replication with cancer derived cells [29]. The cell line itself was harvested from the cervical cancer of the patient Henrietta Lacks and is described as an immortal cell line as a direct result of the cancerous mutations present, which permits them to continually divide. Due to this fact, HeLa is still one of the most widely used cell lines for research surrounding cancer [30–36]. Additionally, of great importance to this project the HeLa cell line is also known to display the folate receptor protein [37,38], ensuring this cell line as a good starting point for biological assays.

For initial screening, the concentrations of polymers HBP4060, $HBP4060_{ethyf}$ and $HBP4060_{pegf}$ were chosen so that a broad spectrum of cytotoxicity measurements can be observed, with further narrowing down of concentrations tested to be performed later, dependant entirely on the results obtained and desired drug concentration. Concentrations were chosen between 1 mg through to 1 µg per ml of stimulant. Cells to be used for the analysis were cultured until ca. 70% confluence was observed via the use of a light microscope. Polymer solutions were then made to the appropriate concentration in Dulbecco’s Phosphate Buffered Saline and were sterilised via the use of 0.2 µm membrane filters to produce a sterile filtrate for cell stimulation. The use of a membrane filter was chosen as a sterilisation technique for a variety of reasons. Furthermore, autoclave would subject the solution to high temperatures and steam to induce sterilization at above 100°C. At this high temperature it is entirely possible that breakdown of polymer bonds (such as disulfide or amide linker bonds) could occur whilst ethylene diamine has been shown to produce toxic fumes within a humid environment and thus this method was not chosen for these reasons. Membrane filteration was then chosen as a benign, safe, affordable and relatively quick method for sterilisation and it has been reported as an acceptable method in order to sterilise compounds. One could argue that the use of

the pore size used could avert larger polymer molecules from being processed such as aggregates etc. and therefore loss of compound in the resultant liquid is expected however this was deemed as a necessary risk as it is believed that autoclaving of the compounds at high temperature and pressure could itself cause breakdown of products. It could be argued that sonication before filtering could be performed to breakdown aggregates and allow for better processing of the polymer, however this was not performed as a pre-sterilisation technique as it was thought that whilst breakdown of aggregated particles would be an advantage there was too greater risk of complete breakdown of the hyperbranched structure itself.

Cells once cultured were then transferred to a 96 well plate at a cell density of 5K cells per well (100 µl volume) and could adhere for a total of 3-4 hours within the incubator. Upon adhering to the plate polymer stimulus was added into the cell media with equal volume (100 µl) to produce the desired concentration of polymer with PBS solution used as the control for the experiment, all of which was performed in triplicate.

After a period of 68 hours MTT solution (5 mg/ml in PBS) was added to each cell containing well and cells were left to metabolise for a further 4 hours, upon this time point purple crystals were distinctly visible at the bottom of each well. Aspiration of the media was performed and dissolution of MTT reagent was performed in 100 µl of DMSO to produce a purple solution for analysis (**Image 4-1**)

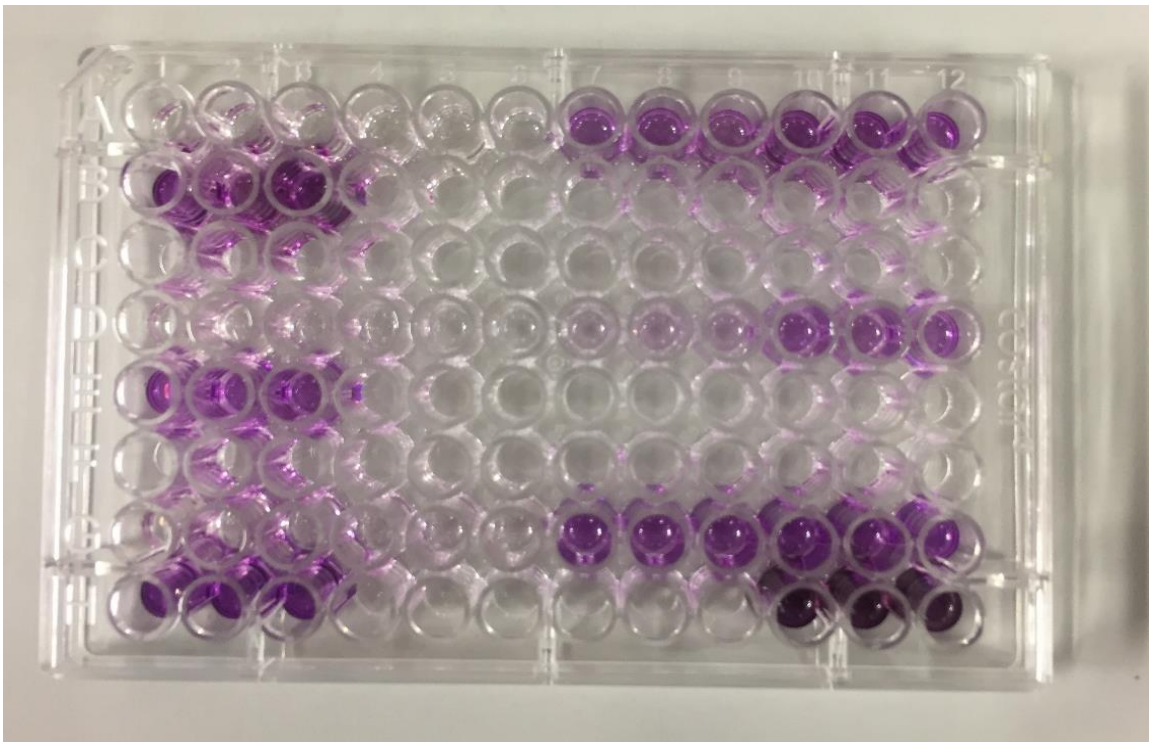

Image 4- 1: Metabolised MTT reagent prepared for UV-Vis analysis

Results from the cytotoxicity experiment can be seen in **Table 4-2** and **Figure 4-4**.

Table 4- 2: MTT cytotoxicity results for HBP4060, HBP4060ethyf and HBP4060pegf (Technical repetitions)

HBP4060			HBP4060ethyf			HBP4060pegf		
Concentration µg/ml	**Cell Survival**	**% error**	**Concentration µg/ml**	**Cell Survival**	**% error**	**Concentration µg/ml**	**Cell Survival**	**% error**
0	100	3	0	100	3	0	100	3
10	58	19	10	34	0.9	10	55	3
50	48	5	50	30	3	50	51	3
100	34	4	100	10	1	100	42	3
500	5	1	500	5	0.3	500	5	0.8
1000	5	1	1000	5	0.3	1000	5	0.2

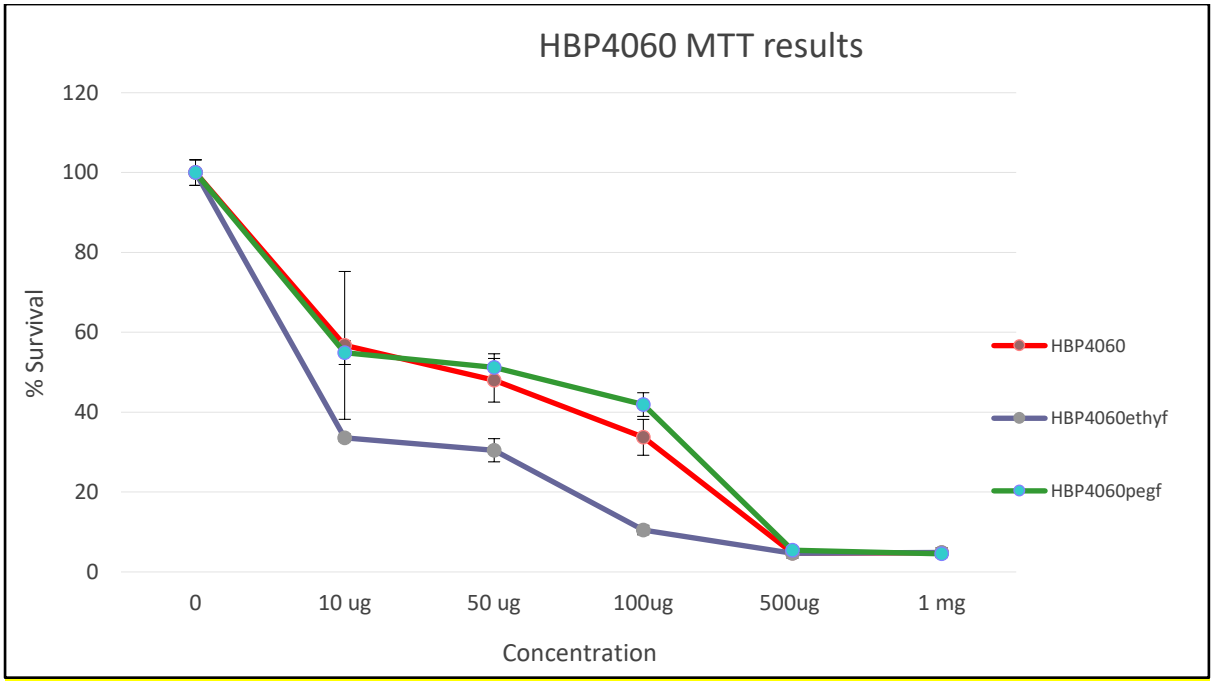

Figure 4- 4: MTT cytotoxicity results for HBP4060, HBP4060ethyf and HBP4060pegf (technical repititions)

The initial screening of polymer toxicity lead to results that were surprising, due to presenting a high overall toxicity of the polymer even up to the lower limit of dosage (10 µg/ml). Furthermore, previous predictions of ethylene diamine possible inducing enhanced toxicity of the polymer were also correlated within the data with polymers conjugated with this linker showing a significant decrease in toxicity in all concentrations above 100 µg, when compared to the naked and peg conjugated sister polymers. The effect of the PEG linker and folate addition did not appear however to induce a higher toxicity when compared to the naked polymer at the concentrations tested.

Whilst this result has been described as an initial sweep there are still a variety of concerns that need addressing so that the polymer can be optimised, and toxicity can be reduced. Firstly, we hypothesised that the use of precipitation, via the hexane ether mixture previously described as a purification method for synthesised polymers may be causing the toxicity observed within HBP4060 (whilst this does not entirely explain toxicity displayed in folate conjugated polymers as these were dialysed post conjugation). It is plausible that ether and hexane molecules used as the anti-solvent for precipitation may be trapped in hydrophobic pockets of the polymer, unable to escape. Therefore, breakdown of the polymer within the cellular

environment could release these molecules inducing toxicity. To put this in perspective, should diethyl ether, hexane or THF be trapped within these pockets the safety data sheets of the compounds were checked, from the readily available download of the respective compound from Fisher Scientific for their half maximal lethal dose LD_{50} toxicity values and the following was found: Diethyl ether (1215 mg/Kg oral, 20 ml/Kg dermal and 32000 ppm inhalation) , Hexane (25 g/Kg oral, 3000 mg/Kg dermal and 48000 ppm inhalation) and THF (1650 mg/Kg oral, >2000 mg/Kg dermal and 180 mg/L (1hr)/ 53.9 mg/L (4hr) inhalation). These values suggest that toxicity is especially a concern when diethyl ether and THF may be trapped within the hydrophobic pockets of compounds, whereas whilst hexane is still imparting toxic effect it is less than the other solvents. However, it was decided that for future proofing of the compound and the synthetic process for scaling up and possible commercialisation there needs to be no doubt that there are no toxic solvents left within the mixture, and thus a switch from precipitation to dialysis was considered at this point of the project for polymer purification.

Furthermore, uptake studies have not yet been performed. There is no conclusive evidence as of yet that the polymer has been up taken into the target cell. Proteins, nutrients and other molecules within the media could interact with the polymer as a side mechanism breaking down or altering polymer structure in a way that could induce toxicity due to interference with the materials needed for cell proliferation. On the other hand, breakdown of the polymer structure could release further small molecules that have unwanted side effects on cell growth. Additionally, it is worth noting that whilst cultured within media and stimulated via polymer during the 72-hr period there is a lack of clearance mechanisms displayed within the human body, such as renal clearance. Therefore, it is a possibility that metabolism of the polymer by cells to release waste products back into the media could interfere with cell proliferation, such as the breakdown of hyperbranched chains releasing thiol containing polymeric chains of lower molecular weight (**Figure 4-5**).

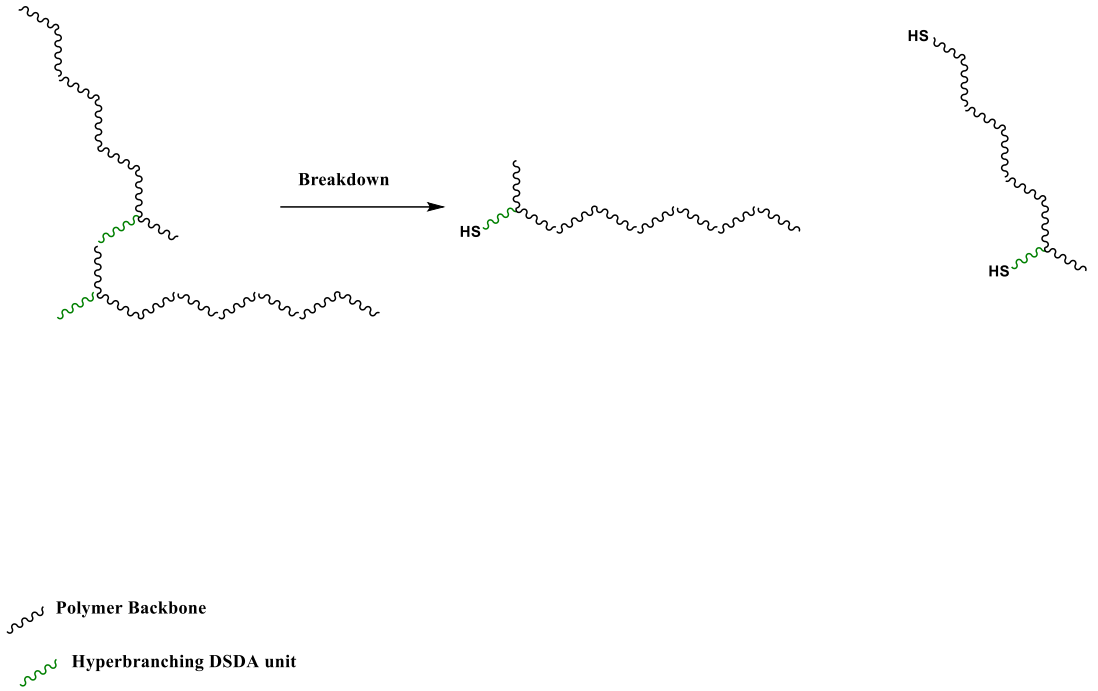

Figure 4- 5: Theoretical breakdown of HBP to form thio-ended chains

Despite the toxicity results obtained displaying undesirable values, the results suggest that this polymer would require drug load and final polymer concentration below that of 10 µg/ ml at the very least to be considered viable for use, whilst precipitation as a purification method should be abolished in favour of dialysis to ensure that no harmful anti-solvents have the possibility of being trapped within polymer molecules with no method of release.

4.4.2: Fluorophore conjugation and cellular uptake

As previously discussed, there was no way at the present time to prove conclusively that the designed polymer had been taken up by cells. Therefore, before further studies can be conducted cell uptake studies were performed to assess further any future considerations and modifications needed before further work. Despite UV activity folic acid and trithiocarbonate functionalities within the polymer lend themselves to very poor fluorescent properties and hence fluorophore conjugation was necessary in order to visualise polymer particles via confocal microscopy. Rhodamine was chosen as the compound of choice for this purpose

due to the fluorescent properties it displays and relative ease of conjugation onto the polymer itself.

In order to prepare rhodamine for conjugation the ethylene diamine form was synthesised utilising the Steglich esterification methodology used previously for folate addition (**Scheme 4-3**).

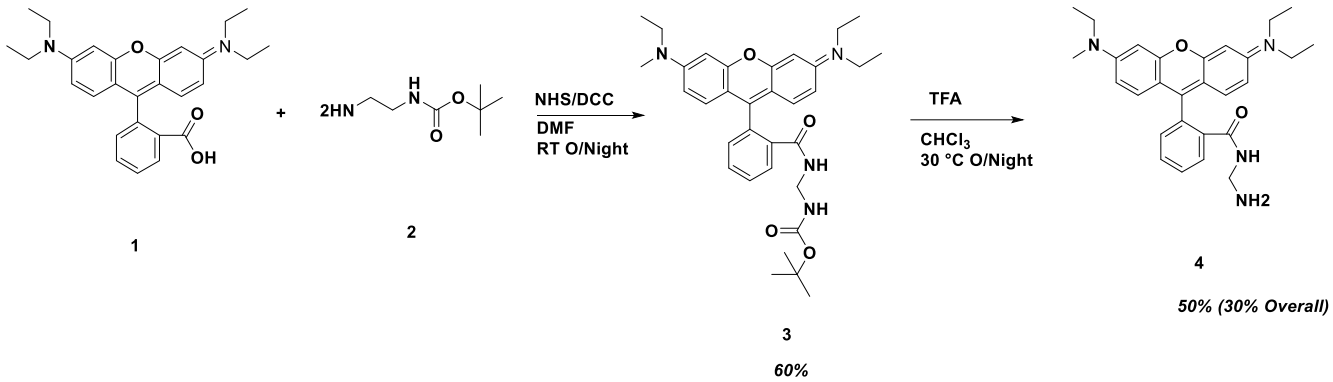

Scheme 4- 3: Synthesis of Rhodamine B ethylene diamine

Rhodamine B (**1**) was initially conjugated to mono-boc protected ethylene diamine (**2**) before deprotection with tri-flouro acetic acid to yield the fluorophore ready for polymer conjugation (**4**) with a 30% overall yield. Conjugation of rhodamine to HBP4060 species was performed twice, on both HBP4060 and HBP4060$_{pegf}$ again via the Steglich esterification to yield HBP4060 variants **C** and **D** (**Scheme 4-4**).

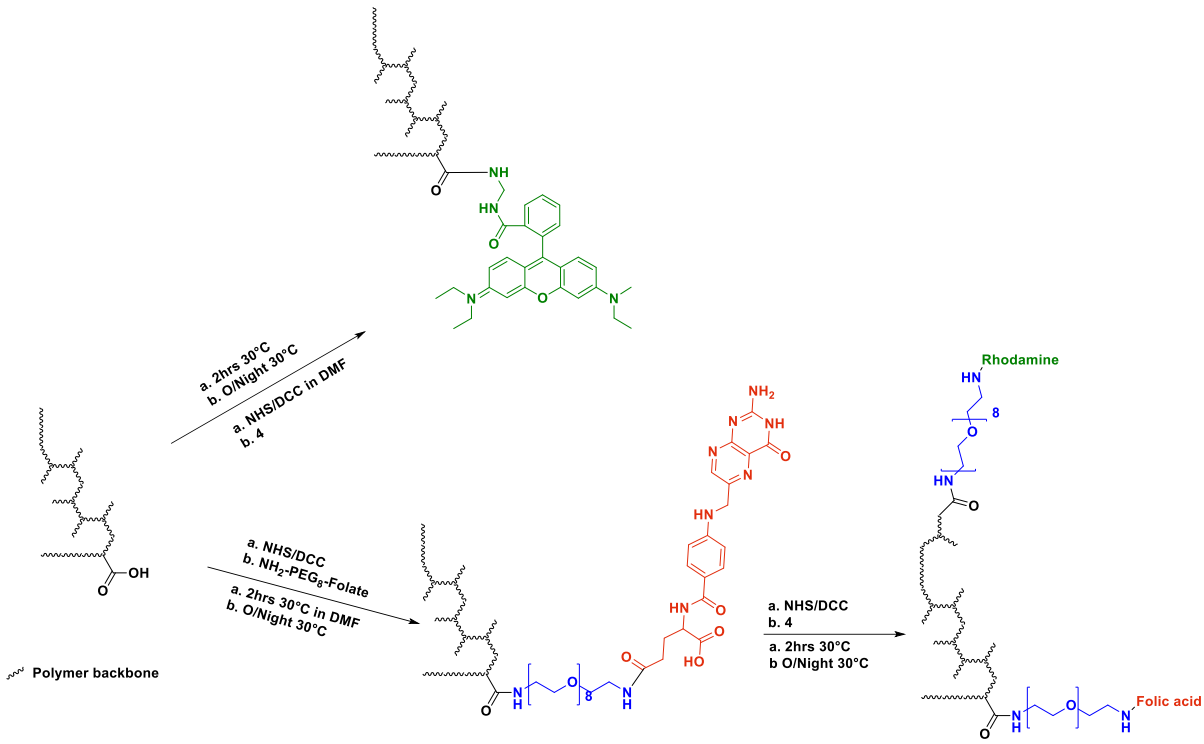

Scheme 4- 4: Synthesis of fluorophore enabled HBP4060

Upon modification of HBP4060 to yield fluorescent properties dialysis was performed in a 5:95 DMF:Water (*v/v*) system with solvent changes every 24 hours until the solution was colourless (4 days for **C** and 5 days for **D**). Freeze drying of the liquid within membrane was then performed to yield an orange powder and a red powder for **C** and **D** respectively.

In order to quantify the amount of rhodamine conjugated onto each polymer UV-Vis analysis was employed, with quantification performed at the λ_{max} of rhodamine (554 nm) in DMF solvent with quartz cuvettes (Table 4-3) and the corresponding calibration curve can be found within chapter two of this thesis.

Table 4- 3: Quantification of Rhodamine content on polymers via UV-Vis absorption spectrometry

Sample	A.U. 554 nm	nMol/mg (Rhodamine/polymer)
HBP4060$_R$	0.3582	648.0
HBP4060$_{pegfR}$	0.0496	89.6

Rhodamine labelled polymers were then used as a treatment towards HeLa cells within a concentration range of 100 µg/ml - 10 µg/ml levels in order to assess the uptake of polymeric material within the first hour after treatment. The concentration range was chosen for two reasons. Firstly, these concentration levels were chosen as they displayed the least toxicity towards cells as evidenced by preliminary MTT results, however anything above 10 µg/ml can still be classified as toxic, although at these concentrations it is expected that sufficient fluorescence will be observed in order to get a good visualisation of fluorescent materials. Polymer were again sterilised with the use of 0.2 µm membrane filters for the same reasons as discussed previously. Cells were plated on cover slips in a 24 well plate at a cell density of approximately 80K cells per well and left to proliferate for 24 hrs before treatment. Controls for the experiment were sterile water, PBS and rhodamine B (100 µg/ml) and cells were treated for a period of 1 hr. After which, media was aspirated, and the cells were fixed in a 4% paraformaldehyde solution (in PBS) before being washed twice with PBS. Nuclei were stained via DAPI (4',6-diamidino-2-phenylindole) in Bovine Serum Albumin and mounting onto microscope slides via ImmunoHistoMount.

Whilst multiple concentrations were dosed only polymers conjugated with Rhodamine at a 100 µg/ml concentration allowed for the production of images with good fluorescent visualisation and meaningful data to be extracted. Comparisons of the Rhodamine control with both polymer samples suggests rhodamine doesn't enter the cell efficiently. Both polymer samples, however, display fluorescent hotspots possibly relating to endosomal transport into the cell, however, it could be argued that this is also a result of aggregate type behaviour from the material itself, however as this is only visible within the cells themselves it could be suggested that this is not the case. Furthermore, it can be suggested via the localisation of the fluorescent signal that there is an accumulation of the polymeric structure within the endoplasmic reticulum within the first hour, however this was not confirmed (**Figure 4-6**).

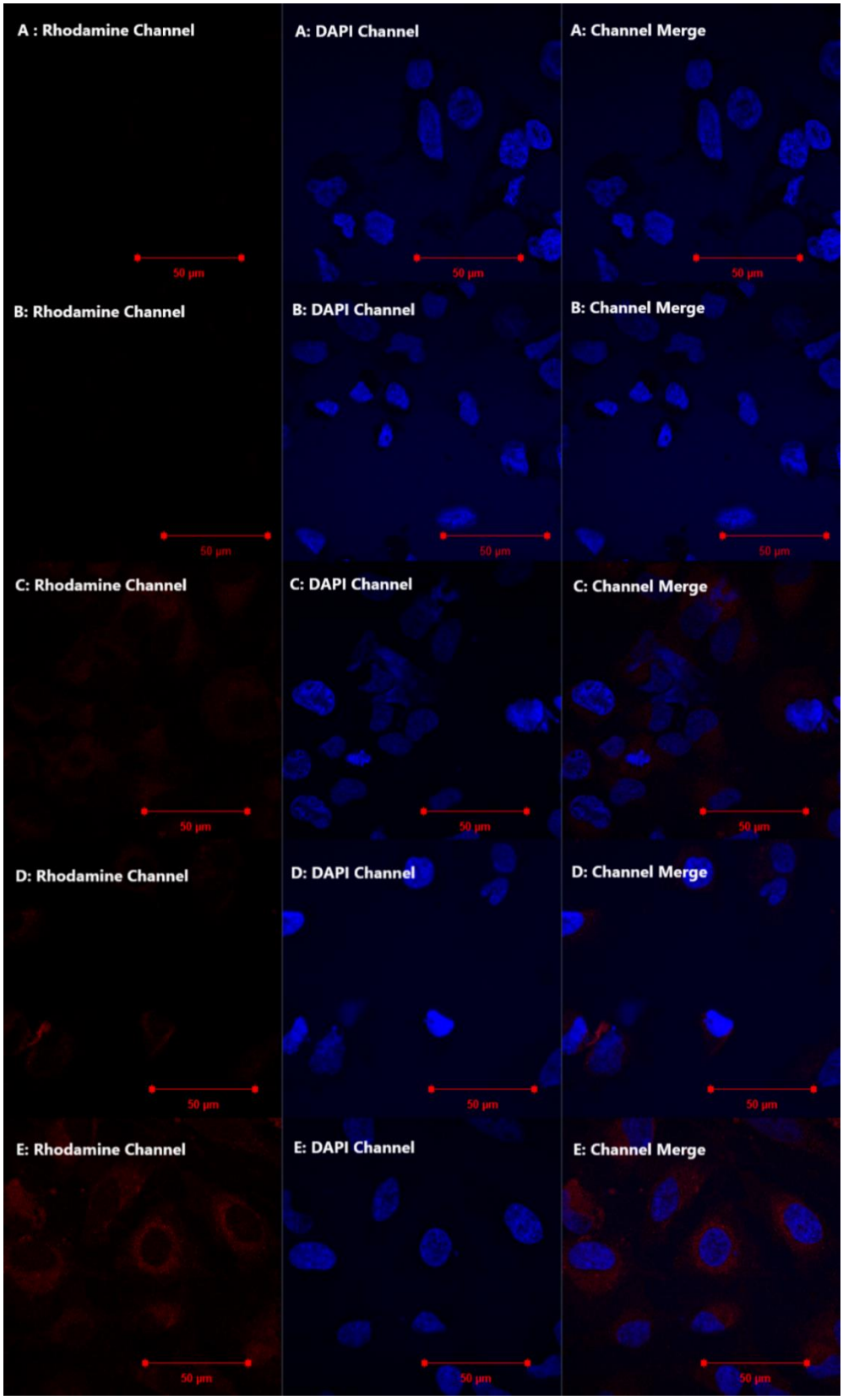

A: PBS B: Water C: Rhodamine 210 nM/ml D: $HBP4060_{pegfR}$ E: $HBP4060_{R}$

Figure 4- 6: Confocal Microscopy of rhodamine containing polymers (63x magnification)

Whilst internalisation has been displayed it is clear from the imagery that folate containing polymer has a much greater barrier to entry. DLS data for both the unlabelled and PEG labelled polymer offer a possible explanation for this phenomenon. It is known that the upper limit for endocytosis is known to be around the 200 nm mark [40]. Whilst internalisation of both polymers is evident it that the uptake doesn't occur in similar quantities. It can be argued that there is a greater amount of rhodamine on $HBP4060_R$ as oppose to the folated variant.. Whilst polymer is approaching the endoplasmic reticulum, much the same as $HBP4060_R$, there is a distinct lack of "tail" or "queue" of rhodamine containing polymers in cell imagery and rather a hotspot surrounding the nucleus.

DLS results presented beforehand predict sizes for HBP4060 ranging from 74.8-337.9 nm. Therefore, in order to assess whether the decrease in uptake of $HBP4060_{pegf}$ was a possible result of a increase in particle size leaving the vehicle too large to facilitate cellular uptake further DLS was performed on $HBP4060_{pegf}$ and from the results obtained it can be shown that the polymeric system is indeed too large to facilitate any efficient cellular uptake with particle diameter ranging from 882 – 1195 nm based on Zave calculations (Table 4-4).

Table 4- 4: DLS data for HBP4060pegf

Entry	Sample	pH	Particle Diameter Zave[ab] (nm)
1	$HBP4060_{pegf}$	7.4	882
		6.8	1195
		5.4	1160
		Dulbecco's PBS	1178

a: Harmonic intensity averaged hydrodynamic particle diameter b: measurements showed a neglible error of ± 0.0005 nm and therefore are omitted.

Furthermore, the graphs obtained from the DLS data suggested multiple polymer populations, most likely as a net result of aggregation due to folate addition, which was not surprising, due to the low solubility of folic acid. Whilst it was observed that, unlike the naked HBP4060 variant of the polymer, there is not the initial drop in particle size as a result of the lowering of the pH of the solution from 7.4 to 6.8 suggesting that the use of PAA carboxyl moieties in the steglich reaction has negatively impacted the smart properties of this polymer. However, as before, data transformations were performed in order to gain a better understanding of the data, as the

Zave is sensitive to slight aggregations transformations in the data to both volume and number averaged particle size can give an indication of the particle diameter with aggregation exempt from calculations. The data from these transformations has been summarised in Table 4-5.

Table 4- 5: DLS data transformations for HBP4060pegf

Entry	Sample	pH	Zave Particle Diameter (nm)	Volume Averaged Diameter (nm)	Number Averaged Diameter (nm)
1	HBP4060pegf	7.4	882.4	463.1 (40.9%) 962.9 (59.1 %)	455.2 (89.7%) 1003.3 (10.3%)
		6.8	1194.5	111.2 (8%) 536.2 (55.2 %) 2398.7 (36.8 %)	109.6 (92.7%) 472.4 (7.2%)
		5.4	1160.1	405.4 (28.5%) 924.7 (71.5%)	402.8 (85.3%) 926.3 (14.7%)
		Dulbecco's PBS	1177.6	703.2	688.7

What can be observed via the data transformations is that the initial reduction in particle size as a result of lowering pH from 7.4 to 6.8 is once again observed with both volume and number averaged paticle size. These transformations therefore suggest that with the introduction of folate onto the polymer there is an increased tendency for aggregation, possibly due to pi-pi stacking of folate moieties in combination with steric effects whilst also an alteration of the hydrophilic/phobic properties of the polymer due to the introduction of folic acid, which is known to be sparingly soluble within aqueous media [20].

Whilst this size difference alone would suggest internalisation of conjugated polymer alone would have a great barrier of entry the effects of further conjugation of rhodamine tag on the overall particle size was not studied for the purpose of this experiment and it can only be hypothesised that the particles would further increase in

size although the % increase of which particle diameter is changed cannot be accurately predicted. Despite these results not presenting a proof of concept of the usefulness of the folate ligand optimism can be obtained via the fact that internalisation of both polymer variants was observed.

4.4.3 Considerations moving forward with the HBP4060 structure

With both MTT and cell uptake bioassays presenting data wholly unsuitable for the use of this compound as a drug delivery vehicle further consideration were needed in order to optimise the structure in order to assess if suitability can be obtained.

Firstly, purification of the synthesised polymer was altered from a precipitation method to a dialysis in pure water, in an attempt to prevent encapsulation of solvent molecules. Secondly, the RAFT mechanism was exploited with increasing feed ratio of RAFT agent compared to the initiator used in order to control the molecular weight. Both points have been discussed in much detail in chapter three in their respective experimental and discussion sections.

Additionally, cytotoxicity is a major issue with the structure and is something that if possible, needs to be reduced further down the line, be it via the use of different purification or preparation methods. Particle size when conjugated onto folic acid is also a major issue, inhibiting efficient internalisation of the polymer, and thus whilst ethylene diamine cannot be used due to toxicity concerns presented via MTT results a smaller PEG based linker should be synthesised and used in order to inhibit the effect of ligand conjugation on particle size.

All the above points were taken into consideration for further studies of this polymer and the biological behaviour of cells stimulated with it. Further work focused on utilising HBP4060_2,3 and 4 and assessment of their suitability for the drug delivery role comparing results obtained with preliminary results obtained via HBP4060.

4.5 HBP4060_2,3&4 – improvements in the modification process

4.5.1. Bio-conjugations of HBP4060_2,3 and 4

As previously mentioned, the sister polymers of HBP4060 were used for analysis of the structure for drug delivery suitability. It would be easy to suggest that the structure itself could be a major issue in the previously studied MTT bioassay invoking cytotoxicity as a result of monomers used. However, all three monomers have previously been used in cell friendly polymer mechanisms for delivery of payloads ranging from drugs to genes. Therefore, the structure was carried forward despite some concerns in order to address considerations relating to size, molecular weight, folate concentration, linker size and uptake efficiency so that a full picture of this polymer can be realised and should it be deemed still unsuitable for this role, alternative uses for the polymer could be realised due to the novel structure and further unstudied properties.

Initially, due to the size concerns of $HBP4060_{pegf}$ two solutions were proposed. Firstly, the PEG linker can be reduced in size without effecting the click chemistry needed in order to conjugate folate. Previously a PEG_8 linker was used although this could readily be reduced to a PEG_4 linker without any concerns of synthesis to a diamine form or the ability to react with either polymer or folic acid. Not only was $HBP4060_{pegf}$ distinctly folate coloured upon conjugation and took a much longer time to dissolve in common solvent such as water, PBS and DMF when compared to the HBP4060 and $HBP4060_{ethyf}$. Whilst solubility itself was not effected in either folate conjugated polymers it could be argued the “folate effect” inhibited an efficient solvation of the polymer end groups hindering dissolution. Therefore, a reduced amount of folate conjugated onto the polymer is expected to reduce both the size and time needed for dissolution without negatively impacting the ability for folate mediated endocytosis to occur.

Therefore, synthesis of PEG-diamine linker was achieved utilising the same methodology as before although a PEG_4 was used instead of a PEG_8 linker. Mono-boc protection and subsequent folate addition before removal of the boc group was performed as previous conjugation experiments displayed this methodology as the most appropriate to achieve greater yield and folate addition to polymers. HBP4060-_2,3 and 4 were then conjugated via the Steglich esterification to the newly formed H_2N-PEG4-folate linker to produce 3 new folate containing polymers.

Quantification of folate on the newly formed polymers was then performed via the UV-Vis method established beforehand at the recorded λ_{max} value of 362 nm. It was interesting to see the relative concentrations of folate on each individual polymer trending alongside molecular weight (and therefore PAA functional group availability). For instance, as polymer decreases in molecular weight there is a much more abundant folate concentration observed via UV (Table 4-6). This is most likely due to the reduced steric hinderance presented by the polymer in solution. As molecular weight decreases so does the repeat units contained within each polymer. Whilst this would reduce the amount of PAA carboxylic acid groups able to react (on a molar to molar ratio between the polymer and the folate linker) there is a greater chance of reaction due to a reduction in complexity of structure and hence an easier route of access.

Table 4- 6: Folate quantification post conjugation on HBP4060_2,3 and 4

Polymer Sample	mg/ml	Abs (362nm)	Folate/polymer (µmol/mg)	Yield (% wt.)
HBP4060_2$_{pegf}$	0.5	0.1154	41	43
HBP4060_3$_{pegf}$	0.5	0.1694	60	56
HBP4060_4$_{pegf}$	0.5	0.2475	88	86

One consideration when cell uptake measurements were taken was the difference in rhodamine concentration between “naked” and folate labelled polymer. This severely restricted any further methods of quantification within cells, such as with FACS, due the variance of fluorophore displayed within each polymer variant. Therefore, in order to address this a change in conjugation order was devised as to ensure that the same amount of fluorophore was present on both folate deficient and folate containing polymer species (**Scheme 4-5**).

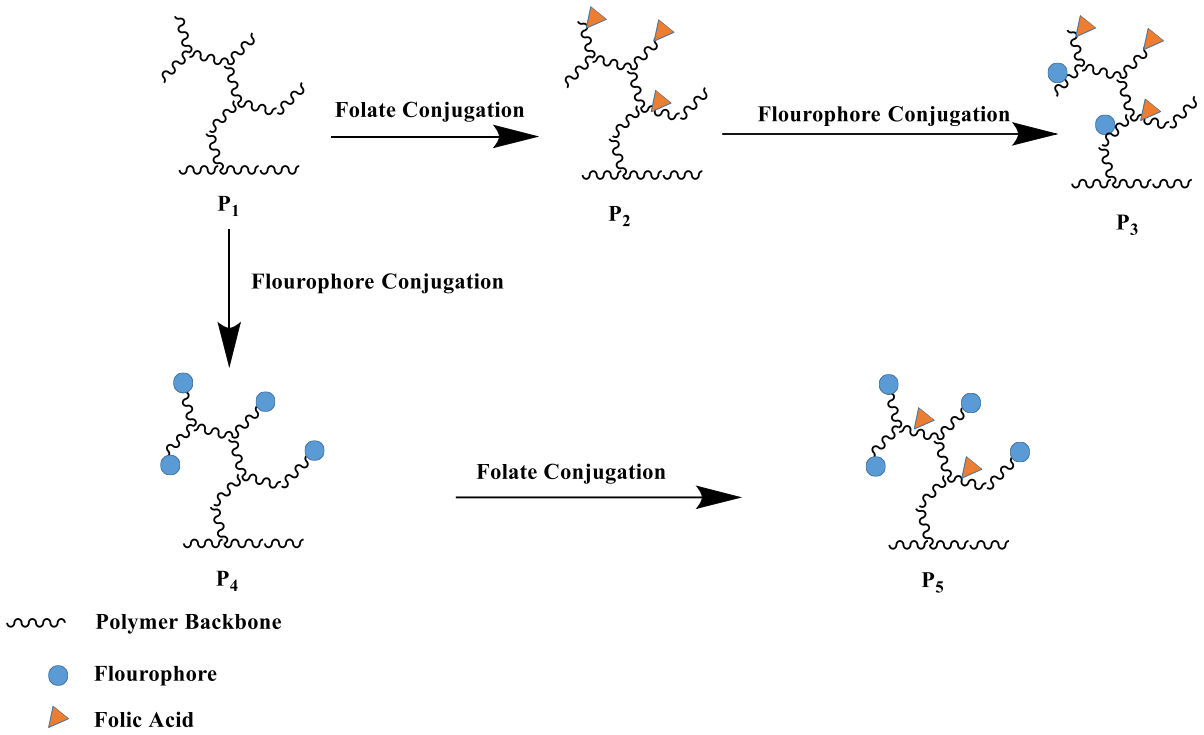

Scheme 4- 5: Methodology to ensure fluorophore levels are constant between folate deficient and folate containing polymer species

Previous attempts to achieve this outcome resulted in a P_3 vs P_4 scenario in which whilst both species were labelled with fluorophore, although concentrations were not identical in the two samples. Thus, by going from $P_1 \rightarrow P_4 \rightarrow P_5$ it can be ensured that the levels of fluorophore are constant between polymers containing folate with those that do not. With future cell uptake experiments therefore, fluorescein (FITC) was first conjugated onto naked polymers before folate conjugation to make two separate batches of folate conjugated polymer (those without fluorophore and those with). The fluorophore was switched from rhodamine for two reasons, firstly, the quantum yield of fluorescein is known to be higher than that of rhodamine. Therefore, a lower amount of dye can be conjugated onto the polymer and yield acceptable results. Furthermore, compatibility with the Flow Cytometry/ Fluorescent Assisted Cell Sorting (FACS) hardware present in the collaborating School of Medical Sciences at Bangor University. FACS was previously unsuitable for use due to both rhodamine concentration in folate present and deficient polymers being distinguishable from one another. FITC was prepared for conjugation onto polymers by first converting the Na salt to the acidified analogue by precipitation with HCl to form the free acid. Secondly, mono-boc ethylene diamine

was conjugated onto the carboxylic acid group and then deprotection was performed to yield fluorescein ethylene diamine (**Scheme 4-6**).

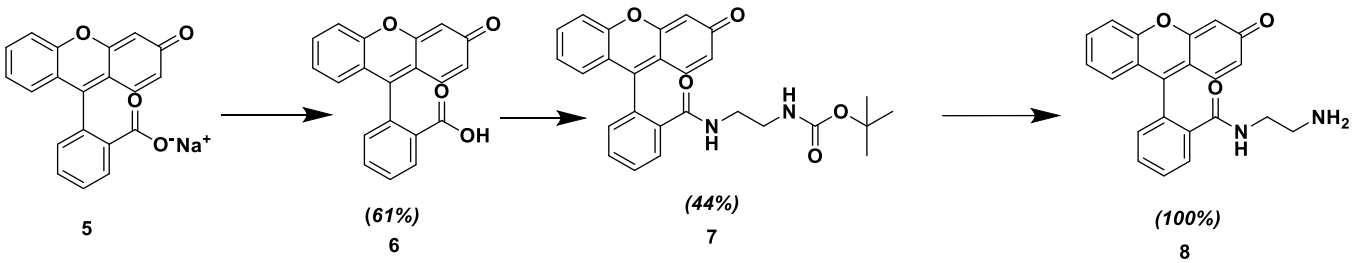

Scheme 4- 6: Synthesis of Fluorescein linker

The FITC linker was then conjugated onto each individual polymer (HBP4060_2, HBP4060_3 and HBP4060_4) via the Steglich esterification once again to produce UV active variants of the polymers. Quantification of fluorescein on the polymers was performed via UV-vis analysis at the corresponding λ_{max} value of 445 nm and the results of the quantification alongside product yield can be seen in **Table 4-7**.

Table 4- 7: HBPfitc FITC quantification via UV-Vis alongside product yield

Entry	Polymer Sample	Mg/ml	Abs (485nm)	Fluorescein/polymer (µmol/mg)	Yield (% wt.)
1	HBP4060_2$_{fitc}$	0.005	0.0157	90	30
2	HBP4060_3$_{fitc}$	0.005	0.0237	136	56
3	HBP4060_4$_{fitc}$	0.005	0.0282	162	58

HBP-FITC conjugates were then subject to linking to the same H_2N-PEG_4-Folate linker as their non fluorescent variants, to produce three fluorescent folate active HBPs, with the folate concentration measured via UV-vis spectroscopy (**Table 4-8**).

Table 4- 8: HBP$_{fitc_pegf}$ folate quantification via UV-Vis alongside product yield

Entry	Polymer Sample	Mg/ml	Abs (362nm)	Folate/polymer (µmol/mg)	Yield (% wt.)
1	HBP4060_2$_{fitc_pegf}$	0.25	0.1037	73	53
2	HBP4060_3$_{fitc_pegf}$	0.5	0.1638	58	66
3	HBP4060_4$_{fitc_pegf}$	0.5	0.0907	32	69

Interestingly, it was apparent that the concentration of folate onto FITC conjugated polymers was observed to be the reverse of FITC conjugations. Whereas in FITC conjugation the efficiency of conjugation was seen to increase as M_w of polymers decreased, folate conjugations decreased in efficiency as M_w decreased. In the initial FITC conjugations the increase in conjugation efficiency was somewhat surprising and a trend observed in folate conjugation was initially expected. This was due to the reduced number of PAA repeat units contained within the polymer chains as a direct result of the lower molecular weight. However, as this hypothesis did not come to fruition it is suggested that due to a lessened steric hindrance for conjugation onto chains this relationship was observed. This in part aids discussion on the relationship seen with folate conjugation decreasing in efficiency as M_w of macromolecules decreases alongside an increase in FITC conjugation. As FITC concentration increases the effects of steric hindrance are negated as there are fewer carboxylic acid groups required for the conjugation available on polymers, either from PAA repeating units or RAFT agent end group. Therefore, the decreasing folate concentration onto polymers is completely understandable.

4.5.2. Cytotoxicity analysis of HBP4060_2,3 and 4

Previously it was mentioned that the cytotoxicity of HBP4060 was concerning for the role of drug delivery vehicle. Therefore, purification methods were shifted from a precipitation-based purification to the much more benign dialysis purification method. MTT analysis was therefore performed on HBP4060_2, HBP4060_3 and HBP4060_4 alongside all folate conjugated variants of these molecules to assess whether purification methods have aided in reducing the overall toxicity of the polymers. The concentrations used were therefore identical to previous studies. It was expected that at high concentrations of polymer (>100 µg/ml) that a high toxicity surpassing 50% cell survival would be observed, mimicking HBP4060 whilst below this value cell survival should increase suggesting less toxicity when compared to HBP4060. The results from the cytotoxicity experiments can be seen in Table 4-9 and Figure 4-7.

Table 4- 9: MTT results for HBP4060_2,3&4 (Biological repeats)

HBP4060_2			**HBP4060_3**			**HBP4060_4**		
Concentration µg/ml	**Cell Survival**	**% error**	**Concentration µg/ml**	**Cell Survival**	**% error**	**Concentration µg/ml**	**Cell Survival**	**% error**
0	100	1E-14	**0**	100	1.00E-14	**0**	100	1.00E-14
10	79	22	**10**	100	23	**10**	88	18
50	37	14	**50**	87	29	**50**	57	16
100	11	2	**100**	26	8	**100**	16	1
500	11	3	**500**	11	3	**500**	11	2
1000	10	2	**1000**	11	3	**1000**	11	2

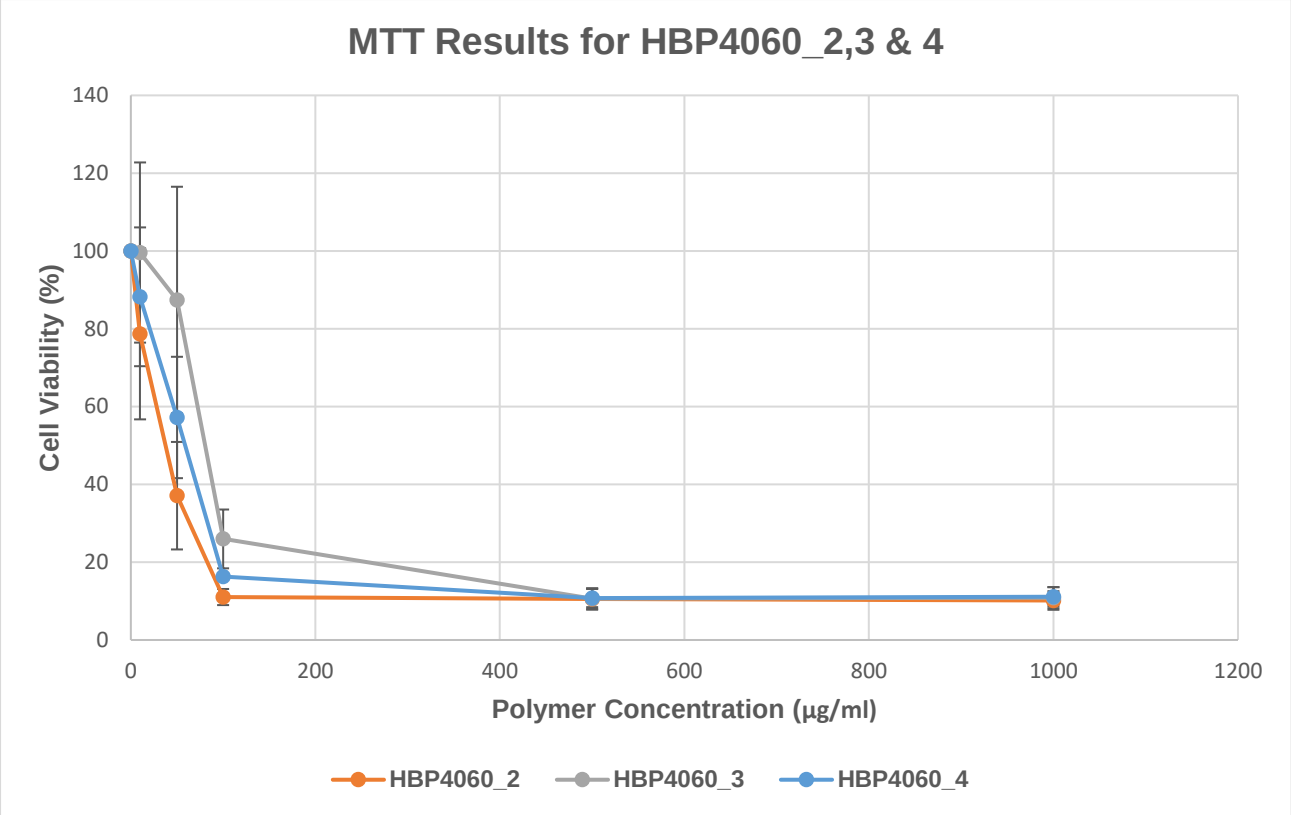

Figure 4- 7: MTT results for HBP4060_2,3&4 (Biological Repeats)

Initially what is observed is all three polymers displayed similar trends to one another as concentration decreases toxicity also decreases, an expected scenario. HBP4060_2 however shows increased toxicity up to a concentration of 50 µg/ml. It is hypothesised that the increased % composition of DMAEMA within this molecule is cause of this toxicity, due to amines present within this repeating unit. However, when concentration is reduced to 10 µg/ml there is no clear case for any of the three samples being regarded as the least toxic sample, due a large variance in cell viability within the measurements. However, it is worth noting that the other samples still display around a 30% increase in cell survival at this concentration when compared to HBP4060. This increase is hypothesised to be a result of the change in purification method previously mentioned. The use of the dialysis method is much more benign in nature than precipitation as there is no introduction of toxic solvents that could be trapped into the polymer precipitate and released into the cells promoting cell death. This result, although at this stage still preliminary, there was a distinct reduction in toxicity of these polymers when compared to HBP4060, although

there is a lack relevance of this within a clinical setting, as polymers still show a cell viability of <25% at 100 µg/ml. The reduction of toxicity when compared to HBP4060 at 10 µg/ml confirmed that any drug loading and cytotoxicity studies concerning polymer drug conjugates must be conducted at this concentration or below to ensure minimal cell death as a result of polymeric species. Furthermore, further work on cell survival assays needs to be performed due to the large variance in survival mentioned. Thus, conducting further research into cell survival below a concentration of 10 µg/ml needs to be conducted to ensure that this polymer is fit for purpose and is a non-toxic drug carrier. The variance in results could be attributed to the HeLa cell line itself (or more specifically the physiological state of the cells at the time of the experiment itself), as experiments were performed on different days. As previously discussed, the results from the MTT assay rely on the capability for the cells to metabolise the MTT reagent and as such is a measurement of metabolization, which can be correlated to the cell viability. Therefore, variance in cell metabolism between biological triplicates could be behind the variance. For the studies all biological protocols were adhered to, and the cells were “split” no more than 4 times post awakening before experiments were conducted ensuring the cells were as fresh as possible upon waking, to negate any metabolic variances. Interestingly, experiment controls yielded little error and consistent results. This would suggest that the variance in metabolism suggested is not being shown and that the variance in cell survival at lower polymer concentrations are a result of polymeric stimulation. This could be due to a result of cell cycle growth arrest or as a result of competition with the MTT reagent itself, whilst pipetting variance and physiological variances are also possible causes. Therefore, further studies at lower concentration of polymer are required in order to provide a narrower window of observation to deduce concentrations at which the polymer can be deemed non-toxic. Furthermore, it could be argued that the variance is a result of technical error between repeats, however in order to negate this a triplicate of triplicates was performed. Each plate was performed in triplicate and cells were split and the plate repeated to give 9 separate measurements per concentration (3 per plate). Therefore, any technical error could be accounted for. It was observed that between plates there was some variance in cell viability (which is accounted for in the error reported). Whilst triplicates within the same plate didn’t show large variance (technical repeats) results between plates did (biological repeats) , except for the

control which always equated to 100% on average. This phenomenon suggests that therefore, much more complex mechanisms are in place for cell death rather than just the introduction of polymer.

In addition to these points there are also limitations within the MTT assay itself when accounting for the cell death. As previously discussed, the results correspond to the activity of mitochondrial reductase protonating and, hence reducing the reagent. It could be argued therefore, that with the results observed that a complimentary colony survival assay should be performed in order to gain a better understanding of the results. In doing this assay this would give a better understanding of the biological impact of the introduction of the synthesised drug delivery system.

Therefore, further in-depth studies are required to assess the mechanism of cell death with respect to polymeric stimulation to fully identify whether this biological effect is a result of cell death. In addition to “naked” polymer toxicity studies all folate containing polymers with peg linkage were tested to assess whether any fluctuations in toxicity could be observed (**Table 4-10** and **Figure 4-8**).

Table 4- 10: MTT results for HBP4060_2pegf, 3pegf & 4pegf (Biological repeats)

HBP4060_2$_{pegf}$			**HBP4060_3$_{pegf}$**			**HBP4060_4$_{pegf}$**		
Concentration µg/ml	**Cell Survival**	**% error**	**Concentration µg/ml**	**Cell Survival**	**% error**	**Concentration µg/ml**	**Cell Survival**	**% error**
0	100	1E-14	**0**	100	1E-14	**0**	100	1E-14
10	115	20	**10**	107	22	**10**	101	10
50	84	12	**50**	95	14	**50**	79	5
100	47	20	**100**	84	19	**100**	18	7
500	6	1	**500**	6	0.3	**500**	6	0.4
1000	6	1	**1000**	6	0.2	**1000**	6	0.4

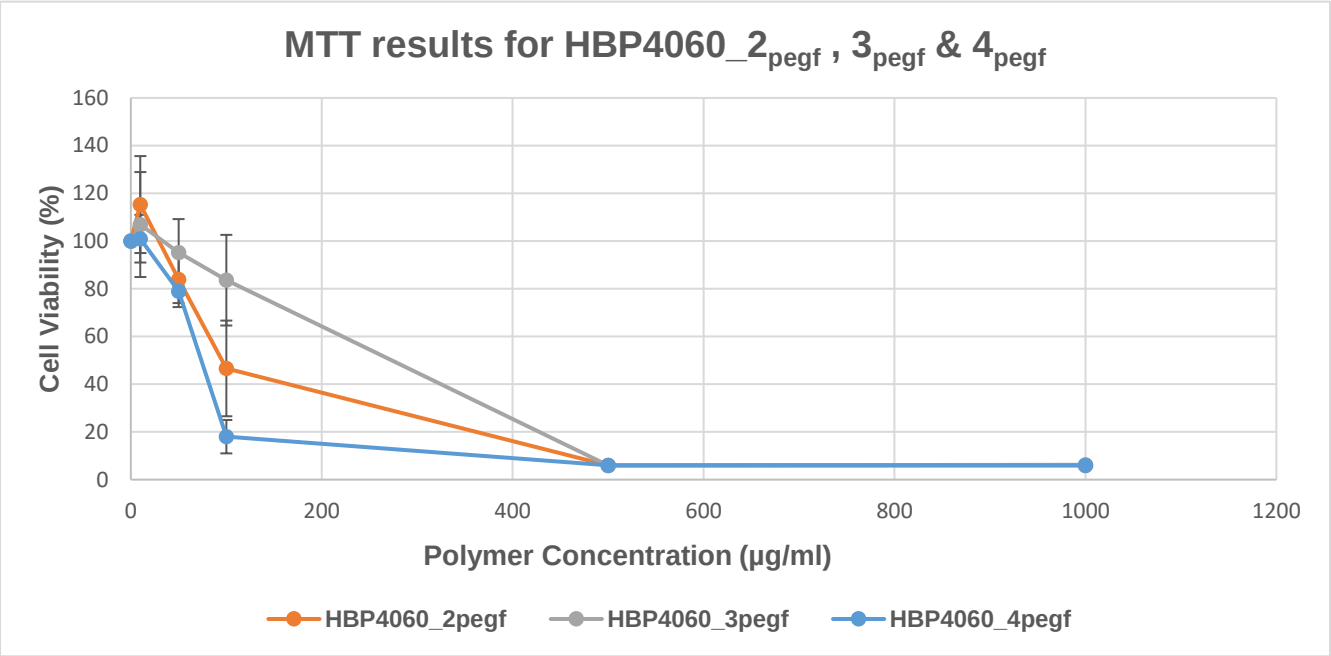

Figure 4- 8: MTT results for HBP4060_2pegf, 3pegf & 4pegf (Biological repeats)

The results of folate conjugated polymers correlated with the previous studies in that cell survival studied with polymer stimulation at a concentration of 50 µg/ml is observed to have the largest increase before peaking at 10 µg/ml. Interestingly however, the behaviour of the HBP4060_3_{pegf} polymer seems to suggest a higher cell tolerance towards this sample with viability upwards of 80% at 100 µg/ml.

However, this result only shows any significant difference with HBP4060_4_{pegf}. The results obtained also somewhat correlate with studies performed on HBP4060 as it was found that $HBP4060_{pegf}$ displayed a similar toxicity profile to the naked polymer alone. All three polymer samples when folate conjugated however displayed little toxicity at the lowest concentration whereas when naked some toxicity (between 15-10% cell death) was still observed. These results are promising as they suggest that both purification and synthetic methods facilitate the production of polymer folate conjugates with low toxicity at concentrations of 10 µg/ml and below. However, once again the variance in cells that are surviving between repeats is large and must be considered an area for refinement. Therefore, to emphasise points made earlier, narrowing of the MTT analysis window is a future consideration in order to better

understand the toxicity profile of this polymer with respect to the HeLa cell line at low concentration.

4.5.3 Cellular uptake assessment of polymers

HBP4060_2 HBP4060_3 and HBP4060_4 (both fitc and fitc_pegf variants) were tested for their ability to be taken up into the HeLa cell line. Previously, the reasoning was discussed for the use of a different fluorophore for greater sensitivity with confocal imaging whilst it was ensured that fluorophore concentration was kept constant throughout both folated and non-folated variants of their respective sample polymer.

Furthermore, in order to assess the role of folic acid within the uptake of polymeric species experiments were run with cells either being cultured within folate containing media or media displaying folate deficiency.

Therefore, by depriving the culturing media of folate it is suggested that a restricted competition for the cellular folate receptor protein an increased uptake of folate containing polymers will be seen in these conditions when compared to cells cultured and stimulated with media containing folic acid. Therefore, any observed increase in the uptake of polymer folate conjugates can be indeed attributed to ligand mediated endocytosis. Confocal imagery can be seen in **Figures 4-9 to 4-14.**

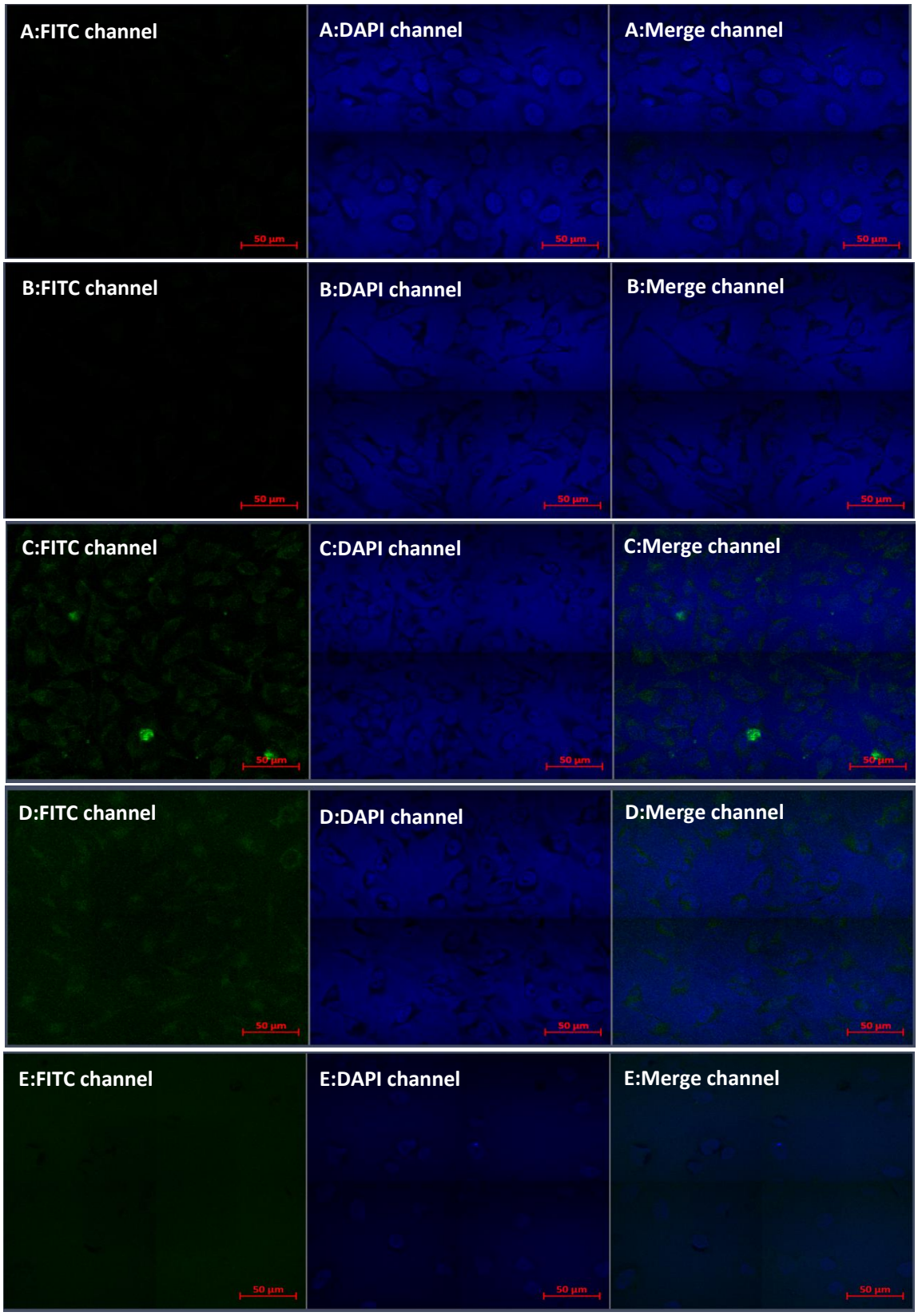

A: Water B:PBS C:FITC D:HBP4060_2$_{FITC}$ E:HBP4060_2$_{FITC_pegf}$

Figure 4- 9: Confocal Microscopy analysis of HP4060_2$_{FITC}$ and HBP4060_2$_{FITC_pegf}$ in folate containing media

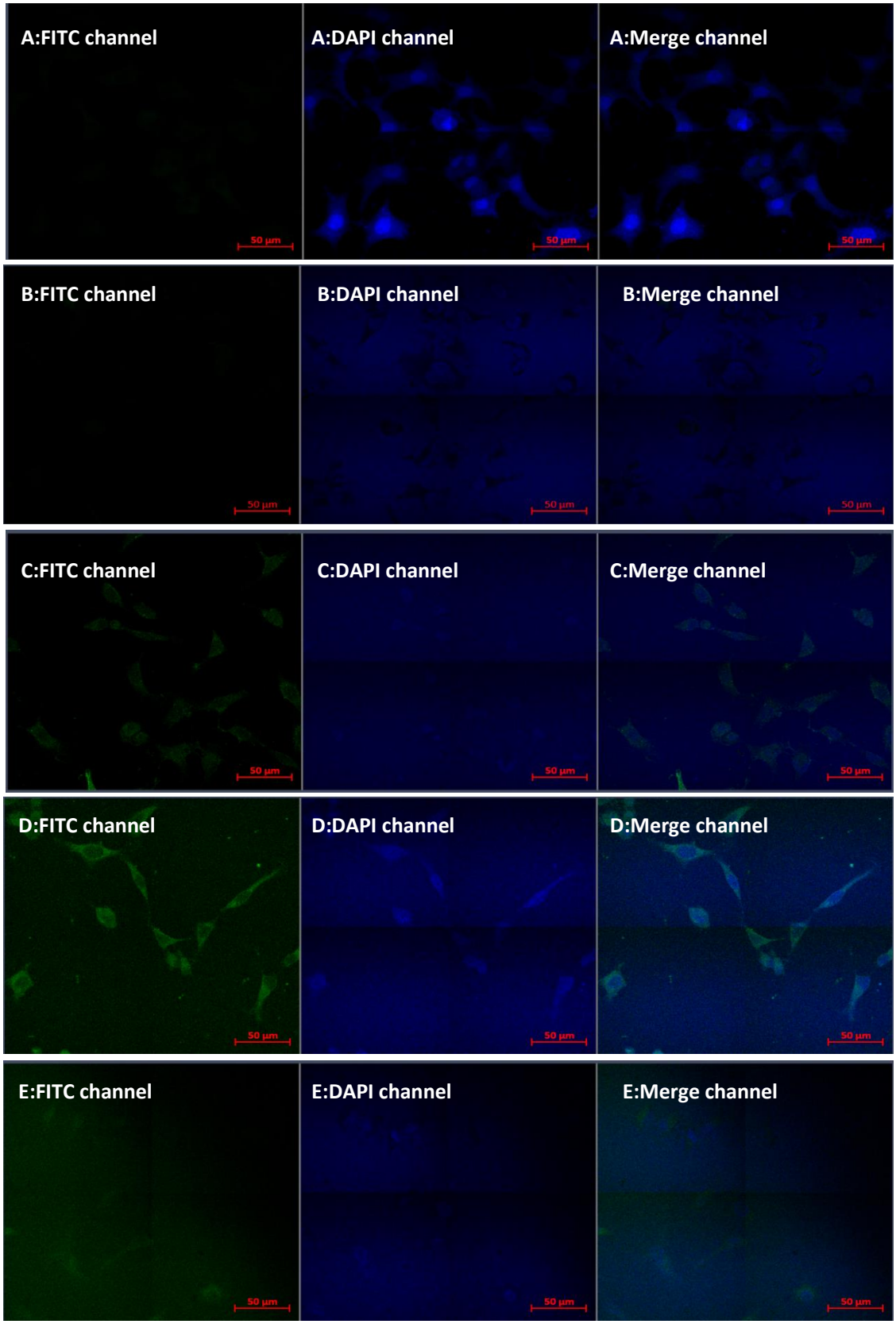

A: Water B:PBS C:FITC D:HBP4060_2_{FITC} E:HBP4060_2_{FITC_pegf}

Figure 4- 10: Confocal Microscopy analysis of HP4060_2_{FITC} and HBP4060_$2_{pegfFITC}$ in folate deficient media

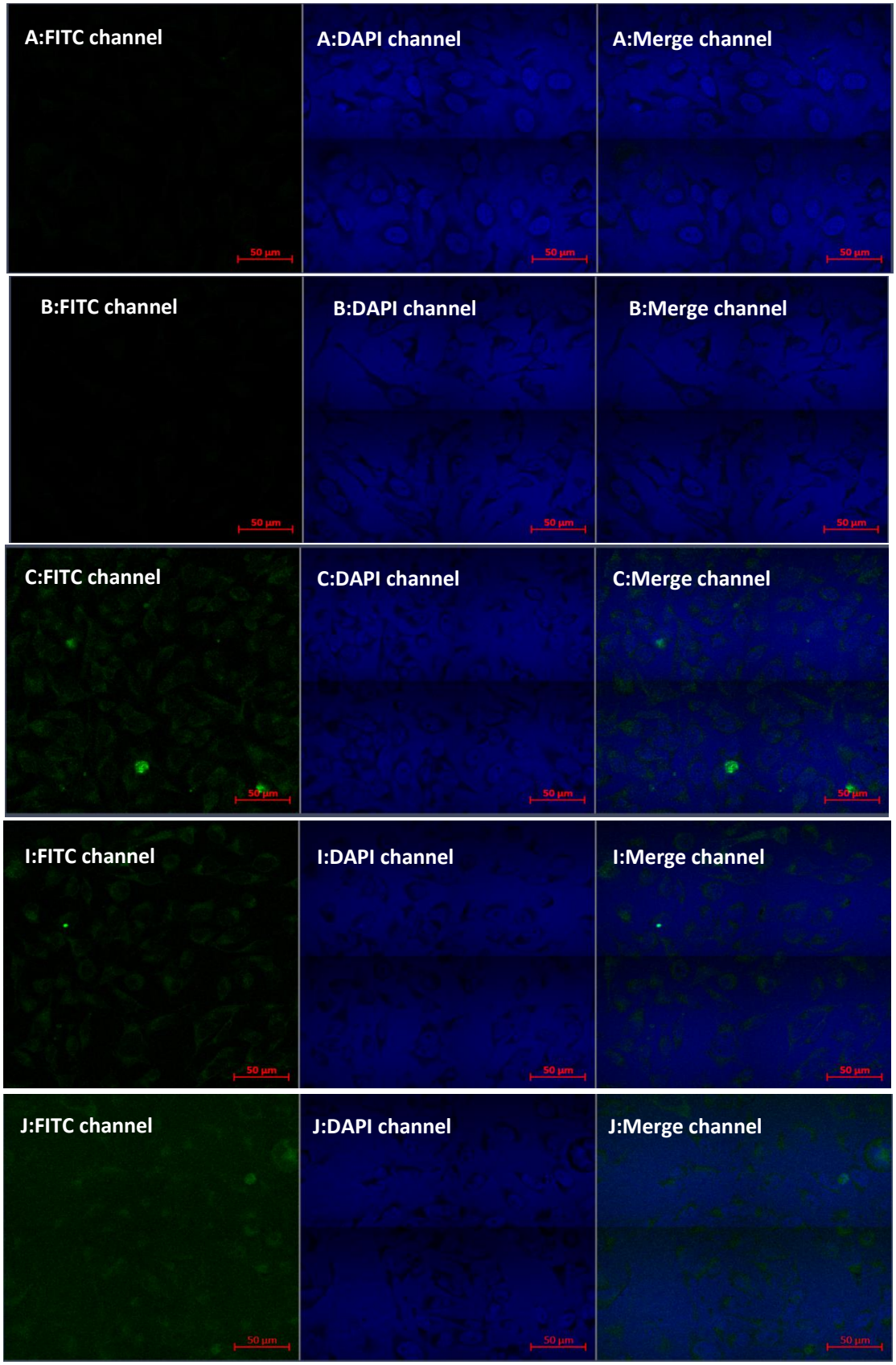

A: Water B:PBS C:FITC I:HBP4060_3_{FITC} J:HBP4060_3_{FITC_pegf}

Figure 4- 11: Confocal Microscopy analysis of HP4060_3_{FITC} and HBP4060_$3_{pegfFITC}$ in folate containing media

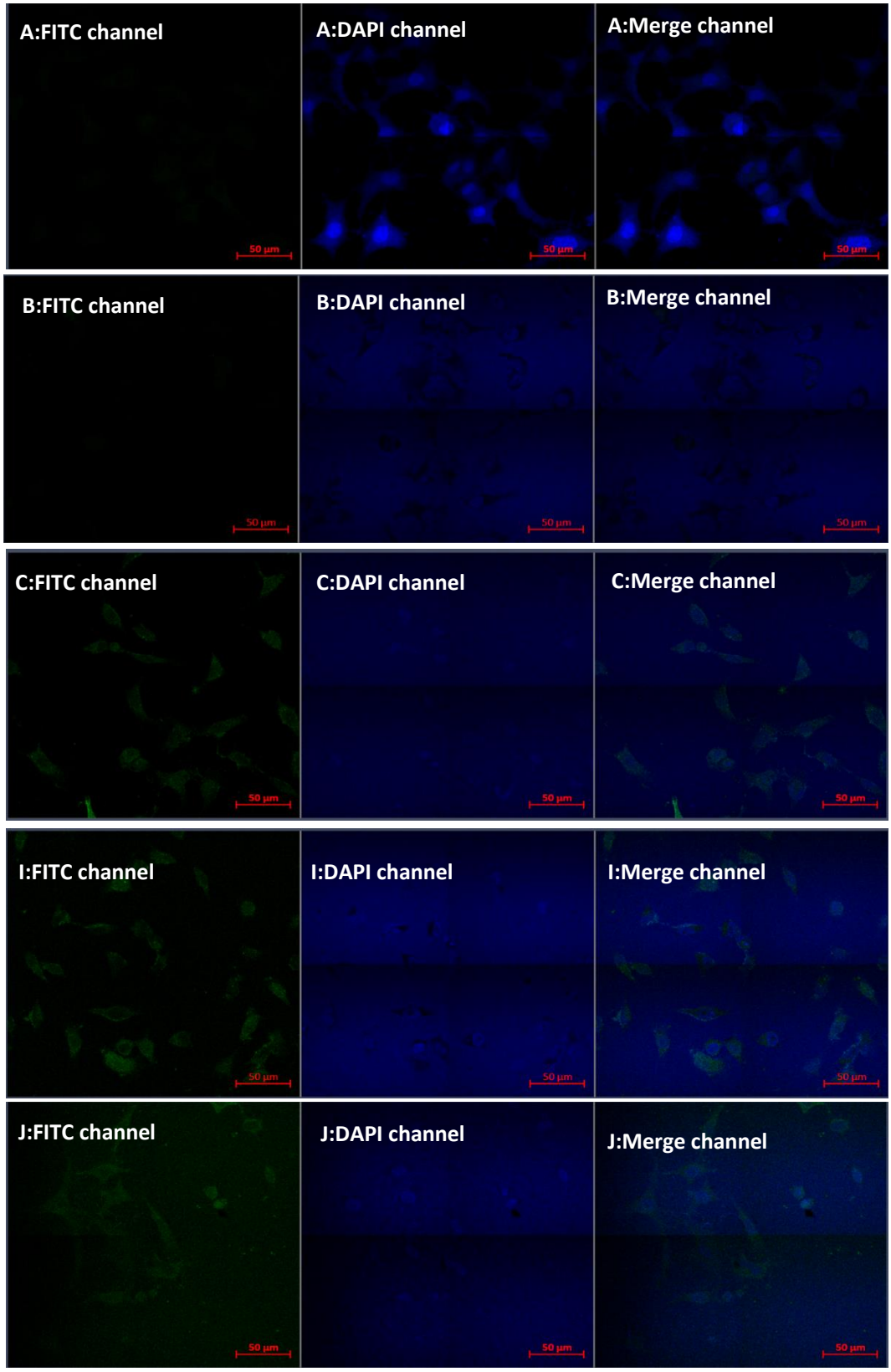

A: Water B:PBS C:FITC I:HBP4060_3$_{FITC}$ J:HBP4060_3$_{FITC_pegf}$

Figure 4- 12: Confocal Microscopy analysis of HP4060_3$_{FITC}$ and HBP4060_3$_{pegfFITC}$ in folate deficient media

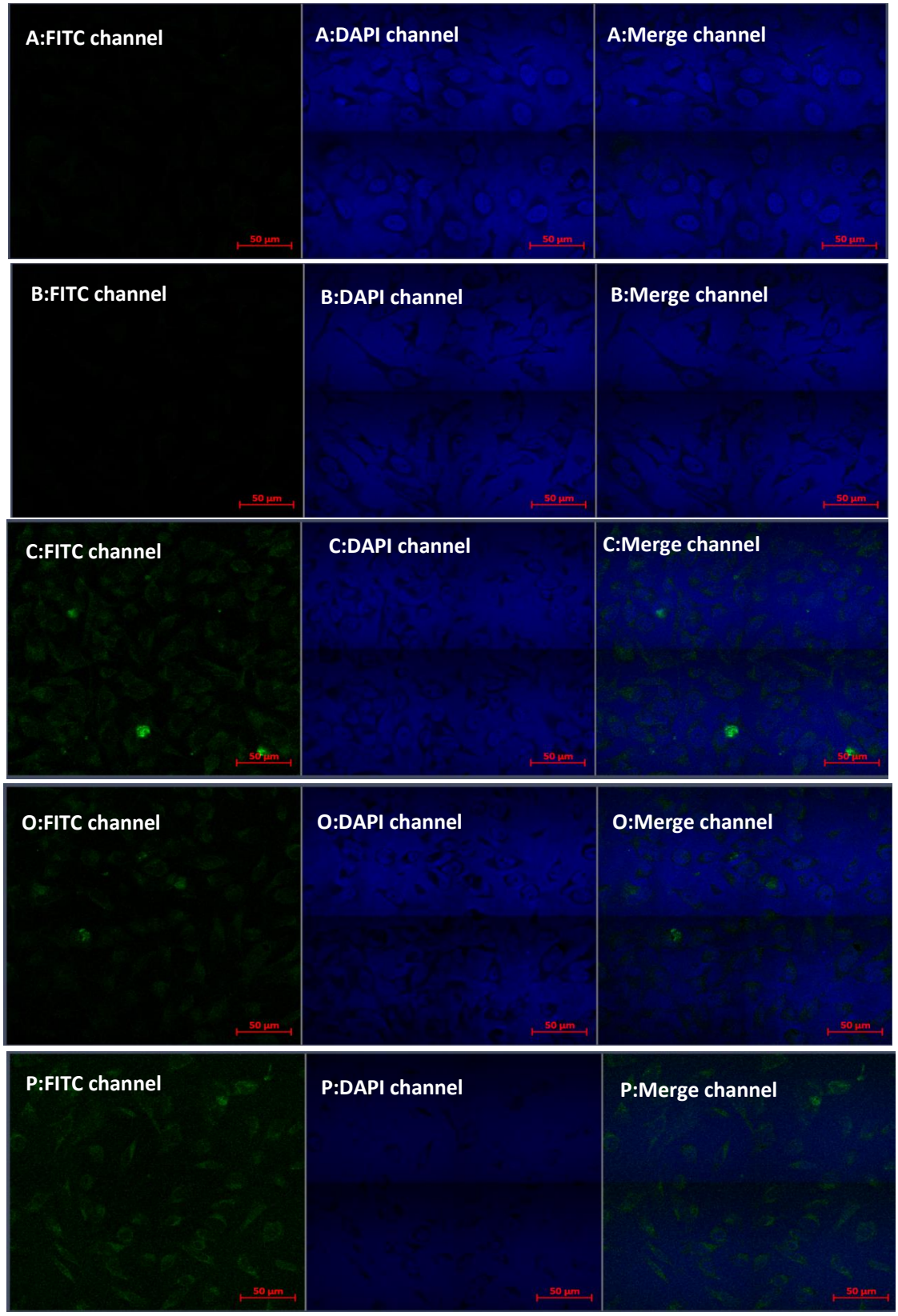

A: Water B:PBS C:FITC O:HBP4060_4$_{FITC}$ P:HBP4060_4$_{FITC_pegf}$

Figure 4- 13: Confocal Microscopy analysis of HP4060_3$_{FITC}$ and HBP4060_3$_{pegfFITC}$ in folate containing media

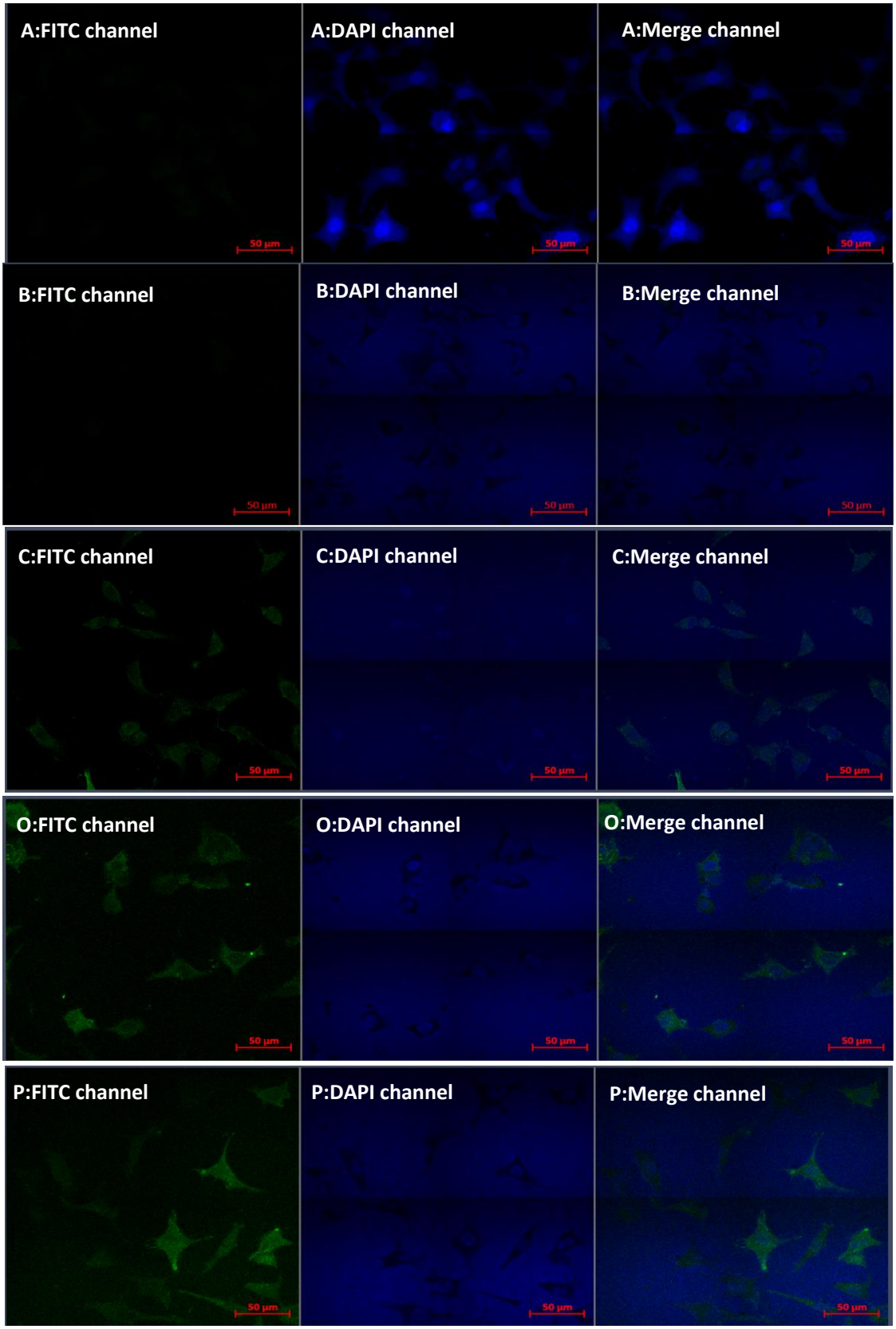

A: Water B:PBS C:FITC O:HBP4060_4_{FITC} P:HBP4060_4_{FITC_pegf}

Figure 4- 14: Confocal Microscopy analysis of HP4060_3_{FITC} and HBP4060_$3_{pegfFITC}$ in folate deficient media

Observations from the confocal data suggest that the polymer is more efficiently taken up into cells when the media is deficient in folate in both naked and folate conjugated forms, as displayed by a higher fluorescence in the samples, suggesting the lack of competition from folic acid for uptake has allowed for greater efficiency in polymeric uptake. In addition, polymer samples HBP4060_3 and HBP4060_4 seem to be up taken better into the cells when folate has been conjugated onto the polymer, supporting the theory that folate mediated endocytosis allows for greater exclusivity in the uptake of dug delivery vehicles, via the folate receptor protein. Additionally, HBP4060_2 in both naked and folated forms was very difficult to visualise due to a lower efficiency of uptake into the cells. This was expected due to the sample displaying the largest diameter of all samples, and confocal has confirmed that the size of the particle has a direct influence on the uptake efficiency.

Furthermore, to gain a better understanding of the uptake efficiency Fluorescence Assisted Cell Sorting (FACS) was performed to see whether there was a notable increase in the polymer population between different variations, cultured within folate containing media. This experiment was conducted with the use of polymers HBP4060_3, HBP4060_3_{pegf} and HBP4060_4 and HBP4060_4_{pegf} and the histograms from the analysis can be seen below (**Figure 4-15**)

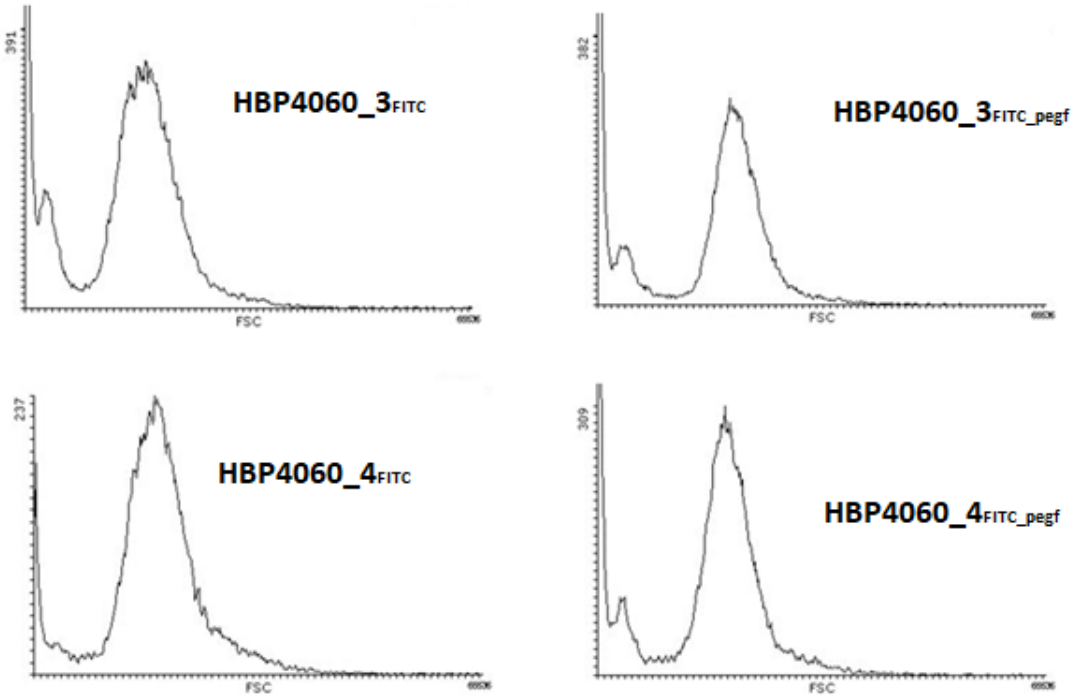

Figure 4- 15: FACS analysis on HeLa cells detecting FITC when treated with either HBP4060_3, HBP4060_3$_{pegf}$

From the FACS analysis it was observed that only HBP4060_4$_{pegf}$ displayed superior uptake when compared to its naked counterpart, with an increase in counts from 237 to 309 whereas HBP4060_3 displayed a similar number of counts to its folate ligated relative (391 to 382). Therefore, this complimentary technique allowed for a better realisation of the uptake, as through confocal microscopy it was difficult to come to a absolute conclusion on whether the folate ligand had facilitated enhanced uptake in either of these two samples, due to the similar fluorescent profiles displayed.

Additionally, DLS was performed on all folate containing polymers tested for uptake within the pH ranges of 7.4, 6.8 and 5.4 to assess size and pH response as a result of folate conjugation, with the expectation that samples that have shown an increased uptake when folate ligated (HBP4060_4) would see a particle diameter of below 200 nm, a key factor in the enhanced uptake via folate mediated endocytosis observed. The results of which are summarised in **Table 4-11** with data transformations presented in **Table 4-12**.

Table 4- 11: DLS data for HBP4060_2pegf, 3pegf & 4pegf

Entry	Sample	pH	Zave Particle Diameter[a] (nm)
1	HBP4060_2_{pegf}	7.4	654
		6.8	661
		5.4	645
2	HBP4060_3_{pegf}	7.4	687
		6.8	345
		5.4	419
3	HBP4060_4_{pegf}	7.4	67
		6.8	66
		5.4	42

a: Harmonic intensity averaged hydrodynamic particle diameter b: measurements showed a neglible error of ± 0.0005 nm and therefore are omitted.

Table 4- 12: DLS data transformations for HBP4060_2pegf, 3pegf & 4pegf

Entry	Sample	pH	Zave Particle Diameter (nm)	Volume Averaged Diameter (nm)	Number Averaged Diameter (nm)
1	HBP4060_2_{pegf}	7.4	654	767	764
		6.8	661	123	69
		5.4	645	123	96
2	HBP4060_3_{pegf}	7.4	687	536 (39.1%) 2448 (60.9%)	500 (98.5 %) 2393 (1.5%)
		6.8	345	31 (45.5%) 143 (54.5%)	31 (98.7%) 138 (1.3%)
		5.4	419	111	86
3	HBP4060_4_{pegf}	7.4	67	8	7
		6.8	66	7	6
		5.4	42	7	6

From the results gathered it is clear to see that the addition of folic acid onto the polymers has caused a increase in the particle diameter in all cases. Additionally, by the Zave only HBP4060_3_{pegf} and HBP4060_$_{4pegf}$ displayed favourable PAA related pH responsiveness, as was seen beforehand in the naked polymers. When the transformations are applied the effects of aggregation are accounted for both HBP4060_2_{pegf} and HBP4060_3_{pegf} display particle sizes too large for endocytosis at the normal accepted physiological pH however when the pH is dropped below this particle shrinkage is seen suggesting that there is promise that these particles could display enhanced uptake within cancer cells due to the Warburg effect with the added advantage of existing within normal physiological pH as too large in diameter to be effectively taken up. Thus, the pH responsive nature of these macromolecules enhance the exclusivity of drug delivery. Interestingly, whilst HBP4060_4_{pegf} displays smart properties at pH 5.4 when observed with the Zave there is no such advantages when transformations are applied suggesting mass aggregation of these particles due to folate ligation.

These results correlate with both confocal microscopy and FACS analysis suggesting that only HBP4060_4_{pegf} would display an enhanced uptake over the naked relative due to the small particle diameter observed.

4.6 Drug (Gemcitabine) loaded HBPs and further toxicity studies

4.6.1 Gemcitabine modification and conjugation

The drug chosen for this study was Gemcitabine. A cytidine analogue gemcitabine's mechanism of action is incorporation within DNA via a replicative DNA polymerase, instead of cytidine and thus the sugar phosphate backbone upon tri-phosphorylation. Once incorporated programmed cell death occurs as a reaction to gemcitabine acting as a chain terminator and thus stalling the DNA replication process as cytidine has been replaced [41–44]. In fact, subtly, the only difference between gemcitabine and its cytidine relative is the replacement of the 2' hydroxyl with a di-fluorine (**Figure 4-16**)

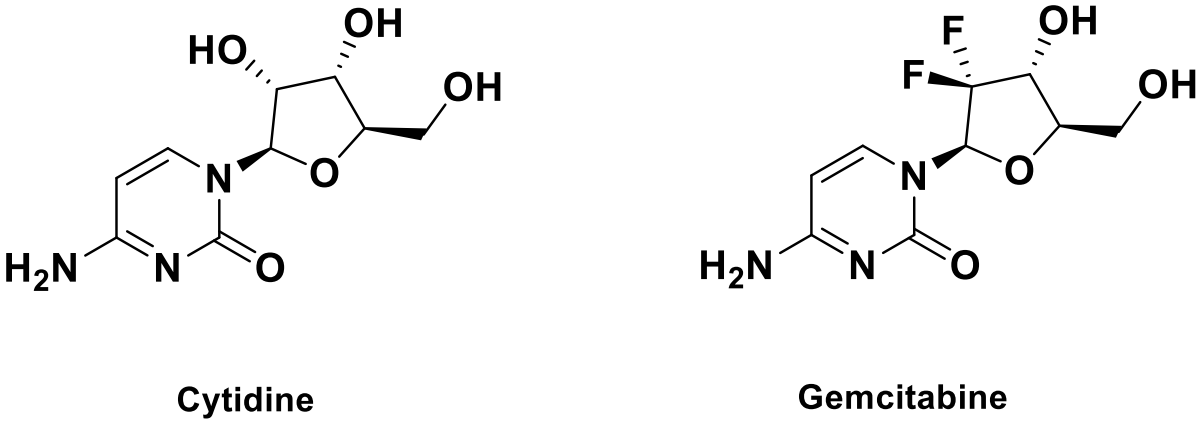

Figure 4- 16: Cytidine and the nucleoside analogue Gemcitabine

For conjugation of the drug to polymer a linker was required. Whilst utilisation of the primary amine group on gemcitabine is possible this was decided against as concerns about steric hinderance and thus payload release were identified, due to the large macromolecular structure of polymeric materials. Therefore, in order to conjugate gemcitabine via the primary amine presented to polymeric materials via

Steglich esterification methods a disulphide linker was produced. Previously, it was discussed that the use of the disulphide bond in the branching agent DSDA opened the hyperbranched polymer up to reduction and bond breakage allowing the large macromolecular structure to be “cut apart” at this bond. Therefore, a s-carboxymethylcysteamine (CTC) linker (**11**) was produced from starting materials thioglycolic acid (**9**) and cysteamine (**10**) via an oxidation with H_2O_2 (**Scheme 4-8**). It is hypothesised that with this linker present there would be a greater chance of drug release and thus bioavailability of the drug within cells, as oppose to direct conjugation onto polymer.

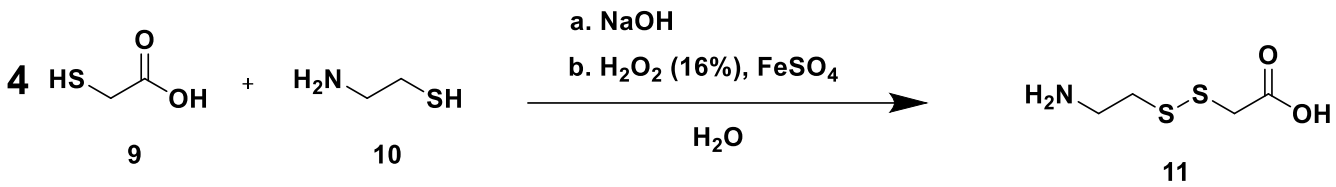

Scheme 4- 7: Synthesis of CTC linker

Firstly, reagents were dissolved in distilled water and neutralisation was performed via the addition of NaOH. Ferrous sulphate was then crudely added as a heaped spatula for use as a redox indicator with hydrogen peroxide subsequently added dropwise with a change of the solution colour from red to yellow indicating reaction completion.

Purification was performed via the use of a Dowex 50 column acidified via HCl with a 50 mmol: acetic acid gradient mobile phase (pH 3 – 5) with increments of an increase of pH by 0.5 every 200 ml. Fractions (ca. 10 ml) were then analysed via TLC (every third fraction) in an ethyl acetate:acetic acid:water (8:2:1) solvent system with a R_f value around 0.2-0.3 the desired compound. Staining was performed via the use of the ninhydrin stain (**Figure 4-17**).

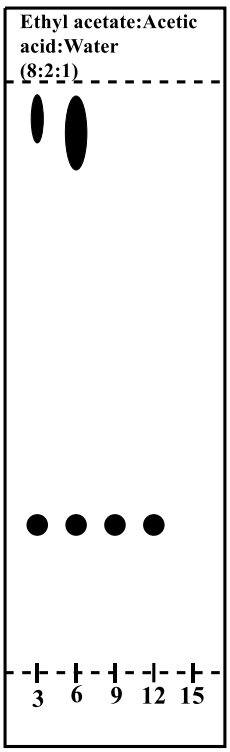

Figure 4- 17: Representative TLC plate for CTC purification

Fractions 9-12 were then taken diluted with water and freeze dried to yield the desired material as a pale-yellow pungent oil. The CTC linker was then BOC protected in aqueous media before conjugation onto gemcitabine to produce a CTC-gemcitabine linker (**Scheme 4-8**).

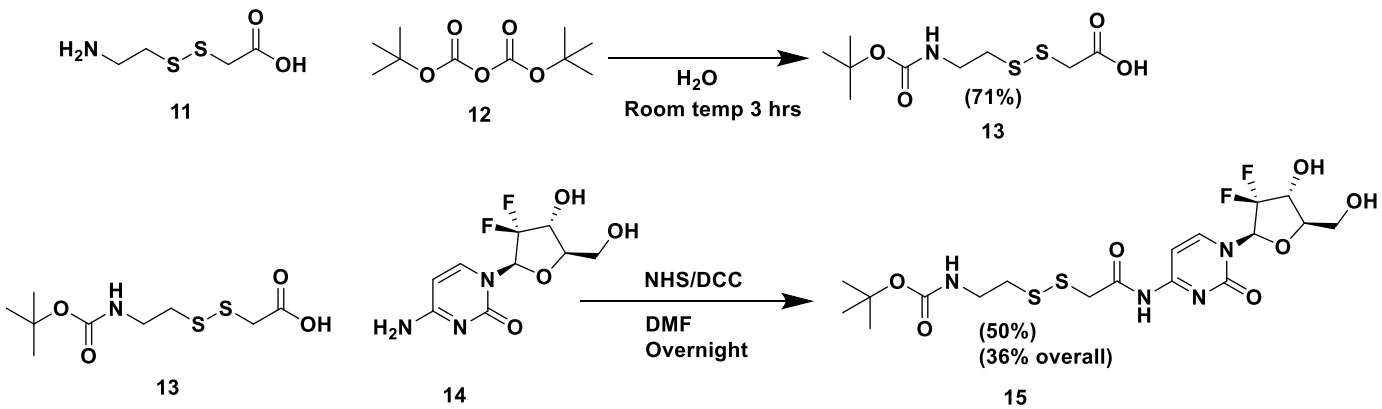

Scheme 4- 8: Synthesis of CTC gemcitabine

BOC de-protection and subsequent steglich esterification onto HBP4060_4_{pegf} then yielded the desired drug conjugate. Purification was performed via dialysis in a DMF:Water (5:95 *v/v %*) solvent system with water changes every 24 hours for a set period of 72 hours. Beforehand it was expected that the quantification of gemcitabine

onto polymers may be cumbersome and hence assuming 100% drug conjugation a concentration of gemcitabine/polymer was expected to be 15 µg gemcitabine / 100 µg polymer. This equates to approximately 570 nmol of gemcitabine per 100 µg of polymer. Throughout the MTT process it was mentioned that 10 µg/ml of polymer would be the upper limit for drug loading. Taking into account this upper limit there would need to be enough gemcitabine within polymeric materials in order to induce the desired therapeutic effect.

Due to the possible difficulties in the quantification of gemcitabine due to folic acid interference upon solvent changes solvent was kept and freeze dried and subjected to UV-Vis analysis in order to assess any leakage of gemcitabine from the dialysis membrane, however no such absorbance was found. Therefore, upon completion of the purification process the liquid retained in the dialysis membrane was freeze dried. Analysis via ^{1}H NMR or UV-Vis for either qualitative or quantitative analysis of gemcitabine was not ideal due to interference with folic acid groups and therefore, the use of FT-IR was chosen as the most suitable method of analysis due to the presence of C-F bonds within gemcitabine. Utilising this method, it was clear to see that there was a presence of gemcitabine within both the CTC-gemcitabine linker and the newly synthesised HBP4060_4$_{pegfctcgemzar}$ (**Figures 4-18 and 4-19**) however quantification of the amount of gemcitabine was not possible on the hardware available.

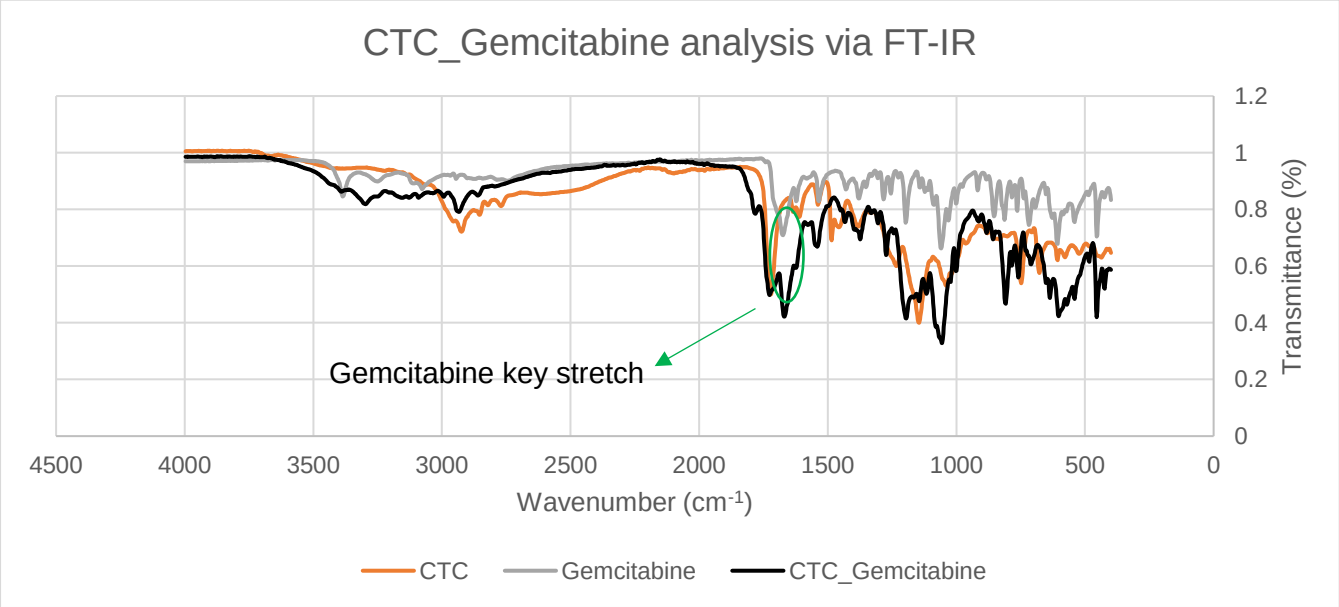

Figure 4- 18: Analysis of synthesised CTC_Gemcitabine linker via FTIR

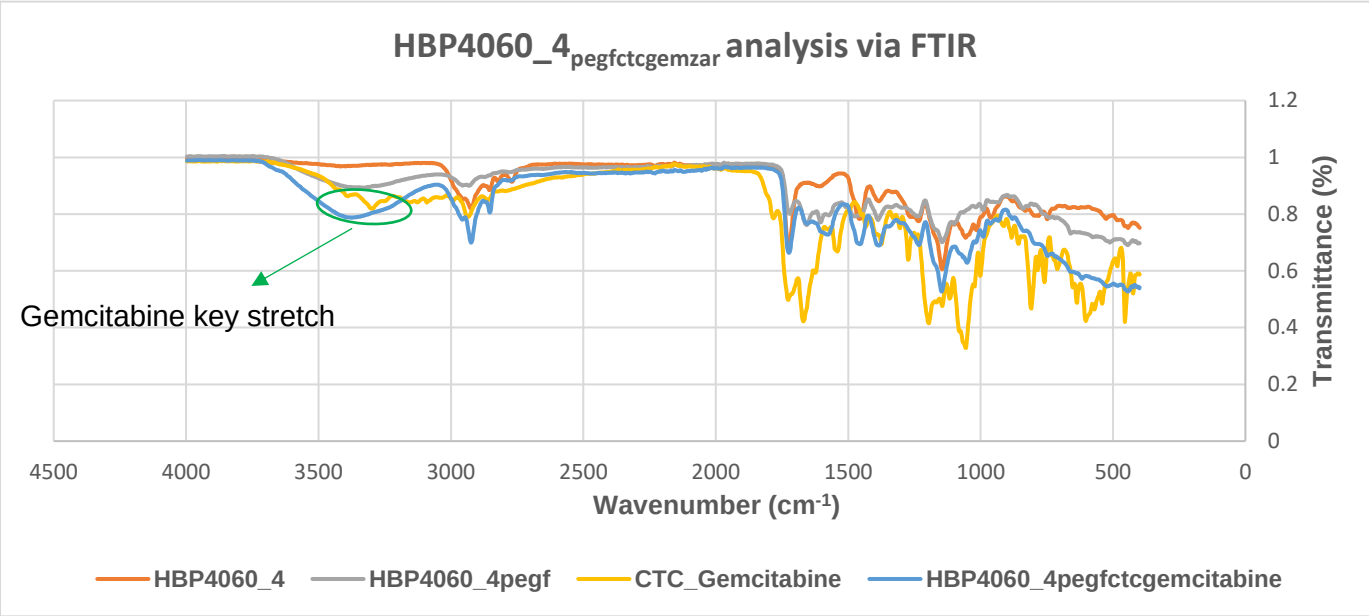

Figure 4- 19: Analysis of synthesised HBP4060_4$_{pegfctcgemzar}$ via FTIR

Whilst the analysis of the CTC linker via FTIR was relatively straightforward elucidating the presence of gemcitabine within the drug loaded polymer post dialysis was more complex. Firstly, the peaks around 1500-2000 cm^{-1} relating to the gemcitabine aromatics was covered by amides within the polymer and folic acid aromaticity. Therefore, looking between 3000 – 4000 cm^{-1} was the best option to avoid any polymeric or folate interference. From here it can be observed the difference in morphology between the broad stretch here for HBP4060_4$_{pegfctcgemzar}$ when compared to HBP4060_4$_{pegf}$. This change in morphology to a much more intense and what appears to be a right-handed shoulder peak suggests the presence of further peaks being hidden within this broad peak, indistinguishable in the current resolution. This leads to the belief that there is indeed the successful conjugation of the linker containing gemcitabine within the polymer itself and thus the sample was taken forward for testing via an MTT assay. In addition, mass spectroscopy cellular uptake experiments were planned to assess the amount of free gemcitabine within cell extracts, whilst gemcitabine has been found to have been present within HBP4060_4$_{pegfctcgemzar}$ the use of this method will hopefully aid in proving that the drug delivery vehicle does indeed contain the drug, by detection of gemcitabine peaks.

Therefore, as no gemcitabine was observed as leakage from the dialysis tubing it was assumed that a concentration of 15 µg gemcitabine / 100 µg polymer was within the final product. This concentration laid the foundation for future MTT assay analysis and mass spec uptake experimental.

4.6.2 Gemcitabine loaded HBP4060_4 cytotoxicity analysis

MTT analysis on HeLa cells was conducted utilising three different sample variants – HBP4060_4pegf, HBP4060_4pegfctcgemzar and free gemcitabine. Concentrations of the samples were set alongside gemcitabine concentrations. For example, if the amount of gemcitabine dosed at cells required 10 µg/ml of drug loaded polymer, this concentration of polymer was used for both drugs loaded, and non-drug loaded polymer variants. The concentrations used for the drug loaded MTT assay are displayed in **Table 4-13.**

Table 4- 13: MTT concentrations for HBP4060_4, HBP4060_4$_{pegf}$, HBP4060_4$_{pegfCTCgemzar}$ and Gemcitabine (Technical repeats)

	Sample name				
Entry	HBP4060	HBP4060$_{pegf}$	HBP4060$_{pegfctcgemzar}$	Gemcitabine	
	Concentration of polymer (µg/ml)			equivalent drug concentration (µg/ml)	Moles of gemcitabine
1	100	100	100	15	18.8 nmol
2	66	66	66	9.9	14.2 nmol
3	49	49	49	7.35	5.7 nmol
4	33	33	33	4.95	3.9 nmol
5	25	25	25	3.75	2.5 nmol

The results obtained suggest that the drug loaded polymer indeed induces a higher cell death, however quite concerningly only at the lowest concentration of treatment. Concerns therefore are drawn with the data above this contradicts previous findings about the toxicity of both polymer naked and folated. Furthermore, the efficiency of the free drug has not been matched, although this is not completely surprising as the HeLa cell line is known to display the nucleoside transporters needed for efficient gemcitabine uptake. (**Figure 4-120 and Table 4-14**).

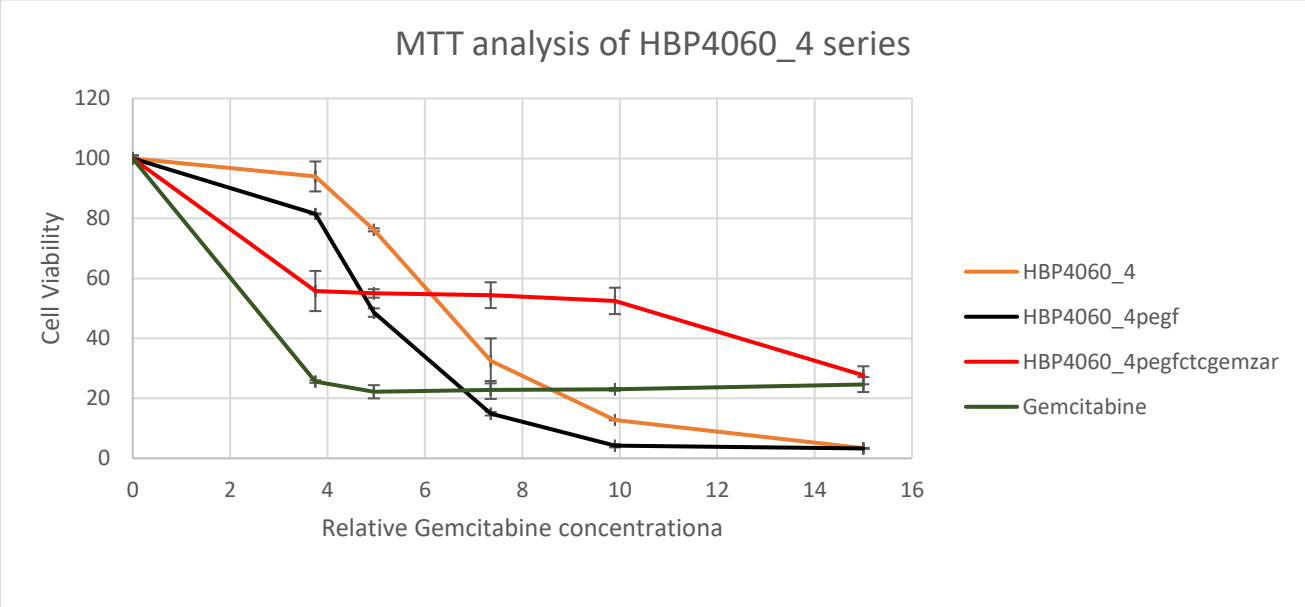

Figure 4- 20: MTT results for HBP4060_4, HBP4060_4$_{pegf}$, HBP4060_4$_{pegfCTCgemzar}$ and Gemcitabine (Technical repeats)

Table 4- 14: MTT results for HBP4060_4, HBP4060_4$_{pegf}$, HBP4060_4$_{pegfCTCgemzar}$ and Gemcitabine

HBP4060_4 (µg/ml)[a]	Cell Viability %	STD dev	HBP4060_4$_{pegf}$ (µg/ml)[a]	Cell Viability %	STD dev	HBP4060_4$_{pegfCTCgemzar}$ (µg/ml)[a^b]	Cell Viability %	STD dev	Gemcitabine (µg/ml)[b]	Cell Viability %	STD dev
100	3.4	0.07	100	3.3	0.07	15	27.7	3	15	24.6	2.5
66	12.8	0.1	66	4.2	0.54	9.9	52.5	4.4	9.9	23	0.47
49	32.5	7.5	49	14.9	0.6	7.35	54.4	4.3	7.35	22.8	3
33	76.2	0.5	33	48.6	1.4	4.95	55	1.4	4.95	22.2	2.2
25	94	5	25	81.5	0.2	3.75	55.8	6.7	3.75	25.6	0.43
0	100	0.99	0	100	0.99	0	100	0.99	0	100	0.99

a: concentration of Drug delivery system a^b: concentration of drug delivery system, where gemcitabine concentration is matched to the free drug b: concentration of the free drug

These results are somewhat promising as they demonstrate the ability of the polymer to firstly be taken up in the cells via confocal imaging techniques whilst also suppression of cell growth has been displayed at low concentrations. Additionally, as previously mentioned there is a direct difference between the toxicity of HBP4060_4 and HBP4060_4_{pegf} in these results compared to the previous MTT studies. Therefore, it is suggested that a more thorough look into the activity of the polymer needs to be explored. Firstly, a colony survival is a must for future studies. Whilst the MTT assay can give an indication of the cytotoxicity of agents there has been throughout this project issues with reproducibility of data and large biological error between batches of HeLa cells used, whilst technical errors have stayed relatively constant (standard deviations are generally seen below 5) This biological error must be reduced by appropriate means. For instance, the use of multiple cell lines for MTT experiments such as the use of MCF7 (breast cancer), HT-29 or T84 which are both colon cancer derived cell lines. Most importantly however, the use of a cell line that does not express nucleoside transporters is paramount. Using these cell lines, a direct comparison can be made between drug loaded polymer and free drug treatments. As a lack of nucleoside transporter would bring a direct barrier to entry for therapeutics, an ideal situation would present drug loaded polymers displaying a significantly greater therapeutic effect compared to their free drug counterparts. Additionally, the MTT assay itself could be complimented alongside a live/dead cell assay (trypan blue or proponium iodide) so that corroboration of results can be obtained. These results suggest that when considering the toxicity of the synthesised polymers there needs to be a lot of future work to be performed.

However, what cannot be concluded at this time is whether the delivery of gemcitabine is due to degradation of the CTC linker within the media and hence free gemcitabine is being delivered to the cells inducing this response. Therefore, mass spectrometry analysis of the cell extracts was performed. This technique allows for the characterisation of compounds within the cell and thus should CTC_gemcitabine linker, or related fragments, be found within the cells it can be argued that the polymer uptake previously observed is directly related to the delivery of drugs without major interference from the linker.

Therefore, this was performed utilising the methanol extraction methodology on cell samples dosed with either CTC_gemcitabine, CTC, gemcitabine, HBP4060_4_{pegf} and HBP4060_$4_{pegfctcgemzar}$, whilst untreated HeLa cells were also extracted.

4.6.3 Cell extract experiments – assessment of Gemcitabine delivery

Mass spec was performed via LC-MS/MS technique in order to quantify the amount of gemcitabine within HeLa cell extracts whilst also trying to detect phosphorylated metabolites of gemcitabine. Gemcitabine is known to be active in both di and tri-phosphorylated forms. Where the di-phosphorylated gemcitabine is known to interact with the deoxycytidine kinase protein restricting the concentration of phosphorylated cytidine products, whilst also inhibiting ribonucleotide reductase, the tri-phosphorylated form replaces cytidine within the DNA of cells inducing programmed cell death. Essentially a multi-pronged attack on the cancerous cells. Therefore, it is of great interest to not only detect whether free gemcitabine is found more regularly within cells but if the detection of phosphorylated products can be obtained in both free gemcitabine samples and samples where drug loaded polymer was dosed at cells, it would demonstrate the ability of the polymeric drug delivery vehicle to deliver drugs at no hinderance to their biological metabolic activity.

Gemcitabine controls were therefore initially run within the mass spectrometer within the ranges of 0.0078 nmol to 10000 nmol and the spectra can be found in the appendix of this thesis, alongside the spectra of untreated HeLa cells (**Appendix 4-S3**). This gave a characteristic gemcitabine peak at a retention time of 1.69 minutes. Therefore, by analysis of both free gemcitabine cell extracted sample and the combi treatment (HBP4060_$4_{pegfctcgemzar}$) an indication of the cell uptake of gemcitabine can be analysed. Whilst the method was run to be quantitative there are numerous factors to be considered when analysing the data so an accurate and reasonable assessment can be made. It must be stressed that the reliability of the quantification is dependent on the same number of cells being seeded and treated and if therefore the same number of cells have been harvested. Furthermore, the extraction efficiency of both treated samples needs to be identical for a reliable quantification.

With these factors considered the quantification performed can still give a good indication of the uptake efficiency and the detection of gemcitabine within the cellular extracts. Furthermore, injections were run in triplicate to determine the error of the machine and to further attempt to increase the accuracy of the results presented. The spectra of both extracts are shown in **Figures 4-21 and 4-22**.

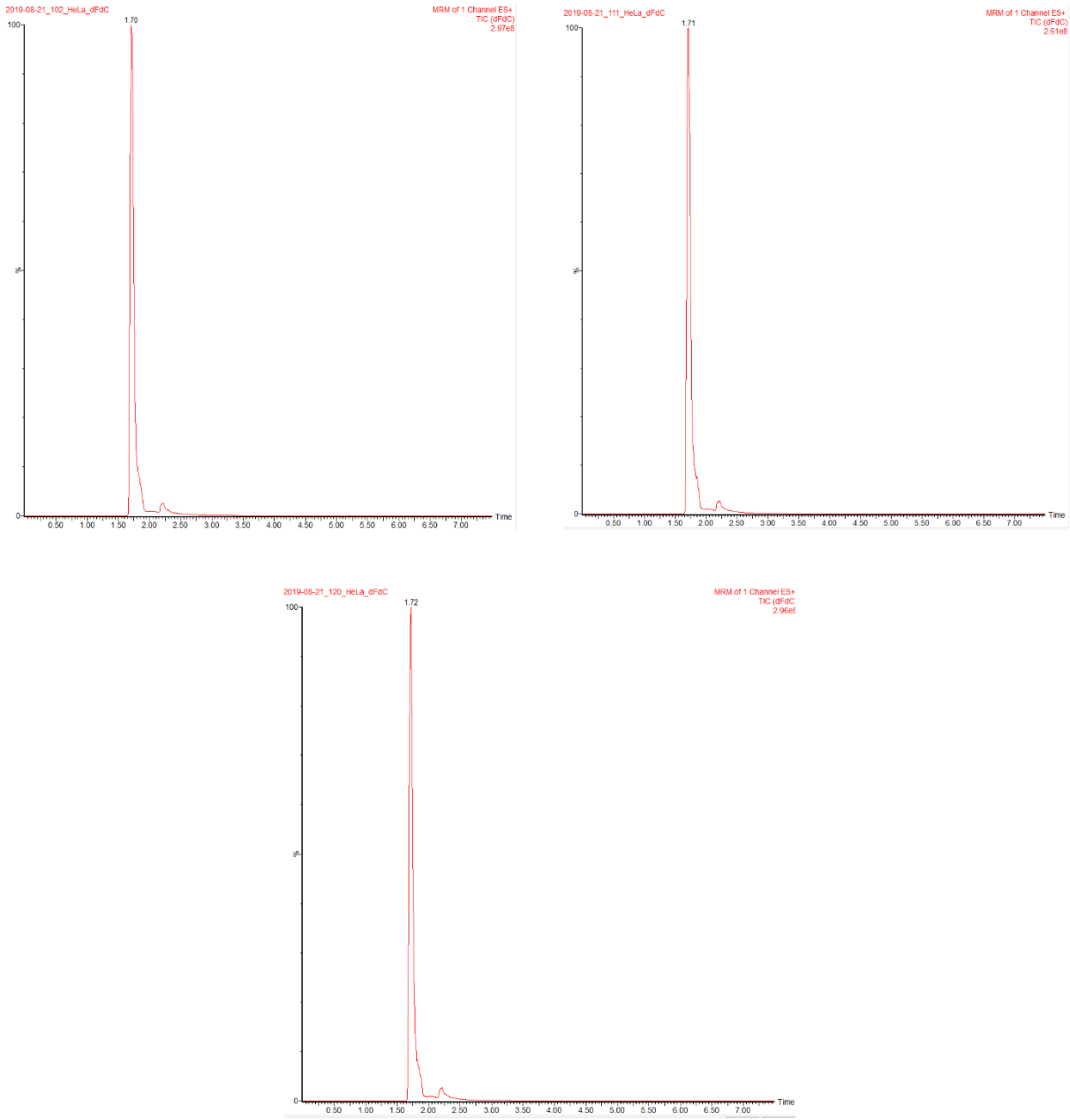

Figure 4- 21: Triplicate mass spectrometry analysis of HeLa dosed with free gemcitabine

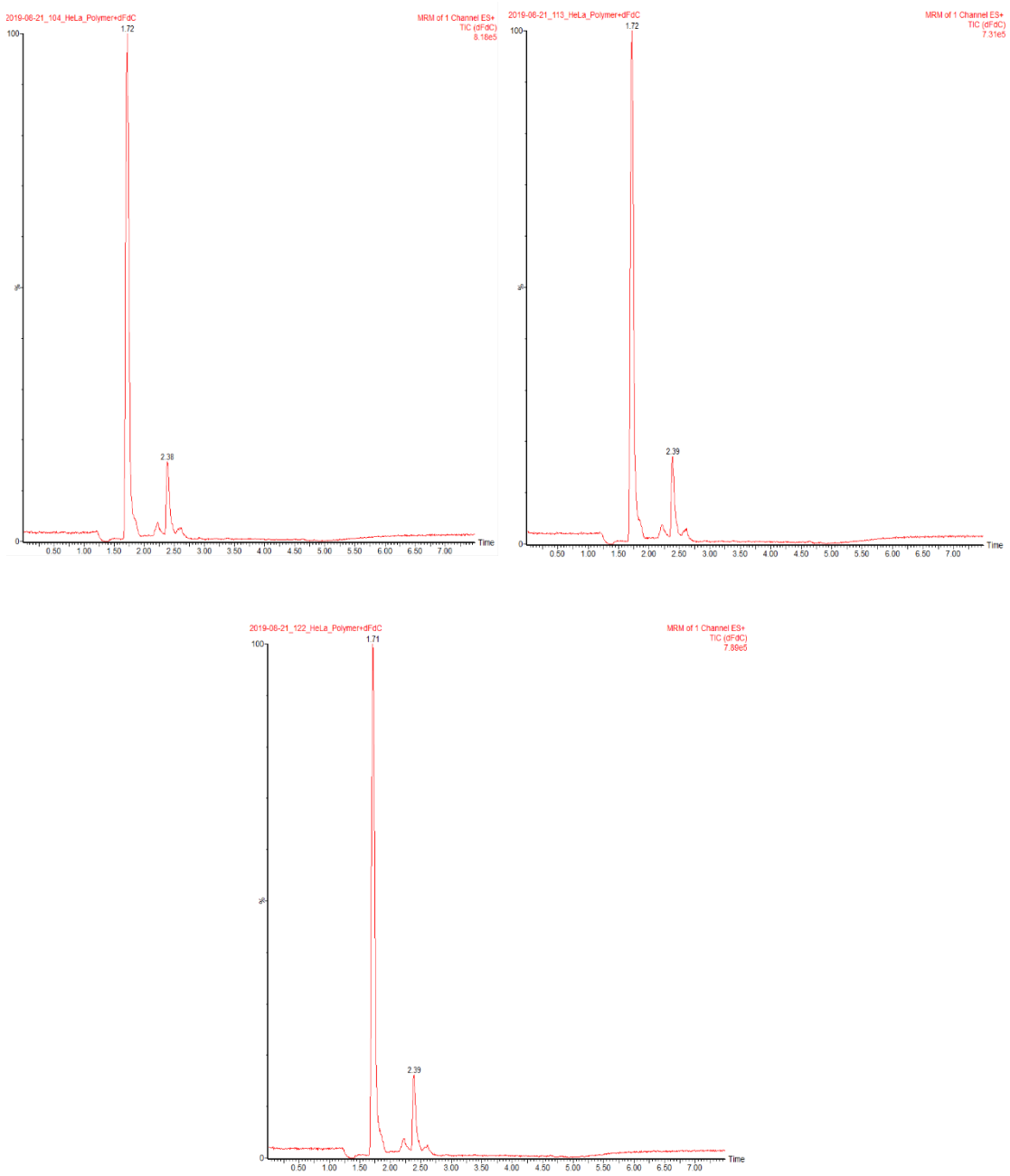

Figure 4- 22: Triplicate mass spectrometry analysis of HeLa dosed with HBP4060_4$_{pegfctcgemzar}$

Firstly, from the spectra alone it is evident that the combi treatment (HBP4060_4$_{pegfctcgemzar}$) was not as efficient as the free gemcitabine alone, with the background peak at 2.38-2.39 much more apparent within the spectra. Comparing peak analysis of the triplicates we also see a huge reduction in gemcitabine detected via the combi treatment, the relative detections of the gemcitabine extracts are shown in **Table 4-15**

Table 4- 15: Gemcitabine detection via LC-MS/MS

Sample Run	**Cell Extraction Detection count**		**% Detection of gemcitabine in the combi treatment compared to the free treatment**
	Free gemcitabine treatment	HBP4060_4$_{pegfctcgemzar}$ (combi)	
1	2.97E+08	8.18E+05	27.54%
2	2.61E+08	7.31E+05	28.01%
3	2.96E+08	7.89E+05	26.66%

From the detected gemcitabine it is evident that there is at least a reduction of 60% in the detection of gemcitabine in the cell extracts of the combi treatment. Whilst the factors considered earlier are still applied there is a clear case to suggest that the increased efficiency in cell death in the free gemcitabine treatments is a direct result of the increased amount of gemcitabine being up taken into these cells. These results suggest that whilst there is uptake into the cells there could be a lack of drug availability due to the increased metabolic complexity needed for the cells to retrieve the free gemcitabine from the polymeric vehicle. Furthermore, these results do not go as far to suggest a method of delivery for the gemcitabine in the combi treatment.

Therefore, to garner further information as to whether the biological activity of the drug is hindered by the drug delivery vehicle, mass spec analysis on the extracts was also performed to assess the presence of phosphorylated metabolites.

Therefore, mono di and tri-phosphate versions of gemcitabine were run as external controls at 10 µmol to assess their retention time and the spectra can be found in the appendix of this thesis, alongside the spectra for the untreated HeLa cell extracts and polymer only treated cell extracts (**Appendix 4-S4**), whilst the results of the controls are summarised in **Table 4-16.**

Table 4- 16: Retention time of gemcitabine metabolite controls

Entry	Control	Retention time (mins)
1	dFdCMP[a]	3.48-3.81
2	dFdCDP[b]	3.27-3.52
3	dFdCTP[c]	2.63-2.75

a: Gemcitabine monophosphate b: gemcitabine diphosphate c: gemcitabine triphosphate

From the results obtained it was found that only cells dosed with free gemcitabine metabolised gemcitabine into any phosphorylated form, whereas the combi treatment displayed only background noise (**Figures 4-23** and **4-24).** This is particularly surprising as free gemcitabine has been detected in the combi treatment. This could be due to timing of the analysis the delivery of gemcitabine to the cells via the use of the polymeric vehicle may take longer than the free drug itself. Thus, when the cell extracts were harvested there was not sufficient time afforded to allow for metabolization.

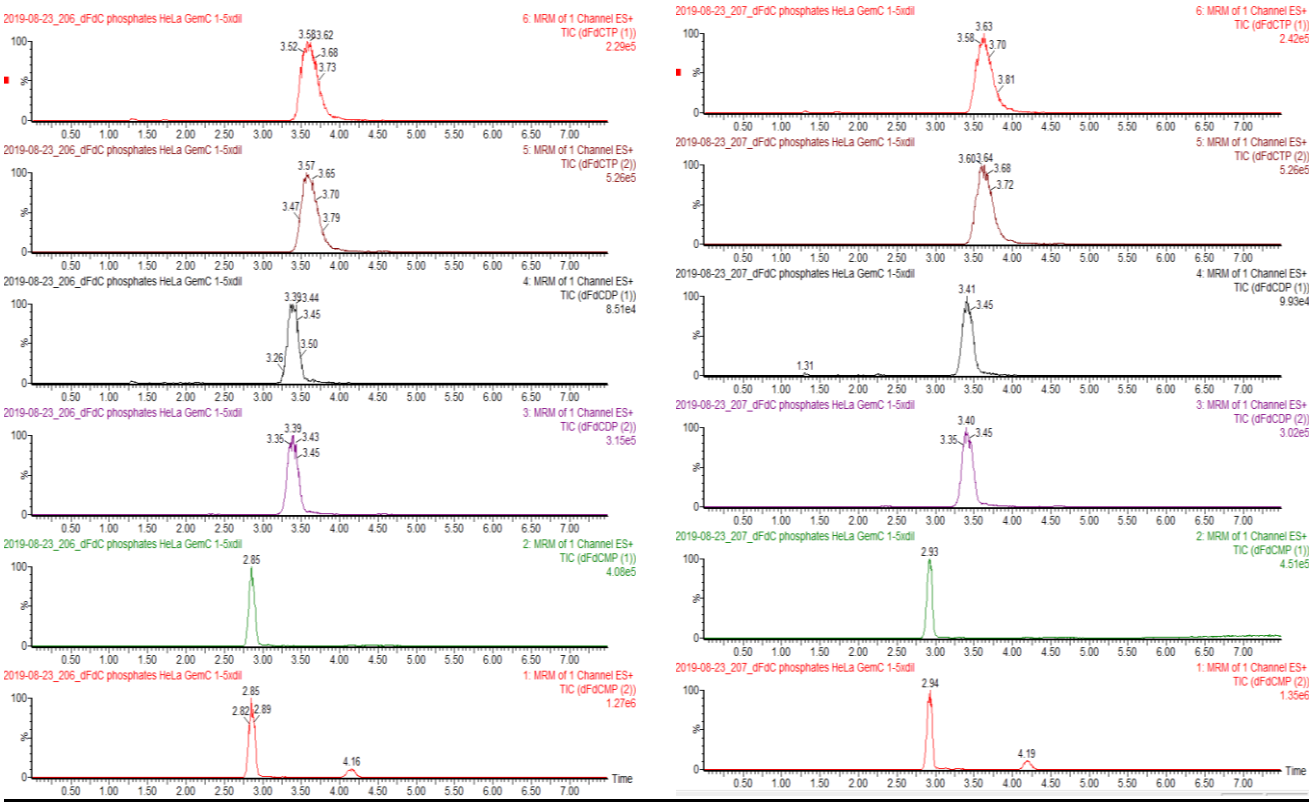

Figure 4- 23: Mass Spectrometry analysis of the presence of gemcitabine metabolites within cell extracts of HeLa cells treated with free gemcitabine

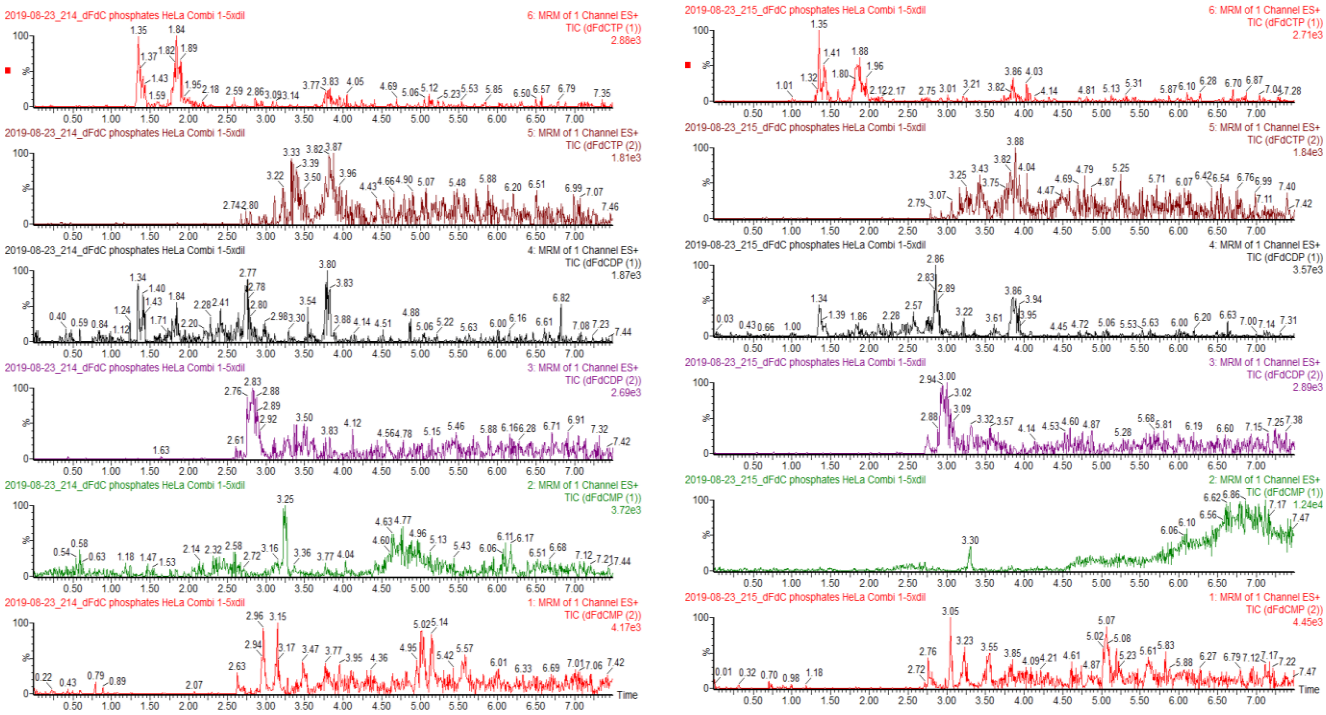

Figure 4- 24: Mass Spectrometry analysis of the presence of gemcitabine metabolites within cell extracts of HeLa cells treated with HBP4060_4$_{pegfctcgemzar}$

From the results of the metabolite analysis it is clear to see that only the cells treated with free gemcitabine were able to metabolise the drug. This leans toward the theory that gemcitabine is not being released within the media from the polymer and introduced into the cell as a free product, although whether methanol extraction could introduce free gemcitabine into the cell was not studied. However, these results do suggest that there is either interference in the biological activity of the gemcitabine from either the polymer itself or the use of a covalent linker. Therefore, the lack of metabolites is concerning for any drug delivery vehicle the need to restrict the metabolic interference of the drug is essential to ensure that the high efficiency of the drug is upheld.

The lack of gemcitabine metabolites was investigated further in order to assess whether there is some hinderance to the activity of the deoxycytidine kinase enzyme. Hypothetically the gemcitabine linker can be broken apart from either the polymer or the drug itself in a variety of ways within the cell. All scenarios of breakage were assessed via full MS on an orbitrap system however no indication of linker was observed, as either a remnant or as a full structure. These results therefore suggest that there could be a breakage of the linker within the media, however this would not account for the lack of gemcitabine metabolites as previously

discussed, as if this was the case there would be no hinderance for gemcitabine to be biologically active. Furthermore, no phosphorylated forms of gemcitabine were observed when either partial or no linker breakage was accounted for, suggesting that the presence of a linker is at the very least preventing phosphorylation. Therefore, it could be possible that the linker should it be cleaved at the disulphide bond as predicted is becoming involved in another biological pathway that has not been studied throughout this project. However, the nature of how free gemcitabine has been observed within the cell extract and why the linker cannot be detected is of concern and thus a plethora of work on these findings is required to come to a rational conclusion.

Additionally, to provide more information as to whether the delivery of the drug could be media induced breakage of the linker, rather than polymeric delivery hindering the system further DLS measurements were made. These were performed for three main reasons: firstly, should the drug delivery system be too large for the delivery of the drug (exceeding 200 nm) then it can be hypothesised that there is breakage of the linker in the media, providing a route for gemcitabine entry, albeit in an altered form with linker residue; secondly, should the particle diameter exceed 200 nm further modifications should be made to the structure to ensure that the particle size can be limited in expansion (such as encapsulation of the drug) and finally, to assess whether the pH responsive nature of the polymer has been negatively impacted by the covalent bonding of gemcitabine via the PAA/RAFT agent carboxyl moieties. These results can be seen in **Table 4-17.**

Table 4- 17: DLS data for HBP4060_4$_{pegfCTCgemzar}$

Entry	Sample	pH	Zave Particle Diameter[a] (nm)
1	HBP4060_4$_{pegfCTCgemzar}$	7.4	61
		6.8	91.8
		5.4	73

a: Harmonic intensity averaged hydrodynamic particle diameter b: measurements showed a neglible error of ± 0.0005 nm and therefore are omitted.

Interestingly, we see that there is a increase in size when pH is decreased to 6.8 before a shrinkage characteristic of PAA based polymers when the pH is dropped again to 5.4, despite still being larger in size than when the polymer was dissolved in pH 7.4 media. This suggests possible aggregation and indeed multiple populations are seen within the spectra. In order to assess further the smart properties when drug loaded data transformations were again performed (**Table 4-18**).

Table 4- 18: DLS data transformations for HBP4060_4$_{pegfCTCgemzar}$

Entry	Sample	pH	Zave Particle Diameter (nm)	Volume Averaged Diameter (nm)	Number Averaged Diameter (nm)
1	HBP4060_4$_{pegfCTCgemzar}$	7.4	61	9	8
		6.8	91.8	13 (98.1 %) 109 (1.8%)	12
		5.4	73	8	7

Indeed, again the same scenario was played out with an initial increase when pH is dropped and then a shrinkage when further acidification of the media was performed, this suggests that there is not just aggregation at play, but a change in the smart characteristics of the polymer, with an increase in size that could be also attributed to the covalent linkage of drug and linker. Pleasingly however, at no point was the polymer observed above the 200 nm threshold for endocytosis suggesting that free gemcitabine found within the cells could be from polymeric delivery.

However, it does not discount the possibility for media breakdown of the structure releasing free gemcitabine into the media and thus cellular transporters bringing gemcitabine intracellular. Furthermore, the ionisation process of the mass spectrometry could also cause linker cleavage from gemcitabine resulting in a false positive of free gemcitabine delivery.

Although, the theory of media breakdown seems unlikely due to the lack of gemcitabine metabolites when the drug delivery carrier is treated towards cells and it

is more likely if breakdown was to occur within the media that there would be alterations to the gemcitabine structure as a result of linker remnants. Leading to the idea that ionisation could have provided a false positive.

Thus, it is suggested that a cell line where transporters such as: MRP5 and ENT1 required for gemcitabine transportation within the cell are knocked down should be subject to this treatment so that any free gemcitabine found within the cell would be a net result of endocytosis of the polymeric vehicle and subsequent drug release intracellular. Thus, exposing the gemcitabine loaded polymer to methanol extraction and subsequent analysis, whether this method releases free gemcitabine from the polymeric carrier could be characterised.

Reflecting on these results and the MTT results therefore there is a case that the polymer can deliver the drug in the free form at the very least into the cells which causes either growth arrest or an increase in cell death when compared to the polymer alone, when the carrier is used at a concentration of 33 µg/ml. However, this is not conclusive as potential drug-linker breakdown with the mass spec ionisation could have led to false positives. Whilst further evidence of a lack of metabolization suggests that much more work is needed to ascertain why this is the case. The focus therefore of the work moving forward must be to assess the mechanism of action of the drug delivery vehicle and therefore the effect on the biological activity of the drug itself, whilst robust toxicity studies need to be performed to understand the biological variance when the toxicity of the polymer is the point of interest.

However, there is some promise for this structure to be enhanced and improved, whilst other drug loading strategies such as ionic interactions and encapsulation need to be assessed in order to deduce the effect of a covalent linker on the drug delivery process and the associated biological metabolism of such drugs.

4.7 Concluding Remarks

The RAFT polymerisation of hyperbranched polymers displayed good controllability with HBP4060 and its sisters chosen for further work and investigation.

To this end it was decided that exploitation of the carboxylic acid present on both RAFT agent end groups and present on HBP4060 repeating units via the well-known steglich esterification technique would be the most efficient route to folic acid addition. Initially HBP4060 was used as a trial molecule for functionalization due to having a superior amount of product mass and due to its much larger particle size it was deemed not as “precious” as HBP4060_2,3 or 4 and therefore experiments can be performed in order to optimize conjugation procedures without risk of needing to produce a second batch of polymer. Two initial experiments were conducted on HBP4060, a random conjugation technique and a controlled conjugation technique. Within the random methodology polymer was dissolved in DMF alongside NHS and DCC, whilst in a separate flask folic acid was dissolved in DMF alongside NHS and DCC for 1 hr. Afterwards, the two mixtures were added together and ethylene diamine added and mixed overnight to form conjugated particles, with a overall folic acid to polymer COOH ratio of 1:2. Initially, upon completion of the reaction it was clear to see precipitated particles reminiscent of the dried of polymer within the now heterogeneous mixture. This suggested cross linking of the polymer molecules and therefore filtration was performed before dialysis within a 2KDa cut-off tube before freeze drying to obtain the final product, in low yield and low folate concentration as characterized by UV-VIS spectroscopy. Therefore, the controlled approach to conjugation required the synthesis of a PEG_8-diamine linker and subsequent mono-boc protection before folate addition via the steglich esterification. Subsequently, the boc protecting group was removed and addition to polymer was performed. This lead to a polymer with a much higher folate concentration post dialysis and a lack of solid precipitate at the end of the reaction. This methodology was then continued with HBP4060_2,3,4 although a smaller PEG_4-diamine linker was used and there was a vastly reduced amount of folate linker used in the synthesis of these folate conjugated polymers as detailed in chapter 4. Thus, DLS was performed on all five polymer variants displaying an increase in particle size and the retention of stimuli responsive nature.

Conjugation of fluorescent markers was performed via rhodamine and FITC, with rhodamine used for HBP4060 polymers linked with or without folate, and this was performed in a controlled manner, through synthesis of rhodamine ethylene diamine in an attempt to conjugate the same amount of rhodamine onto each

polymer for confocal microscopy. However, this did not occur and thus once again modifications were used for the conjugation of marker to HBP4060_2,3 and 4. FITC was chosen for this purpose after trial runs with rhodamine linked polymers displayed technical issues with some equipment causing delays in the project. FITC was conjugated onto each polymer in their naked form. Therefore, further conjugation of folic acid would result in differing amounts of folic acid between polymer batch to polymer batch however most importantly FITC concentrations between the folate labelled and folate defiant polymers of the same batch would remain equal.

Finally, the conjugation of the model drug gemcitabine was performed via the use of a synthesised CTC linker, using the steglich methodology, however issues occurred in the characterization of the amount of drug within the polymer and thus assumptions were performed. Due to the nature of folic acid there was no plausible way of characterising the amount of gemcitabine upon the polymer once purification was performed. Instead, the dialysis water was checked at regular intervals for gemcitabine concentrations to be taken away from the overall feed, however this was not observed. Thus, FTIR analysis was performed to identify gemcitabine within the drug loaded polymer and confirmation of this fact was found within the spectra. In summation, the key points taken away from these sections of work was the following A. controlled conjugation methods via the use of mono-boc protection on a diamine linker provided a greater control and yield over random methodologies with a greater amount of ligand conjugated on the polymer. B. conjugation of folic acid vastly increases the radius of the synthesised polymers however stimuli responsive properties remain. C. for fluorescent marker conjugation in order to obtain the same amount of marker on folate rich and folate deficient versions of the same polymer fluorescent marker conjugation needs to be performed first before folate addition. D. a more thorough characterization of gemcitabine contained within polymers needs to be researched, taking into account folic acid interference, therefore it may be possible to use radioactive gemcitabine to monitor reaction progress or utilise the fluorine atoms present.

A key parameter for the project in the development of a potential drug delivery vehicle is testing that the device itself is not toxic towards human cells, thus adding to the problem of therapeutic toxicity towards cells. Therefore, the well established

immortalised cancer cell line HeLa was used for the purpose of bio-analysis of the polymer properties. Two main assays were performed the MTT assay for cytotoxicity and cellular uptake performed by confocal microscopy. Drug uptake assays were then performed on gemcitabine loaded polymers, with the aid of mass spectroscopy techniques. To summise, all HBP4060 variants tested (folate rich/ folate deficient) and HBP4060_2,3 and 4 variants displayed toxicity values deemed unacceptable at concentrations tested. Therefore, it is of paramount importance that the reasons behind this are explored and rectified. Furthermore, throughout all MTT assays high biological variance was observed, suggesting that these results should be taken with some scepticism. Gemcitabine loaded cells produced interesting MTT results, with gemcitabine producing a steady rate of cell death irrespective of the concentrations used whereas great fluctuations were observed in the polymer gemcitabine treatment whilst naked polymer alone caused cytotoxicity contradictory to previous studies. In terms of cell uptake, confocal microscopy confirmed the use of folate receptor enhances cellular uptake of the polymer, albeit size dependent, with only HBP4060_4_{pegf} displaying these characteristics and only when cells were cultured in folate deficient media, suggesting competition within the media itself is too strong, this was confirmed by FACS analysis, however this data is classed as crude and therefore much further work is needed in order to get better quantification of the actual increase of polymer uptake in to the cells. Drug uptake was monitored via methanol extracts and mass spectroscopy. It was observed that polymer conjugated gemcitabine was taken up by cells in a lower concentration however, it was not able to be metabolised by cells suggesting a plethora of further work is needed within this part of the project, to strengthen the bioanalysis as a whole. Therefore, the conclusions to be taken from this section of work is the following A. polymer toxicity needs to be addressed and show consistent results B. cellular uptake is size dependent and HBP4060_4_{pegf} can be used as a “gold standard” for future works into this structure and the size of which it can be considered too large. C. Cell uptake studies require further work, whilst the images produced and the observations can be taken a much more robust method of quantification is needed, such as fluorescence analysis of cell extracts. D. Gemcitabine is taken into the cell either in the free or polymeric form but the method of which gemcitabine is recovered from the polymer is not well understood, furthermore, there is a lack of metabolization of gemcitabine internalised via the polymer and thus more thorough research is

needed, such as DNA analysis to assess whether gemcitabine itself is producing the cell cytotoxicity.

References

[1] H. Chen, X. Xu, L. Liu, G. Tang, Y. Zhao, Phosphorus Oxychloride as an Efficient Coupling Reagent for the Synthesis of Ester, Amide and Peptide under Mild Conditions, RSC Adv. 3 (2013) 16247–16250. https://doi.org/10.1039/b000000x.

[2] B. Neises, W. Steglich, Simple Method for the Esterification of Carboxylic Acids, Angew. Chemie Int. Ed. English. 17 (1978) 522–524. https://doi.org/10.1002/anie.197805221.

[3] A.B. Lutjen, M.A. Quirk, A.M. Barbera, E.M. Kolonko, Synthesis of (E)-cinnamyl ester derivatives via a greener Steglich esterification, Bioorganic Med. Chem. 26 (2018) 5291–5298. https://doi.org/10.1016/j.bmc.2018.04.007.

[4] R.O. McCourt, E.M. Scanlan, A Sequential Acyl Thiol-Ene and Thiolactonization Approach for the Synthesis of δ-Thiolactones, Org. Lett. 21 (2019) 3460–3464. https://doi.org/10.1021/acs.orglett.9b01271.

[5] C.E. Butterworth, T. Tamura, Folic acid safety and toxicity: A brief review, Am. J. Clin. Nutr. 50 (1989) 353–358. https://doi.org/10.1093/ajcn/50.2.353.

[6] R.. Hillmans, Vitimin B12, folic acid and the treatment of megaloblastic anemias., in: A. Gilman, L. Goodman, T. Rall, F. Murad (Eds.), Goodman Gillman's Pharmalogical Basis Ther., 7th ed., Macmillan, New York, 1985: pp. 1323–1327.

[7] R. Suarez, T. Spies, R. Suarez Jr, THE USE OF FOLIC ACID IN SPRUE, Ann. Intern. Med. 26 (1947) 643–677.

[8] A.R. Hilgenbrink, P.S. Low, Folate receptor-mediated drug targeting: From therapeutics to diagnostics, J. Pharm. Sci. 94 (2005) 2135–2146. https://doi.org/10.1002/jps.20457.

[9] R.J. Lee, P.S. Low, Folate-mediated tumor cell targeting of liposome-entrapped doxorubicin in vitro, BBA - Biochim. Biophsica Acta. 1233 (1995) 134–144. https://doi.org/10.1016/0005-2736(94)00235-H.

[10] B. a Kamen, a Capdevila, Receptor-mediated folate accumulation is regulated by the cellular folate content., Proc. Natl. Acad. Sci. U. S. A. 83 (1986) 5983–7.

https://doi.org/10.1073/pnas.83.16.5983.

[11] G. Pasut, F. Canal, L. Dalla Via, S. Arpicco, F.M. Veronese, O. Schiavon, Antitumoral activity of PEG-gemcitabine prodrugs targeted by folic acid, J. Control. Release. 127 (2008) 239–248. https://doi.org/10.1016/j.jconrel.2008.02.002.

[12] K.R. Kalli, A.L. Oberg, G.L. Keeney, T.J.H. Christianson, P.S. Low, K.L. Knutson, L.C. Hartmann, Folate receptor alpha as a tumor target in epithelial ovarian cancer, Gynecol. Oncol. 108 (2008) 619–626. https://doi.org/10.1016/j.ygyno.2007.11.020.

[13] N. Parker, M.J. Turk, E. Westrick, J.D. Lewis, P.S. Low, C.P. Leamon, Folate receptor expression in carcinomas and normal tissues determined by a quantitative radioligand binding assay, Anal. Biochem. 338 (2005) 284–293. https://doi.org/10.1016/j.ab.2004.12.026.

[14] Y. Lu, E. Sega, C.P. Leamon, P.S. Low, Folate receptor-targeted immunotherapy of cancer: Mechanism and therapeutic potential, Adv. Drug Deliv. Rev. 56 (2004) 1161–1176. https://doi.org/10.1016/j.addr.2004.01.009.

[15] G.L. Zwicke, G.A. Mansoori, C.J. Jeffery, Targeting of Cancer Nanotherapeutics, Nano Rev. 1 (2012) 1–11.

[16] G.M. Van Dam, G. Themelis, L.M.A. Crane, N.J. Harlaar, R.G. Pleijhuis, W. Kelder, A. Sarantopoulos, J.S. De Jong, H.J.G. Arts, A.G.J. Van Der Zee, J. Bart, P.S. Low, V. Ntziachristos, Intraoperative tumor-specific fluorescence imaging in ovarian cancer by folate receptor-α targeting: First in-human results, Nat. Med. 17 (2011) 1315–1319. https://doi.org/10.1038/nm.2472.

[17] Z.G. Le, Z.C. Chen, Y. Hu, Q.G. Zheng, Organic Reactions in Ionic liquids: N-Alkylation of Phthalimide and Several Nitrogen Heterocycles, Synthesis (Stuttg). (2004) 208–212. https://doi.org/10.1055/s-2003-44383.

[18] X.P. Qiu, F.M. Winnik, Facile and efficient one-pot transformation of RAFT polymer end groups via a mild aminolysis/michael addition sequence, Macromol. Rapid Commun. 27 (2006) 1648–1653. https://doi.org/10.1002/marc.200600436.

[19] D. Muller, I. Zeltser, G. Bitan, C. Gilon, Building Units for N-Backbone Cyclic Peptides. 3. Synthesis of Protected N^{α}-(ω-Aminoalkyl)amino Acids and N^{α}-(ω-Carboxyalkyl)amino Acids, J. Org. Chem. 62 (1997) 411–416.

https://doi.org/10.1021/jo961580e.

[20] Z. Wu, X. Li, C. Hou, Y. Qian, Solubility of folic acid in water at pH values between 0 and 7 at temperatures (298.15, 303.15, and 313.15) K, J. Chem. Eng. Data. 55 (2010) 3958–3961. https://doi.org/10.1021/je1000268.

[21] J.E. Young, M.T. Matyska, J.J. Pesek, Liquid chromatography/mass spectrometry compatible approaches for the quantitation of folic acid in fortified juices and cereals using aqueous normal phase conditions, J. Chromatogr. A. 1218 (2011) 2121–2126. https://doi.org/10.1016/j.chroma.2010.09.025.

[22] R. Matias, P.R.S. Ribeiro, M.C. Sarraguça, J.A. Lopes, A UV spectrophotometric method for the determination of folic acid in pharmaceutical tablets and dissolution tests, Anal. Methods. 6 (2014) 3065–3071. https://doi.org/10.1039/c3ay41874j.

[23] P. Chen, W.R. Wolf, LC/UV/MS-MRM for the simultaneous determination of water-soluble vitamins in multi-vitamin dietary supplements, Anal. Bioanal. Chem. 387 (2007) 2441–2448. https://doi.org/10.1007/s00216-006-0615-y.

[24] M.K. Off, A.E. Steindal, A.C. Porojnicu, A. Juzeniene, A. Vorobey, A. Johnsson, J. Moan, Ultraviolet photodegradation of folic acid, J. Photochem. Photobiol. B Biol. 80 (2005) 47–55. https://doi.org/10.1016/j.jphotobiol.2005.03.001.

[25] K. Skrabania, A. Miasnikova, A.M. Bivigou-Koumba, D. Zehm, A. Laschewsky, Examining the UV-vis absorption of RAFT chain transfer agents and their use for polymer analysis, Polym. Chem. 2 (2011) 2074. https://doi.org/10.1039/c1py00173f.

[26] C. Flego, C. Perego, Acetone condensation as a model reaction for the catalytic behavior of acidic molecular sieves: A UV-Vis study, Appl. Catal. A Gen. 192 (2000) 317–329. https://doi.org/10.1016/S0926-860X(99)00410-X.

[27] G. Ciapetti, E. Cenni, L. Pratelli, A. Pizzoferrato, In vitro evaluation of cell/biomaterial interaction by MTT assay, Biomaterials. 14 (1993) 359–364. https://doi.org/10.1016/0142-9612(93)90055-7.

[28] J. V. Merloo, G.J.. Kaspers, J. Cloos, Cell Sensitive Assays: The MTT assay, in: I.A. Creed (Ed.), Cancer Cell Cult. Methods Mol. Biol. (Methods Protoc., 2nd ed., Humana Press, 2011. https://doi.org/10.1007/978-1-61779-080-5.

[29] W. Scherer, J. Syverton, G. Gey, Studies on the propogation in vitro of

Poliomyelitis viruses: IV. Viral multiplication in a stable strain of human malignant epithelial cells (strain HeLa) derived from a Epidermoid Carcinoma of the Cervix, J. Exp. Med. 97 (1951) 695–710.

[30] Z. Wang, B. Xu, L. Zhang, J. Zhang, T. Ma, J. Zhang, X. Fu, W. Tian, Folic acid-functionalized mesoporous silica nanospheres hybridized with AIE luminogens for targeted cancer cell imaging, Nanoscale. 5 (2013) 2065–2072.

[31] C.P. Leamon, P.S. Low, Membrane folate-binding proteins are responsible for folate-protein conjugate endocytosis into cultured cells, Biochem. J. 291 (2015) 855–860. https://doi.org/10.1042/bj2910855.

[32] H.N. Li, F.F. Nie, W. Liu, Q.S. Dai, N. Lu, Q. Qi, Z.Y. Li, Q.D. You, Q.L. Guo, Apoptosis induction of oroxylin A in human cervical cancer HeLa cell line in vitro and in vivo, Toxicology. 257 (2009) 80–85. https://doi.org/10.1016/j.tox.2008.12.011.

[33] J.J.M. Landry, P.T. Pyl, T. Rausch, T. Zichner, M.M. Tekkedil, A.M. Stütz, A. Jauch, R.S. Aiyar, G. Pau, N. Delhomme, J. Gagneur, J.O. Korbel, W. Huber, L.M. Steinmetz, The genomic and transcriptomic landscape of a hela cell line, G3 Genes, Genomes, Genet. 3 (2013) 1213–1224. https://doi.org/10.1534/g3.113.005777.

[34] H.Z. Hu, Y.B. Yang, X.D. Xu, H.W. Shen, Y.M. Shu, Z. Ren, X.M. Li, H.M. Shen, H.T. Zeng, Oridonin induces apoptosis via PI3K/Akt pathway in cervical carcinoma HeLa cell line, Acta Pharmacol. Sin. 28 (2007) 1819–1826. https://doi.org/10.1111/j.1745-7254.2007.00667.x.

[35] D. Berrington, N. Lall, Anticancer activity of certain herbs and spices on the cervical epithelial carcinoma (HeLa) cell line, Evidence-Based Complement. Altern. Med. 2012 (2012). https://doi.org/10.1155/2012/564927.

[36] R. Rahbari, T. Sheahan, V. Modes, P. Collier, C. Macfarlane, R.M. Badge, A novel L1 retrotransposon marker for HeLa cell line identification, Biotechniques. 46 (2009) 277–284. https://doi.org/10.2144/000113089.

[37] Y. Song, W. Shi, W. Chen, X. Li, H. Ma, Fluorescent carbon nanodots conjugated with folic acid for distinguishing folate-receptor-positive cancer cells from normal cells, J. Mater. Chem. 22 (2012) 12568–12573. https://doi.org/10.1039/c2jm31582c.

[38] J.M. Saul, A. Annapragada, J. V. Natarajan, R. V. Bellamkonda, Controlled

targeting of liposomal doxorubicin via the folate receptor in vitro, J. Control. Release. 92 (2003) 49–67. https://doi.org/10.1016/S0168-3659(03)00295-5.

[39] L. Zapor, J. Skowroń, M. Gołofit-Szymczak, The cytotoxicity of some organic solvents on isolated hepatocytes in monolayer culture, Int. J. Occup. Saf. Ergon. 8 (2002) 121–129.

[40] J. Rejman, V. Oberle, I.S. Zuhorn, D. Hoekstra, Size-dependent internalization of particles via the pathways of clathrin- and caveolae-mediated endocytosis, Biochem. J. 377 (2004) 159–169. https://doi.org/10.1042/BJ20031253.

[41] W. Plunkett, P. Huang, Y.Z. Xu, V. Heinemann, R. Grunewald, V. Gandhi, Gemcitabine: metabolism, mechanisms of action, and self-potentiation, Semin. Oncol. 22 (1995) 3—10. http://europepmc.org/abstract/MED/7481842.

[42] J. Ciccolini, C. Serdjebi, G.J. Peters, E. Giovannetti, Pharmacokinetics and pharmacogenetics of Gemcitabine as a mainstay in adult and pediatric oncology: an EORTC-PAMM perspective, Cancer Chemother. Pharmacol. 78 (2016) 1–12. https://doi.org/10.1007/s00280-016-3003-0.

[43] W. Plunkett, P. Huang, C.E. Searcy, V. Gandhi, Gemcitabine: preclinical pharmacology and mechanisms of action, Semin. Oncol. 23 (1996) 3—15. http://europepmc.org/abstract/MED/8893876.

[44] L. De Sousa Cavalcante, G. Monteiro, Gemcitabine: Metabolism and molecular mechanisms of action, sensitivity and chemoresistance in pancreatic cancer, Eur. J. Pharmacol. 741 (2014) 8–16. https://doi.org/10.1016/j.ejphar.2014.07.041.

Chapter Five – Project Direction and Future Work

5.1 Introduction

In this chapter a summarisation of the research conducted, and general conclusions are presented. The main chemical and biological findings are discussed in detail within chapters three and four. In summary this chapter will focus on general discussions alongside the authors insights into the future direction of the project for successive researchers in this area.

5.2 General Discussion and Future Works

Overall, this polymeric structure has great promise with controllability displayed via the RAFT approach and an efficient conjugation method developed utilising RAFT end group functionalization and PAA carboxylic acid functionality. Whilst the project encompassed hurdles in the initial synthesis the use of DMAEMA allowed for not only cationic characteristics to be imparted on the structure but also the successful co-polymerization of a structure containing PAA and DSDA. However, the stumbling blocks surrounding this project are not contained just to the synthetic route taken initially. Further work therefore on the computational chemistry behind polymeric synthesis is required. Computationally, this was not possible to do accurately within the current time frame due to in house issues with GPC hardware and a lack of kinetic data on the monomers utilised. Therefore, it is suggested that a lot of work is performed on kinetically analysing these monomers and RAFT agents

in order to accurately program the experiment in full, to give a better indication of the reaction conditions required to obtain polymers with desirable characteristics.

Future time and work for the completeness of this project needs to be focusing on the biological results and gaining a better understanding and more consistency between the cytotoxicity results, as the toxicity pertaining to polymer-drug conjugates is expected to come from the polymer itself and therefore a lack of consistency between polymer-drug conjugates and polymer cytotoxicity is of great concern Therefore, it would be advised to use other cancerous cell lines such as BT-20 or MCF-7 in order to corroborate whether fluctuations between MTT assays are evident, suggesting better purification of the polymer is required, or a complex mechanism of death. As such, colony survival assays should also be performed to corroborate these results.

Cellular uptake experiments it is advised need further quantification works, with more intense focus on FACS analysis, as this was used briefly for confirmation of uptake via the folate receptor and to assess whether correlation with confocal results was evident. Furthermore, greater FACS analysis would allow investigation into the cell cycle itself and results pertaining to whether cell cycle arrest has occurred. Research into this area would allow conclusions to be drawn as to whether the polymer itself causes growth arrest and thus give a much better indication as to whether toxicity has been imparted through the polymer itself and thus the mechanism at which that occurs can be eluded to. Additionally, the cell cycle can be monitored through both gemcitabine and polymer-gemcitabine treatments as a method to assess whether the mechanism of death is different between the two treatments as mass spectrometry analysis concluded there was a difficulty in metabolising the free gemcitabine produced and thus, toxicity through this treatment is not well understood.

Whilst confocal microscopy can provide quantitative data, there is a requirement for vast image capture and analysis, of which there was insufficient time throughout this project to perform. By production of a greater number of images,

there would be capability to asses in a quantitative manner much more accurately the amount of fluorescent containing substance entering the cell. This would be performed over regular time intervals (such as 1 hr , 6 hrs, 12 hr, 24 hr etc). As the images captured throughout this project were at a set time point there was a lack of images demonstrating the mechanism of entry of compounds, whilst also no indication of the time frame required for these materials to enter the cell. This data, if obtained would then allow more efficient experimental planning as optimal time frames for cellular entry would be known.

In the same vein, methanol extractions can be performed on the cells at regular intervals before mass spec analysis in order to assess the time frame needed for free gemcitabine to become apparent in the treated cells. This is also important in the case of polymer-drug treatments. It was observed that free gemcitabine was available to these cells albeit in a lower concentration. Therefore, by analysis at different time points of these treated cells it can be deduced whether the gemcitabine released has accrued sufficient time in order to metabolise, and if so then investigations into the metabolic arrest observed can be conducted.

It is the authors opinion that the following points need to be addressed therefore in any future work carrying this project forward.

- There needs to be an increased reliance on computational chemistry and a greater understanding of the kinetic profiles of the monomers in question. This would therefore eliminate the trial and error performed in the project with regards to polymer synthesis, saving time and money and allowing resources to be deployed in a more appropriate manner
- The synthetic route towards PEG-diamine needs to be optimised in order to provide a better yield for the reactions. Therefore, different purification methods such as column chromatography could be utilised with a more appropriate solvent system in order to increase yield and reduce the amount of time needed to produce this molecule.
- A sophisticated method for the quantification of gemcitabine conjugated to polymers needs to be addressed. Due to folic acid interference there was a

lack of a method other than analysis of dialysis water to asses the amount of gemcitabine conjugated to polymers. Thus, there was no indication as to the amount of drug within polymers leading to estimates for future work.

- Biologically, the toxicity results need greater investigation at different time points in order to better understand the mechanism of action of the polymer-drug conjugate, with FACS analysis and confocal analysis expanded upon in order to understand any cell growth arrest and uptake mechanisms in action with respect to the drug delivery vehicle.

A much more sophisticated mass spectrometry procedure is needed. There was no evidence of the disulfide linker within results and thus a mechanism of gemcitabine release could not be concluded. Furthermore, due to a lack of metabolites of gemcitabine within polymer-drug treatment it is suggested DNA analysis is performed on both free gemcitabine and polymer-drug treatments to assess whether gemcitabine is being incorporated into DNA leading to toxicity of the drug. It is suggested therefore that should these objectives be met then this project would be in a much stronger state scientifically and this material, which is believed to have potential can be assessed much more accurately for its commercial and clinical potential.